

SHOCK DYNAMICS

FLUID MECHANICS AND ITS APPLICATIONS

Volume 11

Series Editor: R. MOREAU

MADYLAM

Ecole Nationale Supérieure d'Hydraulique de Grenoble

Boîte Postale 95

38402 Saint Martin d'Hères Cedex, France

Aims and Scope of the Series

The purpose of this series is to focus on subjects in which fluid mechanics plays a fundamental role.

As well as the more traditional applications of aeronautics, hydraulics, heat and mass transfer etc., books will be published dealing with topics which are currently in a state of rapid development, such as turbulence, suspensions and multiphase fluids, super and hypersonic flows and numerical modelling techniques.

It is a widely held view that it is the interdisciplinary subjects that will receive intense scientific attention, bringing them to the forefront of technological advancement. Fluids have the ability to transport matter and its properties as well as transmit force, therefore fluid mechanics is a subject that is particularly open to cross fertilisation with other sciences and disciplines of engineering. The subject of fluid mechanics will be highly relevant in domains such as chemical, metallurgical, biological and ecological engineering. This series is particularly open to such new multidisciplinary domains.

The median level of presentation is the first year graduate student. Some texts are monographs defining the current state of a field; others are accessible to final year undergraduates; but essentially the emphasis is on readability and clarity.

For a list of related mechanics titles, see final pages.

Zhaoyuan Han and Xiezhen Yin

*Department of Mechanics
University of Science and Technology
Hefei, Anhui, China*

Shock Dynamics



Science Press
BEIJING



SPRINGER-SCIENCE+BUSINESS MEDIA, B.V.

Library of Congress Cataloging-in-Publication Data

Han, Z.

Shock dynamics / by Z. Han and X. Yin.

p. cm. -- (Fluid mechanics and its applications ; v. 11)

Includes bibliographical references and index.

ISBN 978-90-481-4159-3 ISBN 978-94-017-2995-6 (eBook)

DOI 10.1007/978-94-017-2995-6

1. Shock waves. 2. Gas dynamics. I. Yin, X. II. Title.

III. Series.

QC168.85.S45H36 1992

533'.293--dc20

92-10614

ISBN 978-90-481-4159-3

All Rights Reserved

© 1993 Springer Science+Business Media Dordrecht

Originally published by Kluwer Academic Publishers in 1993

No part of the material protected by this copyright notice may be reproduced or utilized in any form or by any means, electronic or mechanical, including photocopying, recording or by any information storage and retrieval system, without written permission from the copyright owner.

Preface

This book was written as a graduate student course—Shock Dynamics. Up to now, the first author has taught this course to the graduate students in the field of Fluid Mechanics, Department of Modern Mechanics, University of Science and Technology of China for seven times.

In the spring semester 1989, during his visit to the United States, the first author taught this course to the graduate students of Department of Mathematics, University of Colorado at Denver. At the same time, he gave a series of four lectures on Shock Dynamics to the graduate students of Department of Aerospace Engineering Sciences, University of Colorado at Boulder.

In 1991, during the first author's visit to Japan, he gave some lectures on Shock Dynamics in Tohoku University, University of Tokyo and Kyushu University.

The dynamic phenomena of shock waves such as propagation, diffraction, reflection, refraction and interaction of shock waves may be studied by using experimental methods, numerical calculations and theoretical analyses.

Although the detailed flow patterns of phenomena of shock motion can be obtained by using experimental methods and numerical calculations of solving Euler Equation or Navier-Stokes Equation, for example, the diffractions of shock waves by wedges form various phenomena of reflection—RR, SMR, CMR and DMR, we also need to analyse the process of the formation of shock waves in various phenomena of diffraction, reflection and interaction by using theoretical methods.

The shock dynamic method is a simple, fast and useful theoretical method, which can be used not only to calculate shock waves, but also to analyse the formation of shock waves. Particularly, the theory of disturbance propagating on shock surface which was presented by Whitham (1957) provides us with such a possibility to analyse complicated phenomena of shock diffraction and interaction. This book will introduce and explain basic concepts, methods, equations, and applications of shock dynamics systematically.

According to the development of shock dynamics, the problems investigated can be divided into two types, i.e., shock propagating into a quiescent gas and a moving gas. The former describes the interaction of a moving shock with a stationary body, while the latter describes the interaction of a moving shock with a moving body, of course, including a moving shock propagating through

a nonuniform disturbed flow field. It is evident that the kind of problems on the propagation and interaction of shock in moving gases is more widespread.

For the case of a uniform quiescent gas ahead of a shock, Chester (1954), Chisnell (1957), and Whitham (1958) obtained all the same relation that shock Mach number varies with the cross-sectional area along a tube by means of different ways, respectively. Then Whitham (1957,1959) extended the relation which originally applies to solid wall tube to the ray tube in flow field, and established two- and three-dimensional equations of geometrical shock dynamics.

For the case of a nonuniform quiescent gas ahead of a shock, Whitham(1957), Collins and Chen(1970), Catherasoo and Sturtevant(1983) derived the two-dimensional geometrical relations and area relation along a ray tube. In this book, the authors give a set of three- dimensional equations of shock dynamics.

For the case of a moving gas ahead of a shock, it can be divided into uniform flow and nonuniform flow. Chester(1960) derived the area relation. Whitham(1968) derived two-dimensional equations of shock dynamics denoted by the function of shock surface, α , for a uniform flow ahead of a shock, by using a transformation of coordinates. On the basis of Whitham's work, Han and Yin (1989A) obtained two- dimensional equations denoted by shock Mach number and shock wave angle, and then obtained two-dimensional equations of shock dynamics for a nonuniform flow ahead of a shock. Next, Han and Yin (1989B) derived three- dimensional equations of shock dynamics for a nonuniform flow ahead of a shock. In this book, the authors give the relations for disturbances propagating on shock surface under the condition of a moving gas ahead of a shock.

This book consists of three parts:

Part 1 (Chapters 1, 2, 3 and 4) explains the equations of shock dynamics for quiescent uniform and nonuniform gases ahead of shocks and their applications.

Part 2 (Chapters 5, 6 and 7) explains the equations of shock dynamics for uniform and nonuniform flows ahead of shocks and their applications.

Part 3 (Chapters 8, 9 and 10) introduces Mach reflection of shock in the case of steady, pseudosteady and unsteady flows, the shock refraction at gas interface and the interaction between shocks.

The authors express their acknowledgment and gratitude to the professors, colleagues and their students for their advice and suggestions. They would like to express their thanks to Prof. S. F. McCormick, Prof. C. Y. Chow and Prof. K. Gustafson, University of Colorado, USA for their kind invitation and arrangement for the first author teaching and lecturing in their University. They also express their thanks to Prof. K. Takayama for his kind invitation and ar-

rangement for the first author to visit Tohoku University, Japan, and to Prof. B. E. Milton, University of New South Wales, Australia for the very helpful discussion and cooperative research in the field of shock dynamics. Thanks are also due to Prof. Y. Aihara, Prof. K. Matsuo, and Prof. F. Higashino for their kind invitations for lecturing of the first author in their Universities.

Next, the authors would like to give thanks to their friends and colleagues in China, Prof. Hongru Yu, Prof. Hanxin Zhang, Prof. Dun Huang, and Prof. Jihai Wang for their supports and the meaningful discussions in the field of shock wave interaction and shock dynamics.

Finally, the authors wish to give thanks to the National Natural Science Foundation Committee of China for the supporting of their research in the field of shock dynamics.

The authors welcome suggestions and comments from the interested readers of this book.

Zhaoyuan Han and Xiezhen Yin

Hefei, Anhui, P.R. China

May 16, 1992

TABLE OF CONTENTS

Preface	(i)
Introduction One-Dimensional Unsteady Gasdynamics	(1)
§ 1 Sound wave and speed of sound	(1)
§ 2 Some basic concepts and expressions	(3)
§ 3 One-dimensional, unsteady, homoentropic flow in a constant cross sectional tube	(7)
§ 4 One-dimensional, unsteady flow in the general case	(14)
§ 5 Formation of shock wave from a simple wave	(17)
Part 1. Shock Dynamics for a Quiescent Gas Ahead of a Shock Wave	
Chapter 1. Relation Between M and A for a Uniform Quiescent Gas Ahead of a Shock Wave	(21)
§ 1.1 Shock wave of variable strength	(21)
§ 1.2 Chisnell's method	(24)
§ 1.3 Whitham's method	(30)
§ 1.4 Milton's modified relation	(38)
Chapter 2. Two-Dimensional Equations of Shock Dynamics for a Uniform Quiescent Gas Ahead of a Shock Wave	
§ 2.1 Fundamental concepts	(42)
§ 2.2 Two-dimensional equations of shock dynamics	(45)
§ 2.3 The disturbances propagating on the shock	(46)
§ 2.4 Transformation of curvilinear orthogonal coordinate system into rectangular coordinate system	(48)
§ 2.5 Shock-expansion and shock-compression	(50)
§ 2.6 Theory of sound	(60)
§ 2.7 Shock-shock	(62)
Chapter 3. Three-Dimensional Equations of Shock Dynamics for a Uniform Quiescent Gas Ahead of a Shock Wave	
§ 3.1 Three-dimensional equations of shock dynamics	(68)
§ 3.2 The various forms of differential equations for a uniform quiescent gas ahead of a shock	(72)
§ 3.3 Analogy of shock diffraction with steady supersonic flow	(75)
§ 3.4 The shock-shock relations in the case of three-dimensional flow	(79)

§ 3.5 Diffraction by a cone	(82)
§ 3.6 Diffraction by a circular cylinder or a sphere	(87)
§ 3.7 Diffraction by a thin or slender body	(92)
§ 3.8 Internal conical diffraction	(102)
§ 3.9 A set of simple, useful equations for external conical diffraction	(105)
§ 3.10 Different behaviour of the triple point locus of internal and external conical diffractions	(110)

Chapter 4. Equations of Shock Dynamics for a Nonuniform

Quiescent Gas Ahead of a Shock Wave (118)

§ 4.1 Area relation along a tube	(118)
§ 4.2 Two-dimensional equations in the orthogonal curvilinear coordinates	(120)
§ 4.3 Three-dimensional equations for nonuniform quiescent gas	(121)
§ 4.4 The various forms of differential equations	(123)
§ 4.5 Characteristic relations	(125)

Part 2. Shock Dynamics for a Moving Gas Ahead of a Shock Wave

Chapter 5. Two-Dimensional Equations for a Uniform Moving

Gas Ahead of a Shock Wave (135)

§ 5.1 Two frames of reference	(135)
§ 5.2 Two-dimensional equations denoted by the function $\alpha(x,y)$	(138)
§ 5.3 Two-dimensional equations denoted by shock Mach number M and shock angle θ (Han and Yin, 1989A)	(142)
§ 5.4 The behavior of shock propagating into the uniform flow	(144)
§ 5.5 Characteristic relations in the rectangular coordinates	(148)
§ 5.6 Application of theory of sound to regular reflection over a wedge	(151)
§ 5.7 Formation of a reflected shock wave	(153)
§ 5.8 Basic relations for the calculation of reflected shock	(155)
§ 5.9 First disturbance point and last disturbance point	(158)
§ 5.10 The equations for axially-symmetrical flow	(161)

Chapter 6. One- and Two-Dimensional Equations for a

Nonuniform Moving Gas Ahead of a Shock Wave (165)

§ 6.1 One-dimensional area relation for a nonuniform, steady flow ahead of a shock	(165)
§ 6.2 Basic idea for establishing the two-dimensional equations	

of shock dynamics	(168)
§ 6.3 Transformation of coordinates in any small region	(169)
§ 6.4 Two-dimensional equations denoted by the function $\alpha(x,y)$ for small region	(172)
§ 6.5 Two-dimensional equations denoted by shock Mach number M and shock angle θ for a small region	(175)
§ 6.6 The area relation along ray tube in moving frame	(176)
§ 6.7 The equations in stationary frame of reference for entire flow field	(178)
§ 6.8 Shock wave-vortex interaction	(187)

Chapter 7. Three-Dimensional Equations for a Nonuniform Moving Gas Ahead of a Shock Wave

.....	(191)
§ 7.1 Three-dimensional shock propagating into a nonuniform flow field	(191)
§ 7.2 Transient transformation of coordinates in three-dimensional flow	(193)
§ 7.3 Three-dimensional equations in rectangular coordinates	(198)
§ 7.4 Three-dimensional equations in cylindrical coordinates	(202)
§ 7.5 Three-dimensional equations in spherical coordinates	(207)
§ 7.6 The equations in the case of axially-symmetrical and self-similar flow field	(210)
§ 7.7 Shock-shock relations in the case of a moving gas ahead of a shock	(212)
§ 7.8 The application of the equations of shock dynamics to 'shock- on-shock interaction'	(217)

Part 3. Dynamic Phenomena of Shock Waves

Chapter 8. Reflections of Shock Waves in Steady and Pseudosteady Flows

.....	(233)
§ 8.1 Introduction	(233)
§ 8.2 Flow patterns	(237)
§ 8.3 Some basic concept and analytic method	(241)
§ 8.4 Transition criteria $RR \rightleftharpoons MR$ in steady and pseudosteady flows	(246)
§ 8.5 CMR, DMR and their transition	(250)
§ 8.6 Calculation of χ and χ'	(253)
§ 8.7 Effect of viscosity in pseudosteady flow	(257)
§ 8.8 von Neumann paradox of weak Mach reflection	(262)

Chapter 9. Reflections of Shock Waves in Unsteady Flow	(264)
§ 9.1 Introduction	(264)
§ 9.2 Shock reflection on a cylindric surface	(264)
§ 9.3 Prediction of transition RR \rightarrow MR on cylindric convex surface	(268)
§ 9.4 Prediction of transition MR \rightarrow RR on cylindric concave surface	(273)
§ 9.5 Reflection of plane shock on double wedge	(278)
Chapter 10. Refractions of Shock Waves at Interface Between Different Media and Interaction Between Shocks	(280)
§ 10.1 Introduction	(280)
§ 10.2 Flow patterns of shock refraction and their shock polars	(280)
§ 10.3 Refraction of moving shock at slip surface	(289)
§ 10.4 Application of shock dynamics to shock refraction	(292)
§ 10.5 Numerical shock dynamics	(297)
§ 10.6 Interaction between shocks	(300)
References	(310)
Nomenclature	(315)
Index	(317)

Introduction One-Dimensional Unsteady Gasdynamics

As a basis, this chapter introduces one-dimensional, unsteady, continuous flow of gasdynamics, in which the behaviour, concepts and relations of small amplitude wave (sound wave) and large amplitude wave are discussed.

§ 1 Sound wave and speed of sound

Sound wave is an infinitesimal pressure wave (or call it small disturbance wave), which may be generated by means of vibrating a tuning fork, where the vibrated tuning fork is regarded as a source of sound.

In this book, however, we are interested in so-called compression sound wave and rarefaction sound wave, which may be initiated by means of pushing or pulling a piston with a very low constant speed in a tube of constant cross-sectional area (as shown in Figs. 1 and 2, respectively). Why does pushing or pulling the piston with a very low constant speed generate a compression sound wave or a rarefaction sound wave? This is because the uniform flow field ahead of the piston is disturbed, and such a small disturbance propagates with the speed of sound. We will discuss this as follows.

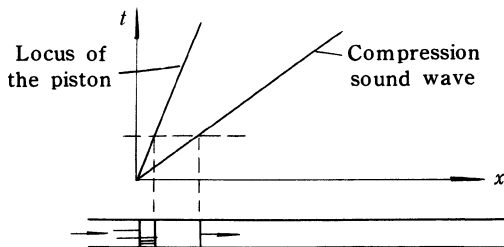


Fig. 1 Compression sound wave

In the case of one-dimensional, ideal, and homoentropic flow, we have the following basic equations of gasdynamics, that is, continuity equation, Euler equation, energy and state equations (we will discuss the flow field and equations in next section)

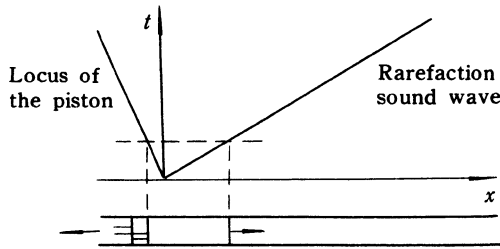


Fig.2 Rarefaction sound wave

$$\begin{cases} \frac{\partial \rho}{\partial t} + \rho \frac{\partial u}{\partial x} + u \frac{\partial \rho}{\partial x} = 0 \\ \frac{\partial u}{\partial t} + u \frac{\partial u}{\partial x} + \frac{1}{\rho} \frac{\partial p}{\partial x} = 0 \\ p = p(\rho) \end{cases} \quad (1)$$

where p , ρ , and u are the pressure, density, and flow velocity of gas particle, respectively. The third expression of the equations (1) can be obtained by combination of the energy equation with the state equation in the case of homoentropic flow.

In the case of small perturbations, pressure, density and flow velocity can be expressed as

$$\begin{cases} p = p_0 + p' \\ \rho = \rho_0 + \rho' \\ u = u' \end{cases} \quad (2)$$

where the prime denotes small perturbations; "0" denotes undisturbed quantities.

By substituting (2) into (1), retaining first order terms, we obtain

$$\begin{cases} \frac{\partial p'}{\partial t} + \rho_0 \frac{\partial u'}{\partial x} = 0 \\ \rho_0 \frac{\partial u'}{\partial t} + a_0^2 \frac{\partial \rho'}{\partial x} = 0 \end{cases} \quad (3)$$

where $a_0^2 = \frac{dp'}{d\rho'} = \frac{dp}{d\rho}$, a_0 is the speed of sound. From the equations (3), a wave equation is obtained

$$\frac{\partial^2 \rho'}{\partial t^2} - a_0^2 \frac{\partial^2 \rho'}{\partial x^2} = 0 \quad (4)$$

The solution of the equation (4) is given as

$$\rho' = f_1(x - a_0 t) + f_2(x + a_0 t) \quad (5)$$

where f_1 and f_2 are arbitrary functions. $x - a_0 t = \text{constant}$ corresponds to right-traveling wave; $x + a_0 t = \text{constant}$ corresponds to left-traveling wave, that is, the infinitesimal pressure wave propagates with the speed of sound, a_0 .

The expression for the speed of sound can be written as a partial derivative at constant entropy

$$a_0^2 = \left(\frac{\partial p}{\partial \rho} \right)_s \quad (6)$$

This is a general expression, which is valid even if sound wave propagates in a non-homoentropic flow field. Since the propagation of sound wave is rapid and the variations in pressure and temperature are small, the process may be considered as both reversible and adiabatic, and therefore, isentropic.

For a perfect gas, the relation between pressure and density in an isentropic process is given by

$$p / \rho^\gamma = \text{constant} \quad (7)$$

or

$$\frac{dp}{p} = \gamma \frac{d\rho}{\rho} \quad (8)$$

Substituting (8) into (6), we obtain

$$\left(\frac{\partial p}{\partial \rho} \right)_s = \gamma R T \quad (9)$$

or

$$a^2 = \sqrt{\gamma \frac{p}{\rho}} = \sqrt{\gamma R T} = \sqrt{\gamma \frac{R_u}{\mu} T} \quad (10)$$

where γ is ratio of specific heats, R is gas constant, $R_u = 8314.3 \text{ J/Kg mol} \cdot \text{K}$ is universal gas constant, μ is molecular weight. The speed of sound in air is of the order of 340m / sec, and in hydrogen, of the order of 1300m / sec.

§ 2 Some basic concepts and expressions

Before further discussion of one-dimensional, unsteady flow, we explain here some basic concepts and expressions, which are important for us to describe an unsteady flow field.

1. *The meaning of the expression for $\frac{dQ}{dt} = 0$*

Q in the total derivative is a quantity, which may be entropy s , pressure p ,

density ρ , velocity u or their combination.

For one-dimensional, unsteady flow, any quantity Q can be expressed as a function of x and t , where x and t are independent variables, that is, $Q = Q(x, t)$.

We first consider entropy s . If the function $s = s(x, t)$ is given, it is easy for us to find the partial derivatives $\frac{\partial s}{\partial t}$ and $\frac{\partial s}{\partial x}$, but how do we find the total derivative $\frac{ds}{dt}$? And what does $\frac{ds}{dt}$ mean? We know that there are two viewpoints for describing fluid flow, that is, particle (material) viewpoint and field (spatial) viewpoint. The former is to follow gas particle to see the change in entropy s (or other quantities). In this description, the coordinates of gas particles are considered to be a function of time. For a particular particle, we have $x = x(t)$. The latter is a field description, in which, we do not follow any particle to see the change in entropy s . We observe the change in entropy s at fixed spatial coordinates with time t , or keep time t constant to see the change in entropy s with spatial coordinates.

The total derivative $\frac{ds}{dt}$ can be expanded as

$$\frac{ds}{dt} = \frac{\partial s}{\partial t} + \frac{\partial s}{\partial x} \frac{dx}{dt} \quad (11)$$

In one-dimensional, unsteady flow, the differential equation of particle path can be written as

$$\frac{dx}{dt} = u \quad (12)$$

Substituting (12) into (11), we obtain

$$\frac{ds}{dt} = \frac{\partial s}{\partial t} + u \frac{\partial s}{\partial x} \quad (13)$$

If the functions $s = s(x, t)$ and $u = u(x, t)$ are given, from the relation (13), $\frac{ds}{dt}$ can be obtained.

The meaning of $\frac{ds}{dt}$ is the change in the entropy of a gas particle along a particle path.

Next, we want to make an extension of the above concept to any curves, for example, wave lines.

Quantity Q here may be p , ρ , a , u or their combination, which can be expressed as

$$Q = Q(x, t) = Q[x(t), t] \quad (14)$$

Taking derivative of function Q with respect to t , we obtain

$$\frac{dQ}{dt} = \frac{\partial Q}{\partial t} + \frac{\partial Q}{\partial x} \frac{dx}{dt} \quad (15)$$

Here $\frac{dx}{dt}$ may be written, for example, in the following forms

$$\begin{cases} \frac{dx}{dt} = u \\ \frac{dx}{dt} = a \\ \frac{dx}{dt} = u \pm a \\ \frac{dx}{dt} = W_s \pm a \end{cases} \quad (16)$$

where W_s is shock speed.

If $\frac{dQ}{dt}$ is expressed as $\frac{\partial Q}{\partial t} + (u + a)\frac{\partial Q}{\partial x}$, and $\frac{dQ}{dt} = 0$, the quantity Q remains constant along a right traveling pressure wave, and if $\frac{dQ}{dt} = \frac{\partial Q}{\partial t} + (u - a)\frac{\partial Q}{\partial x} = 0$, Q remains constant along a left traveling pressure wave.

2. Homoentropic, isentropic and non-isentropic flow field

In the case of unsteady flow, the flow fields may be divided into three types: homoentropic, isentropic and non-isentropic flows.

The flow field of some continuous pressure waves propagating in a constant cross-sectional tube is usually considered as a homoentropic flow field. In this case, the heat transfer and viscosity of gas may be neglected.

The expression for entropy is given as

$$s = \text{constant entire flow field} \quad (17)$$

In one-dimensional, unsteady flow, we have $\frac{\partial s}{\partial t} = 0$, $\frac{\partial s}{\partial x} = 0$.

In three dimensional flow, we have

$$\frac{\partial s}{\partial t} = 0, \quad \frac{\partial s}{\partial x} = 0, \quad \frac{\partial s}{\partial y} = 0, \quad \frac{\partial s}{\partial z} = 0.$$

The flow field behind a moving shock wave of variable strength is usually regarded as an isentropic flow field.

In this case, the expression for entropy is

$$\frac{ds}{dt} = 0 \quad (18)$$

It means that the entropy of a gas particle remains constant during the process of motion of the particle, but different particles have the different values of entropy as shown in Fig.3.

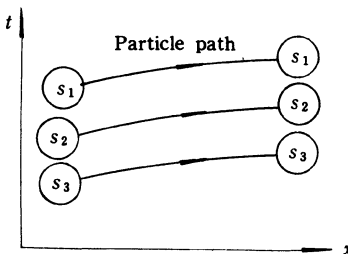


Fig. 3 The isentropic flow

In the case of isentropic flow, the partial derivatives of entropy are not equal to zero

$$\frac{\partial s}{\partial t} \neq 0, \quad \frac{\partial s}{\partial x} \neq 0 \quad (19)$$

In more general case, that is, non-isentropic flow, the expression for entropy is expressed as

$$\frac{ds}{dt} \neq 0 \quad (20)$$

In this case, we usually consider the viscosity on the wall of tube, the heat transfer and the change in cross-sectional area of tube. We will discuss this later.

3. Expressions for the derivatives of pressure and density

It should be noted that under different conditions, that is, different flow fields, the expressions for the relationship between p and ρ are different.

We first consider the relation between total derivatives of p and ρ .

For non-isentropic flow, p is the function of ρ and s , $p = p(\rho, s)$, we have

$$\frac{dp}{dt} = \left(\frac{\partial p}{\partial \rho} \right)_s \frac{d\rho}{dt} + \left(\frac{\partial p}{\partial s} \right)_\rho \frac{ds}{dt} = a^2 \frac{d\rho}{dt} + \left(\frac{\partial p}{\partial s} \right)_\rho \frac{ds}{dt} \quad (21)$$

For isentropic flow, $p = p(\rho, s)$ and $\frac{ds}{dt} = 0$, we have

$$\frac{dp}{dt} = a^2 \frac{d\rho}{dt} \quad (22)$$

For homoentropic flow, we have the same relation as (22).

Next we consider the partial derivatives of p and ρ .

For non-isentropic flow, we have

$$\begin{cases} \frac{\partial p}{\partial t} = a^2 \frac{\partial \rho}{\partial t} + \left(\frac{\partial p}{\partial s} \right)_\rho \frac{\partial s}{\partial t} \\ \frac{\partial p}{\partial x} = a^2 \frac{\partial \rho}{\partial x} + \left(\frac{\partial p}{\partial s} \right)_\rho \frac{\partial s}{\partial x} \end{cases} \quad (23)$$

For isentropic flow, we have the same relations as (23).

For homoentropic flow, $\frac{\partial s}{\partial t} = 0$ and $\frac{\partial s}{\partial x} = 0$, we obtain

$$\begin{cases} \frac{\partial p}{\partial t} = a^2 \frac{\partial \rho}{\partial t} \\ \frac{\partial p}{\partial x} = a^2 \frac{\partial \rho}{\partial x} \end{cases} \quad (24)$$

§ 3 One-dimensional, unsteady, homoentropic flow in a constant cross-sectional tube

In this section, we will consider the flow field in a constant cross-sectional tube, in which there are some continuous pressure waves without the restriction of small perturbations; but no shock waves and contact surfaces (discontinuities), propagating in a constant cross-sectional tube. If the friction and heat transfer are ignored and the gas is taken as a perfect gas, the problem becomes a homoentropic flow.

The flows mentioned above may be divided into three types, double-wave flows, simple-wave flows and steady-state flows.

In double-wave flows, there are both right-traveling and left-traveling waves.

In simple-wave flows, either right-traveling or left-traveling waves, but not both, are present.

In steady-state flows, there are no pressure waves.

1. Double wave flows

A set of one-dimensional, homoentropic, unsteady equations is given as follows

$$\begin{cases} \frac{\partial \rho}{\partial t} + \rho \frac{\partial u}{\partial x} + u \frac{\partial \rho}{\partial x} = 0 \\ \frac{\partial u}{\partial t} + u \frac{\partial u}{\partial x} + \frac{1}{\rho} \frac{\partial p}{\partial x} = 0 \\ p = p(\rho) \end{cases} \quad (25)$$

From the equations (25), we can obtain

$$\left[\frac{\partial u}{\partial t} + (u + a) \frac{\partial u}{\partial x} \right] + \frac{a}{\rho} \left[\frac{\partial \rho}{\partial t} + (u + a) \frac{\partial \rho}{\partial x} \right] = 0 \quad (26)$$

and

$$\left[\frac{\partial u}{\partial t} + (u - a) \frac{\partial u}{\partial x} \right] - \frac{a}{\rho} \left[\frac{\partial \rho}{\partial t} + (u - a) \frac{\partial \rho}{\partial x} \right] = 0 \quad (27)$$

Since the flow field is homoentropic and the speed of sound, a , is only a function of ρ , $\frac{a}{\rho} d\rho$ must be a total differential, that is,

$$d \left[\int \frac{a}{\rho} d\rho \right] = \frac{a}{\rho} d\rho \quad (28)$$

Expanding (28), we obtain

$$\begin{cases} \frac{\partial}{\partial t} \int \frac{a}{\rho} d\rho = \frac{a}{\rho} \frac{\partial \rho}{\partial t} \\ \frac{\partial}{\partial x} \int \frac{a}{\rho} d\rho = \frac{a}{\rho} \frac{\partial \rho}{\partial x} \end{cases} \quad (29)$$

Substituting (29) into (26) and (27), respectively, we obtain

$$\begin{cases} \left[\frac{\partial}{\partial t} + (u + a) \frac{\partial}{\partial x} \right] \left(u + \int \frac{a}{\rho} d\rho \right) = 0 \\ \left[\frac{\partial}{\partial t} + (u - a) \frac{\partial}{\partial x} \right] \left(u - \int \frac{a}{\rho} d\rho \right) = 0 \end{cases} \quad (30)$$

According to relation (15), the meaning of relations (30) may be interpreted as follows: The quantity $\left(u + \int \frac{a}{\rho} d\rho \right)$ remains constant along each pressure wave of $\frac{dx}{dt} = u + a$; $\left(u - \int \frac{a}{\rho} d\rho \right)$ remains constant along each pressure wave of $\frac{dx}{dt} = u - a$. In other words, $\left(u + \int \frac{a}{\rho} d\rho \right)$ on the wave front of $\frac{dx}{dt} = u + a$ is kept constant during the motion of the wave; for $\left(u - \int \frac{a}{\rho} d\rho \right)$ on the wave front of $\frac{dx}{dt} = u - a$, similar explanation can be made.

The relations (30) can be written in another form

$$\begin{cases} u + \int \frac{a}{\rho} d\rho = K_1 & \text{along } \frac{dx}{dt} = u + a \\ u - \int \frac{a}{\rho} d\rho = K_2 & \text{along } \frac{dx}{dt} = u - a \end{cases} \quad (31)$$

where K_1 and K_2 are referred to as Riemann Invariables.

Under the conditions of perfect gas and homoentropic flow, by using the

first and second thermodynamic laws, we have

$$\int \frac{a}{\rho} d\rho = \frac{2a}{\gamma - 1} \quad (32)$$

Substituting (32) into (31), we obtain

$$\begin{cases} u + \frac{2a}{\gamma - 1} = K_1 & \text{along } \frac{dx}{dt} = u + a \\ u - \frac{2a}{\gamma - 1} = K_2 & \text{along } \frac{dx}{dt} = u - a \end{cases} \quad (33)$$

The first expressions in (31) and (33) represent the right-traveling waves, while the second expressions represent the left-traveling waves.

Next, we will discuss simple wave flows in detail.

2. Simple wave flows

In the equations (30), there are two equations, which represent two types of waves, i.e., the right-traveling waves and the left-traveling waves. If one of the Riemann Invariables is a constant over the entire flow field, for example, $\frac{\partial}{\partial t} \left(u - \frac{2a}{\gamma - 1} \right) = 0$, $\frac{\partial}{\partial x} \left(u - \frac{2a}{\gamma - 1} \right) = 0$, which means that there is only one type of waves here propagating in the flow field, the relations for perfect gas become

$$\begin{cases} \left[\frac{\partial}{\partial t} + (u + a) \frac{\partial}{\partial x} \right] \left(u + \frac{2a}{\gamma - 1} \right) = 0 \\ u - \frac{2a}{\gamma - 1} = \text{constant} \quad \text{entire flow field} \end{cases} \quad (34)$$

From the equations (34), we find that there are only the right-traveling waves (a family of waves) which propagate in a constant cross-sectional tube.

Next, we will analyse the behaviour and formation of simple wave.

By substituting the second expression of (34) into the first one, we obtain

$$\begin{cases} \frac{\partial u}{\partial t} + (u + a) \frac{\partial u}{\partial x} = 0 \\ \frac{\partial a}{\partial t} + (u + a) \frac{\partial a}{\partial x} = 0 \end{cases} \quad (35)$$

or $\left[\frac{\partial}{\partial t} + (u + a) \frac{\partial}{\partial x} \right] (u + a) = 0 \quad (36)$

It follows from (35) and (36) that u , a , $(u + a)$, therefore p , ρ remain constant along $\frac{dx}{dt} = u + a$, that is, the wave lines of simple wave are a family of straight lines. The expressions for simple wave can be expressed as

$$\begin{cases} x = (u + a)t + F(u) \\ u - \int \frac{a}{\rho} d\rho = \text{constant} \end{cases} \quad \text{entire flow field} \quad (37)$$

or for perfect gas

$$\begin{cases} x = (u + a)t + F(u) \\ u - \frac{2a}{\gamma - 1} = \text{constant} \end{cases} \quad \text{entire flow field} \quad (38)$$

where $F(u)$ is an arbitrary function.

In order to examine the change of wave form while a simple wave moves forward, we need to identify the sign of expression for $\frac{d(u+a)}{d\rho}$. We only consider the right-traveling waves here

$$\frac{d(u+a)}{d\rho} = \frac{du}{d\rho} + \frac{da}{d\rho} = \frac{du}{d\rho} + \frac{d}{d\rho} \left(\frac{\partial p}{\partial \rho} \right)_s^{\frac{1}{2}} \quad (39)$$

From the second expression of (37), the perfect gas and homoentropic relation, the expression (39) can be rewritten as

$$\frac{d(u+a)}{d\rho} = \frac{a}{\rho} + \frac{1}{2a} \frac{d}{d\rho} \left(\frac{\gamma p}{\rho} \right) = \frac{(\gamma + 1)a}{2\rho} > 0 \quad (40)$$

Next we explain the formation of simple wave. Simple wave may be divided into right-traveling compression wave, right-traveling rarefaction wave, left-traveling compression wave and left-traveling rarefaction wave. A lot of manner can be used for generating simple wave. What we use here is the motion of a piston in a tube for generating compression wave and rarefaction wave as shown in Fig.4 and Fig.5.

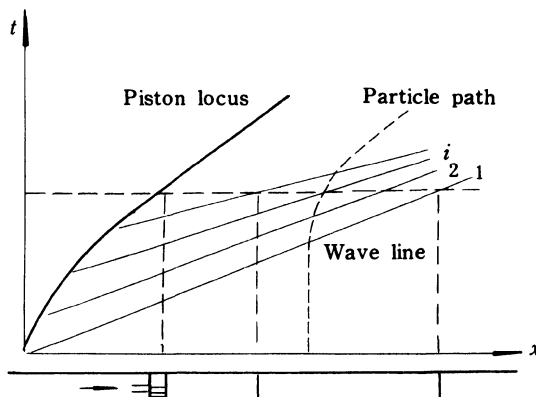


Fig.4 Compression wave

Initially, the air in front of the piston and the piston itself are at rest. Of course, the boundary condition for the air on the surface of the piston is satisfied.

We now push the piston rightward. The piston is gradually accelerated to a certain value of velocity, and then is kept this velocity continuously to move forward. A right-traveling compression wave is generated, which is illustrated by Fig. 4. The piston locus is divided into two parts, the curved locus and straight locus. The compression wave is generated at the curved part of the piston locus. However, there is no wave which is initiated at the straight locus, because the boundary condition on the surface of the piston is satisfied. The flow pattern is shown in the $x-t$ plane, where the piston locus, wave lines and particle path are illustrated.

Now we consider the generation of the rarefaction wave. The piston is gradually accelerated leftward, the same thing will be done, a right-traveling rarefaction wave is generated on the right of the piston (as shown in Fig.5).

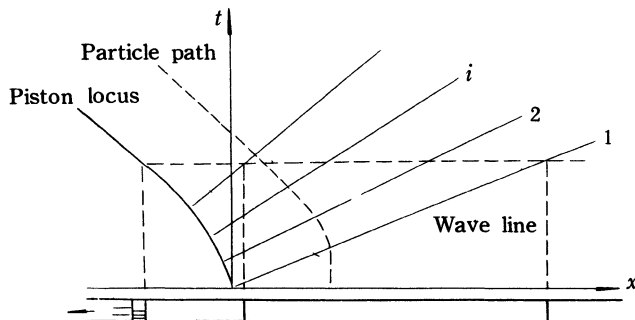


Fig.5 Rarefaction wave

By using the relations (40) and (37), that is,

$$\frac{d(u + a)}{d\rho} > 0 \quad \text{and} \quad du = \frac{a}{\rho} d\rho$$

we can analyse the behaviour of the above compression wave and rarefaction wave as follows.

For the compression wave, we have

$$dp > 0, \quad d\rho > 0, \quad d(u + a) > 0, \quad du > 0 \quad (41)$$

Therefore

$$\left(\frac{dx}{dt}\right)_2 = (u_2 + a_2) > \left(\frac{dx}{dt}\right)_1 = (u_1 + a_1) \quad (42)$$

For the rarefaction wave, we have

$$dp < 0, \quad d\rho < 0, \quad d(u + a) < 0, \quad du < 0 \quad (43)$$

Therefore

$$\left(\frac{dx}{dt}\right)_2 = (u_2 + a_2) < \left(\frac{dx}{dt}\right)_1 = (u_1 + a_1) \quad (44)$$

where subscripts 1 and 2 represent the distance waves as shown in Fig. 4 and Fig. 5, respectively.

According to the relations (41), (42), (43), and (44), the following conclusions can be obtained:

- (1) In compression waves, the wave lines are convergent; in rarefaction waves, the wave lines are divergent, as time progresses.
- (2) In compression waves, the particle path bends toward the wave line; in rarefaction waves, the particle path bends away from the wave line.
- (3) The region of rarefaction wave always broadens, while the region of compression wave always narrows, that is, the compression wave form always steepens.

The above mentioned is concerned with the right-traveling waves, as for the left-traveling waves, the similar manner of analysis can be made.

Next we will give the definition of right-traveling and left-traveling waves, which is important for us to analyse the behaviour of the continuous pressure waves.

What is a right-traveling or left-traveling wave? The definition does not depend on whether the wave is traveling rightward or leftward, if observing at a fixed coordinates (for example, on the ground). In order to make this concept clear, we have to define the front side of wave and back side of wave.

The front side of a wave is defined as the side into which a gas particle enters; the back side, the side from which a gas particle leaves.

For the right-traveling wave, the gas particle always enters into the wave front from the right-hand side of it, in other words, the front side of wave is always on the right hand side of wave line.

For the left-traveling wave, the gas particle always enters into the wave front from the left-hand side of it.

The expression for the right-traveling wave and left-traveling wave is given

as

$$\frac{dx}{dt} = u \pm a$$

where the upper sign represents the right-traveling wave, the lower sign represents the left-traveling wave.

According to the equations (38) and the corresponding left-traveling wave equations (which are negligible), the basic relations can be written as

$$\frac{a_2}{a_1} = 1 \pm \frac{\gamma - 1}{2} \left(\frac{u_2 - u_1}{a_1} \right) \quad (45)$$

$$\frac{p_2}{p_1} = \left[1 \pm \frac{\gamma - 1}{2} \left(\frac{u_2 - u_1}{a_1} \right) \right]^{\frac{2\gamma}{\gamma - 1}} \quad (46)$$

$$\frac{\rho_2}{\rho_1} = \left[1 \pm \frac{\gamma - 1}{2} \left(\frac{u_2 - u_1}{a_1} \right) \right]^{\frac{1}{\gamma - 1}} \quad (47)$$

where "+" denotes the right-traveling wave, and "-" denotes the left-traveling wave; "1" denotes the front side of wave and "2" denotes the back side of wave.

If the flow field in the front side of wave is at rest, and "0" is used as the subscript of the parameters in the flow field in the front side, M denotes the flow Mach number in the flow field in the back side, namely $M = \frac{u_2}{a_2}$, a , p , and T are the speed of sound, pressure and temperature in the back side, respectively, then the relations (45), (46) and (47) for the left-traveling wave can be written as

$$\frac{a_0}{a} = 1 + \frac{\gamma - 1}{2} M \quad (48)$$

$$\frac{p_0}{p} = \left(1 + \frac{\gamma - 1}{2} M \right)^{\frac{2\gamma}{\gamma - 1}} \quad (49)$$

$$\frac{T_0}{T} = \left(1 + \frac{\gamma - 1}{2} M \right)^2 \quad (50)$$

In order to see the differences between one-dimensional, unsteady and steady flows, we write one-dimensional, steady, homoentropic (isentropic) relations as

$$\frac{a_0}{a} = \left(1 + \frac{\gamma - 1}{2} M^2 \right)^{\frac{1}{2}} \quad (51)$$

$$\frac{p_0}{p} = \left(1 + \frac{\gamma - 1}{2} M^2 \right)^{\frac{\gamma}{\gamma - 1}} \quad (52)$$

$$\frac{T_0}{T} = 1 + \frac{\gamma - 1}{2} M^2 \quad (53)$$

It is interesting to see that if $M = 5$, $\gamma = 1.4$, for example, for the steady flow, $\frac{p_0}{p} = 529$, $\frac{T_0}{T} = 6$, but for the unsteady flow, $\frac{p_0}{p} = 128$, $\frac{T_0}{T} = 4$. The behaviour of the unsteady flow mentioned above is sometimes useful to perform some hypersonic experiments for avoiding condensation of air.

§ 4. One-dimensional, unsteady flow in the general case

In this section, we will discuss the general case of one-dimensional, unsteady flow including isentropic flow and non-isentropic flow, in a constant cross-sectional area tube and a variable cross-sectional area tube.

1. Basic equations

In the general case, one-dimensional, unsteady governing equations are expressed as

$$\begin{cases} \frac{\partial p}{\partial t} + \rho \frac{\partial u}{\partial x} + u \frac{\partial \rho}{\partial x} = - \frac{\rho u}{A} \frac{dA}{dx} \\ \frac{\partial u}{\partial t} + u \frac{\partial u}{\partial x} + \frac{1}{\rho} \frac{\partial p}{\partial x} = - f \\ \frac{\partial s}{\partial t} + u \frac{\partial s}{\partial x} = \frac{uf + q}{T} \\ p = p(\rho, s) \end{cases} \quad (54)$$

where f is the frictional force per unit mass of gas, q is the heat transfer rate per unit mass of gas, T is the temperature of gas, A is the cross-sectional area of a tube.

The equations (54) represent one-dimensional, non-isentropic, unsteady flow in the tube with variable cross-sectional area, in which heat transfer and frictional force on the wall surface of tube are considered.

Under the condition of the isentropic flow in constant cross-sectional area tube, that is, heat transfer and friction being negligible, the equation can be simplified to

$$\left\{ \begin{array}{l} \frac{\partial p}{\partial t} + \rho \frac{\partial u}{\partial x} + u \frac{\partial \rho}{\partial x} = 0 \\ \frac{\partial u}{\partial t} + u \frac{\partial u}{\partial x} + \frac{1}{\rho} \frac{\partial p}{\partial x} = 0 \\ \frac{\partial s}{\partial t} + u \frac{\partial s}{\partial x} = 0 \\ p = p(\rho, s) \end{array} \right. \quad (55)$$

As mentioned already, for example, the flow field behind a moving shock, neglecting the heat transfer and friction, may be regarded as an isentropic flow, in which two cases are included, namely the flow in a constant cross-sectional area tube, and the flow in a variable cross-sectional area tube. The difference between them is only the term of the right-hand side of the continuity equations as expressed in the equations (54) and (55), and we will discuss this later.

2. Characteristic curves in isentropic and non-isentropic flows

We know that in the case of homoentropic flow, there are two families of waves, in other words, two families of characteristics. But in isentropic and non-isentropic flows, the situation is different from that of homoentropic flow, that is, there are three families of characteristics.

We first derive the characteristic relations expressed by du and dp under the condition of isentropic flow in a constant cross-sectional area tube.

From the equations (55) and expression (22), we have

$$\frac{1}{\rho a} \frac{\partial p}{\partial t} + \frac{u}{\rho a} \frac{\partial p}{\partial x} + a \frac{\partial u}{\partial x} = 0 \quad (56)$$

$$\frac{1}{\rho} \frac{\partial p}{\partial x} + \frac{\partial u}{\partial t} + u \frac{\partial u}{\partial x} = 0 \quad (57)$$

By combining the equation (56) with the equation (57), we obtain

$$\left[\frac{\partial u}{\partial t} + (u + a) \frac{\partial u}{\partial x} \right] + \frac{1}{\rho a} \left[\frac{\partial p}{\partial t} + (u + a) \frac{\partial p}{\partial x} \right] = 0 \quad (58)$$

$$\left[\frac{\partial u}{\partial t} + (u - a) \frac{\partial u}{\partial x} \right] - \frac{1}{\rho a} \left[\frac{\partial p}{\partial t} + (u - a) \frac{\partial p}{\partial x} \right] = 0 \quad (59)$$

$$\frac{\partial s}{\partial t} + u \frac{\partial s}{\partial x} = 0 \quad (60)$$

or

$$\left\{ \begin{array}{l} \left(\frac{du}{dt} \right)_I + \frac{1}{\rho a} \left(\frac{dp}{dt} \right)_I = 0 \\ \left(\frac{du}{dt} \right)_{II} - \frac{1}{\rho a} \left(\frac{dp}{dt} \right)_{II} = 0 \end{array} \right. \quad (61)$$

$$\left\{ \begin{array}{l} \left(\frac{du}{dt} \right)_I + \frac{1}{\rho a} \left(\frac{dp}{dt} \right)_I = 0 \\ \left(\frac{du}{dt} \right)_{II} - \frac{1}{\rho a} \left(\frac{dp}{dt} \right)_{II} = 0 \end{array} \right. \quad (62)$$

$$\left\{ \begin{array}{l} \left(\frac{ds}{dt} \right)_{III} = 0 \end{array} \right. \quad (63)$$

or

$$\left\{ \begin{array}{ll} du + \frac{1}{\rho a} dp = 0 & \text{along } \frac{dx}{dt} = u + a \end{array} \right. \quad (64)$$

$$\left\{ \begin{array}{ll} du - \frac{1}{\rho a} dp = 0 & \text{along } \frac{dx}{dt} = u - a \end{array} \right. \quad (65)$$

$$\left\{ \begin{array}{ll} ds = 0 & \text{along } \frac{dx}{dt} = u + a \end{array} \right. \quad (66)$$

where I, II, and III denote the first, second, and third families of characteristics, respectively.

It follows from above characteristic relations that there are three families of characteristics in isentropic flow. The first family represents the right-traveling pressure waves, and the second represents the left-traveling pressure waves. These two families of characteristics mean that the disturbance waves of pressure propagate in the flow field with the local speed of sound relative to the flow ahead of it. The third family represents the particle paths, which means that the disturbance of entropy propagates in the flow field with the velocity of gas particle, in other words, the velocity of the propagation of entropy is the same as that of gas particle.

It should be noted that if the characteristic relations are expressed by du and $d\rho$, the results are complicated, because

$$\frac{1}{\rho a} \left(\frac{dp}{dt} \right)_I = \frac{a}{\rho} \left(\frac{d\rho}{dt} \right)_I + \frac{1}{\rho} \left(\frac{\partial p}{\partial s} \right)_{\rho} \frac{\partial s}{\partial x} \quad (67A)$$

$$\frac{1}{\rho a} \left(\frac{dp}{dt} \right)_{II} = \frac{a}{\rho} \left(\frac{d\rho}{dt} \right)_{II} - \frac{1}{\rho} \left(\frac{\partial p}{\partial s} \right)_{\rho} \frac{\partial s}{\partial x} \quad (67B)$$

Substituting the relations (67A) and (67B), into (61) and (62), respectively, we obtain

$$\left\{ \begin{array}{l} \left(\frac{du}{dt} \right)_I + \frac{a}{\rho} \left(\frac{d\rho}{dt} \right)_I = - \frac{1}{\rho} \left(\frac{\partial p}{\partial s} \right)_{\rho} \frac{\partial s}{\partial x} \\ \left(\frac{du}{dt} \right)_{II} - \frac{a}{\rho} \left(\frac{d\rho}{dt} \right)_{II} = - \frac{1}{\rho} \left(\frac{\partial p}{\partial s} \right)_{\rho} \frac{\partial s}{\partial x} \\ \left(\frac{ds}{dt} \right)_{III} = 0 \end{array} \right. \quad (68)$$

Next, we will derive the characteristic relations under the condition of a non-isentropic flow in a variable cross-sectional tube.

For the first expression of equations (54), the continuity equation, with the consideration of the relation (23), can be rewritten as

$$\frac{1}{\rho a} \left(\frac{\partial p}{\partial t} \right) + \frac{u}{\rho a} \left(\frac{\partial p}{\partial x} \right) + a \frac{\partial u}{\partial x} = \frac{1}{\rho a} \left(\frac{\partial p}{\partial s} \right)_p \left(\frac{ds}{dt} \right)_{\text{III}} - \frac{ua}{A} \frac{dA}{dx} \quad (69)$$

The second expression of equations (54) is written as

$$\frac{1}{\rho} \frac{\partial p}{\partial x} + \frac{\partial u}{\partial t} + u \frac{\partial u}{\partial x} = -f \quad (70)$$

Combining the equation (70) with the equation (69) and considering the third expression of equations (54), we can obtain the characteristic relations as follows

$$\begin{aligned} \left(\frac{du}{dt} \right)_I + \frac{1}{\rho a} \left(\frac{dp}{dt} \right)_I &= \frac{1}{\rho a} \left(\frac{\partial p}{\partial s} \right)_p \left(\frac{ds}{dt} \right)_{\text{III}} \\ &\quad - \frac{ua}{A} \frac{dA}{dx} - f \quad \text{along } \frac{dx}{dt} = u + a \end{aligned} \quad (71)$$

$$\begin{aligned} \left(\frac{du}{dt} \right)_{\text{II}} - \frac{1}{\rho a} \left(\frac{dp}{dt} \right)_{\text{II}} &= - \frac{1}{\rho a} \left(\frac{\partial p}{\partial s} \right)_p \left(\frac{ds}{dt} \right)_{\text{III}} \\ &\quad + \frac{ua}{A} \frac{dA}{dx} - f \quad \text{along } \frac{dx}{dt} = u - a \end{aligned} \quad (72)$$

$$\left(\frac{ds}{dt} \right)_{\text{III}} = \frac{uf + q}{T} \quad \text{along } \frac{dx}{dt} = u \quad (73)$$

If the flow is isentropic in a variable cross sectional area tube, the above equations (71)–(73) can be expressed as follows

$$\left\{ \begin{array}{ll} \left(\frac{du}{dt} \right)_I + \frac{1}{\rho a} \left(\frac{dp}{dt} \right)_{\text{II}} &= - \frac{ua}{A} \frac{dA}{dx} \quad \text{along } \frac{dx}{dt} = u + a \\ \left(\frac{du}{dt} \right)_{\text{II}} - \frac{1}{\rho a} \left(\frac{dp}{dt} \right)_{\text{II}} &= \frac{ua}{A} \frac{dA}{dx} \quad \text{along } \frac{dx}{dt} = u - a \\ \left(\frac{ds}{dt} \right)_{\text{III}} &= 0 \quad \text{along } \frac{dx}{dt} = u \end{array} \right. \quad (74)$$

The equations (74) will be used in Chapter 1.

§ 5 Formation of shock wave from a simple wave

It follows from the relation (40), $\frac{d}{dp}(u + a) > 0$, that for the right-traveling compression simple wave, the velocity of wave at higher pressure point is greater than that at lower pressure point, and therefore a compression wave steepens as it progresses, finally the higher pressure parts of the wave overtake the lower pressure parts to form a shock wave, a contact surface and a reflected wave (as shown in Fig. 6). Of course, this is a simple case of forming shock wave.

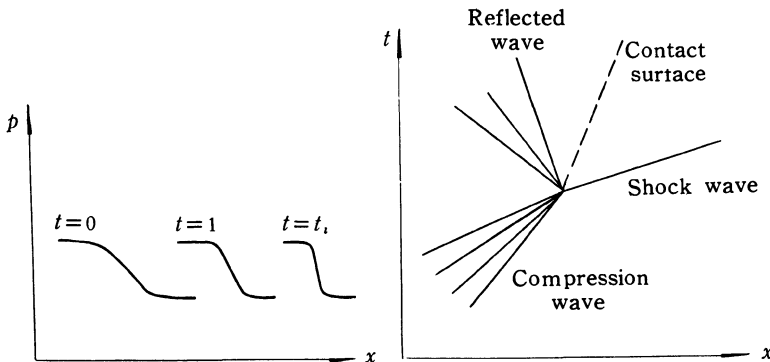


Fig.6 Formation of shock wave from a simple compression wave

For the left-traveling compression wave, a relation similar to the relation (40) can be found, and similar results of formation of shock wave will be obtained.

If the assumption that a shock wave is formed at the front of compression wave is made, we can find the location and time of shock formation.

From the relations (38), taking the derivative of x with respect to u , we obtain

$$\frac{\partial x}{\partial u} \Big|_{u=0} = \left(1 + \frac{da}{du} \right) t + F'(u) \Big|_{u=0} = 0 \quad (75)$$

$$t = -\frac{2}{\gamma + 1} F'(0), \quad x = -\frac{2a_0}{\gamma + 1} F'(0) + F(0) \quad (76)$$

So far, we have only discussed one-dimensional unsteady, continuous flow. In the next chapter, we will first briefly introduce one-dimensional, unsteady, moving shock, and then explain the basis of shock dynamics, the relation between shock Mach number and cross-sectional area of tube, $A = f(M)$.

Part 1 Shock Dynamics for a Quiescent Gas Ahead of a Shock Wave

Chapter 1 Relation Between M and A for a Uniform Quiescent Gas Ahead of a Shock Wave

In this chapter, we will explain the basis of shock dynamics—CCW relation. So-called CCW relation is that Chester(1954), Chisnell(1957), and Whitham (1958) obtained the same relation between shock Mach number M and cross-sectional area A in a tube for a uniform quiescent gas ahead of a shock by using three different methods.

we only introduce Chisnell's method, Whitham's method, and Milton's modified relation here.

First of all, we discuss a shock traveling with a variable speed through a nonuniform medium.

§ 1.1 Shock wave of variable strength

1. The case of constant strength

We know that if a shock of constant strength moves into a region of constant fluid properties in a tube, the shock must travel with a constant speed. If a moving frame of reference (moving coordinate system) which travels with the same speed as the shock is used, the unsteady phenomenon of the shock motion may become a steady one.

Choose a control volume in a tube as shown in Fig. 1.1.

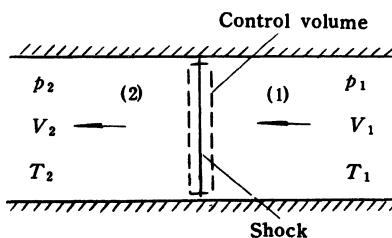


Fig. 1.1 Moving coordinate system attached to shock

The basic equations in integral form for any control volume can be written as follows

The continuity equation

$$\frac{\partial}{\partial t} \int_{\tau} \rho d\tau + \int_s \rho \vec{V} \cdot \vec{n} ds = 0 \quad (1.1)$$

The momentum equation

$$\frac{\partial}{\partial t} \int_{\tau} \rho \vec{V} d\tau + \int_s \rho \vec{V} (\vec{V} \cdot \vec{n}) ds = \sum \vec{F} \quad (1.2)$$

The energy equation

$$\frac{\partial}{\partial t} \int_{\tau} \rho \left(\frac{V^2}{2} + \varepsilon \right) d\tau + \int_s \rho \vec{V} \left(\frac{V^2}{2} + h \right) \vec{n} ds = q \quad (1.3)$$

The state equation (for perfect gas)

$$p = \rho R T \quad (1.4)$$

where p , ρ , T , ε and q , are pressure, density, temperature, internal energy, and heat, respectively; R is a gas constant; \vec{V} is the velocity; \vec{n} is the unit vector of the outward normal to the surface of the control volume.

Under the condition of an adiabatic steady flow of a perfect gas, above equations may be simplified to

$$\begin{cases} \int \rho \vec{V} \cdot \vec{n} ds = 0 \\ \int \rho \vec{V} (\vec{V} \cdot \vec{n}) ds = \sum \vec{F} \\ \int \rho \vec{V} \left(\frac{V^2}{2} + h \right) \vec{n} ds = 0 \\ p = \rho R T \end{cases} \quad (1.5)$$

In the case of ideal gas and the control volume chosen as shown in Fig. 1.1, the equation (1.5) can be written in the following form

$$\begin{cases} \rho_1 V_1 = \rho_2 V_2 \\ p_1 + \rho_1 V_1^2 = p_2 + \rho_2 V_2^2 \\ h_1 + \frac{V_1^2}{2} = h_2 + \frac{V_2^2}{2} \\ p = \rho R T \end{cases} \quad (1.6)$$

where V_1 and V_2 are the velocities in the moving frame which is attached to the moving shock.

If the stationary coordinate system which is attached to the tube is used, the flow velocities, u_1 and u_2 , are different from those in (1.6). But such thermodynamic properties as the pressure, density, temperature, and speed of sound are not influenced by the transformation of coordinate system. The rela-

tions between the flow velocities in the two frames can be expressed as

$$\begin{cases} V_1 = W_s \\ V_2 = W_s \pm (u_1 - u_2) \end{cases} \quad (1.7)$$

where W_s represents the velocity of the shock relative to the gas ahead of the shock. The upper sign refers to the right-traveling shock waves, and the lower sign to the left-traveling shock waves, as shown in Fig. 1.2. u_1 and u_2 are the flow velocities ahead of and behind the shock wave in the stationary coordinate system, respectively.

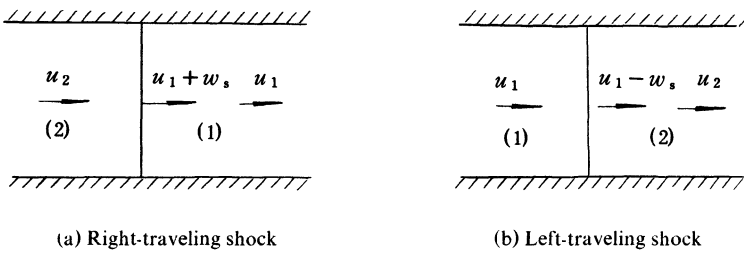


Fig. 1.2 Moving shock in stationary coordinate system.

The flow Mach number, M_1 , may be expressed in terms of the shock Mach number, M_s ,

$$M_1 = \frac{V_1}{a_1} = \frac{W_s}{a_1} = M_s \quad (1.8)$$

From the relation (1.6) and the expressions (1.7) and (1.8), we can obtain

$$\frac{u_2 - u_1}{a_1} = \pm \frac{2}{\gamma + 1} \left(M_s - \frac{1}{M_s} \right) \quad (1.9)$$

$$\frac{p_2}{p_1} = \frac{2\gamma}{\gamma + 1} M_s^2 - \frac{\gamma - 1}{\gamma + 1} \quad (1.10)$$

$$\frac{\rho_2}{\rho_1} = \frac{(\gamma + 1) M_s^2}{(\gamma - 1) M_s^2 + 2} \quad (1.11)$$

$$\frac{T_2}{T_1} = \frac{\left[2\gamma M_s^2 - (\gamma - 1) \right] \left[(\gamma - 1) M_s^2 + 2 \right]}{(\gamma + 1)^2 M_s^2} \quad (1.12)$$

2. The case of variable strength

The relations (1.9), (1.10), (1.11), and (1.12) are derived under the condition of the shock of constant strength. We want to ask: whether can we use the

above relations to the case of the shock of variable strength?

It is evident that because of the variable strength, the shock moves with variable speed. We cannot obtain a steady flow by means of the transformation from the stationary frame into the moving one as mentioned above.

In the control volume with an unsteady flow, we have

$$\frac{\partial \rho}{\partial t} \neq 0, \quad \frac{\partial V}{\partial t} \neq 0, \quad \frac{\partial p}{\partial t} \neq 0 \dots \quad (1.13)$$

But when the control surfaces which are in parallel with the shock front approach to the shock surface infinitely, we can obtain

$$\begin{cases} \int_{\tau} \rho d\tau \rightarrow 0 \\ \int_{\tau} \rho \vec{V} d\tau \rightarrow 0 \\ \int_{\tau} \rho \left(\frac{V^2}{2} + \varepsilon \right) d\tau \rightarrow 0 \end{cases} \quad (1.14)$$

$$\begin{cases} \frac{\partial}{\partial t} \int_{\tau} \rho d\tau \rightarrow 0 \\ \frac{\partial}{\partial t} \int_{\tau} \rho \vec{V} d\tau \rightarrow 0 \\ \frac{\partial}{\partial t} \int_{\tau} \rho \left(\frac{V^2}{2} + \varepsilon \right) d\tau \rightarrow 0 \end{cases} \quad (1.15)$$

Considering expression (1.15), we can obtain a set of all the same equations as (1.5), that is, the equations (1.6) for the case of constant strength can be extended to the case of variable strength at each instant of time.

But for a moving body with a variable speed, the above extension does not apply.

§ 1.2 Chisnell's method

If a shock moves along a channel (or a tube) with a small area change, the shock itself and the flow behind it are perturbed. But, in the method presented by Chisnell, the re-reflected disturbances generated by nonuniformity behind the shock are neglected. This type of propagation of shock is called "free propagating". Obviously, based on this assumption, the problems to be investigated may be simplified to a great extent.

Fig. 1.3 shows a shock wave moving along a tube with a small area change.

When a shock, which is called incident shock, travels through a tube with a small area change, the strength of the incident shock changes, and at the same time a family of reflected continuous waves and contact surfaces are generated.

Finally a transmitted shock with constant strength forms, when the area change of the tube has passed.

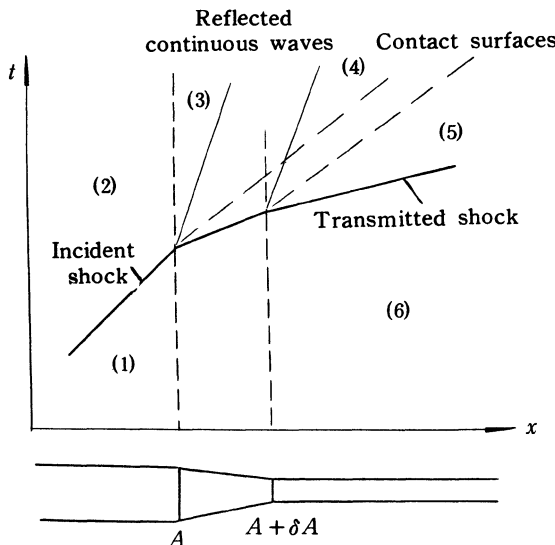


Fig. 1.3 A shock moves along a tube with a small area change

In the $x-t$ plane, the flow fields can be divided into six regions (or five regions) and corresponding relations can be written as follows across the incident shock from region (1) to region (2), across the transmitted shock from region (6) to region (5), through the area change between region (2) and region (3), across the contact surfaces from region (5) to region (4), across the reflected continuous waves from region (3) to region (4).

Next, the relation between the shock strength and the cross-sectional area of the tube (or channel) is derived.

1. The relations for the incident shock

The moving shock relations are used to the incident shock

$$u_2 = (\xi - 1) \left\{ \frac{2p_1}{\rho_1 [(\gamma - 1) + (\gamma + 1)\xi]} \right\}^{\frac{1}{2}} \quad (1.16)$$

$$M_2 = (\xi - 1) \left\{ \frac{2}{\gamma \xi [(\gamma + 1) + (\gamma - 1)\xi]} \right\}^{\frac{1}{2}} \quad (1.17)$$

where u_2 , M_2 are the flow velocity and flow Mach number in region 2,

respectively. ξ is the shock strength (pressure ratio), which can be expressed as follows

$$\xi = \frac{p_2}{p_1} \quad (1.18)$$

2. The relations for the transmitted shock

The parameters in region 6 is the same as those in region 1, so the strength of the transmitted shock can be expressed by

$$\xi + \delta\xi = \frac{p_5}{p_6} = \frac{p_5}{p_1} \quad (1.19)$$

$$u_5 = (\xi + \delta\xi - 1) \left\{ \frac{2p_1}{\rho_1 [(\gamma - 1) + (\gamma + 1)(\xi + \delta\xi)]} \right\}^{\frac{1}{2}} \quad (1.20)$$

3. The relations for the steady flow between region 2 and region 3

The relations of one-dimensional steady flow are written as

$$\frac{p_3}{p_2} = 1 - \frac{\gamma M_2^2}{M_2^2 - 1} \frac{\delta A}{A} \quad (1.21)$$

$$\frac{u_3}{u_2} = 1 + \frac{1}{M_2^2 - 1} \frac{\delta A}{A} \quad (1.22)$$

4. The relations for the reflected continuous waves

The simple wave relations are written as

$$\frac{p_4}{p_3} = \left[1 - \frac{\gamma - 1}{2} \left(\frac{u_4 - u_3}{a_3} \right) \right]^{\frac{2\gamma}{\gamma - 1}} \quad (1.23)$$

Retaining only the terms of first order quantities, we can obtain

$$\left(\frac{p_4}{p_3} - 1 \right) = -\gamma M_3 \left(\frac{u_4}{u_3} - 1 \right) \quad (1.24)$$

5. The relations on the two sides of the contact surface

$$p_4 = p_5 \quad (1.25)$$

$$u_4 = u_5 \quad (1.26)$$

From the relations (1.18), (1.19), (1.21), and (1.25), and retaining only first order terms, we can obtain

$$\left(\frac{p_4}{p_3} - 1 \right) = \frac{\delta\xi}{\xi} + \frac{\gamma M_2^2}{M_2^2 - 1} \frac{\delta A}{A} \quad (1.27)$$

From the relations (1.16), (1.20), (1.22), and (1.26), retaining only first order terms, we obtain

$$\left(\frac{u_4}{u_3} - 1 \right) = \frac{\delta\xi}{\xi - 1} - \frac{(\gamma + 1)\delta\xi}{2[(\gamma - 1) + (\gamma + 1)\xi]} - \frac{1}{M_2^2 - 1} \frac{\delta A}{A} \quad (1.28)$$

Substituting the relations (1.27) and (1.28) into the relation (1.24), we have

$$\begin{aligned} & \frac{\delta\xi}{\xi} + \frac{\gamma M_2^2}{M_2^2 - 1} \frac{\delta A}{A} \\ &= -\gamma M_3 \left\{ \frac{\delta\xi}{\xi - 1} - \frac{(\gamma + 1)\delta\xi}{2[(\gamma - 1) + (\gamma + 1)\xi]} - \frac{1}{M_2^2 - 1} \frac{\delta A}{A} \right\} \end{aligned} \quad (1.29)$$

Letting $\delta A \rightarrow 0$, $M_3 \rightarrow M_2$, and substituting the relation (1.17) into (1.29), we obtain

$$-\frac{1}{A} \frac{dA}{d\xi} = \frac{1}{(\xi - 1)K(\xi)} \quad (1.30)$$

where $K(\xi)$ is a slowly varying function

$$\begin{aligned} K(\xi)^{-1} &= 1 + \frac{\xi - 1}{\gamma\xi} - \frac{(\gamma + 1)(\xi - 1)}{2[(\gamma - 1) + (\gamma + 1)\xi]} \\ &+ (\xi - 1) \left\{ \frac{2}{\gamma\xi[(\gamma + 1) + (\gamma - 1)\xi]} \right\}^{\frac{1}{2}} \times \left\{ 1 - \frac{(\gamma + 1)(\xi - 1)}{2[(\gamma + 1)\xi + (\gamma - 1)]} \right. \\ &\quad \left. + \frac{(\gamma + 1) + (\gamma - 1)\xi}{2(\xi - 1)} \right\} \end{aligned} \quad (1.31)$$

For strong shocks, $(\xi - 1) \approx \xi \gg 1$

$$\begin{aligned} K^{-1} &= 1 + \frac{1}{\gamma} - \frac{1}{2} + \left[\frac{2}{\gamma(\gamma - 1)} \right]^{\frac{1}{2}} \left[1 - \frac{1}{2} + \frac{\gamma - 1}{2} \right] \\ &= \frac{1}{2} + \frac{1}{\gamma} + \left[\frac{\gamma}{2(\gamma - 1)} \right]^{\frac{1}{2}} \\ K &= 0.3941 \text{ (for } \gamma = 1.4) \end{aligned}$$

For weak shocks, $\xi \rightarrow 1$

$$\begin{aligned} K^{-1} &= 1 + \left\{ \frac{2}{\gamma[(\gamma + 1) + (\gamma - 1)]} \right\}^{\frac{1}{2}} \cdot \left[\frac{(\gamma + 1) + (\gamma - 1)}{2} \right] \\ K &= 0.5 \end{aligned}$$

If shock strength is denoted by shock Mach number M_s , the following relations can be used

$$\xi = \frac{p_2}{p_1} = \frac{2\gamma}{\gamma+1} M_s^2 - \frac{\gamma-1}{\gamma+1} \quad (1.32)$$

$$d\xi = \frac{4\gamma}{\gamma+1} M_s dM_s \quad (1.33)$$

Substituting (1.32) and (1.33) into (1.30), we obtain

$$-\frac{dA}{A} = \frac{2M_s dM_s}{(M_s^2 - 1)K(M_s)} \quad (1.34)$$

where $K(M_s)$ can be obtained by means of substituting (1.32) into (1.31).

Finally, we will discuss the so-called "Free-Propagating".

As mentioned already, if a moving shock travels through a tube with a variable cross section, the shock itself and the flow field behind it are disturbed, that is, in the process of the shock propagating, the shock strength and the shape of shock front will change. Such changes of the shock will generate some reflected disturbances. These disturbances include continuous waves and contact surfaces.

At the same time, the changes in the strength and shape of the shock form a nonuniform flow field behind the shock. While the reflected disturbances move into the nonuniform flow field, the re-reflected disturbances occur, some of which will overtake the shock and make its strength and shape changes further (as shown in Fig. 1.4).

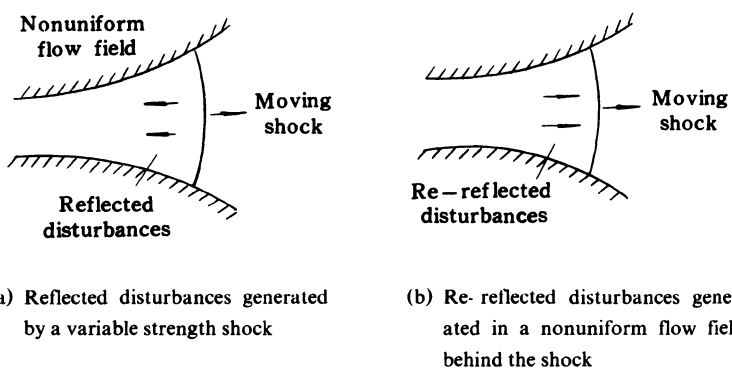


Fig. 1.4 Reflected and re-reflected disturbances

There are three types of re-reflected disturbances which are generated in the

flow field behind the shock.

(1) The continuous waves reflected by the shock wave with variable strength moving through the varying cross-sectional area tube generate the first type of re-reflected waves. Among them, the waves which have the same direction as the shock wave (for example, both the shock wave and re-reflected waves are right-traveling waves) can catch up with the shock wave.

(2) The contact discontinuity generated by the change of strength of the shock moving through the varying cross-sectional area tube form the second type of re-reflected waves. Among them, the same direction waves as the shock can catch up with the shock wave.

(3) Interaction of reflected continuous waves generated by the shock wave with the contact discontinuity can form the third type of re-reflected waves.

Figure 1.5 shows the interaction of the reflected continuous wave with the contact discontinuity.

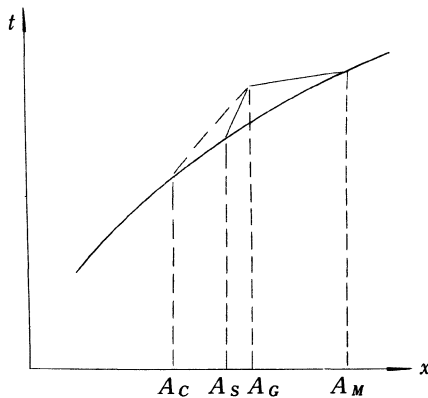


Fig. 1.5 Interaction of the reflected continuous wave generated at A_S with the contact discontinuity generated at A_C

In Fig. 1.5, we neglect the first and second type of re-reflected disturbance waves generated by the reflected continuous waves and the contact discontinuity moving through a small area change and only remain the third type of re-reflected wave generated by the interaction of the reflected wave formed at A_S with the contact discontinuity formed at A_C .

Some results of the calculation show that the three types of the re-reflected disturbances may be canceled out one another, so we may neglect the re-reflected disturbances, that is, as a good approximation, the influence of the three types of re-reflected disturbance waves on the shock wave may be neglected.

This is the so-called “free propagating” idea.

Certainly, further studies of the above re-reflected phenomenon are needed.

§ 1.3 Whitham's method

When a shock wave moves through a variable area tube as shown in Fig. 1.6, a nonuniform, isentropic flow field behind the moving shock is formed. There are three families of characteristics in the flow field, that is, characteristics C^+ , characteristics C^- , and characteristics P which are the particle paths. The following relations describe the three families of characteristics

$$dp + \rho a^2 u \frac{dA}{A} = 0 \quad \text{along } C^+ \quad \frac{dx}{dt} = u + a \quad (1.35)$$

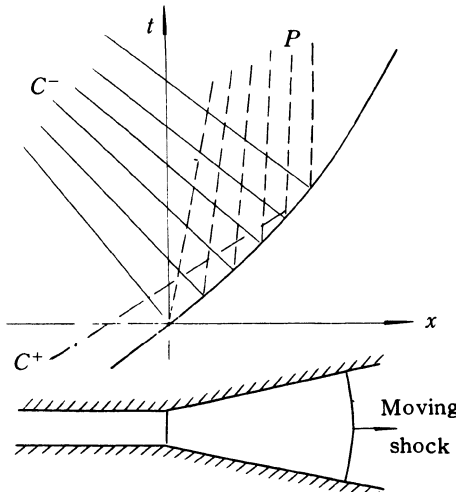


Fig. 1.6 A Shock wave moving through a variable area tube shown in $x-t$ plane

$$dp - \rho a^2 u \frac{dA}{u - a} = 0 \quad \text{along } C^- \quad \frac{dx}{dt} = u - a \quad (1.36)$$

$$dp - a^2 d\rho = 0 \quad \text{along } P \quad \frac{dx}{dt} = u \quad (1.37)$$

From the physical point of view, the negative characteristics labelled as C^- are generated by the variable strength shock, that is, as mentioned already in Introduction, the negative characteristics are the reflected disturbance waves.

The positive characteristics labelled as C^+ have the same direction as the shock wave. If the re-reflected disturbance waves are neglected, the positive characteristics only play a subsidiary role.

Next, we will derive the relation between the shock strength and the cross-sectional area of the tube.

The basic idea is presented as follows(Whitham, 1958).

We know that the relation

$$dp + \rho adu + \frac{\rho a^2 u}{u+a} dA = 0$$

is valid along a characteristic C^+ . Now, let the above relation be also valid along the moving shock. The moving shock relations are given as follows

$$\left\{ \begin{array}{l} p_2 = p_1 \left(\frac{2\gamma}{\gamma+1} M^2 - \frac{\gamma-1}{\gamma+1} \right) \\ \rho_2 = \rho_1 \frac{(\gamma+1)M^2}{(\gamma-1)M^2 + 2} \\ u_2 = \frac{2a_1}{\gamma+1} \left(M - \frac{1}{M} \right) \\ a_2 = a_1 \frac{[2\gamma M^2 - (\gamma-1)]^{\frac{1}{2}} [(\gamma-1)M^2 + 2]^{\frac{1}{2}}}{(\gamma+1)M} \end{array} \right. \quad (1.38)$$

where M is the shock Mach number, and its subscript s is omitted for convenience.

From the relation (1.38), we obtain

$$dp_2 = p_1 \frac{4\gamma}{\gamma+1} M dM \quad (1.39)$$

$$du_2 = \frac{2a_1}{\gamma+1} \left(1 + \frac{1}{M^2} \right) dM \quad (1.40)$$

$$\rho_2 a_2 = \frac{\rho_1 a_1 M}{\mu} \quad (1.41)$$

where $\mu = \left[\frac{(\gamma-1)M^2 + 2}{2\gamma M^2 - (\gamma-1)} \right]^{\frac{1}{2}}$, which represents the Mach number for the propagation of a moving shock relative to the flow field behind it. From (1.38) and (1.41), we have

$$\frac{\rho_2 a_2^2 u_2}{u_2 + a_2} = \frac{2\rho_1 a_1^2 \mu (M^2 - 1) [2\gamma M^2 - (\gamma-1)]}{\{2\mu(M^2 - 1) + [(\gamma-1)M^2 + 2]\} (\gamma+1)} \quad (1.42)$$

Substituting (1.39), (1.40),(1.41), and (1.42) into(1.35), we can obtain the relation between the shock Mach number and the cross-sectional area

$$\frac{2MdM}{(M^2 - 1)K(M)} + \frac{dA}{A} = 0 \quad (1.43)$$

where $K(M) = \left[2(2\mu + 1 + M^{-2})^{-1} \left(1 + \frac{2}{\gamma+1} \frac{1-\mu^2}{\mu} \right)^{-1} \right]$

For strong shocks ($M \rightarrow \infty$)

$$K(M) = 0.3941 (\gamma = 1.4)$$

For weak shocks ($M \rightarrow 1$)

$$K(M) = 0.5$$

It follows the from the above results that the relation (1.43) is all the same as the relation (1.30). Whitham obtained exactly the same results as Chisnell's.

Integrating (1.43), we can get

$$A = C \exp \left[- \int \frac{2MdM}{(M^2 - 1)K(M)} \right] = Cf(M)$$

Letting $C = \frac{A_0}{f(M_0)}$, we have

$$\frac{A}{A_0} = \frac{f(M)}{f(M_0)} \quad (1.44)$$

where

$$\begin{aligned} f(M) = & \exp \left\{ - \left\{ \ln \left(\frac{M^2 - 1}{M} \right) + \frac{1}{\gamma} \ln \left(M^2 - \frac{\gamma - 1}{2\gamma} \right) \right. \right. \\ & + \ln \left(\frac{1 - \mu}{1 + \mu} \right) + \left(\frac{\gamma - 1}{2\gamma} \right)^{\frac{1}{2}} \ln \left[\mu + \left(\frac{\gamma - 1}{2\gamma} \right)^{\frac{1}{2}} \right] \\ & - \left(\frac{\gamma - 1}{2\gamma} \right)^{\frac{1}{2}} \ln \left[\mu - \left(\frac{\gamma - 1}{2\gamma} \right)^{\frac{1}{2}} \right] \\ & + \left[\frac{2}{\gamma(\gamma - 1)} \right]^{\frac{1}{2}} \ln \left[\left(M^2 + \frac{2}{\gamma - 1} \right)^{\frac{1}{2}} + \left(M^2 - \frac{\gamma - 1}{2\gamma} \right)^{\frac{1}{2}} \right] \\ & \left. \left. + \left[\frac{1}{2(\gamma - 1)} \right]^{\frac{1}{2}} \tan^{-1} \left\{ \frac{[4\gamma - (\gamma - 1)^2]M^2 - 4(\gamma - 1)}{4\gamma^{\frac{1}{2}}(\gamma - 1)[M^2 + \frac{2}{\gamma - 1}]^{\frac{1}{2}}[M^2 - \frac{\gamma - 1}{2\gamma}]^{\frac{1}{2}}} \right\} \right\} \right\} \end{aligned}$$

If the shock is very strong, or very weak, or the change of shock strength in a narrow region, $K(M)$ may be regarded as a constant, the relation (1.44) can be written as follows

$$A(M^2 - 1)^{\frac{1}{k}} = \text{constant} \quad (1.45)$$

The relation (1.45) is very simple for engineering calculation.

Next, we must investigate why the relation (1.35) which is valid along a C^+ can be used to the shock wave, that is,

$$dp + \rho a u du + \frac{\rho a^2 u}{u+a} \frac{dA}{A} = 0 \quad \text{along} \quad \frac{dx}{dt} = u + a \quad (1.35)$$

can be written as

$$dp + \rho a u du + \frac{\rho a^2 u}{u+a} \frac{dA}{A} = 0 \quad \text{along} \quad \frac{dx}{dt} = W \quad (1.46)$$

where W is the shock speed.

We make a discussion for this question as follows.

The characteristics C^+ are in the flow field behind the shock wave, so $dp = dp_2$, $du = du_2$, $\rho_2 = \rho$... in (1.35).

The relation (1.35) can be re-written as

$$\left(\frac{\partial p}{\partial x} + \frac{1}{u+a} \frac{\partial p}{\partial t} \right) + \rho a \left(\frac{\partial u}{\partial x} + \frac{1}{u+a} \frac{\partial u}{\partial t} \right) + \frac{\rho a^2 u}{u+a} \frac{1}{A} \frac{dA}{dx} = 0 \quad (1.47)$$

The relation (1.46) can also be expressed as

$$\left(\frac{\partial p}{\partial x} + \frac{1}{W} \frac{\partial p}{\partial t} \right) + \rho a \left(\frac{\partial u}{\partial x} + \frac{1}{W} \frac{\partial u}{\partial t} \right) + \frac{\rho a^2 u}{u+a} \frac{1}{A} \frac{dA}{dx} = 0 \quad (1.48)$$

That the relation (1.35), or (1.47), can be used to the shock wave means

$$(1.48) - (1.47) = \left(\frac{1}{W} - \frac{1}{u+a} \right) (p_t + \rho au_t) = 0 \quad (1.49)$$

or (1.48)–(1.47) is very small.

At first sight, it seems that the first factor $\left(\frac{1}{W} - \frac{1}{u+a} \right)$ is very small, namely, C^+ is very close to the shock wave. Although $\left(\frac{1}{W} - \frac{1}{u+a} \right) \rightarrow 0$ for weak shock ($M \rightarrow 1$), it tends to be 0.274 (for $\gamma = 1.4$) as $M \rightarrow \infty$. In fact, it is the smallness of the second factor in (1.49) which leads to the high accuracy (Whitham, 1958).

When the shock wave is strong (or not weak), the characteristics C^+ does not close to the shock wave.

In order to prove $(p_t + \rho au_t)$ is very small, first we use Chester's small perturbation theory.

It should be noted that there is no such assumptions that $p_2 - p_1$ is small,

the so-called small perturbation is that $\Delta p_2, \Delta u_2 \dots$ are small.

In the case of small perturbation, letting $\rho = \rho_2 + \rho'$, $u = u_2 + u'$, $p = p_2 + p'$, $A = A_0 + A'$, we obtain the basic equations as

$$\begin{cases} \rho_t + u_2 \rho_x + \rho_2 u_x + \rho_2 u_2 \frac{A'(x)}{A_0} = 0 \\ u_t + u_2 u_x + \frac{1}{\rho_2} p_x = 0 \\ p_t + u_2 p_x - a_2^2 (\rho_t + u_2 \rho_x) = 0 \end{cases} \quad (1.50)$$

where the prime is omitted for convenience.

It follows from equations (1.50) that

$$C^+ \left[\frac{\partial}{\partial t} + (u_2 + a_2) \frac{\partial}{\partial x} \right] (p + \rho_2 a_2 u) + \rho_2 a_2^2 u_2 \frac{A'(x)}{A_0} = 0 \quad (1.51)$$

$$C^- \left[\frac{\partial}{\partial t} + (u_2 - a_2) \frac{\partial}{\partial x} \right] (p - \rho_2 a_2 u) + \rho_2 a_2^2 u_2 \frac{A'(x)}{A_0} = 0 \quad (1.52)$$

$$P \left[\frac{\partial}{\partial t} + u_2 \frac{\partial}{\partial x} \right] (p - a_2^2 \rho) = 0 \quad (1.53)$$

Let $\varphi = p + \rho_2 a_2 u$, $c_0 = u_2 + a_2$

$\beta = x + c_0 t$, $\alpha = x - c_0 t$

then, from (1.51)

$$\frac{\partial}{\partial \beta} \left(c_0 \varphi + \rho_2 a_2^2 u_2 \frac{A}{A_0} \right) = 0 \quad (1.54)$$

or

$$p + \rho_2 a_2 u = - \frac{\rho_2 a_2^2 u_2}{u_2 + a_2} \frac{A}{A_0} + F[x - (u_2 + a_2)t] \quad (1.55)$$

Since here p is p' , u is $u' \dots$, the following solution can be obtained

$$\begin{aligned} (p - p_2) + \rho_2 a_2 (u - u_2) + \frac{\rho_2 a_2^2 u_2}{u_2 + a_2} \frac{A - A_0}{A_0} \\ = F[x - (u_2 + a_2)t] \end{aligned} \quad (1.56)$$

Similarly, for the left-traveling waves C^- , we have

$$\begin{aligned} (p - p_2) - \rho_2 a_2 (u - u_2) + \frac{\rho_2 a_2^2 u_2}{u_2 - a_2} \frac{A - A_0}{A_0} \\ = G[x - (u_2 - a_2)t] \end{aligned} \quad (1.57)$$

and for the particle paths P , we have

$$(p - p_2) - a_2^2(\rho - \rho_2) = H(x - u_2 t) \quad (1.58)$$

where F , G , and H are arbitrary functions.

From (1.56), (1.57) and (1.58), the general solution of the equations (1.50) is obtained

$$\begin{aligned} p - p_2 &= -\frac{\rho_2 a_2^2 u_2^2}{u_2^2 - a_2^2} \frac{A(x) - A_0}{A_0} + F[x - (u_2 + a_2)t] \\ &\quad + G[x - (u_2 - a_2)t] \end{aligned} \quad (1.59)$$

$$\begin{aligned} u - u_2 &= \frac{a_2^2 u_2}{u_2^2 - a_2^2} \frac{A(x) - A_0}{A_0} + \frac{1}{\rho_2 a_2} F[x - (u_2 + a_2)t] \\ &\quad - \frac{1}{\rho_2 a_2} G[x - (u_2 - a_2)t] \end{aligned} \quad (1.60)$$

$$\rho - \rho_2 = \frac{p - p_2}{a_2^2} + H(x - u_2 t) \quad (1.61)$$

It follows from the above results that the disturbances can be divided into four parts: the first is from the area change of the tube, the second is the disturbances propagating along the characteristics C^+ , the third is the disturbances propagating along the characteristics C^- , and the fourth is the disturbances propagating along the particle paths P . The entropy changes are represented by the function H . It is interesting to note that the changes in p and u do not depend directly on H .

(1.56) can be used for proving $p_t + \rho_2 a_2 u_t = 0$, with the following procedure.

The boundary condition serves to determine the function F .

We know that all C^+ originate from the uniform region.

Substituting the values of pressure, density, velocity, and cross-sectional area in the uniform region ($p = p_2$, $\rho = \rho_2$, $u = u_2$, $A = A_0$) into (1.56), we can obtain

$$F[x - (u_2 + a_2)t] = 0 \quad (1.62)$$

Now, taking a partial derivative of (1.56) with respect to t , we obtain

$$p_t + \rho_2 a_2 u_t = 0 \quad (1.63)$$

In the general case, we have

$$p_t + \rho_2 a_2 u_t = -(u_2 + a_2)F[x - (u_2 + a_2)t] \quad (1.64)$$

That is,

$$p_1 + \rho_2 a_2 u_1 = \text{constant along } \frac{dx}{dt} = u_2 + a_2 \quad (1.65)$$

The case we discussed above is small disturbance for the shock wave.

When the disturbances are not small, we may expect that in any small region the small perturbation theory holds for variations about some local value. Then for each local region, $p_1 + \rho a u_1$ remains constant on a C^+ .

From Fig. 1.7, we can discuss the problem further.

Under the conditions of small disturbances and the characteristic C^+ originated from the uniform region, we have

$$p_1 + \rho_2 a_2 u_1 = 0 \quad \text{along each } C^+$$

Under the conditions of small disturbances and characteristic C^+ originated from the nonuniform region, we have

$$p_1 + \rho_2 a_2 u_2 = \text{constant} \quad \text{along each } C^+$$

Under the conditions of finite disturbances and characteristic C^+ originated from the nonuniform region, we have

$$p_1 + \rho a u_1 = \text{constant} \quad \text{along each } C^+$$

For each local region, we consider that the small perturbation theory holds.

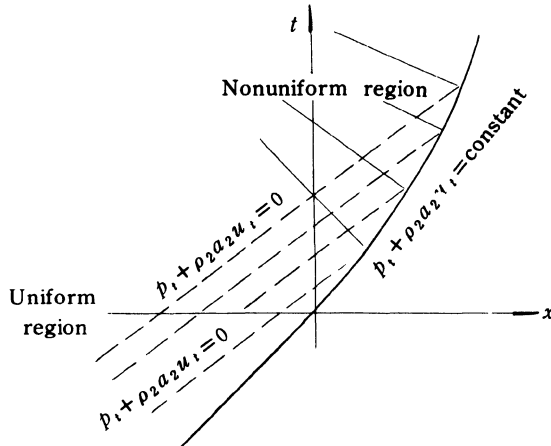


Fig. 1.7 $p_1 + \rho a u_1$ remains constant on C^+

If the small disturbances in the whole finite region do not accumulate, roughly speaking, we may obtain

$$p_t + \rho a u_t = 0 \quad \text{along each } C^+ \text{ or everywhere behind the shock.}$$

That is, the above relation is valid for all characteristics C^+ originated from the uniform region (where $p_t + \rho_2 a_2 u_2 = 0$ in the whole uniform region).

Thus we have proved that $(p_t + \rho a u_t)$ is very small, and the relation of the characteristics C^+ can be used to the shock wave.

Next, a simple form of the expression for $K(M)$ in the case of diatomic gases will be given. As shown already in the relation (1.43), $K(M)$ is a complicated mathematical function, so the function $f(M)$ in the relation (1.44) has many terms.

Milton (1975) found that the shape of the variation of function $K(M)$ follows a simple form which approaches that of a hyperbola. An appropriate hyperbola will provide a good approximation in the moderate strength range. For $\gamma = 1.4$, $K_a(M)$ may be expressed as follows

$$K_a(M) = 0.394 \left[1 + \frac{0.107}{M - 0.600} \right] \quad (1.66)$$

where $K_a(M)$ is a hyperbolic function which approaches $K(M)$. The maximum error is 0.92% at $M = 1.30$.

The equation (1.43), with $K_a(M)$ replacing $K(M)$, becomes

$$\frac{dA}{A} = \frac{-2M(M - 0.600)dM}{0.394(M^2 - 1.000)(M - 0.493)} \quad (1.67)$$

Integration of (1.67) follows simply to give

$$A(M - 1.000)^{2.004} \cdot (M + 1.000)^{2.719} \cdot (M - 0.493)^{0.354} = \text{constant} \quad (1.68)$$

Up to now, we have already discussed the CCW relation. This relation is a very simple one for calculation, but, as we know, the error is that the re-reflected disturbances in the flow behind the incident shock are not considered. This description is so-called that of a freely propagating shock, that is, as mentioned already, the shock wave is not affected by the re-reflected disturbances.

Since 1960, many researchers have studied the problem about the re-reflected disturbances in the flow behind the incident moving shock. Rosciszewski (1960) and Oshima *et al.* (1965) have formulated the error involved in using CCW approximation and obtained correction terms. Yousaf (1974) have presented an exact formulation of the strength of the disturbances overtaking the shock, and the equation (1.43) may be modified to the following form

$$\frac{dA}{A}(1+\lambda) = \frac{-2MdM}{K(M)(M^2 - 1)} \quad (1.69)$$

where λ is an integral containing in its integrand the five interaction terms.

Milton (1975) has obtained a useful, simple relation between M and A in the case of strong shocks. Itoh *et al.* (1981), on the basis of Milton's modified relation, has extended this relation to the general case. Next section, we will explain Milton's modification.

§ 1.4 Milton's modified relation

As mentioned already in § 1.3, in Whitham's method, substitution of the Rankine-Hugoniot conditions at the main shock front into the characteristic C^+ , that is,

$$du + \frac{1}{\rho a} dp + \frac{ua}{u+a} \frac{dA}{A} = 0 \quad \text{on } C^+$$

gives the equation (1.43). This neglects the interaction terms (as shown in Fig. 1.8a).

Milton describes the flow pattern of the motion of a shock wave through a slowly varying cross-sectional area tube as follows: The incident shock is disturbed by the flow behind it, and a reflected shock, contact surface and Mach stem are formed (as shown in Fig. 1.8b).

Line 32 follows characteristic C^+ , but values along it differ from those given by the characteristic identity (1.35) due to the interactions of the reflected shock and the contact surface. Line 31 is not a characteristic, but connects an arbitrary point 3 in the region just prior to the formation of the reflected shock to point 1.

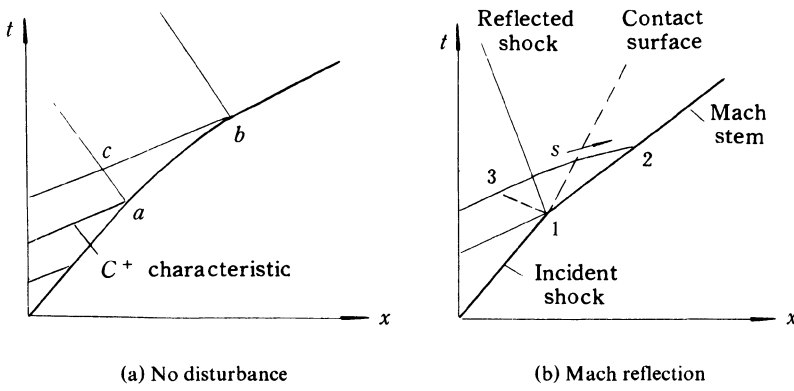


Fig. 1.8 Milton's description

The correction terms on the shock front can be written as

$$(d\zeta)_1^2 = (d\zeta)_3^2 + (d\zeta)_1^3 \quad (1.70)$$

where

$$d\zeta = du + \frac{1}{\rho a} dp + \frac{ua}{u+a} d(\ln A)$$

On line 31, the incident shock is undisturbed and du , dp , and $d(\ln A)$ are all zero, making $(d\zeta)_1^3$ zero, and therefore

$$(d\zeta)_1^2 = (d\zeta)_3^2 \quad (1.71)$$

In order to obtain values for the disturbance terms on line 32, the function $d\zeta$ is assumed, as an approximation, to be continuous, but is not equal to zero.

By integrating between the end points, points 2 and 3, and differentiating with respect to s in the characteristic direction, we have

$$\frac{d}{ds} \int_3^2 d\zeta = \frac{d\zeta_2}{ds} - \frac{d\zeta_3}{ds} + \varepsilon + \sigma \quad (1.72)$$

where

$$\varepsilon = \int_3^2 \frac{\partial}{\partial s} \left(\frac{1}{\rho a} \right) dp$$

and

$$\sigma = \int_3^2 \frac{\partial}{\partial s} \left(\frac{ua}{u+a} \right) d(\ln A)$$

At either end of 23, the line represents a true characteristic and the characteristic identity holds, so $\frac{d\zeta_2}{ds}$ and $\frac{d\zeta_3}{ds}$ equal zero. Of course, in the undisturbed case, $d\zeta = 0$ or $\frac{d\zeta}{ds} = 0$ holds for whole line 23, that is, ε and σ also vanish. But in the disturbed case, ε and σ are not equal to zero, and this is the reason for generating correction terms (or interaction terms). The expression for this can be written as

$$(d\zeta)_1^2 = (\varepsilon + \sigma)ds \quad (1.73)$$

or

$$du_2 + \frac{dp_2}{\rho_2 a_2} + \frac{u_2 a_2}{u_2 + a_2} d(\ln A) = (\varepsilon + \sigma)ds \quad (1.74)$$

where the subscript 2 represents the flow immediately behind the moving shock.

Now substituting the Rankine–Hugoniot conditions on the shock front, which is the same as Whitham's method in § 1.3, we obtain

$$\frac{dA}{A} = -\frac{2MdM}{(M^2 - 1)K(M)} + \frac{u_2 + a_2}{u_2 a_2} (\varepsilon + \sigma)ds \quad (1.75)$$

Next we will find ε and σ . The expression (1.72) can be rewritten as follows

$$d\varepsilon = \frac{\partial}{\partial s} \left(\frac{1}{\rho a} \right) dp \quad (1.76)$$

$$d\sigma = \frac{\partial}{\partial s} \left(\frac{ua}{u + a} \right) d(\ln A) \quad (1.77)$$

or

$$-\frac{de}{dp} = -\frac{\partial}{\partial s} \left(\frac{1}{\rho a} \right) = \left(\frac{1}{\rho a^2} \right) \frac{\partial a}{\partial s} + \left(\frac{1}{\rho^2 a} \right) \frac{\partial \rho}{\partial s} \quad (1.78)$$

$$-\frac{d\sigma}{d(\ln A)} = -\frac{\partial}{\partial s} \left(\frac{ua}{u + a} \right) = \frac{u^2 \left(\frac{\partial a}{\partial s} \right) + a^2 \left(\frac{\partial u}{\partial s} \right)}{(u + a)^2} \quad (1.79)$$

The evaluation can be made in the region upstream of the reflected shock and at the main shock front. At point 3, $\frac{\partial a_3}{\partial s}$, $\frac{\partial \rho_3}{\partial s}$, and $\frac{\partial u_3}{\partial s}$ are all zero, making $\left(\frac{de}{dp} \right)_3$ and $\left(\frac{d\sigma}{d(\ln A)} \right)_3$ also zero. At point 2, it has been assumed that variations in the s direction can be approximated by variations in the shock front direction, that is, the Rankine–Hugoniot conditions on the shock front can be used to the relations (1.76) and (1.77), or, (1.78) and (1.79). Under the condition of strong shocks, Milton obtained

$$\varepsilon = -\frac{1}{2} \left[\frac{\gamma - 1}{2\gamma} \right]^{\frac{1}{2}} \frac{1}{\rho_1 a_1 M^2} (p_2 - p_3) \frac{dM}{ds} \quad (1.80)$$

$$\sigma = \frac{2}{\gamma + 1} \frac{[2\gamma(\gamma - 1)]^{\frac{1}{2}} + \gamma(\gamma - 1)}{[(2\gamma / (\gamma - 1))^{\frac{1}{2}} + 2]^2} a_1 \cdot \ln \left(\frac{A_2}{A_3} \right) \frac{dM}{ds} \quad (1.81)$$

where the subscript 1 represents the flow condition ahead of the main shock, the subscript 2 represents the flow condition behind the disturbed shock (Mach stem), whose Mach number is M , and the subscript 3 represents the flow condition ahead of the reflected shock, which just corresponds to the flow condition behind the incident shock, whose Mach number is M_0 . The cross-sectional areas of the upstream ray tube and the ray tube behind the Mach

stem are A_3 and A_2 , which correspond to A and A_0 , respectively. According to the moving shock wave relations, we have

$$(p_2 - p_3) / p_1 = \left(\frac{2\gamma}{\gamma + 1} \right) \left(M^2 - M_0^2 \right) \quad (1.82)$$

$$\frac{u_2 + a_2}{u_2 a_2} = \frac{\gamma + 1}{a_1 M} \cdot \frac{[2\gamma(\gamma - 1)]^{\frac{1}{2}} + 2}{2[2\gamma(\gamma - 1)]^{\frac{1}{2}}} \quad (1.83)$$

Substituting relations (1.82), (1.83), (1.80), and (1.81) into relation (1.75), we obtain the correction terms

$$\begin{aligned} \left(\frac{u_2 + a_2}{u_2 a_2} \right) (\varepsilon + \sigma) ds &= -\frac{1}{2\gamma} \left\{ \left[\frac{\gamma(\gamma - 1)}{2} \right]^{\frac{1}{2}} + 1 \right\} \cdot \left[1 - \frac{M_0^2}{M^2} \right] \frac{dM}{M} \\ &\quad - \frac{1}{2} \ln \left(\frac{A_0}{A} \right) \frac{dM}{M} \end{aligned} \quad (1.84)$$

Milton's modified relation between M and A is given as follows

$$\frac{dA}{A} = - \left[\frac{2M}{K(M)(M^2 - 1)} + \frac{\eta}{M} \right] dM \quad (1.85)$$

where $K(M)$ is the same as that in relation (1.43), and

$$\eta = \frac{1}{2\gamma} \left\{ \left[\frac{\gamma(\gamma - 1)}{2} \right]^{\frac{1}{2}} + 1 \right\} \left\{ 1 - \frac{M_0^2}{M^2} \right\} + \frac{1}{2} \ln \frac{A_0}{A}$$

For $\gamma = 1.4$,

$$\eta = 0.546 \left[1 - \left(\frac{M_0}{M} \right)^2 \right] + \frac{1}{2} \ln \frac{A_0}{A} \quad (1.86)$$

Itoh *et al.* have extended Milton's results to the general case, and the expression for η is

$$\begin{aligned} \eta &= \left(1 - \frac{M_0^2}{M^2} \right) \frac{(F + 2B)E}{(M^2 - 1)BD} + \frac{1}{2} \ln \left(\frac{A_0}{A} \right) \cdot \\ &\quad \frac{D^{\frac{3}{2}}(M^2 + 1) + 4(M^2 - 1)^2 F}{(M^2 - 1)DE} \end{aligned} \quad (1.87)$$

where

$$\begin{aligned} B &= 2\gamma M^2 - (\gamma - 1), \quad C = (\gamma - 1)M^2 + 2, \\ D &= BC, \quad E = 2(M^2 - 1) + \sqrt{D}, \\ F &= (\gamma - 1)(1 + \gamma M^4) \end{aligned}$$

In the case of strong shocks, $M_0 \rightarrow \infty$, the expression (1.87) reduces to (1.85). The expressions above are useful for calculations.

Chapter 2 Two-Dimensional Equations of Shock Dynamics for a Uniform Quiescent Gas Ahead of a Shock Wave

§ 2.1 Fundamental concepts

The equations of shock dynamics consist of the geometrical relations and the ray tube area relation, which can be expressed in orthogonal curvilinear coordinates or rectangular coordinates. Whitham(1957) established the two-dimensional equations and the corresponding relations for the disturbance propagating on shock surface in the case of a quiescent gas ahead of a shock. This chapter is written on the basis of Whitham's and Skews' results(Whitham, 1957 and 1973; Skews, 1967).

The geometrical relations correspond to the kinematic relation of shock dynamics.

The ray tube area relation corresponds to the kinetic relation of shock dynamics.

What is the ray?

What is an orthogonal curvilinear coordinate system?

Which we will discuss in this section.

1. Rays and orthogonal curvilinear coordinate system

When a shock wave (plane shock or curved shock) moves forward through a uniform quiescent medium, for some reasons (for example, shock diffraction by a body), the shape of the shock will change.

How to describe and represent the successive positions of the curved shock? It is convenient for us to use an orthogonal curvilinear coordinate system for describing the shock motion.

We define that the rays are the orthogonal trajectories of the curved shock at successive time, which are shown in Fig. 2.1

In Fig. 2.1, the positions of the shock wave are shown as full lines and the rays are shown as broken lines. The networks consist of the curved shock and rays.

The curvilinear coordinates (α, β) are introduced such that the shock positions are represented by the curves with $\alpha = \text{constant}$ and the rays are represented by the curves with $\beta = \text{constant}$, that is,

$\alpha = \text{constant}$ along a shock at any given time

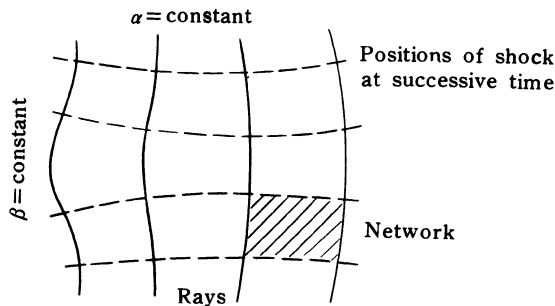


Fig. 2.1 Positions of curved shock and rays

$\beta = \text{constant}$ along a ray

The successive positions of the curved shock are described by a family of the curves with $\alpha = \text{constant}$, and the rays are described by a family of the curves with $\beta = \text{constant}$. The shock positions can be given by the following expression

$$\alpha(x, y) = a_1 t \quad (2.1)$$

where a_1 is the speed of sound in the uniform region ahead of the shock. Obviously, at any given time,

$$\alpha(x, y) = \text{constant}$$

From expression (2.1), we may ask such a question: Does the curved shock travel with the speed of sound?

The answer is No!

2. The line elements

It should be noted that the increments are different from the line elements in this orthogonal curvilinear coordinate system.

From (2.1), we have

$$d\alpha = a_1 dt \quad (2.2)$$

where $d\alpha$ is not the distance the curved shock travels through.

$d\alpha$ and $d\beta$ are called the increments.

$M d\alpha$ and $A d\beta$ are called the line elements.

$M d\alpha$ is the distance along a ray between the shock positions given by α and $\alpha + d\alpha$.

$A d\beta$ is the distance along a curved shock between two rays β and $\beta + d\beta$.

M and A are called coefficients for the line elements.

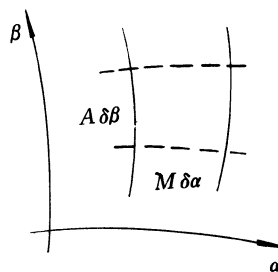


Fig. 2.2 Line elements in shock dynamics

Next, we will analyse the physical significances of M and A ,

$$Md\alpha = Ma_1 dt = W_s dt \quad (2.3)$$

From (2.3), $Md\alpha$ (or $W_s dt$) is the distance that the curved shock travels through, so W_s must be the shock speed and M must be the shock Mach number.

Two neighbouring rays construct a tube or a channel, which is called the ray tube. Obviously, $A d\beta$ is the width of a ray tube. A is proportional to the width of the ray tube (or the ray tube area), because $d\beta = \text{constant}$ along the ray tube.

3. The relationship between the ray and the particle path behind the shock wave

An important idea for shock dynamic theory which was presented by Whitham is to extend the relation between M and A (CCW relation), which originally applies to the solid wall tube, to the ray tube. Of course, we may ask a question:

Can we regard a ray tube as a solid wall tube?

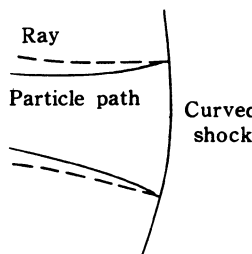


Fig. 2.3 Ray and particle path

We know that under the condition of a quiescent gas ahead of a shock, the shock requires the induced flow immediately behind to be normal to it, but the particle paths will deviate from the ray as the distance from the shock increases in general (as shown in Fig. 2.3). So a definite approximation is involved.

However, in the problem of diffraction along a curved wall, the wall itself has to be both a ray and a particle path along its entire length, so there is some additional resistance to keep the particle paths from the deviation from the rays.

§ 2.2 Two-dimensional equations of shock dynamics

1. The geometrical relationship

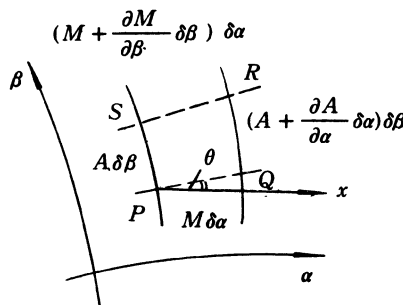


Fig. 2.4 Neighbouring α and β curves

We now derive the geometrical relationship in the orthogonal curvilinear coordinate system. From Fig. 2.4, we have

$$\begin{aligned}\delta\theta &= \frac{QR - PS}{PQ} = \frac{\frac{\partial A}{\partial \alpha} \delta\alpha \cdot \delta\beta}{M \delta\alpha} = \frac{1}{M} \frac{\partial A}{\partial \alpha} \delta\beta \\ \frac{\partial \theta}{\partial \beta} &= \frac{1}{M} \frac{\partial A}{\partial \alpha}\end{aligned}\quad (2.4)$$

where θ is the angle between the ray and x -axis.

Similarly, we can obtain

$$\frac{\partial \theta}{\partial \alpha} = -\frac{1}{A} \frac{\partial M}{\partial \beta} \quad (2.5)$$

From the equations (2.4) and (2.5), we get

$$\frac{\partial}{\partial \alpha} \left(\frac{1}{M} \frac{\partial A}{\partial \alpha} \right) + \frac{\partial}{\partial \beta} \left(\frac{1}{A} \frac{\partial M}{\partial \beta} \right) = 0 \quad (2.6)$$

The equations (2.4) and (2.5), or equation (2.6) are the geometrical rela-

tions of shock dynamics, which have nothing to do with the flow condition and only depend on the geometrical condition.

2. The ray tube area relationship

The equation (2.6) is the first relation between the shock Mach number and ray tube cross-sectional area. In order to find the strength, orientation, and shape of the shock at any given time, we need to establish the second equation which describes the relationship between M and A . If gasdynamics is applied for the purpose, the problem concerned becomes complicated.

In shock dynamics, a simple, approximate method is presented, that is, the relation

$$\frac{dA}{A} = - \frac{2MdM}{(M^2 - 1)K(M)} \quad (2.7)$$

can be used to the ray tube.

Combining (2.6) and (2.7), we have

$$\begin{cases} \frac{\partial}{\partial\alpha} \left(\frac{1}{M} \frac{\partial A}{\partial\alpha} \right) + \frac{\partial}{\partial\beta} \left(\frac{1}{A} \frac{\partial M}{\partial\beta} \right) = 0 \\ A = A(M) \end{cases} \quad (2.8)$$

Substituting the second equation of (2.8) into the first one, we can get a second-order hyperbolic equation for M .

§ 2.3 The disturbances propagating on the shock

In this section, a new concept, the disturbances or waves propagating on the shock, will be presented. These waves are nonlinear waves, which could make the shock change its strength and shape.

In the preceding section, we have known that the equation (2.8) is a second-order hyperbolic equation, so there are two families of characteristics.

Substituting (2.7) into (2.4) and (2.5), we get two equations with two unknown variables $M(\alpha, \beta)$ and $\theta(\alpha, \beta)$,

$$\frac{\partial\theta}{\partial\beta} - \frac{A'(M)}{M} \frac{\partial M}{\partial\alpha} = 0 \quad (2.9)$$

$$\frac{\partial\theta}{\partial\alpha} + \frac{1}{A(M)} \frac{\partial M}{\partial\beta} = 0 \quad (2.10)$$

where $A'(M) = \frac{dA}{dM}$, $\frac{\partial A}{\partial\alpha} = A'(M) \frac{\partial M}{\partial\alpha}$

Now, we introduce a speed of disturbance, $c(M)$, and then find out the expression for $c(M)$. By using the procedure of (2.9) $\times c \pm$ (2.10), we can obtain the following expressions

$$\left(\frac{\partial \theta}{\partial \alpha} + c \frac{\partial \theta}{\partial \beta} \right) - c \frac{A'(M)}{M} \frac{\partial M}{\partial \alpha} + \frac{1}{A} \frac{\partial M}{\partial \beta} = 0 \quad (2.11)$$

$$\left(\frac{\partial \theta}{\partial \alpha} - c \frac{\partial \theta}{\partial \beta} \right) + c \frac{A'(M)}{M} \frac{\partial M}{\partial \alpha} + \frac{1}{A} \frac{\partial M}{\partial \beta} = 0 \quad (2.12)$$

$\frac{dM}{Ac}$ is a total differential, so we have

$$d \left[\int \frac{dM}{Ac} \right] = \frac{dM}{Ac} \quad (2.13)$$

or

$$\frac{\partial}{\partial \alpha} \int \frac{dM}{Ac} = \frac{1}{Ac} \frac{\partial M}{\partial \alpha} \quad (2.14)$$

$$\frac{\partial}{\partial \beta} \int \frac{dM}{Ac} = \frac{1}{Ac} \frac{\partial M}{\partial \beta} \quad (2.15)$$

Substituting (2.14) and (2.15) into (2.11) and (2.12), we get

$$\left(\frac{\partial \theta}{\partial \alpha} + c \frac{\partial \theta}{\partial \beta} \right) - c \frac{A'(M)}{M} Ac \frac{\partial}{\partial \alpha} \int \frac{dM}{Ac} + c \frac{\partial}{\partial \beta} \int \frac{dM}{Ac} = 0 \quad (2.16)$$

$$\left(\frac{\partial \theta}{\partial \alpha} - c \frac{\partial \theta}{\partial \beta} \right) + c \frac{A'(M)}{M} Ac \frac{\partial}{\partial \alpha} \int \frac{dM}{Ac} + c \frac{\partial}{\partial \beta} \int \frac{dM}{Ac} = 0 \quad (2.17)$$

Letting $-c \frac{A'(M)}{M} Ac = 1$, we get

$$c = \sqrt{-\frac{M}{A'(M)A}} \quad (2.18)$$

and

$$\begin{cases} \left(\frac{\partial \theta}{\partial \alpha} + c \frac{\partial \theta}{\partial \beta} \right) + \left(\frac{\partial}{\partial \alpha} + c \frac{\partial}{\partial \beta} \right) \int \frac{dM}{Ac} = 0 \\ \left(\frac{\partial \theta}{\partial \alpha} - c \frac{\partial \theta}{\partial \beta} \right) - \left(\frac{\partial}{\partial \alpha} - c \frac{\partial}{\partial \beta} \right) \int \frac{dM}{Ac} = 0 \end{cases} \quad (2.19)$$

The relations (2.19) can be written as

$$\begin{cases} \left(\frac{\partial}{\partial \alpha} + c \frac{\partial}{\partial \beta} \right) \left(\theta + \int \frac{dM}{Ac} \right) = 0 \\ \left(\frac{\partial}{\partial \alpha} - c \frac{\partial}{\partial \beta} \right) \left(\theta - \int \frac{dM}{Ac} \right) = 0 \end{cases} \quad (2.20)$$

or

$$\theta + \int \frac{dM}{Ac} = \text{constant along } \frac{d\beta}{d\alpha} = c(M) \quad (2.21)$$

$$\theta - \int \frac{dM}{Ac} = \text{constant along } \frac{d\beta}{d\alpha} = -c(M) \quad (2.22)$$

From (2.21) and (2.22), we find that $\left(\theta + \int \frac{dM}{Ac} \right)$ and $\left(\theta - \int \frac{dM}{Ac} \right)$ are

Riemann invariants, and $c(M)$ is the speed of nonlinear disturbance wave on the shock in the α, β plane.

From the expression (2.18), we know that in order to obtain the real characteristics, it is necessary that $A'(M) < 0$.

In fact, the true speed of disturbance wave propagating along the shock front is $\frac{Ad\beta}{dt}$ (or $a_1 A c$).

§ 2.4 Transformation of curvilinear orthogonal coordinate system into rectangular coordinate system

1. The transformation of independent variables

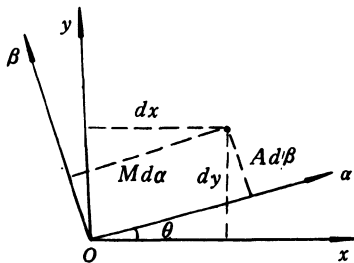


Fig. 2.5 Relations among $M d\alpha$, $Ad\beta$, dx and dy

From Fig. 2.5, we have

$$Md\alpha = dx\cos\theta + dy\sin\theta \quad (2.23)$$

$$Ad\beta = -dx\sin\theta + dy\cos\theta \quad (2.24)$$

or

$$d\alpha = \frac{\cos\theta}{M} dx + \frac{\sin\theta}{M} dy \quad (2.25)$$

$$d\beta = -\frac{\sin\theta}{A} dx + \frac{\cos\theta}{A} dy \quad (2.26)$$

On the other hand, we have

$$d\alpha = \frac{\partial\alpha}{\partial x} dx + \frac{\partial\alpha}{\partial y} dy \quad (2.27)$$

$$d\beta = \frac{\partial\beta}{\partial x} dx + \frac{\partial\beta}{\partial y} dy \quad (2.28)$$

In comparison of (2.25) and (2.26) with (2.27) and (2.28), respectively, we get

$$\frac{\partial\alpha}{\partial x} = \frac{\cos\theta}{M}, \quad \frac{\partial\alpha}{\partial y} = \frac{\sin\theta}{M} \quad (2.29)$$

$$\frac{\partial \beta}{\partial x} = -\frac{\sin\theta}{A}, \quad \frac{\partial \beta}{\partial y} = \frac{\cos\theta}{A} \quad (2.30)$$

Similarly, we can obtain

$$\frac{\partial x}{\partial \alpha} = M\cos\theta, \quad \frac{\partial x}{\partial \beta} = -A\sin\theta \quad (2.31)$$

$$\frac{\partial y}{\partial \alpha} = M\sin\theta, \quad \frac{\partial y}{\partial \beta} = A\cos\theta \quad (2.32)$$

2. The characteristic relations in rectangular coordinates

The relation between two coordinates can be written as follows

$$x = x(\alpha, \beta) \quad (2.33)$$

$$y = y(\alpha, \beta) \quad (2.34)$$

If we use the relation along the characteristic $\frac{d\beta}{d\alpha} = c$, the above relations can be written as

$$x = x[\alpha, \beta(\alpha)] \quad (2.35)$$

$$y = y[\alpha, \beta(\alpha)] \quad (2.36)$$

Their derivatives can be expressed in the following forms

$$\frac{dx}{d\alpha} = \frac{\partial x}{\partial \alpha} + \frac{\partial x}{\partial \beta} \frac{d\beta}{d\alpha} \quad (2.37)$$

$$\frac{dy}{d\alpha} = \frac{\partial y}{\partial \alpha} + \frac{\partial y}{\partial \beta} \frac{d\beta}{d\alpha} \quad (2.38)$$

Substituting $\frac{d\beta}{d\alpha} = c$, (2.31), (2.32) into (2.37) and (2.38), we get

$$\frac{dx}{d\alpha} = M\cos\theta - A\sin\theta \cdot c \quad (2.39)$$

$$\frac{dy}{d\alpha} = M\sin\theta + A\cos\theta \cdot c \quad (2.40)$$

In the $x - y$ plane, the characteristic can be expressed as

$$\frac{dy}{dx} = \frac{\frac{dy}{d\alpha}}{\frac{dx}{d\alpha}} = \frac{\sin\theta + \cos\theta \frac{Ac}{M}}{\cos\theta - \sin\theta \frac{Ac}{M}} \quad (2.41)$$

Letting $\frac{Ac}{M} = \tan v$ and substituting it into (2.41), we get

$$\frac{dy}{dx} = \frac{\sin(\theta + v)}{\cos(\theta + v)} = \tan(\theta + v) \quad (2.42)$$

Similarly, for $\frac{d\beta}{d\alpha} = -c$, we can obtain

$$\frac{dy}{dx} = \tan(\theta - v) \quad (2.43)$$

Finally, we get the following characteristic relations in rectangular coordinate system

$$\theta + \int \frac{dM}{Ac} = \text{constant along } \frac{dy}{dx} = \tan(\theta + v) \quad (2.44)$$

$$\theta - \int \frac{dM}{Ac} = \text{constant along } \frac{dy}{dx} = \tan(\theta - v) \quad (2.45)$$

§ 2.5 Shock-expansion and shock-compression

1. Physical analysis

We now start with the problem of the diffraction of a plane shock along a curved wall. The curved walls may be convex or concave. In gasdynamics, the above phenomenon of diffraction can be analysed as follows.

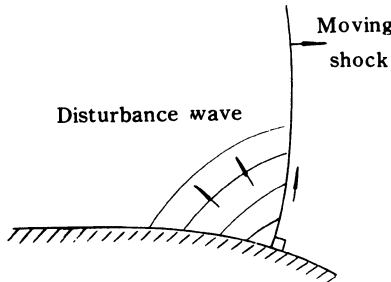


Fig 2.6 The cylindrical disturbance waves generated on curved wall surface

The gas flow induced by the moving shock (plane shock or deforming shock) is disturbed by the convex or concave wall, and a lot of cylindrical disturbance waves are generated on the places of wall surface where directions of the wall change. These cylindrical waves (in two dimensional flow, sound wave is cylindrical) propagate with the local speed of sound relative to the local flow. When these waves catch up with the moving shock, the strength and shape of the shock will change (as shown in Fig 2.6).

Above analysis is from the gasdynamic viewpoint.

Next, we start from the shock dynamic viewpoint to analyse the propagation of disturbance wave along the shock surface. This analysis is analogous to that of one-dimensional waves propagating in a tube. The displacement of the

wall, that is, the change of the wall direction, corresponds to a piston motion in a shock tube. The displacement of the convex wall corresponds to pulling the foot of the shock and the displacement of the concave wall corresponds to pushing the foot of the shock. The pulling and pushing will send out a lot of disturbance waves along the shock.

The convex corner produces a so-called expansion wave. We call it shock-expansion, which represents the propagation of an expansion wave on the shock. The concave corner corresponds to producing a so-called compression wave on the shock. We call it shock-compression.

As mentioned in § 2.3, the speed of the disturbance wave propagating along the shock is $\frac{Ad\beta}{dt}$ ($= a_1 A c$), which is denoted by W_d , that is,

$$W_d = \frac{Ad\beta}{dt} = a_1 A c \quad (2.46)$$

Substituting (1.43) and (2.18) into (2.46), we can obtain

$$W_d = a_1 \left[\frac{1}{2} (M^2 - 1) K(M) \right]^{\frac{1}{2}} \quad (2.47)$$

From the expression (2.47), it is evident that the speed of disturbance wave is, of course, not constant, but varies with the shock strength (shock Mach number) in the case of a uniform gas ahead of shock, where the speed of sound a_1 is given as a constant. The stronger the local strength of the curved shock wave is, the faster the disturbance wave on the shock propagates. So the disturbance wave is a nonlinear wave.

2. Diffraction of plane shock over convex curved wall

In the general case, that is, the diffraction of a plane shock propagating through a channel, the disturbance waves propagate in both directions (as shown in Fig. 2.7).

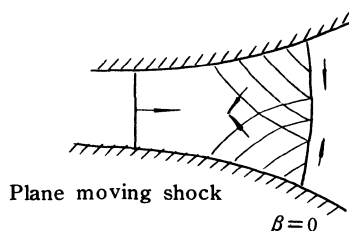


Fig. 2.7 Disturbance waves in both directions

The characteristic relations are written as

for upward waves

$$\theta + \int \frac{dM}{Ac} = J_+ \quad \text{along } \frac{dy}{dx} = \tan(\theta + v) \quad (2.48)$$

$$\left(\frac{d\beta}{d\alpha} = c \right)$$

for downward waves

$$\theta - \int \frac{dM}{Ac} = J_- \quad \text{along } \frac{dy}{dx} = \tan(\theta - v) \quad (2.49)$$

$$\left(\frac{d\beta}{d\alpha} = -c \right)$$

where J_+ and J_- are constants.

In the special case, that is, in the case of simple waves, either upward or downward waves, but not both, are present. In this case, a family of the characteristics are straight lines.

Next, we will discuss the case of the upward simple wave.

From the relations (2.21) and (2.22), considering that there is only upward waves, we have

$$\left\{ \theta + \int_1^M \frac{dM}{Ac} = \text{constant along } \frac{dy}{dx} = \tan(\theta + v) \right. \quad (2.50)$$

$$\left. \theta - \int_1^M \frac{dM}{Ac} = \text{constant everywhere} \right. \quad (2.51)$$

Combining (2.50) and (2.51), we find that

$$\theta = \text{constant} \quad \text{along } \frac{dy}{dx} = \tan(\theta + v) \quad (2.52)$$

$$\int_1^M \frac{dM}{Ac} = \text{constant} \quad \text{along } \frac{dy}{dx} = \tan(\theta + v) \quad (2.53)$$

From (2.53), we get

$$M = \text{constant} \quad \text{along } \frac{dy}{dx} = \tan(\theta + v) \quad (2.54)$$

We know that

$$\tan v = \frac{Ac}{M} = \frac{1}{M} \left[\frac{1}{2} (M^2 - 1) K(M) \right]^{\frac{1}{2}} \quad (2.55)$$

Substituting (2.54) into (2.55), we can obtain

$$v = \text{constant} \quad \text{along } \frac{dy}{dx} = \tan(\theta + v) \quad (2.56)$$

and

$$\frac{dy}{dx} = \tan(\theta + v) = \text{constant} \quad (2.57)$$

Therefore, the family of the characteristics are straight lines.

Integrating the relation (2.57), we get

$$\int_{y_w}^y dy = \tan(\theta + v) \int_{x_w}^x dx$$

or

$$y - y_w = (x - x_w) \tan(\theta + v) \quad (2.58)$$

where subscript w is the value of the wall surface.

From (2.52) and (2.54), we know that in the case of simple waves, the strength and orientation of the shock remain constant along each characteristic, that is, the shock Mach number M and the orientation of shock, θ , remain constant in the points $a, a_1, a_2\dots$ or the points $b, b_1, b_2\dots$ and so on. The points a, b, c, d, e represent the points on the wall surface. Thus, the relation (2.58) can be written as

$$y - y_w = (x - x_w) \tan(\theta_w + v_w) \quad (2.59)$$

where

$$\begin{aligned} \tan v_w &= \left(\frac{Ac}{M} \right)_w = \frac{1}{M_w} \left[\frac{(M_w^2 - 1)K(M_w)}{2} \right]^{\frac{1}{2}} \\ \tan \theta_w &= \left(\frac{dy}{dx} \right)_w \end{aligned}$$

where $\left(\frac{dy}{dx} \right)_w$ is the slope of the tangent to the wall surface and θ_w is the angle between the tangent to the wall surface and x -axis (as shown in Fig. 2.8).

In the region of simple wave on the shock, the expression (2.51) can be used for finding M and θ , while the relation (2.50) is no significance. This is because (2.50) only applies to the case along each characteristic where M and θ are constants.

According to the initial and boundary conditions, $M = M_0$, $\theta_0 = 0$, for $\alpha = 0$, $0 < \beta < \infty$; $\theta = \theta_w$ for $\beta = 0$, $0 < \alpha < \infty$ (if the plane shock can be considered as the initial condition), we can obtain

$$\theta - \int_1^M \frac{dM}{Ac} = \theta_0 - \int_1^{M_0} \frac{dM}{Ac} \quad (2.60)$$

or

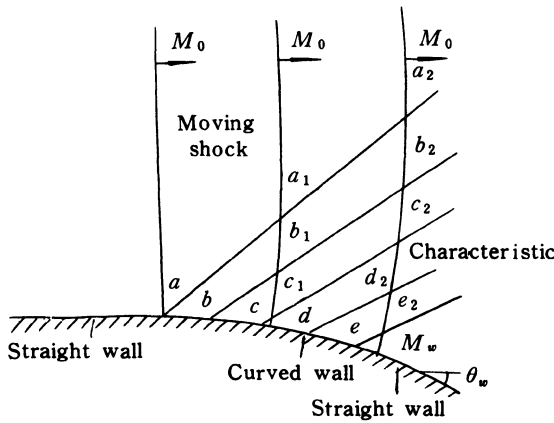


Fig. 2.8 The simple wave on the shock

$$\theta = \int_{M_0}^M \frac{dM}{Ac} \quad (2.61)$$

If the relation (2.61) is used to the surface of the curved wall, it can be written in the following form

$$\theta_w = \int_{M_0}^{M_w} \frac{dM}{Ac} \quad (2.62)$$

We sum up the expressions for simple waves as follows

$$\begin{cases} \theta = \int_{M_0}^M \left[\frac{2}{(M^2 - 1)K(M)} \right]^{\frac{1}{2}} dM + \theta_0 \\ y - y_w = (x - x_w) \tan(\theta_w + v_w) \end{cases} \quad (2.63)$$

If the initial strength of shock M_0 , the angle of shock wave θ_0 , and the curves of the wall are given, we can find out the shock Mach numbers on the wall surface, M_{w1}, M_{w2}, \dots , by using (2.62), and then can obtain the characteristics originated from the points on the surface of the curved wall by using (2.59). Finally, starting the calculation from the intersection point of the plane moving shock with the first characteristic by using M_{w1} and θ_{w1} , we can obtain the strength and angle of the whole curved shock at any given time.

3. Diffraction of a plane shock around a convex sharp corner

In Fig. 2.8, the surface of the wall includes three parts — straight wall,

curved wall, and straight wall. Now if the curved wall diminishes to zero, we will obtain a sharp corner as shown in Fig. 2.9.

(1) The regions on the shock (as shown in Fig. 2.9)

The shock can be divided into three regions.

The undisturbed region where the first disturbance (corresponding to the characteristic originated at the point a in Fig. 2.8) does not arrive.

The region between the first and last disturbances.

The region where the last disturbance has passed (the last disturbance corresponds to the characteristic originated at the point e in Fig. 2.8).

It follows from Fig. 2.8 that the first disturbance is originated at the point where the straight wall begins to bend and the last disturbance is originated at the point where the curved wall stops bending. By comparing Fig. 2.9 with Fig. 2.8, we find that in the case of diffraction around a convex sharp corner, the first and last disturbances are originated at the same point.

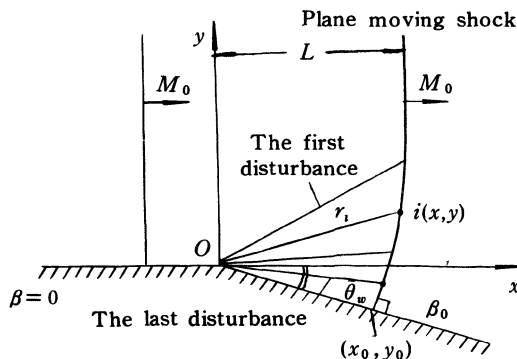


Fig. 2.9 The regions on shock divided by the first disturbance and the last disturbance

The first disturbance can be expressed as

$$\begin{aligned} \frac{dy}{dx} &= \tan(\theta_0 + v_0) = \tan v_0 \\ &= \frac{1}{M_0} \left[\frac{1}{2} (M_0^2 - 1) K(M_0) \right]^{\frac{1}{2}} \end{aligned} \quad (2.64)$$

For strong shocks

$$\begin{aligned} M_0 &\rightarrow \infty & K(M_0) &\rightarrow 0.3941 \\ n &= 2 / K(M_0) = 5.0743 \end{aligned}$$

$$\tan v_0 = \frac{dy}{dx} = \frac{1}{\sqrt{n}}, \quad v_0 = 23.94^\circ$$

where v_0 is the angle between the first disturbance and x -axis.

The last disturbance can be expressed as

$$\frac{dy}{dx} = \tan(\theta_w + v_w) \quad (2.65)$$

where $\tan v_w = \frac{1}{M_w} \left[\frac{1}{2} (M_w^2 - 1) K(M_w) \right]^{\frac{1}{2}}$

For strong shocks

$$M_w \rightarrow \infty, \quad v_w = 23.94^\circ,$$

$$\frac{dy}{dx} = \tan(\theta_w + 23.94^\circ)$$

Any disturbance in the region between the first and the last disturbances can be calculated by the following relations

$$\begin{cases} \theta_i = \int_{M_0}^{M_i} \left[\frac{2}{(M^2 - 1)K(M)} \right]^{\frac{1}{2}} dM \\ \theta_i + v_i = \omega_i \\ \tan v_i = \frac{1}{M_i} \left[\frac{1}{2} (M_i^2 - 1) K(M_i) \right]^{\frac{1}{2}} \end{cases} \quad (2.66)$$

If any point on the shock is specified, that is, the angle ω_i between the characteristic i and x -axis is given, the strength and orientation of the shock at the specified point, M_i and θ_i can be determined.

The shape of the disturbed shock can be obtained by using the following relation

$$r_i = \left(\frac{M_i}{M_0} \right) \frac{L}{\cos(\omega_i - \theta_i)} \quad (2.67)$$

where r_i is the distance between the origin O and the point i on the shock surface, L is the distance the plane shock travels from the origin O to the position considered.

(2) The expression for the shape of shock front

In this sub-section, our purpose is to derive the expression for the shape of shock front under the condition of strong shocks, if the angle of deflection of the wall, θ_w , and the strength of plane shock, M_0 , are given.

The distance along the surface of the wall (along $\beta = 0$) can be expressed as

$$s = \int_0^s ds = \int_0^\alpha M d\alpha = \int_0^\alpha M_w d\alpha \quad (2.68)$$

$$x_0(\alpha) = M_w \alpha \cos \theta_w \quad (2.69)$$

$$y_0(\alpha) = M_w \alpha \sin \theta_w \quad (2.69)$$

There are following relations along the shock (along $\alpha = a_1 t = \text{constant}$, namely, partial derivative with respect to β , $\frac{\partial}{\partial \beta}$)

$$\frac{\partial x}{\partial \beta} = -A \sin \theta \quad (2.70)$$

$$\frac{\partial y}{\partial \beta} = A \cos \theta \quad (2.71)$$

From (2.68), (2.69), (2.70) and (2.71), we can obtain the expressions for the coordinates of any point on the shock front as follows

$$x = x_0(\alpha) - \int_0^\beta A \sin \theta d\beta \quad (2.72)$$

$$y = y_0(\alpha) + \int_0^\beta A \cos \theta d\beta \quad (2.73)$$

By using the ray tube area relation

$$\frac{A}{A_0} = \frac{f(M)}{f(M_0)} \quad (2.74)$$

where

$$f(M) = \exp \left[- \int \frac{2M dM}{(M^2 - 1) K(M)} \right],$$

and taking $A_0 = 1$, we can obtain

$$A = \frac{f(M)}{f(M_0)} \quad (2.75)$$

Substituting (2.68), (2.69), and (2.75) into (2.72) and (2.73), we get

$$x = M_w \alpha \cos \theta_w - \int_0^\beta \frac{f(M)}{f(M_0)} \sin \theta d\beta \quad (2.76)$$

$$y = M_w \alpha \sin \theta_w + \int_0^\beta \frac{f(M)}{f(M_0)} \cos \theta d\beta \quad (2.77)$$

The expressions (2.76) and (2.77) are the expressions for the shape of shock front in the general cases.

For special case of strong shocks, we have

$$\frac{dA}{A} = \frac{-2MdM}{(M^2 - 1)K(M)} = -n \frac{dM}{M} \quad (2.78)$$

or

$$\frac{A}{A_0} = \left(\frac{M_0}{M}\right)^n, \quad A_0 = 1 \quad (2.79)$$

The expressions (2.76) and (2.77) can be written as

$$x = \alpha M_w \cos\theta_w - \int_0^\beta \left(\frac{M_0}{M}\right)^n \sin\theta d\beta \quad (2.80)$$

$$y = \alpha M_w \sin\theta_w + \int_0^\beta \left(\frac{M_0}{M}\right)^n \cos\theta d\beta \quad (2.81)$$

From $\beta=0$ to $\beta=\beta_c$, $M=M_w = \text{constant}$, and $\theta=\theta_w$, where the subscript c represents the position of the last distance wave, we get

$$\begin{aligned} \frac{x}{M_0 \alpha} &= \frac{M_w}{M_0} \cos\theta_w - \frac{1}{M_0 \alpha} \int_0^{\beta_c} \left(\frac{M_0}{M}\right)^n \sin\theta d\beta \\ &\quad - \frac{1}{M_0 \alpha} \int_{\beta_c}^\beta \left(\frac{M_0}{M}\right)^n \sin\theta d\beta \end{aligned} \quad (2.82)$$

$$\begin{aligned} \frac{y}{M_0 \alpha} &= \frac{M_w}{M_0} \sin\theta_w + \frac{1}{M_0 \alpha} \int_0^{\beta_c} \left(\frac{M_0}{M}\right)^n \cos\theta d\beta \\ &\quad + \frac{1}{M_0 \alpha} \int_{\beta_c}^\beta \left(\frac{M_0}{M}\right)^n \cos\theta d\beta \end{aligned} \quad (2.83)$$

or

$$\begin{aligned} \frac{x}{M_0 \alpha} &= \frac{M_w}{M_0} \cos\theta_w - \left(\frac{M_0}{M_w}\right)^n \sin\theta_w \left(\frac{\beta_c}{M_0 \alpha}\right) \\ &\quad - \frac{1}{M_0 \alpha} \int_{\beta_c}^\beta \left(\frac{M_0}{M}\right)^n \sin\theta_w d\beta \end{aligned} \quad (2.84)$$

$$\begin{aligned} \frac{y}{M_0 \alpha} &= \frac{M_w}{M_0} \sin\theta_w + \left(\frac{M_0}{M_w}\right)^n \cos\theta_w \left(\frac{\beta_c}{M_0 \alpha}\right) \\ &\quad + \frac{1}{M_0 \alpha} \int_{\beta_c}^\beta \left(\frac{M_0}{M}\right)^n \cos\theta_w d\beta \end{aligned} \quad (2.85)$$

By means of the transformation of variables from β to θ , namely,

$$\theta = \frac{\sqrt{n}}{n+1} \ln \left(\frac{\beta \sqrt{n}}{\alpha M_0} \right) \quad (2.86)$$

$$\frac{M}{M_0} = \left(\frac{\beta \sqrt{n}}{\alpha M_0} \right)^{\frac{1}{n+1}} \quad (2.87)$$

we can obtain

$$\frac{x}{M_0 \alpha} = e^{\frac{\theta_w}{\sqrt{n}}} \cos \theta_w - \frac{1}{\sqrt{n}} e^{\frac{\theta_w}{\sqrt{n}}} \sin \theta_w - \frac{n+1}{n} \int_{\theta_w}^{\theta} e^{\frac{\theta}{\sqrt{n}}} \sin \theta d\theta \quad (2.88)$$

$$\frac{y}{M_0 \alpha} = e^{\frac{\theta_w}{\sqrt{n}}} \sin \theta_w + \frac{1}{\sqrt{n}} e^{\frac{\theta_w}{\sqrt{n}}} \cos \theta_w + \frac{n+1}{n} \int_{\theta_w}^{\theta} e^{\frac{\theta}{\sqrt{n}}} \cos \theta d\theta \quad (2.89)$$

Integrating (2.88) and (2.89) and rearranging, we get

$$\frac{x}{M_0 \alpha} = -e^{\frac{\theta}{\sqrt{n}}} \left(\frac{1}{\sqrt{n}} \sin \theta - \cos \theta \right) \quad (2.90)$$

$$\frac{y}{M_0 \alpha} = e^{\frac{\theta}{\sqrt{n}}} \left(\frac{1}{\sqrt{n}} \cos \theta + \sin \theta \right) \quad (2.91)$$

Letting $\tan \lambda = \sqrt{n}$, $\sin \lambda = \sqrt{\frac{n}{n+1}}$, we finally obtain

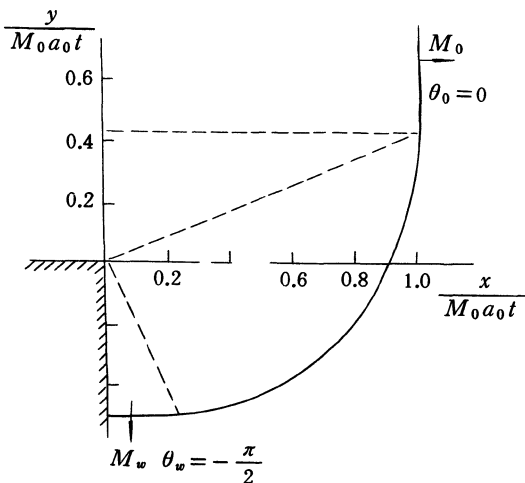


Fig. 2.10 The diffraction of shock around a 90° convex corner

$$\left\{ \begin{array}{l} \frac{x}{M_0 \alpha} = \left(\frac{n+1}{n} \right)^{\frac{1}{2}} e^{\frac{\theta}{\sqrt{n}}} \sin(\lambda - \theta) \\ \frac{y}{M_0 \alpha} = \left(\frac{n+1}{n} \right)^{\frac{1}{2}} e^{\frac{\theta}{\sqrt{n}}} \cos(\lambda - \theta) \end{array} \right. \quad (2.92)$$

$$\left\{ \begin{array}{l} \frac{x}{M_0 \alpha} = \left(\frac{n+1}{n} \right)^{\frac{1}{2}} e^{\frac{\theta}{\sqrt{n}}} \sin(\lambda - \theta) \\ \frac{y}{M_0 \alpha} = \left(\frac{n+1}{n} \right)^{\frac{1}{2}} e^{\frac{\theta}{\sqrt{n}}} \cos(\lambda - \theta) \end{array} \right. \quad (2.93)$$

$$\theta_w \leq \theta \leq 0$$

§ 2.6 Theory of sound

In 1967, Skews made the experiments on the diffraction of a shock around a sharp corner and gave a relation for the first disturbance propagating along the shock by using the theory of sound.

The diffraction of a plane shock around a sharp corner is shown in Fig. 2.11. The flow induced by the plane shock is disturbed by the sharp corner, and the sound waves are produced continuously, some parts of which catch up with the shock and make it deform. But it is difficult to calculate the deforming shock by using the theory of sound, so the only thing we can do is to find out the point where first sound wave overtakes the shock.

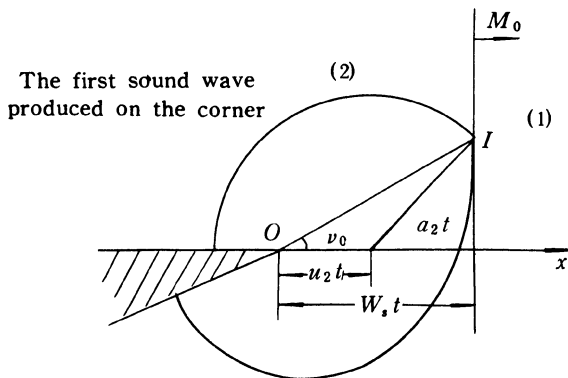


Fig. 2.11 The first sound wave is produced on sharp corner

The first sound wave produced on the sharp corner propagates in the flow field behind the plane shock with the local speed of sound (as shown in Fig. 2.11).

In Fig. 2.11 the centre of the sound circle moves with the gas flow in region 2, v_0 is the angle between IO and x -axis, the straight line IO is drawn from the tip of the sharp corner to the point where the first sound wave intersects with

the moving shock. u_2 , a_2 , and W_s are the flow velocity, the speed of sound behind the moving shock, and the shock speed, respectively.

We have the following relations

$$\tan v_0 = \frac{\left[(a_2 t)^2 - (W_s t - u_2 t)^2 \right]^{\frac{1}{2}}}{W_s t} \quad (2.94)$$

$$\left(\frac{a_2}{a_1} \right)^2 = \frac{\left[2\gamma M_0^2 - (\gamma - 1) \right] \left[(\gamma - 1) M_0^2 + 2 \right]}{(\gamma + 1)^2 M_0^2} \quad (2.95)$$

$$\frac{u_2}{a_1} = \frac{2}{\gamma + 1} \left(M_0 - \frac{1}{M_0} \right) \quad (2.96)$$

Substituting (2.95) and (2.96) into (2.94), we get

$$\tan v_0 = \left\{ \frac{(M_0^2 - 1) \left[(\gamma - 1) M_0^2 + 2 \right]}{(\gamma + 1) M_0^4} \right\}^{\frac{1}{2}} \quad (2.97)$$

For strong shocks

$$M_0 \rightarrow \infty, \tan v_0 = \left(\frac{\gamma - 1}{\gamma + 1} \right)^{\frac{1}{2}},$$

$$v_0 = 22.21^\circ, \quad (\text{for } \gamma = 1.4).$$

Next, Let's make a comparison between Skews' relation (2.97) and Whitham's relation (2.64), namely,

$$\tan v_0 = \left[\frac{1}{2} \left(M_0^2 - 1 \right) K(M_0) \right]^{\frac{1}{2}} / M_0 \quad (2.64)$$

Substituting the function $K(M)$ into (2.64), we can obtain Whithams' expression for v_0 as

$$\tan v_0 = \frac{1}{M_0} \left[\frac{(M_0^2 - 1)}{\left(2\mu + 1 + \frac{1}{M_0^2} \right) \left(1 + \frac{2}{\gamma + 1} \frac{1 - \mu^2}{\mu} \right)} \right]^{\frac{1}{2}} \quad (2.98)$$

where

$$\mu = \left[\frac{(\gamma - 1) M_0^2 + 2}{2\gamma M_0^2 - (\gamma - 1)} \right]^{\frac{1}{2}}$$

The comparison between both theories is shown in Table 2.1.

Table 2.1 The comparison between $(v_0)_{\text{Whitham}}$ and $(v_0)_{\text{Skews}}$

M_0	1	2	3	5	7	10	∞
$(v_0)_w$	0	21.74 °	23.15 °	23.71 °	23.83 °	23.89 °	23.94 °
$(v_0)_s$	0	27.94 °	25.64 °	23.66 °	22.98 °	22.60 °	22.21 °

Finally, we make a comparison between the two speeds of the first disturbances along the shock front.

We have the following relations for the speeds of the first disturbances along the shock

$$\begin{aligned} (W_d)_{\text{Skews}} &= W_s (\tan v_0)_{\text{Skews}} \\ &= a_1 \left\{ \frac{(M_0^2 - 1) \left[(\gamma - 1)M_0^2 + 2 \right]}{(\gamma + 1)M_0^2} \right\}^{\frac{1}{2}} \end{aligned} \quad (2.99)$$

$$(W_d)_{\text{Whitham}} = a_1 \left[\frac{1}{2} \left(M_0^2 - 1 \right) K(M_0) \right]^{\frac{1}{2}} \quad (2.100)$$

§ 2.7 Shock-Shock

1. The formation of shock-shock

Starting with the relations of a simple wave propagating along the shock given in § 2.5, we now discuss the behavior of the diffraction of the plane shock around convex and concave curved walls to see how the disturbance waves propagate along the shock.

The relations are rewritten as

$$\theta = \int_{M_0}^M \left[\frac{2}{(M^2 - 1)K(M)} \right]^{\frac{1}{2}} dM \quad (2.101)$$

$$\theta_w = \int_{M_0}^{M_w} \left[\frac{2}{(M^2 - 1)K(M)} \right]^{\frac{1}{2}} dM \quad (2.102)$$

$$W_d = a_1 \left[\frac{1}{2} (M^2 - 1) K(M) \right]^{\frac{1}{2}} \quad (2.103)$$

For the diffraction of the plane shock with Mach number M_0 along a convex curved wall, the shock is weakened by the shock-expansion wave.

From (2.102), we can see that for $\theta_w < 0$

$$M_0 > M_i > M_w \quad (2.104)$$

From (2.103), we get

$$W_d(M_0) > W_d(M_i) > W_d(M_w) \quad (2.105)$$

where subscript i represents any of the points on the curved shock.

Therefore, the curved part of the shock increases (as shown in Fig. 2.12).

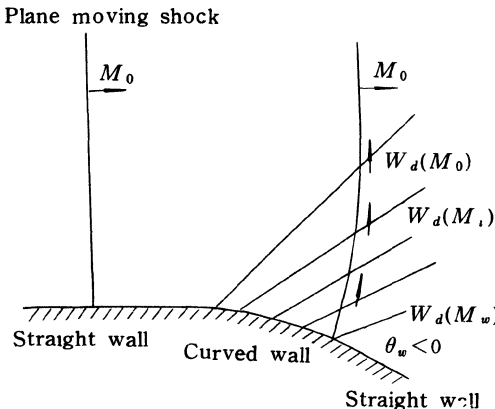


Fig. 2.12 Convex curved wall, $W_d(M_w) < W_d(M_i) < W_d(M_0)$, shock-expansion forms

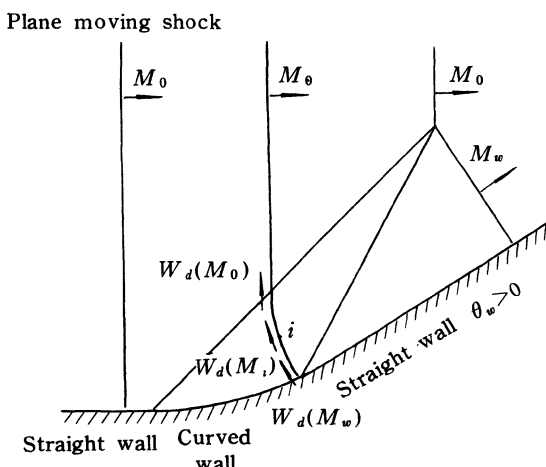


Fig. 2.13 Concave curved wall, $W_d(M_w) > W_d(M_i) > W_d(M_0)$, shock-shock forms from shock-compression

For the diffraction of the plane shock along a concave curved wall, the shock is strengthened by the shock-compression.

From (2.102), we get

$$\theta_w > 0, M_0 < M_i < M_w \quad (2.106)$$

From (2.103), we get

$$W_d(M_0) < W_d(M_i) < W_d(M_w) \quad (2.107)$$

Therefore, the curved part of shock diminishes. Finally, the last disturbance wave overtakes the first one, the curved part of the shock vanishes and a shock-shock forms(as shock in Fig. 2.13).

If a plane shock diffracts around a wedge, the shock-shock forms suddenly as shown in Fig. 2.14.

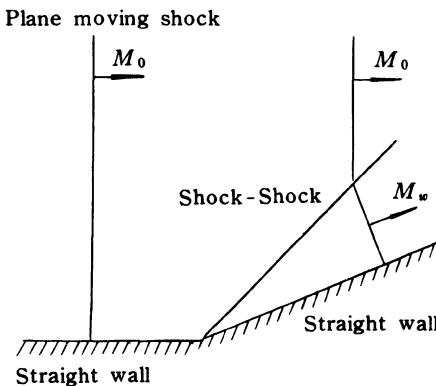


Fig. 2.14 Diffraction by a wedge, shock-shock forms

2. Shock-Shock relations

In the cases of the shock-expansion or shock-compression, we regard these disturbances as continuous waves propagating along the shock, and the continuous waves will make the strength and orientation of the shock change gradually.

In the case of the shock-shock, we may imagine that there is a discontinuous wave which propagates along the shock, and this discontinuous wave may be called shock-shock, which will change the strength and orientation of the shock suddenly.

In Fig. 2.15, M_0 is the shock Mach number for an undisturbed shock; M_1 is the shock Mach number for a disturbed shock. θ_0 represents the direction of the ray of the undisturbed shock and θ_1 represents the direction of

the ray of the disturbed shock.

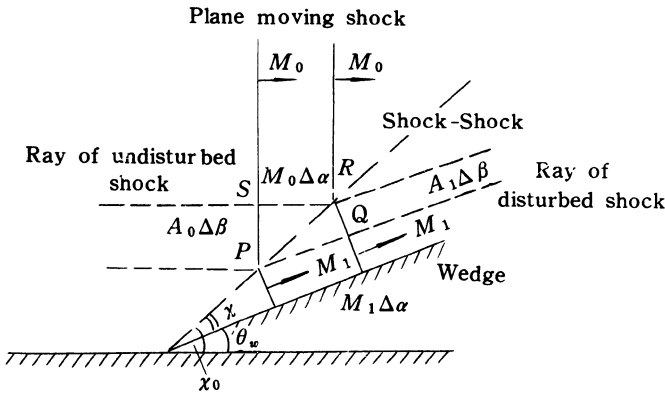


Fig. 2.15 Diffraction of shock by a wedge

From the shock-ray network $PQRS$, the following can be obtained

$$(A_0 \triangle \beta)^2 + (M_0 \triangle \alpha)^2 = (A_1 \triangle \beta)^2 + (M_1 \triangle \alpha)^2$$

or

$$\left(\frac{\triangle \beta}{\triangle \alpha}\right)^2 = -\frac{M_1^2 - M_0^2}{A_1^2 - A_0^2} \quad (2.108)$$

Let $\frac{\triangle \beta}{\triangle \alpha}$ represent the velocity of the shock-shock and the symbol C denote $\frac{\triangle \beta}{\triangle \alpha}$. We get

$$C = \sqrt{-\frac{M_1^2 - M_0^2}{A_1^2 - A_0^2}} \quad (2.109)$$

Next, we will derive the relation for the change of orientation of the shock

$$\cot(\theta_1 - \theta_0) = \tan(\angle RPS + \angle RPQ) = \frac{\frac{M_0}{A_0} \frac{1}{C} + \frac{A_1}{M_1} C}{1 - \frac{M_0}{M_1} \frac{A_1}{A_0}}$$

Substituting (2.109) into the above expression, we get

$$\cot(\theta_1 - \theta_0) = \frac{A_1 M_1 + A_0 M_0}{(A_0^2 - A_1^2)^{\frac{1}{2}} (M_1^2 - M_0^2)^{\frac{1}{2}}} \quad (2.110)$$

It is evident that when $M_1 \rightarrow M_0$, $\theta_1 \rightarrow \theta_0$, $A_1 \rightarrow A_0$, we can obtain the same results as those in § 2.3

$$\begin{cases} c = \sqrt{-\frac{M}{A'(M) \cdot A}} \\ d\theta = \frac{dM}{Ac} \end{cases}$$

The angle between the shock-shock trace and the surface of wall (or the x -axis), χ (or χ_0), can be expressed as follows

$$\tan(\chi_0 - \theta_0) = \frac{A_0 \triangle \beta}{M_0 \triangle \alpha} = \frac{A_0}{M_0} \left(\frac{M_0^2 - M_1^2}{A_1^2 - A_0^2} \right)^{\frac{1}{2}} \quad (2.111)$$

$$\tan(\chi_0 - \theta_1) = \frac{A_1 \triangle \beta}{M_1 \triangle \alpha} = \frac{A_1}{M_1} \left(\frac{M_0^2 - M_1^2}{A_1^2 - A_0^2} \right)^{\frac{1}{2}} \quad (2.112)$$

where $(\chi_0 - \theta_1) = \chi$, $(\theta_1 - \theta_0) = \theta_w$.

3. Diffraction by a wedge

In the problem that a plane shock diffracts around a wedge, the Mach number of the shock, M_0 , and the wedge angle, θ_w , are usually given. We want to find out the Mach number of the disturbed shock, M_w , and the angle between the shock-shock trace and the surface of the wedge, χ .

From (2.110) and (2.112), letting $M_1 = M_w$, $\theta_0 = 0$, $\theta_1 = \theta_w$, $A_1 = A_w$, we get

$$\tan \chi = \frac{A_w}{M_w} \left(\frac{M_w^2 - M_0^2}{A_0^2 - A_w^2} \right)^{\frac{1}{2}} \quad (2.113)$$

$$\tan \theta_w = \frac{\left(M_w^2 - M_0^2 \right)^{\frac{1}{2}} (A_0^2 - A_w^2)^{\frac{1}{2}}}{A_w M_w + A_0 M_0} \quad (2.114)$$

$$\frac{A_w}{A_0} = \frac{f(M_w)}{f(M_0)} \quad (2.115)$$

where

$$f(M) = \exp \left[- \int \frac{2M dM}{(M^2 - 1) K(M)} \right].$$

Substituting (2.115) into (2.113) and (2.114), we get

$$\tan \chi = \frac{f(M_w)}{f(M_0)} \left\{ \frac{1 - \left(\frac{M_0}{M_w} \right)^2}{1 - \left[\frac{f(M_w)}{f(M_0)} \right]^2} \right\}^{\frac{1}{2}} \quad (2.116)$$

$$\tan \theta_w = \left(\frac{M_w}{M_0} \right) \frac{\left[1 - \left(\frac{M_0}{M_w} \right)^2 \right]^{\frac{1}{2}} \left\{ 1 - \left[\frac{f(M_w)}{f(M_0)} \right]^2 \right\}^{\frac{1}{2}}}{1 + \frac{f(M_w)}{f(M_0)} \frac{M_w}{M_0}} \quad (2.117)$$

From (2.116) and (2.117), we can find out χ and M_w .

For strong shocks, we have

$$\frac{A_w}{A_0} = \left(\frac{M_0}{M_w} \right)^n \quad (2.118)$$

and the expressions (2.116) and (2.117) are written as

$$\tan \chi = \left(\frac{M_0}{M_w} \right)^n \left[\frac{1 - \left(\frac{M_0}{M_w} \right)^2}{1 - \left(\frac{M_0}{M_w} \right)^{2n}} \right]^{\frac{1}{2}} \quad (2.119)$$

$$\tan \theta_w = \left(\frac{M_w}{M_0} \right) \frac{\left[1 - \left(\frac{M_0}{M_w} \right)^2 \right]^{\frac{1}{2}} \left[1 - \left(\frac{M_0}{M_w} \right)^{2n} \right]^{\frac{1}{2}}}{\left[1 + \left(\frac{M_0}{M_w} \right)^{n-1} \right]} \quad (2.120)$$

From (2.119), it follows that the angle χ only depends on the ratio of M_0 to M_w in the case of strong shocks.

Chapter 3 Three-Dimensional Equations of Shock Dynamics for a Uniform Quiescent Gas Ahead of a Shock Wave

Chapter 3 is very important for the whole book, which is the basis of the following chapters 4, 5, 6, and 7. In this chapter, we first discuss the three-dimensional equations and shock-shock relations for a uniform quiescent gas ahead of a shock (Whitham, 1959); then explain the external diffractions, the diffraction by a cone (Whitham, 1959; Han, Milton, and Takayama, 1992), diffraction by a cylinder or a sphere (Bryson and Gross, 1961), diffraction by a thin or slender body (Whitham, 1959); finally explain the internal diffraction along a conically contracting channel (Milton, 1971; Han, Milton, and Takayama, 1992).

§ 3.1 Three-dimensional equations of shock dynamics

For the three-dimensional problem, it is difficult to use the orthogonal curvilinear coordinates (α , β and the third coordinate, say, γ). So we revert to the Cartesian coordinates (x , y , z).

As mentioned already in Chapter 2, the equations of shock dynamics consist of the geometric relations, which represent the kinematic relations, and the area relation along a ray tube, which represents the kinetic relation.

1. The relation between the shock Mach number M and function α

In the case of three-dimensional flow, the shock positions can be expressed as

$$\alpha(x, y, z) = a_1 t \quad (3.1)$$

where a_1 is the speed of sound in the uniform region ahead of the shock.

The expression (3.1) can also be written as

$$S(x, y, z, t) = a_1 t - \alpha(x, y, z) = 0 \quad (3.2)$$

Differentiating (3.2) with t , we get

$$\frac{\partial S}{\partial t} + \nabla S \cdot \vec{W} = 0 \quad (3.3)$$

where \vec{W} is the velocity of a moving surface, $\nabla|S|$ is the normal to the moving

surface.

If the moving surface is a shock wave, (3.3) can be expressed as

$$a_1 - \nabla \alpha \cdot \vec{W}_s = 0 \quad (3.4)$$

where \vec{W}_s is the velocity of the moving shock surface, $\nabla \alpha$ is the normal to the shock.

It is evident for the quiescent gas ahead of the shock that \vec{W}_s has the same direction as $\nabla \alpha$, that is

$$\vec{W}_s \cdot \nabla \alpha = |\vec{W}_s| \cdot |\nabla \alpha| \quad (3.5)$$

where $|\vec{W}_s|$ is the magnitude of \vec{W}_s , which equals W_s . Therefore, we can obtain

$$W_s = \frac{a_1}{|\nabla \alpha|} \quad (3.6)$$

The shock Mach number can be expressed as

$$M = \frac{1}{|\nabla \alpha|} \quad (3.7)$$

2. The unit vector for the ray direction, \vec{i}

As mentioned already in Chapter 2, the rays are the orthogonal trajectories of the curved shock at successive time, so the direction of the ray is consistent with that of the normal to the shock at any point. It is convenient for us to introduce a unit vector \vec{i} for the ray direction.

$$\vec{i} = \frac{\nabla \alpha}{|\nabla \alpha|} \quad (3.8)$$

3. The divergence of \vec{i}

What is the meaning of $\operatorname{div} \vec{i}$?

We will prove that the increases in cross-sectional area along a ray tube are related to the divergence of the unit vector \vec{i} by some expression.

First of all, we will prove the following relation

$$\nabla \cdot \left(\frac{\vec{i}}{A} \right) = 0 \quad (3.9)$$

The divergence theorem is applied to the volume V , which is surrounded with the surfaces of the ray tube and the two successive shock positions as shown in Fig. 3.1. We have

$$\int_V \nabla \cdot \left(\frac{\vec{i}}{A} \right) dV = \int_{S_1 + S + S_2} \frac{\vec{i} \cdot \vec{n}}{A} dS \quad (3.10)$$

where S refers to the side surface of the ray tube, S_1 and S_2 refer to the surfaces of the ends, and \vec{n} is the outward normal. Since

$$\text{on } S_1, \quad \vec{i}_1 \cdot \vec{n}_1 = -1$$

$$\text{on } S_2, \quad \vec{i}_2 \cdot \vec{n}_2 = +1$$

$$\text{on } S, \quad \vec{i} \cdot \vec{n} = 0$$

(3.10) can be written as

$$\int_V \nabla \cdot \left(\frac{\vec{i}}{A} \right) dV = \int_{S_2} \frac{dS}{A} - \int_{S_1} \frac{dS}{A} \quad (3.11)$$

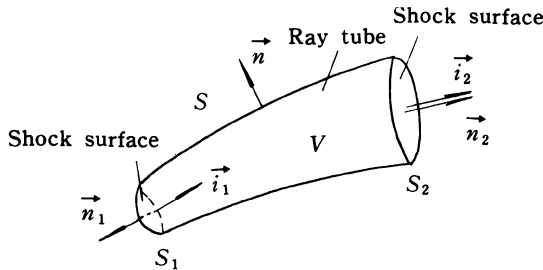


Fig. 3.1 The volume surrounded with the surfaces of the ray tube and the two successive shock positions

On the right-hand side of (3.11), both integrals tend to the same value as the diameter of the ray tube diminishes to zero. Therefore, we have

$$\int_V \nabla \cdot \left(\frac{\vec{i}}{A} \right) dV = 0 \quad (3.12)$$

Since the ray tube can be taken arbitrarily, we get

$$\nabla \cdot \left(\frac{\vec{i}}{A} \right) = 0 \quad (3.13)$$

The relation (3.13) can be rewritten as

$$\nabla \cdot \vec{i} - \vec{i} \cdot \frac{\nabla A}{A} = 0 \quad (3.14)$$

or

$$\nabla \cdot \vec{i} = \vec{i} \cdot \frac{\nabla A}{A} = \frac{1}{A} \frac{dA}{ds_r} \quad (3.15)$$

where $\frac{dA}{ds_r}$ is the derivative of A with respect to s_r , which is the length along

the ray.

It follows from (3.15) that the divergence of the unit vector \vec{i} is the relative increment in A along the ray tube.

Comparing relation (3.13) with the continuity equation in gasdynamics, namely,

$$\frac{\partial \rho}{\partial t} + \operatorname{div}(\rho \vec{V}) = 0 \quad (3.16)$$

we find out that $\operatorname{div} \vec{i}$ is something like $\operatorname{div} \vec{V}$ in the continuity equation. From (3.16), we get

$$\nabla \cdot \vec{V} = -\frac{1}{\rho} \frac{d\rho}{dt} \quad (3.17)$$

The divergence of the flow velocity is the relative decrease in density ρ .

So relation (3.13) may be regarded as the kinematic relation in shock dynamics.

Substituting (3.7) into (3.8), we get

$$\vec{i} = M \nabla \alpha \quad (3.18)$$

Substituting (3.18) into (3.13), we can obtain

$$\nabla \cdot \left(\frac{M}{A} \nabla \alpha \right) = 0 \quad (3.19)$$

Similarly, the area relation along the ray tube is given as

$$\frac{A}{A_0} = \frac{f(M)}{f(M_0)} \quad (3.20)$$

where

$$f(M) = \exp \left[- \int \frac{2MdM}{(M^2 - 1)K(M)} \right]$$

It should be noted that the relation (3.13) has been obtained under the condition of the diameter of the ray tube diminishing to zero, so the definition of A may need a little amplification, that is, the ratio of the cross-sectional area at any location along the ray tube to the area at a standard reference section can be introduced, so that as the maximum diameter of the ray tube tends to zero, this ratio of any area to the reference area could approach a finite limit. For any infinitesimal ray tube, A is now proportional to the cross-sectional area of the ray tube rather than being the area itself. However, the relation (3.20) is still valid, because only the ratio of areas appears in (3.20).

Summarizing the above relations, we can obtain the three-dimensional equations of shock dynamics denoted by a function $\alpha(x, y, z)$ for a uniform quiescent gas ahead of a shock as follows

$$\begin{cases} \nabla \cdot \left(\frac{M}{A} \nabla \alpha \right) = 0 \\ M = \frac{1}{|\nabla \alpha|} \\ A = A(M) \end{cases} \quad (3.21)$$

where $A = A(M)$, namely, $\frac{dA}{A} = \frac{-2MdM}{(M^2 - 1)K(M)}$.

§ 3.2 The various forms of differential equations for a uniform quiescent gas ahead of a shock

(3.21) are the equations in vectorial form, which can be expressed in various forms in plane flow and axially-symmetric flow.

1. The equations in plane flow

The equations in the plane flow case can be described by the function α or by the shock Mach number M and the angle θ . From the equations (3.21), we can obtain

$$\begin{cases} \frac{\partial}{\partial x} \left(\frac{M}{A} \frac{\partial \alpha}{\partial x} \right) + \frac{\partial}{\partial y} \left(\frac{M}{A} \frac{\partial \alpha}{\partial y} \right) = 0 \\ M = \left(\alpha_x^2 + \alpha_y^2 \right)^{-\frac{1}{2}} \\ A = A(M) \end{cases} \quad (3.22)$$

We know that, under the condition of uniform quiescent gas ahead of the shock, the unit vector of the normal to the shock, \vec{n} , is equal to \vec{i} , so

$$\vec{i} = \vec{n} = M \nabla \alpha = M \frac{\partial \alpha}{\partial x} \vec{e}_x + M \frac{\partial \alpha}{\partial y} \vec{e}_y \quad (3.23)$$

and we have another expression for \vec{n}

$$\vec{n} = \cos \theta \vec{e}_x + \sin \theta \vec{e}_y \quad (3.24)$$

where \vec{e}_x and \vec{e}_y are the unit vectors in the directions of x and y axes, respectively. From (3.23) and (3.24), we get

$$\frac{\partial \alpha}{\partial x} = \frac{\cos \theta}{M}, \quad \frac{\partial \alpha}{\partial y} = \frac{\sin \theta}{M} \quad (3.25)$$

The relations (3.25) are just the same as (2.29).

Substituting (3.25) into the first expression of (3.22) and noting that $\frac{\partial}{\partial y} \left(\frac{\partial \alpha}{\partial x} \right) = \frac{\partial}{\partial x} \left(\frac{\partial \alpha}{\partial y} \right)$, we can obtain the following equations denoted by M

and θ

$$\begin{cases} \frac{\partial}{\partial x} \left(\frac{\cos\theta}{A} \right) + \frac{\partial}{\partial y} \left(\frac{\sin\theta}{A} \right) = 0 \\ \frac{\partial}{\partial x} \left(\frac{\sin\theta}{M} \right) - \frac{\partial}{\partial y} \left(\frac{\cos\theta}{M} \right) = 0 \\ A = A(M) \end{cases} \quad (3.26)$$

We now transfer the equations (3.26) from the rectangular coordinates into the curvilinear orthogonal coordinates.

From (2.29) and (2.30), we get

$$\begin{cases} \frac{\partial}{\partial x} = \frac{\cos\theta}{M} \frac{\partial}{\partial \alpha} - \frac{\sin\theta}{A} \frac{\partial}{\partial \beta} \\ \frac{\partial}{\partial y} = \frac{\sin\theta}{M} \frac{\partial}{\partial \alpha} + \frac{\cos\theta}{A} \frac{\partial}{\partial \beta} \end{cases} \quad (3.27)$$

Substituting (3.27) into the first expression of the equations (3.26), we have

$$\frac{\partial}{\partial x} \left(\frac{\cos\theta}{A} \right) + \frac{\partial}{\partial y} \left(\frac{\sin\theta}{A} \right) = -\frac{1}{MA^2} \frac{\partial A}{\partial \alpha} + \frac{1}{A^2} \frac{\partial \theta}{\partial \beta} = 0$$

or

$$-\frac{1}{M} \frac{\partial A}{\partial \alpha} + \frac{\partial \theta}{\partial \beta} = 0 \quad (3.28)$$

Substituting (3.27) into the second expression of the equations (3.26), we have

$$\frac{\partial}{\partial x} \left(\frac{\sin\theta}{M} \right) - \frac{\partial}{\partial y} \left(\frac{\cos\theta}{M} \right) = \frac{1}{M^2} \frac{\partial \theta}{\partial \alpha} + \frac{1}{AM^2} \frac{\partial M}{\partial \beta} = 0$$

or

$$\frac{1}{A} \frac{\partial M}{\partial \beta} + \frac{\partial \theta}{\partial \alpha} = 0 \quad (3.29)$$

The equations (3.28) and (3.29) are all the same as the equations (2.4) and (2.5), respectively.

Summarizing the above equations, we get

$$\begin{cases} \frac{\partial \theta}{\partial \beta} - \frac{1}{M} \frac{\partial A}{\partial \alpha} = 0 \\ \frac{\partial \theta}{\partial \alpha} + \frac{1}{A} \frac{\partial M}{\partial \beta} = 0 \\ A = A(M) \end{cases} \quad (3.30)$$

2. The equations in axially-symmetric flow

From the equations (3.21), we can obtain axially-symmetric equations denoted by the function $\alpha(x, r)$ as follows

$$\begin{cases} \frac{\partial}{\partial r} \left(r \frac{M}{A} \alpha_r \right) + \frac{\partial}{\partial x} \left(r \frac{M}{A} \alpha_x \right) = 0 \\ M = \left(\alpha_x^2 + \alpha_r^2 \right)^{-\frac{1}{2}} \\ A = A(M) \end{cases} \quad (3.31)$$

If the equations are directly expressed with M and θ , there are two cases:

(1) The diffraction of a plane moving shock around a cone (or any other revolution body) as shown in Fig. 3.2.

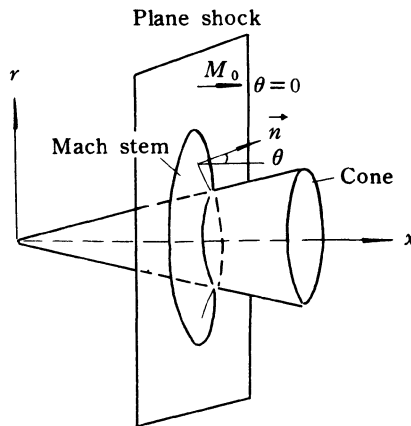


Fig. 3.2 The diffraction of a plane moving shock around a cone

The unit vector of the normal to the shock can be expressed as

$$\vec{n} = M \alpha_x \vec{e}_x + M \alpha_r \vec{e}_r \quad (3.32)$$

$$\vec{n} = \cos\theta \vec{e}_x + \sin\theta \vec{e}_r, \quad (3.33)$$

where \vec{e}_x and \vec{e}_r are the unit vectors in the directions of x and r axes respectively.

From (3.32) and (3.33), we get

$$\alpha_r = \frac{\sin\theta}{M}, \quad \alpha_x = \frac{\cos\theta}{M} \quad (3.34)$$

Substituting (3.34) into the first expression of (3.31) and noting $\frac{\partial}{\partial r}(\alpha_x) = \frac{\partial}{\partial x}(\alpha_r)$, we get

$$\begin{cases} \frac{\partial}{\partial r} \left(\frac{r \sin \theta}{A} \right) + \frac{\partial}{\partial x} \left(\frac{r \cos \theta}{A} \right) = 0 \\ \frac{\partial}{\partial x} \left(\frac{\sin \theta}{M} \right) - \frac{\partial}{\partial r} \left(\frac{\cos \theta}{M} \right) = 0 \\ A = A(M) \end{cases} \quad (3.35)$$

(2) The diffraction of a spherical shock over a horizontal plane as shown in Fig. 3.3 .

We have

$$\alpha_r = \frac{\cos \theta}{M}, \quad \alpha_x = \frac{\sin \theta}{M} \quad (3.36)$$

and

$$\begin{cases} \frac{\partial}{\partial r} \left(\frac{r \cos \theta}{A} \right) + \frac{\partial}{\partial x} \left(\frac{r \sin \theta}{A} \right) = 0 \\ \frac{\partial}{\partial x} \left(\frac{\cos \theta}{M} \right) - \frac{\partial}{\partial r} \left(\frac{\sin \theta}{M} \right) = 0 \\ A = A(M) \end{cases} \quad (3.37)$$

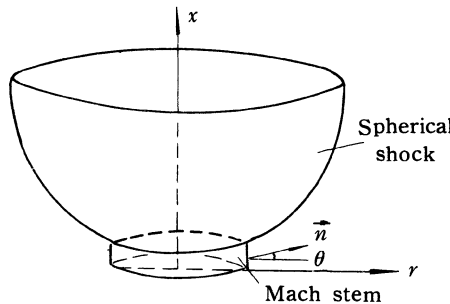


Fig. 3.3 The diffraction of a spherical shock over a plane

§ 3.3 Analogy of shock diffraction with steady supersonic flow

1. The analogy between the two kinematic equations

The two phenomena, namely, the diffraction of a moving shock by a body (wedge, cone and so on) and the irrotational, steady, supersonic flow passing a body can be immediately analogous to each other (Whitham, 1959).

First of all, let us make a comparison of the velocity potential function with the function of shock surface.

In the irrotational flow, we have

$$\vec{V} = \nabla \varphi \quad (3.38)$$

Taking the absolute value on both sides of (3.38), we have

$$V = |\nabla \varphi| \quad (3.39)$$

where \vec{V} is the vector of velocity, φ is the velocity potential function. The relations (3.38) and (3.39) correspond to the following relations

$$\frac{\vec{i}}{M} = \nabla \alpha \quad (3.40)$$

$$\frac{1}{M} = |\nabla \alpha| \quad (3.41)$$

From (3.38), (3.39), (3.40), and (3.41), we get that φ corresponds to α , V corresponds to $\frac{1}{M}$.

Next, let us make a comparison of the continuity equation with the kinematic relation of shock dynamics.

In the case of steady flow, we have the continuity equation in the following form

$$\nabla \cdot (\rho \vec{V}) = 0 \quad (3.42)$$

where ρ is the density.

Substituting (3.38) into (3.42), we have

$$\nabla \cdot (\rho \nabla \varphi) = 0 \quad (3.43)$$

The relations (3.42) and (3.43) correspond to

$$\nabla \cdot \left(\frac{\vec{i}}{A} \right) = 0 \quad (3.44)$$

$$\nabla \cdot \left(\frac{M}{A} \nabla \alpha \right) = 0 \quad (3.45)$$

From (3.43) and (3.45), we get that ρ corresponds to $\frac{M}{A}$.

It should be noted that the two phenomena are not all the same, and the difference is that (3.45) is always hyperbolic, while (3.43) may be hyperbolic or elliptic depending on whether the flow is supersonic or subsonic (Whitham, 1959).

Combining the equation (3.43) and the Euler equation, we can obtain

$$(a^2 - \varphi_x^2)\varphi_{xx} + (a^2 - \varphi_y^2)\varphi_{yy} + (a^2 - \varphi_z^2)\varphi_{zz} - 2\varphi_x \varphi_y \varphi_{xy} - 2\varphi_y \varphi_z \varphi_{yz} - 2\varphi_x \varphi_z \varphi_{xz} = 0 \quad (3.46)$$

where a is the speed of sound.

Expanding (3.45), we get

$$\frac{\partial}{\partial x} \left(\frac{M}{A} \frac{\partial \alpha}{\partial x} \right) + \frac{\partial}{\partial y} \left(\frac{M}{A} \frac{\partial \alpha}{\partial y} \right) + \frac{\partial}{\partial z} \left(\frac{M}{A} \frac{\partial \alpha}{\partial z} \right) = 0 \quad (3.47)$$

or

$$\begin{aligned} \alpha_{xx} + \alpha_{yy} + \alpha_{zz} - AM^2 \frac{d}{dM} \left(\frac{M}{A} \right) (\alpha_x^2 \alpha_{xx} + \alpha_y^2 \alpha_{yy} + \alpha_z^2 \alpha_{zz} + \\ 2\alpha_x \alpha_y \alpha_{yx} + 2\alpha_x \alpha_z \alpha_{zx} + 2\alpha_y \alpha_z \alpha_{yz}) = 0 \end{aligned} \quad (3.48)$$

It follows from the equations (3.46) and (3.48) that it is possible for us to use gasdynamic method for solving shock dynamic problem. We will discuss this in § 3.7. Finally, let us discuss the two-dimensional flow.

The flow velocity V and flow angle θ are unknown variables. The velocity potential φ and stream function ψ can be used as the independent variables, we have

$$V = V(\varphi, \psi) \quad (3.49)$$

$$\theta = \theta(\varphi, \psi) \quad (3.50)$$

(3.49) and (3.50) correspond to $M = M(\alpha, \beta)$, $\theta = \theta(\alpha, \beta)$ in the shock diffraction.

By using the same method as that in Chapter 2, we have

$$\begin{cases} \frac{\partial \theta}{\partial \varphi} - \frac{\rho}{V} \frac{\partial V}{\partial \psi} = 0 \\ \frac{\partial \theta}{\partial \psi} - V \frac{\partial}{\partial \varphi} \left(\frac{1}{\rho V} \right) = 0 \end{cases} \quad (3.51)$$

The equations (3.51) correspond to

$$\begin{cases} \frac{\partial \theta}{\partial \alpha} + \frac{1}{A} \frac{\partial M}{\partial \beta} = 0 \\ \frac{\partial \theta}{\partial \beta} - \frac{1}{M} \frac{\partial A}{\partial \beta} = 0 \end{cases} \quad (3.52)$$

From the equations (3.51) and (3.52), we find that φ corresponds to α , ψ corresponds to β , V corresponds to $\frac{1}{M}$, flow angle θ corresponds to the shock wave angle θ , and ρ correspond to $\frac{M}{A}$.

2. The analogy between the two boundary conditions

(1) At infinity

$$\vec{V} = \vec{V}_\infty = V_\infty \vec{e}_x + 0 \vec{e}_y + 0 \vec{e}_z = \frac{\partial \varphi}{\partial x} \vec{e}_x \quad (3.53)$$

From (3.53), we get

$$\frac{d\varphi}{dx} = V_\infty, \quad \varphi \sim V_\infty x \quad (3.54)$$

The above relation is the boundary condition at infinity for the flow passing a body.

In the problem of the diffraction of a plane shock by a body, the initial condition for the undisturbed plane shock can be written as

$$\begin{cases} \vec{i} = M_0 \nabla \alpha = M_0 \left(\frac{\partial \alpha}{\partial x} \vec{e}_x + \frac{\partial \alpha}{\partial y} \vec{e}_y + \frac{\partial \alpha}{\partial z} \vec{e}_z \right) \\ \vec{i} = \vec{e}_x \end{cases} \quad (3.55)$$

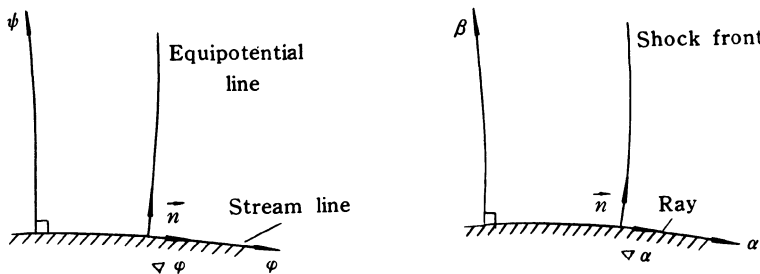
From (3.55), we can obtain

$$M_0 \frac{\partial \alpha}{\partial x} = 1 \quad \text{or} \quad \frac{d\alpha}{dx} = \frac{1}{M_0} \quad (3.56)$$

Integrating (3.56), we get

$$\alpha \sim \frac{x}{M_0} \quad (3.57)$$

(2) On the surface of the body (or curved wall)



(a) The streamline and equipotential line

(b) The shock front and ray

Fig. 3.4 The analogy between shock dynamics and gas dynamics

In the problem of the flow passing a body, the equipotential line is normal to the streamline, and the surface of the body is one of the streamlines, $\nabla \varphi$ is the normal to the equipotential line, \vec{n} is the outward normal to the surface of the body, we have (for inviscid flow)

$$\vec{n} \cdot \nabla \varphi = \frac{\partial \varphi}{\partial n} = 0 \quad (3.58)$$

or

$$V_n = 0 \quad (\text{on the surface}) \quad (3.59)$$

In the problem of the diffraction of the shock over a curved wall (or around a body), we have

$$\vec{n} \cdot \nabla \alpha = \frac{\partial \alpha}{\partial n} = 0 \quad (3.60)$$

where $\nabla \alpha$ is the normal to the shock front, \vec{n} has the same meaning as (3.58).

§ 3.4 The shock-shock relations in the case of three-dimensional flow

There are two independent relations across the shock-shock. One describes the behaviour of the tangential derivatives of α , while the other describes the conservation of flux of $M \nabla \alpha / A$.

1. Tangential derivatives of α

Since the portions of the shock cannot break at any given time, the value of α along the shock is the same even across the discontinuity of the surface of the shock-shock and the tangential derivatives of α on the two sides of the surface of the shock-shock must be equal, which can be written as

$$\vec{n}_{ss} \times (\nabla \alpha)_0 = \vec{n}_{ss} \times (\nabla \alpha)_1 \quad (3.61)$$

where \vec{n}_{ss} is the unit vector normal to the surface of the shock-shock, $\nabla \alpha$ is the normal to the shock front. The subscripts 0 and 1 denote values on the two sides of the surface of the shock-shock.

Since $\nabla \alpha = \frac{\vec{i}}{M}$, the relation (3.61) can be expressed as

$$\frac{\vec{n}_{ss} \times \vec{i}_0}{M_0} = \frac{\vec{n}_{ss} \times \vec{i}_1}{M_1} \quad (3.62)$$

2. Normal derivatives of α

The normal derivatives of α on the two sides of the surface of the shock-shock are not equal, but the flux of $\frac{M \nabla \alpha}{A}$ is conserved across the surface of the shock-shock. A narrow ray tube (as shown in Fig. 3.5), which intersects a small portion of the surface of the shock-shock, is chosen, and the expression for the normal derivatives of α will be derived as follows.

\vec{i}_0 and \vec{i}_1 are the unit vectors along the directions of the ray on the two sides of the shock-shock, respectively. A_0 and A_1 are the corresponding cross-sectional areas of the ray tube, A_{ss} is the surface of the shock-shock, which is cut out by the ray tube. We have the following relations

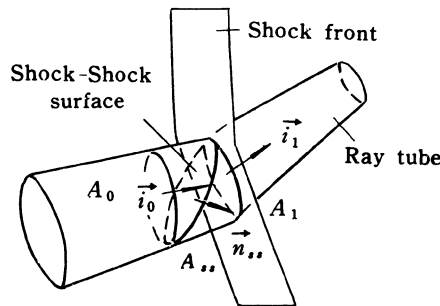


Fig. 3.5 A narrow ray tube intersects the surface of shock-shock

$$\begin{cases} A_{ss} \vec{n} \cdot \vec{i}_0 = A_0 \\ A_{ss} \vec{n} \cdot \vec{i}_1 = A_1 \end{cases} \quad (3.63)$$

From the relations (3.63), we get

$$\frac{\vec{n}_{ss} \cdot \vec{i}_0}{A_0} = \frac{\vec{n}_{ss} \cdot \vec{i}_1}{A_1} \quad (3.64)$$

Substituting $\vec{i} = M \nabla \alpha$ into (3.64), we get

$$\frac{M_0}{A_0} \vec{n}_{ss} \cdot (\nabla \alpha)_0 = \frac{M_1}{A_1} \vec{n}_{ss} \cdot (\nabla \alpha)_1 \quad (3.65)$$

It follows from (3.65) that the normal derivatives of α , namely $\vec{n}_{ss} \cdot (\nabla \alpha)_{1,2}$, are not equal, but the flux of $\frac{M \nabla \alpha}{A}$ is conserved across the surface of shock-shock.

Summarizing the above relations, we obtain a set of the shock-shock relations for the three-dimensional flow as follows

$$\left\{ \begin{array}{l} \frac{\vec{n}_{ss} \times \vec{i}_0}{M_0} = \frac{\vec{n}_{ss} \times \vec{i}_1}{M_1} \\ \frac{\vec{n}_{ss} \cdot \vec{i}_0}{A_0} = \frac{\vec{n}_{ss} \cdot \vec{i}_1}{A_1} \\ \frac{A_1}{A_0} = \frac{f(M_1)}{f(M_0)} \end{array} \right. \quad (3.66)$$

As mentioned already in § 3.3, $\nabla \alpha$ corresponds to \vec{V} , M / A corresponds to ρ in steady supersonic flow. We can find out the following analogies: relation (3.61) corresponds to the continuity of tangential velocity across an oblique

shock wave and relation (3.65) corresponds to the conservation of mass flux.

3. Comparison of relations (3.61) and (3.65) with those in two-dimensional case

In the two-dimensional case, the vectors $\vec{n}_{ss} \times \vec{i}_0$ and $\vec{n}_{ss} \times \vec{i}_1$ have the same direction which is normal to the surface of the figure (as shown in Fig. 3.6). The unit vector in this direction is denoted by \vec{v} . The first expression of (3.66) can be written as

$$\frac{\cos\chi_0}{M_0} \vec{v} = \frac{\cos\chi}{M_1} \vec{v} \quad (3.67)$$

or

$$\frac{\cos\chi_0}{M_0} = \frac{\cos\chi}{M_1} \quad (3.68)$$

(3.68) can be rewritten in the following form

$$\frac{M_0}{\cos\chi_0} = \frac{M_1}{\cos\chi} = M_{ss} \quad (3.69)$$

where $M_{ss} = W_{ss} / a$, W_{ss} is the speed of the shock along the shock-shock locus, and a is the speed of sound in the region ahead of the shock.

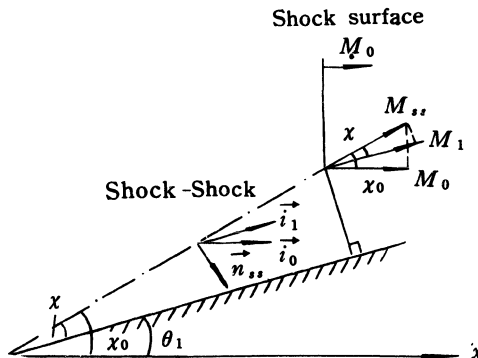


Fig. 3.6 The two-dimensional case

It follows from (3.69) that the portions of shock on the two sides of the shock-shock have the same velocity along the shock-shock locus.

According to the definition of χ_0 and χ , given in Chapter 2, (3.68) can be expressed as

$$\frac{\cos\chi_0}{M_0} = \frac{\cos(\chi_0 - \theta_1)}{M_1} \quad (3.70)$$

In the more general case, we have

$$\frac{\cos(\chi_0 - \theta_0)}{M_0} = \frac{\cos(\chi_0 - \theta_1)}{M_1} \quad (3.71)$$

From (3.64), we get

$$\frac{\sin(\chi_0 - \theta_0)}{A_0} = \frac{\sin(\chi_0 - \theta_1)}{A_1} \quad (3.72)$$

From (3.71) and (3.72), we can obtain

$$\tan(\theta_1 - \theta_0) = \frac{(M_1^2 - M_0^2)^{\frac{1}{2}}(A_0^2 - A_1^2)^{\frac{1}{2}}}{A_1 M_1 + A_0 M_0} \quad (3.73)$$

$$\tan(\chi_0 - \theta_0) = \frac{A_0}{M_0} \left(\frac{M_1^2 - M_0^2}{A_0^2 - A_1^2} \right)^{\frac{1}{2}} \quad (3.74)$$

It follows that the relations (3.73) and (3.74) are all the same as those in Chapter 2.

By using the similar procedure, we can prove that the relations (3.71) and (3.72), or the relations (3.73) and (3.74) are also suitable for the shock-shock surface in the axially-symmetric case.

§ 3.5 Diffraction by a cone

The diffraction of a plane shock by a cone which will be discussed below means that the normal to the shock is coincident with the axis of the cone, so the problem is not only axially-symmetric, but also self-similar.

1. Axially-symmetric equations

From § 3.2, we have

$$\begin{cases} \frac{\partial}{\partial x} \left(\frac{\sin\theta}{M} \right) - \frac{\partial}{\partial r} \left(\frac{\cos\theta}{M} \right) = 0 \\ \frac{\partial}{\partial r} \left(\frac{r\sin\theta}{A} \right) + \frac{\partial}{\partial x} \left(\frac{r\cos\theta}{A} \right) = 0 \\ A = A(M) \end{cases} \quad (3.75)$$

By introducing a similarity variable η , and setting

$$\eta = \tan^{-1} \frac{r}{x} \quad (3.76)$$

we get

$$\frac{\partial}{\partial r} = \frac{\partial}{\partial \eta} \frac{\partial \eta}{\partial r} = \frac{x}{x^2 + r^2} \frac{d}{d\eta} \quad (3.77)$$

$$\frac{\partial}{\partial x} = \frac{\partial}{\partial \eta} \frac{\partial \eta}{\partial x} = -\frac{r}{x^2 + r^2} \frac{d}{d\eta} \quad (3.78)$$

Substituting (3.77) and (3.78) into the first expression of (3.75), we get

$$\tan \eta \frac{d}{d\eta} \left(\frac{\sin \theta}{M} \right) + \frac{d}{d\eta} \left(\frac{\cos \theta}{M} \right) = 0$$

or

$$\frac{1}{M} \frac{dM}{d\eta} = \tan(\eta - \theta) \frac{d\theta}{d\eta} \quad (3.79)$$

Substituting (3.77) and (3.78) into the second expression of (3.75), we get

$$-\frac{1}{A} \frac{dA}{d\eta} = \cot(\eta - \theta) \left[\frac{d\theta}{d\eta} + \frac{\tan \theta}{\sin \eta \cos \eta (1 + \tan \eta \cdot \tan \theta)} \right] \quad (3.80)$$

The area relation, $A = A(M)$, is written as

$$-\frac{1}{A} \frac{dA}{d\eta} = \frac{2M}{(M^2 - 1)K(M)} \frac{dM}{d\eta} \quad (3.81)$$

The relations (3.79), (3.80), and (3.81) constitute a set of equations in which there is no length scale, and both M and θ are the functions of the single variable η .

Substituting (3.81) into (3.80), we can eliminate A , thus having the following equations which only include unknown variables M and θ ,

$$\begin{cases} \frac{d\theta}{d\eta} = \frac{\tan \theta \cdot \cot(\eta - \theta) \cdot (M^2 - 1)K(M)}{\sin \eta \cos \eta (1 + \tan \eta \cdot \tan \theta)[2M^2 \tan(\eta - \theta) - (M^2 - 1)K(M)\cot(\eta - \theta)]} \\ \frac{1}{M} \frac{dM}{d\eta} = \tan(\eta - \theta) \frac{d\theta}{d\eta} \end{cases} \quad (3.82)$$

It follows from (3.82) that in the case of diffraction by a cone, $\frac{d\theta}{d\eta} \neq 0$, the Mach stem is a curve. By using a similar way, for the diffraction by a wedge, we obtain $\frac{d\theta}{d\eta} = 0$ from the equations (3.26), that is, the Mach stem is a straight.

2. Boundary conditions and the procedure for finding solutions

The diffraction of a plane moving shock by a cone is shown in Fig. 3.7.

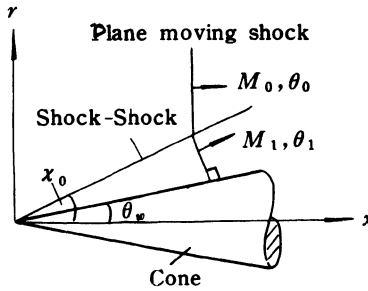


Fig. 3.7 The diffraction by a cone

The discontinuous disturbance wave propagates along the shock front, which can reach to $\eta = \chi_0$, but χ_0 has not been known yet.

The boundary conditions are given as follows:

The shock-shock relations derived in § 3.4 can be used at $\eta = \chi_0$. On the surface of the cone, the curved shock (Mach stem) is normal to the surface, namely

$$\left\{ \begin{array}{l} \theta = \theta_1, \quad M = M_1, \\ \tan \theta_1 = \frac{(M_1^2 - M_0^2)^{\frac{1}{2}} \left[1 - \left(\frac{f(M_1)}{f(M_0)} \right)^2 \right]^{\frac{1}{2}}}{\left[M_0 + \frac{f(M_1)}{f(M_0)} \cdot M_1 \right]} \\ \tan \chi_0 = \frac{f(M_1)}{f(M_0)} \left[\frac{1 - \left(\frac{M_0}{M_1} \right)^2}{1 - \left(\frac{f(M_1)}{f(M_0)} \right)^2} \right]^{\frac{1}{2}} \end{array} \right. \quad \text{at } \eta = \chi_0, \quad (3.83)$$

where

$$f(M) = \exp \left[- \int \frac{2MdM}{(M^2 - 1)K(M)} \right]$$

$$\theta = \theta_\omega \quad \text{on the surface of the cone, } \eta = \theta_\omega \quad (3.84)$$

The procedure for finding M and θ along the Mach stem is given as follows

(1) M_0 , θ_0 , and θ_ω are given.

(2) A value for M_1 is chosen, χ_0 and θ_1 can be found from (3.83).

- (3) The equations (3.82) are integrated from $\eta = \chi_0$ down to the surface of the cone, $\eta = \theta_\omega$.
(4) If $\theta \neq \theta_\omega$ at $\eta = \theta_\omega$, another value for M_1 will be chosen until the boundary condition (3.84) is satisfied, and thus we can obtain χ_0 and all values for M and θ along the disturbed curved shock.

3. The solutions for the case of strong shocks

For strong shocks, the following $A - M$ relation can be used

$$\frac{A}{A_0} = \left(\frac{M_0}{M}\right)^n, \quad n = 5.0743 \quad (3.85)$$

and the problem may be simplified considerably.

From equations (3.82), setting $\frac{M}{M_0} = R$, we have

$$\begin{cases} \frac{d\theta}{d\eta} = \frac{\tan\theta}{\sin\eta\cos\eta(1 + \tan\eta\tan\theta)[n\tan^2(\eta - \theta) - 1]} \\ \frac{1}{R} \frac{dR}{d\eta} = \tan(\eta - \theta) \frac{d\theta}{d\eta} \end{cases} \quad (3.86)$$

and the boundary conditions are given as follows

$$\begin{cases} \tan\theta_1 = \frac{(R_1^2 - 1)^{\frac{1}{2}}(1 - R_1^{-2n})^{\frac{1}{2}}}{1 + R_1^{1-n}} \\ \tan\chi_0 = \left(\frac{R_1^2 - 1}{1 - R_1^{-2n}}\right)^{\frac{1}{2}} \end{cases} \quad \eta = \chi_0 \quad (3.87)$$

$$\theta = \theta_\omega \quad \eta = \theta_\omega \quad (3.88)$$

The same procedure as mentioned before can be used for finding the solutions of equations (3.86). We thus can obtain $\theta(\eta)$ and $R(\eta)$.

The position of shock wave at any time can be found from the solutions, $\theta(\eta)$ and $R(\eta)$, without any further integration.

Next, we want to find out $\frac{x}{M_0\alpha}$ and $\frac{r}{M_0\alpha}$.

Letting

$$\alpha = \frac{xf(\eta)}{M_0} \quad (3.89)$$

and taking derivative of α with respect to x , we get

$$\frac{\partial\alpha}{\partial x} = \frac{1}{M_0} \left[f(\eta) + x \frac{df(\eta)}{d\eta} \frac{\partial\eta}{\partial x} \right] \quad (3.90)$$

Noting $\eta = \tan^{-1} \frac{r}{x}$, we have

$$\frac{\partial \alpha}{\partial x} = \frac{1}{M_0} [f(\eta) - \sin \eta \cos \eta f'(\eta)] \quad (3.91)$$

where $f'(\eta) = \frac{df(\eta)}{d\eta}$. From (3.34), we have

$$\frac{\partial \alpha}{\partial x} = \frac{\cos \theta}{M_0 R} \quad (3.92)$$

Combining (3.91) and (3.92), we get

$$f(\eta) = \frac{\cos \theta}{R} + \sin \eta \cos \eta f'(\eta) \quad (3.93)$$

Taking derivative of α with respect to r , we get

$$\frac{\partial \alpha}{\partial r} = \frac{\cos^2 \eta}{M_0} f'(\eta) \quad (3.94)$$

From (3.34), we have

$$\frac{\partial \alpha}{\partial r} = \frac{\sin \theta}{M_0 R} \quad (3.95)$$

Combining (3.94) and (3.95), we get

$$f'(\eta) = \frac{\sin \theta}{R \cos^2 \eta} \quad (3.96)$$

Substituting (3.96) into (3.93), we get

$$f(\eta) = \frac{\cos \theta + \sin \theta \tan \eta}{R} \quad (3.93)$$

Now, we have already determined the unknown function $f(\eta)$ in (3.89), and thus we obtain

$$\begin{cases} \frac{x}{M_0 \alpha} = \frac{1}{f(\eta)} = \frac{R}{\cos \theta + \sin \theta \cdot \tan \eta} \\ \frac{r}{M_0 \alpha} = \frac{x \cdot \tan \eta}{M_0 \alpha} = \frac{R \cdot \tan \eta}{\cos \theta + \sin \theta \cdot \tan \eta} \end{cases} \quad (3.97)$$

It should be noted that the calculation for strong shocks only depends on the shock Mach number ratio M / M_0 , that is, one calculation gives the solution for a given cone which applies to all shock Mach number M_0 .

The shape of the Mach stem of the diffraction of a cone can also be obtained by using the following relation, which is similar to the relation (2.67),

$$R_i = \left(\frac{M_i}{M_0} \right) \cos(\eta_i - \theta_i) L \quad (3.98)$$

where R_i is the distance between the tip of the cone and the point i on the shock, L is the distance the plane travels through.

§ 3.6 Diffraction by a circular cylinder or a sphere

The application of the equations of shock dynamics to the diffraction by a circular cylinder and a sphere was carried out by Bryson and Gross (1961).

1. The assumptions

The difficulty is to find the solution at the nose for diffraction of a plane moving shock by a circular cylinder or a sphere, because the theory can hardly handle the regular reflection, in which the disturbance wave has not disturbed the shock.

In order to find out the solution at the nose, two assumptions are adopted as follows.

First of all, in the range where the angle between the shock front and the surface of the body is from 0° to 45° , the regular reflection of the plane shock on the surface may occur, which may be regarded as a Mach reflection with an extremely small Mach stem.

Secondly, in this range, the small Mach stem is assumed straight and radial.

2. Diffraction by a circular cylinder

The diffraction of a plane moving shock by a circular cylinder is shown in Fig. 3.8, where the radius of the cylinder is normalized to unity.

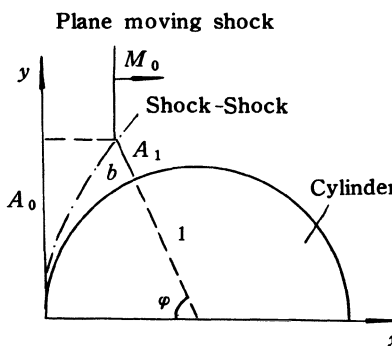


Fig. 3.8 The diffraction of a plane moving shock by a circular cylinder

First of all, we want to find the function of the Mach stem α .

For the plane moving shock, we have

$$\alpha = a_1 t = a_1 \frac{x}{W} = \frac{x}{M_0} \quad (3.99)$$

The distance x that the plane shock travels through can be expressed as

$$x = 1 - (1 + b)\cos\varphi \quad (3.100)$$

where b is the length of Mach stem. Substituting (3.100) into (3.99), we get

$$\alpha = [1 - (1 + b)\cos\varphi] / M_0 \quad (3.101)$$

We know that there is the same value for α along the moving shock across the shock-shock discontinuity at any given time, that is, we have the same relation as (3.101) for the Mach stem.

In the present case, since the function $\alpha = \alpha(b, \varphi)$ is given, there are the two following equations which can be used for finding the solution of the diffraction by a circular cylinder,

$$\begin{cases} \frac{1}{M} = |\nabla \alpha| \\ A = A(M) \end{cases} \quad (3.102)$$

From the first relation of (3.102), we write

$$\nabla \alpha = \frac{\partial \alpha}{\partial r} \vec{e}_r + \frac{\partial \alpha}{\partial \varphi} \vec{e}_\varphi \quad (3.103)$$

Owing to the Mach stem being straight and radial (α remains constant along the shock wave including the Mach stem which has the same direction as the radial), we have

$$\nabla \alpha = \frac{\partial \alpha}{\partial \varphi} \vec{e}_\varphi$$

and

$$\frac{1}{M_1} = |\nabla \alpha| = \frac{\partial \alpha}{\partial \varphi} = \frac{1}{(1 + \frac{b}{2})} \frac{d\alpha}{d\varphi} \quad (3.104)$$

where M_1 is the shock Mach number for the Mach stem.

The second expression of (3.102) can be written as

$$\frac{b}{(1 + b)\sin\varphi} = \frac{f(M_1)}{f(M_0)} \quad (3.105)$$

where b and $(1 + b)\sin\varphi$ are the two areas along the ray tube.

Substituting (3.101) into (3.104) and combining (3.105), we obtain a set of

equations for finding the length of Mach stem b which is the function of angle φ ,

$$\begin{cases} \frac{M_0}{M_1} = \frac{1}{(1 + \frac{b}{2})} \frac{d}{d\varphi} [1 - (1 + b)\cos\varphi] \\ \frac{b}{(1 + b)\sin\varphi} = \frac{f(M_1)}{f(M_0)} \end{cases} \quad (3.106)$$

For strong shocks, (3.105) can be written as

$$\frac{b}{(1 + b)\sin\varphi} = \left(\frac{M_0}{M_1} \right)^n \quad (3.107)$$

where $n = \frac{2}{K(M)} = 5.0743$

or

$$\frac{M_0}{M_1} = \left[\frac{b}{(1 + b)\sin\varphi} \right]^{\frac{1}{n}} \quad (3.108)$$

Substituting (3.108) into the first expression of (3.106), we get

$$\left[\frac{b}{(1 + b)\sin\varphi} \right]^{\frac{1}{n}} = \frac{1}{(1 + \frac{b}{2})} \frac{d}{d\varphi} [1 - (1 + b)\cos\varphi] \quad (3.109)$$

Solving for $\frac{db}{d\varphi}$, we obtain the following ordinary differential equation for b

$$\frac{db}{d\varphi} = (1 + b)\tan\varphi - \frac{(1 + \frac{b}{2})}{\cos\varphi} \left[\frac{b}{(1 + b)\sin\varphi} \right]^{\frac{1}{n}} \quad (3.110)$$

For small φ , which means that the reflection of the plane shock on the surface of the nose is regular, the Mach stem is equal to zero. Thus we have

$$\frac{db}{d\varphi} \ll 1 \quad (3.111)$$

(3.110) can be rewritten as

$$(\sin\varphi)^{\frac{1}{n}} \cos\varphi \frac{db}{d\varphi} = (1 + b)(\sin\varphi)^{\frac{n+1}{n}} - \left(1 + \frac{b}{2} \right) \left(\frac{b}{1 + b} \right)^{\frac{1}{n}} \quad (3.112)$$

After simplification, the following relation can be obtained

$$b = \sin^{\frac{n+1}{n}} \varphi \quad (3.113)$$

Next, let us find the relation of the shock-shock locus and the angle χ_0 . From Fig. 3.8, we can obtain the relation of the shock-shock locus as

$$\begin{cases} y = (1 + b)\sin\varphi \\ x = 1 - (1 + b)\cos\varphi \end{cases} \quad (3.114)$$

The slope of the tangent to the shock-shock locus can be expressed as

$$\tan\chi_0 = \left(\frac{dy}{dx}\right)_{s,s} = \frac{\frac{dy}{d\varphi}}{\frac{dx}{d\varphi}} = \frac{(b + 1)\cos\varphi + \sin\varphi\frac{db}{d\varphi}}{(b + 1)\sin\varphi - \cos\varphi\frac{db}{d\varphi}} \quad (3.115)$$

For strong shocks, in the range of small φ , substituting (3.113) into (3.108), we can obtain $M_1(\varphi)$. Substituting (3.113) into (3.114) and (3.115), we get

$$\begin{cases} y = (1 + \sin^{n+1}\varphi)\sin\varphi \\ x = 1 - (1 + \sin^{n+1}\varphi)\cos\varphi \end{cases} \quad (3.116)$$

and

$$\tan\chi_0 = \cot\varphi \quad (3.117)$$

For the general case, we can solve b from equation (3.110), then substitute it into (3.108), (3.114) and (3.115) to find out $M_1 = f(\varphi)$, $y = f_1(\varphi)$, $x = f_2(\varphi)$ and $\chi_0 = f_3(\varphi)$.

3. Diffraction by a sphere

In the case of the diffraction of a plane shock by a sphere, we have the same function of α as that in the diffraction by a circular cylinder,

$$\alpha = [1 - (1 + b)\cos\varphi] / M_0 \quad (3.118)$$

Similarly, the equations (3.102) can be used for finding the solution of the diffraction by a sphere.

For the same reason, we can obtain

$$\nabla\alpha = \frac{1}{r} \frac{d\alpha}{d\varphi} \vec{e}_\varphi \quad (3.119)$$

and

$$\frac{1}{M_1} = \frac{1}{(1 + \frac{b}{2})} \frac{d\alpha}{d\varphi} \quad (3.120)$$

where M_1 is the shock Mach number for annular Mach shock (as shown in Fig. 3.9).

In the present case, the flow is axially-symmetric about the x -axis, the strength of the Mach shock along the annulus remains constant. The difference

between the diffractions by a circular cylinder and by a sphere is that for the former, $A_0 = (1+b)\sin\varphi$, $A_1 = b$; and for the latter, $A_0 = \pi[(1+b)\sin\varphi]^2$, $A_1 = [2\pi(1+\frac{b}{2})\sin\varphi] \cdot b$.

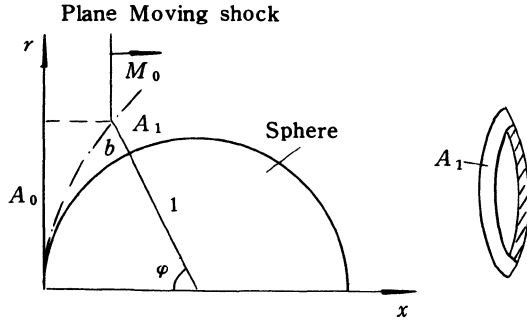


Fig. 3.9 The diffraction by a sphere

Therefore, the area relation along the ray tube can be written as

$$\frac{2b(1+\frac{b}{2})}{(b+1)^2\sin\varphi} = \frac{f(M_1)}{f(M_0)} \quad (3.121)$$

Substituting (3.118) into (3.120) and then combining (3.121), we get a set of equations as follows

$$\begin{cases} \frac{M_0}{M_1} = \frac{1}{(1+\frac{b}{2})} \frac{d}{d\varphi} [1 - (1+b)\cos\varphi] \\ \frac{2b(1+\frac{b}{2})}{(b+1)^2\sin\varphi} = \frac{f(M_1)}{f(M_0)} \end{cases} \quad (3.122)$$

For strong shocks, we have

$$\left(\frac{M_0}{M_1}\right) = \left[\frac{2b(1+\frac{b}{2})}{(b+1)^2\sin\varphi} \right]^{\frac{1}{n}} \quad (3.123)$$

Substituting (3.123) into the first expression of (3.122), we get

$$\frac{db}{d\varphi} = (1+b)\tan\varphi - \frac{\left(1+\frac{b}{2}\right)}{\cos\varphi} \left[\frac{2\left(1+\frac{b}{2}\right)b}{(b+1)^2\sin\varphi} \right]^{\frac{1}{n}} \quad (3.124)$$

For small φ , we have

$$\frac{db}{d\varphi} \ll 1 \quad (3.125)$$

(3.124) can be written as

$$b = \frac{1}{2} \sin^{n+1} \varphi \quad (3.126)$$

By comparing (3.126) with (3.113), we find out

$$b_s = \frac{1}{2} b_c \quad (3.127)$$

where b_s is the length of Mach shock for the diffraction by a sphere at the plane $x = r$, b_c is the length of Mach stem for the diffraction by a circular cylinder.

From (3.127), we find that it is the three-dimensional effect that makes $b_s < b_c$.

§ 3.7 Diffraction by a thin or slender body

In this section, we will discuss the problems on the diffraction of a plane shock by a thin or slender body. The linearized theory or the method of small perturbations, which has been used for finding the solution in the problems of subsonic or supersonic flow passing through a thin or a slender body, can be extended to the diffraction problems. So we first make a review on the perturbation velocity potential.

1. Linear differential equation for the perturbation velocity potential

In this section, the linear differential equation for perturbation velocity potential is simply given as follows. In incompressible flow, the flow passes through a thin body, we can obtain

$$\frac{\partial^2 \varphi'}{\partial x^2} + \frac{\partial^2 \varphi'}{\partial y^2} + \frac{\partial^2 \varphi'}{\partial z^2} = 0 \quad (3.128)$$

In axially-symmetrical flow, we have

$$\frac{\partial^2 \varphi'}{\partial r^2} + \frac{1}{r} \frac{\partial \varphi'}{\partial r} + \frac{\partial^2 \varphi'}{\partial x^2} = 0 \quad (3.129)$$

where φ' is the perturbation velocity potential.

The solution for (3.129) has the following form

$$\varphi' = -\frac{1}{4\pi} \int_0^L \frac{q(\xi) d\xi}{\sqrt{(x - \xi)^2 - r^2}} \quad (3.130)$$

where L is the length of the body, $q(\xi)$ is the function to be determined according to the boundary condition on the surface of the body. $S(\xi)$ is the cross-sectional area of the body. We can get

$$U_{\infty} S'(\xi) = q(\xi) \quad (3.131)$$

where U_{∞} is the free stream velocity.

Substituting (3.131) into (3.130), we get

$$\varphi' = -\frac{U_{\infty}}{4\pi} \int_0^L \frac{S'(\xi)}{\sqrt{(x-\xi)^2 + r^2}} d\xi \quad (3.132)$$

Taking the derivatives of φ' with respect to x and r , respectively, we get

$$V'_{,x} = \frac{\partial \varphi'}{\partial x} = \frac{U_{\infty}}{4\pi} \int_0^L \frac{(x-\xi)S'(\xi)d\xi}{[(x-\xi)^2 + r^2]^{\frac{3}{2}}} \quad (3.133)$$

$$V'_{,r} = \frac{\partial \varphi'}{\partial r} = \frac{U_{\infty}r}{4\pi} \int_0^L \frac{S'(\xi)d\xi}{[(x-\xi)^2 + r^2]^{\frac{3}{2}}} \quad (3.134)$$

Under the condition of the compressible flow, we can make the transformation of the corresponding equations (subsonic and supersonic flow) into Laplace's equation which is the same as (3.128) or (3.129), and find out the solution by using about the same method as above stated already.

2. Linear differential equation for the perturbation α' and its solution (Whitham, 1959)

In § 3.3, we have derived the equations for α , (3.47) and (3.48). Now the linearization of the equations is made as follows.

We know that a plane shock can be expressed as

$$\alpha = \frac{x}{M_0} \quad (3.135)$$

As small perturbation to a plane shock is made, the expression for α can be written as

$$\alpha = \frac{1}{M_0} (x + \alpha') \quad (3.136)$$

where α' is the small perturbation to the plane shock. Taking derivatives of (3.136), we have

$$\begin{cases} \alpha_x = \frac{1}{M_0} (1 + \alpha'_x), & \alpha_{xx} = \frac{1}{M_0} \alpha'_{xx} \\ \alpha_y = \frac{1}{M_0} \alpha'_y, & \alpha_{yy} = \frac{1}{M_0} \alpha'_{yy} \\ \alpha_z = \frac{1}{M_0} \alpha'_z, & \alpha_{zz} = \frac{1}{M_0} \alpha'_{zz} \end{cases} \quad (3.137)$$

Substituting (3.137) into (3.48) and neglecting the second order terms, we get

$$\alpha'_{xx} + \alpha'_{yy} + \alpha'_{zz} - M^2 \left(1 - \frac{M}{A} \frac{dA}{dM} \right) \frac{\alpha'_{xx}}{M^2} = 0 \quad (3.138)$$

Next, we make the linearization of the following equation

$$M = \frac{1}{|\nabla \alpha|} = (\alpha_x^2 + \alpha_y^2)^{-\frac{1}{2}} \quad (3.139)$$

Expanding (3.139) and then substituting the expressions for α_x and α_y of (3.137) into it, we get

$$M = M_0 - M_0 \alpha'_x + O(\alpha'^2_x) \quad (3.140)$$

Expanding $\frac{M}{A}$ in the vicinity of M_0 , we get

$$\frac{M}{A} = \left(\frac{M}{A} \right)_0 + \left[\frac{d}{dM} \left(\frac{M}{A} \right) \right]_{M=M_0} (M - M_0) \quad (3.141)$$

From (3.140) and (3.141), we have

$$\frac{M}{A} = \left(\frac{M}{A} \right)_0 + \left[\frac{d}{dM} \left(\frac{M}{A} \right) \right]_{M=M_0} (-M_0 \alpha'_x) \quad (3.142)$$

and

$$\frac{dA}{dM} = \left(\frac{dA}{dM} \right)_0 + \left[\frac{d}{dM} \left(\frac{dA}{dM} \right) \right]_{M=M_0} (-M_0 \alpha'_x) \quad (3.143)$$

Substituting (3.142) and (3.143) into (3.138), we can obtain the linearized equation for perturbation α' as

$$\alpha'_{yy} + \alpha'_{zz} - B^2 \alpha'_{xx} = 0 \quad (3.144)$$

where

$$B^2 = \left(-\frac{M}{A} \frac{dA}{dM} \right)_{M=M_0}$$

In the axially-symmetrical case, we have

$$\alpha'_{rr} + \frac{1}{r} \alpha'_r - B^2 \alpha'_{xx} = 0 \quad (3.145)$$

By using the aerodynamic method as stated before, we can obtain

$$\alpha'(x, r) = -\frac{1}{2\pi} \int_0^{x-Br} \frac{S'(\xi) d\xi}{\sqrt{(x-\xi)^2 - B^2 r^2}} \quad (3.146)$$

$$\alpha'_x(x, r) = -\frac{1}{2\pi} \int_0^{x-Br} \frac{S''(\xi) d\xi}{\sqrt{(x-\xi)^2 - B^2 r^2}} \quad (3.147)$$

$$\alpha'_r(x, r) = \frac{1}{2\pi r} \int_0^{x-Br} \frac{S''(\xi)(x-\xi) d\xi}{\sqrt{(x-\xi)^2 - B^2 r^2}} \quad (3.148)$$

where $S(x)$ is the cross-sectional area of the slender body, which is assumed as a continuous function of x .

We now make some explanation about the solutions (3.146), (3.147) and (3.148).

The diffraction of a shock by a body corresponds to a supersonic flow past a body. We have the linearized equation for perturbation potential and its solution in the case of supersonic flow as follows

$$\frac{\partial^2 \phi'}{\partial r^2} + \frac{1}{r} \frac{\partial \phi'}{\partial r} - B^2 \frac{\partial^2 \phi'}{\partial x^2} = 0 \quad (3.149)$$

$$\phi'(x, r) = -\frac{1}{2\pi} \int_0^{x-Br} \frac{q(\xi) d\xi}{\sqrt{(x-\xi)^2 - B^2 r^2}} \quad (3.150)$$

where $B = \sqrt{M_\infty^2 - 1}$.

We know that the point (x, r) in the plane $x - r$ cannot be disturbed by the perturbation sources which are located in the points $\xi > x - Br$. The disturbance wave is expressed as

$$\frac{dr}{dx} = \frac{1}{\sqrt{M_\infty^2 - 1}} \quad (3.151)$$

This disturbance is along Mach cone (as shown in Fig. 3.10). Therefore the upper limit of the integral (3.150) is taken as $\xi = x - Br$.

In the problem of the diffraction, the upper limit of the integrals (3.146),

(3.147), and (3.148) is likewise taken as $\xi = x - Br$, since only the disturbances originated in the point $\xi < x - Br$ can influence the point (x, r) on the shock surface as shown in Fig. 3.11.

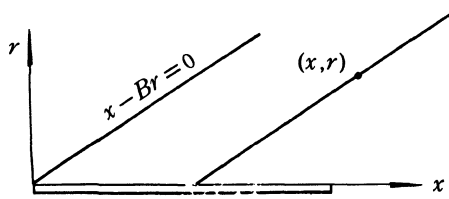


Fig. 3.10 The range of the disturbances in the supersonic flow field

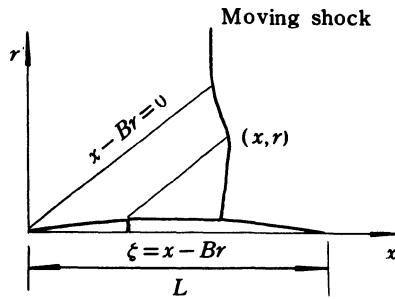


Fig. 3.11 The range of the disturbances on the shock

What is the meaning of B ?

We know that the characteristics in the plane $x - r$ can be expressed as

$$\frac{dr}{dx} = \tan(\theta \pm v) \quad (3.152)$$

where $\tan v = \frac{Ac}{M} = \sqrt{\left(-\frac{A}{M} \frac{dM}{dA} \right)}$.

In Fig. 3.11, we can see that all disturbance lines have the same slope as

$$\frac{dr}{dx} = \frac{1}{B} = \sqrt{\left(-\frac{A}{M} \frac{dM}{dA} \right)}_{M=M_0} \quad (3.153)$$

It follows from (3.153) that in the approximation of linearization, the characteristics degenerate into a family of parallel lines (including shock-shock trace).

When $(x - Br)/r$ is small, namely, the point $\xi \rightarrow 0$, $x \approx Br$, the solutions (3.147) and (3.148) can be simplified to

$$\alpha'_x = -\frac{F(x - Br)}{\sqrt{2Br}} \quad (3.154)$$

$$\alpha'_r = \frac{BF(x - Br)}{\sqrt{2Br}} \quad (3.155)$$

where $F(x) = \frac{1}{2\pi} \int_0^x \frac{S''(\xi)d\xi}{\sqrt{x - \xi}}$.

From (3.140), we get

$$\alpha'_x = -\frac{M - M_0}{M_0} \quad (3.156)$$

From (3.154) and (3.156), we get

$$\frac{M - M_0}{M_0} = \frac{F(x - Br)}{\sqrt{2Br}} \quad (3.157)$$

From (3.34), we have

$$\alpha_r = \frac{\sin\theta}{M} \quad (3.158)$$

Taking derivative of (3.136) with respect to r , we get

$$\alpha_r = \frac{1}{M_0} \alpha'_r \quad (3.159)$$

Substituting (3.140) into (3.158), noting $\sin\theta \approx \theta$ when θ is small, we get

$$\alpha_r = \frac{\theta}{M_0(1 - \alpha'_x)} \quad (3.160)$$

It is important to notice that α'_x and α'_r are not of the same order near the body, but away from the body, α'_x and α'_r are of the same order.

From (3.155), (3.159), and (3.160), we get

$$\theta = \frac{BF(x - Br)}{\sqrt{2Br}} \quad (3.161)$$

In order to derive the expression for the shock-shock trace, an improved method could be used. We introduce a function $\tau(x, r)$, which gives a more accurate approximation to the true characteristic than the line $\tau = x - Br$.

Expanding the relation of the true characteristic (3.152) in the vicinity of M_0 , θ_0 ($\theta_0 = 0$), we have

$$\frac{dx}{dr} = \cot(\theta + v) = \cot v_0 + \left[\frac{\partial}{\partial \theta} \cot(\theta + v) \right]_{M=M_0, \theta=\theta_0} \Delta \theta \\ + \left[\frac{\partial}{\partial M} \cot(\theta + v) \right]_{M=M_0, \theta=\theta_0} \Delta M \quad (3.162)$$

In (3.162),

$$\left[\frac{\partial}{\partial \theta} \cot(\theta + v) \right]_{M=M_0, \theta=\theta_0} = \left[\frac{\partial}{\partial(\theta+v)} \cot(\theta + v) \cdot \frac{\partial}{\partial \theta} (\theta + v(M)) \right]_{M=M_0, \theta=\theta_0} = -\frac{1}{\sin^2 v_0} \quad (3.163)$$

$$\left[\frac{\partial}{\partial M} \cot(\theta + v) \right]_{M=M_0, \theta=\theta_0} = -\frac{1}{\sin^2 v_0} \left(\frac{dv}{dM} \right)_{M=M_0} \quad (3.164)$$

In (3.163) and (3.164), M and θ are independent variables.

Substituting (3.163) and (3.164) into (3.162), we get

$$\frac{dx}{dr} = \cot(\theta + v) = \cot v_0 - \frac{1}{\sin^2 v_0} \left[\theta + \left(\frac{dv}{dM} \right)_0 (M - M_0) \right] \quad (3.165)$$

Now the improved solution can be expressed as

$$\begin{cases} \frac{M - M_0}{M_0} = \frac{F(\tau)}{\sqrt{2Br}} \\ \theta = \frac{BF(\tau)}{\sqrt{2Br}} \end{cases} \quad (3.166)$$

It should be noted that (3.166) is different from (3.157) and (3.161).

Substituting (3.166) into (3.165), we have

$$\frac{dx}{dr} = B - (1 + B^2) \left[\frac{BF(\tau)}{\sqrt{2Br}} + \left(\frac{dv}{dM} \right)_0 \frac{M_0 F(\tau)}{\sqrt{2Br}} \right] \quad (3.167)$$

Rearranging (3.167), we get

$$\frac{dx}{dr} = B - \frac{1}{2} k F(\tau) r^{-\frac{1}{2}} \quad (3.168)$$

where

$$k = (2B)^{\frac{1}{2}} (1 + B^2) \left[1 + \frac{M_0}{B} \left(\frac{dv}{dM} \right)_{M=M_0} \right]$$

By integration of (3.168), noting $\tau = \text{constant}$ on the characteristic curve, we get

$$x = Br - kF(\tau)r^{\frac{1}{2}} + \tau \quad (3.169)$$

(3.169) is the equation of the characteristic curves .

Next, we will find the equation of the shock-shock trace.

A function $G(r)$ is introduced(Wang, 1984), and the shock-shock curve can be expressed as

$$x = Br - G(r) \quad (3.170)$$

In order to determine the function $G(r)$, we differentiate (3.170) with respect to r , and thus we get

$$\frac{dx}{dr} = B - G'(r) \quad (3.171)$$

Since the discontinuity of the shock-shock is weak, the direction of the shock-shock can be regarded as the average direction of the characteristics ahead of and behind the discontinuity.

From (3.168), we get the direction of the shock-shock as

$$\frac{dx}{dr} = \frac{1}{2} \left[B + \left(B - \frac{1}{2} kF(\tau)r^{-\frac{1}{2}} \right) \right] \quad (3.172)$$

By comparison of (3.172) with (3.171), we get

$$G'(r) = \frac{1}{4} kF(\tau)r^{-\frac{1}{2}} \quad (3.173)$$

By comparison of (3.169) with (3.170), we get

$$G(r) = kF(\tau)r^{\frac{1}{2}} - \tau \quad (3.174)$$

Taking the derivative of (3.174) with respect to r , and comparing (3.173), we get

$$\frac{1}{4} kF(\tau) \frac{1}{\sqrt{r}} \frac{dr}{d\tau} + kF'(\tau)\sqrt{r} - 1 = 0 \quad (3.175)$$

Rearranging (3.175), we get

$$d\left(\frac{1}{2} kF^2(\tau) \cdot \sqrt{r}\right) = F(\tau)d\tau \quad (3.176)$$

Taking the integral of (3.176) from 0 to τ , we get

$$r = \left[\frac{2}{kF^2(\tau)} \int_0^\tau F(\tau')d\tau' \right]^2 \quad (3.177)$$

Substituting (3.177) into (3.174), we can obtain the expression for $G(r)$ and then can obtain the expression for the shock-shock trace from (3.170).

3. Diffraction by slender cone

As an example, we are going to find the solution for the diffraction of a plane shock by a slender cone.

By using the above results and the method which has been used in the supersonic aerodynamics, we can obtain the solution of equation (3.145) as

$$\alpha' = -\frac{1}{2\pi} \int_0^{\text{ch}^{-1}\frac{x}{Br}} S'(x - Br\text{ch}\lambda)d\lambda \quad (3.178)$$

$$\alpha'_x = -\frac{1}{2\pi} \int_0^{\text{ch}^{-1}\frac{x}{Br}} S''(x - Br\text{ch}\lambda)d\lambda \quad (3.179)$$

$$\alpha'_{,r} = -\frac{1}{2\pi} \int_0^{\text{ch}^{-1}\frac{x}{Br}} S''(x - Br\text{ch}\lambda)(-B\text{ch}\lambda)d\lambda \quad (3.180)$$

where $\lambda = \text{ch}^{-1}\left(\frac{x - \xi}{Br}\right)$.

For the slender cone, the cross-sectional area S can be expressed as

$$S(x) = \pi r^2(x) = \pi(x \cdot \tan\theta_w)^2 = \pi\theta_w^2 x^2 \quad (3.181)$$

where θ_w is semi-angle of the cone. Taking the derivative of (3.181), we have

$$S'(x) = 2\pi\theta_w^2 x \quad (3.182)$$

$$S''(x) = 2\pi\theta_w^2 \quad (3.183)$$

Substituting (3.182) and (3.183) into (3.178), (3.179), and (3.180), respectively, we can get

$$\alpha' = x\theta_w^2 \left[\frac{\sqrt{\left(\frac{x}{Br}\right)^2 - 1}}{\frac{x}{Br}} - \text{ch}^{-1}\left(\frac{x}{Br}\right) \right] \quad (3.184)$$

$$\alpha'_x = -\theta_w^2 \text{ch}^{-1}\left(\frac{x}{Br}\right) \quad (3.185)$$

$$\alpha'_{,r} = B\theta_w^2 \sqrt{\left(\frac{x}{Br}\right)^2 - 1} \quad (3.186)$$

At $\frac{x}{Br} = 1$, that is, $x - Br = 0$

$$\begin{cases} \alpha' = 0, & \alpha'_x = 0, & \alpha'_r = 0 \\ M = M_0, \theta = 0 \end{cases} \quad (3.187)$$

At the surface of the cone,

$$\frac{x}{Br} = \frac{x}{Bx \cdot \tan \theta_w} = \frac{1}{B\theta_w} \quad (3.188)$$

$$\alpha'_x = -\theta_w^2 \operatorname{ch}^{-1}\left(\frac{1}{B\theta_w}\right) = -\theta_w^2 \ln\left(\frac{2}{B\theta_w}\right) \quad (3.189)$$

$$\alpha'_r = B\theta_w^2 \sqrt{\left(\frac{1}{B\theta_w}\right)^2 - 1} = \theta_w \left[1 - B^2 \theta_w^2\right]^{\frac{1}{2}} \quad (3.190)$$

Retaining the first order terms of (3.190), we get

$$\alpha'_r = \theta_w \quad (3.191)$$

The Mach number at the surface of the slender cone can be written as

$$\frac{M_w - M_0}{M_0} = -\alpha'_x - \frac{1}{2} \alpha'^2_r + O(\alpha'^2_x) \quad (3.192)$$

Substituting (3.189) and (3.191) into (3.192), we get

$$\frac{M_w - M_0}{M_0} = \theta_w^2 \ln\left(\frac{2}{B\theta_w}\right) - \frac{1}{2} \theta_w^2 + O\left(\theta_w^4 \ln^2 \frac{1}{\theta_w}\right) \quad (3.193)$$

Next, we are going to derive the shock-shock curve and the relation across it. First of all, we derive the expression for $F(\tau)$ as follows

$$F(\tau) = \frac{1}{2\pi} \int_0^\tau \frac{S''(\xi) d\xi}{\sqrt{\tau - \xi}} = 2\theta_w^2 \tau^{\frac{1}{2}} \quad (3.194)$$

Substituting (3.194) into (3.177), we have

$$r = \left[\frac{1}{k\theta_w^2 \tau^{\frac{3}{2}}} \right]^2 \quad (3.195)$$

Rearranging (3.195), we get

$$\tau = \frac{9k^2 \theta_w^4 r}{4} \quad (3.196)$$

Substituting (3.196) into (3.174), we get

$$G(r) = \frac{3}{4} k^2 \theta_w^4 r \quad (3.197)$$

Substituting (3.197) into (3.170), we can obtain the expression for the shock-shock trace as

$$x = Br - \frac{3}{4} k^2 \theta_w^4 r \quad (3.198)$$

Differentiating (3.198), we can obtain the shock-shock angle χ as

$$\cot\chi = \frac{dx}{dr} = B - \frac{3}{4} k^2 \theta_w^4 \quad (3.199)$$

where $B = \cot v_0$.

Substituting the expression for k into (3.199), we get

$$\cot\chi = \cot v_0 - \frac{3}{2} B(B^2 + 1)^2 \left[1 + \frac{M_0}{B} \left(\frac{dv}{dM} \right)_{M=M_0} \right]^2 \theta_w^4 \quad (3.200)$$

Substituting $F(\tau)$ into (3.166), we get θ_1 and M_1 at shock-shock as

$$\theta_1 = 3B(B^2 + 1) \left[1 + \frac{M_0}{B} \left(\frac{dv}{dM} \right)_{M=M_0} \right] \theta_w^4 \quad (3.201)$$

$$\frac{M_1 - M_0}{M_0} = 3(B^2 + 1) \left[1 + \frac{M_0}{B} \left(\frac{dv}{dM} \right)_{M=M_0} \right] \theta_w^4 \quad (3.202)$$

Up to now, we have already discussed the problems on diffraction by a thin or slender body.

§ 3.8 Internal conical diffraction

In this section, we will discuss the internal conical diffraction, that is, the internal diffraction of a plane shock along a conically contracting channel. Our purpose is to find the triple-point locus (shock-shock locus) in the case of Mach reflection.

Summarizing the previous sections in this chapter, we find that there are two ways in which the shock dynamic theory can be applied for finding the triple-point loci in the diffractions. One is to use equations (3.21) directly after making some reasonable assumptions, for example, the Mach stem may be regarded as straight and normal to the reflecting surface (Bryson, and Gross, 1961; Milton, 1971). With this condition which immediately defines the rays and noting that the shock surface function α has the same value along both the undisturbed and disturbed shocks, a set of useful, simplified equations can be established. The alternative is to use the shock-shock relations coupled with an axially-symmetric equation for local area ratio (Whitham, 1959; Setchell, 1972;

Duong, 1982; Duong, and Milton, 1985). This requires a continuous evaluation of ray direction. In this section, the first method is used as it provides simple equations which give a clear interpretation of the phenomena (Milton, 1971).

The internal diffraction of a plane shock along a conically contracting channel is shown in Fig. 3.12. Assuming, for an approximate solution that the Mach stem is straight and normal to the wall, a set of axisymmetrical equations can be derived as follows.

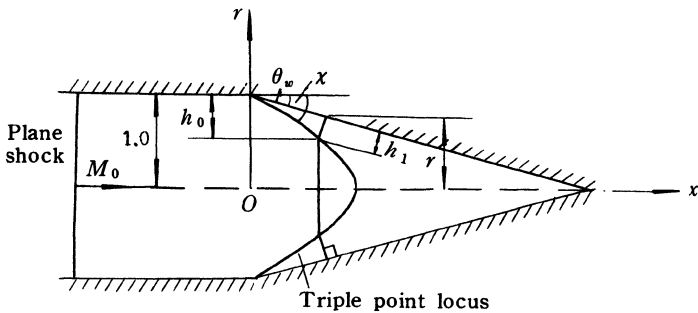


Fig. 3.12 The internal diffraction of a plane shock along a conically contracting channel

The areas of the rays of undisturbed and disturbed shock waves can be expressed as

$$\begin{cases} A_0 = 2\pi h_0 \left(1 - \frac{h_0}{2} \right) \\ A_1 = 2\pi h_1 \left(r - \frac{h_1}{2} \cos\theta \right) \end{cases} \quad (3.203)$$

where subscripts "0" and "1" denote the parameters of the undisturbed and disturbed shocks, respectively. r is the radius of the cone, which is measured from the centre line to the foot of the Mach stem. The radius of the cylinder is taken as 1. h_0 and h_1 are the distances from the wall surface to the ray. θ is the angle between the normal to the disturbed shock and x -axis, $\theta = \theta_w$.

h_0 and h_1 can be written as

$$\begin{cases} h_0 = \frac{1-r}{\sin\theta} \cdot \frac{\sin\chi}{\cos(\chi-\theta)} \\ h_1 = \frac{1-r}{\sin\theta} \cdot \frac{\sin(\chi-\theta)}{\cos(\chi-\theta)} \end{cases} \quad (3.204)$$

where χ is the angle between the triple-point locus and x -axis, which refers to χ_0 , the subscript "0" is omitted for convenience.

Substituting the equations (3.204) into the equations (3.203), the area ratio can be obtained as follows

$$\frac{A_1}{A_0} = \frac{\sin(\chi - \theta)}{\sin\chi} \left[\frac{r - \frac{(1-r)\tan(\chi-\theta)}{2}}{1 - \frac{(1-r)}{2} \frac{\tan\theta}{\sin\chi}} \right] \quad (3.205)$$

For the shock kinematics, α can be written as

$$\alpha = \frac{x}{M_0} = \frac{(1-r)\cos\chi}{M_0 \sin\theta \cdot \cos(\chi - \theta)} \quad (3.206)$$

where x is the coordinate of the triple point in the x direction (as shown in Fig. 3.13).

Differentiating with respect to r and noting that $\chi = \chi(r)$, we get

$$\frac{d\alpha}{dr} = -\frac{1}{M_0 \sin\theta} \left[\frac{\cos\chi}{\cos(\chi - \theta)} - \frac{(1-r)\sin\theta}{\cos^2(\chi - \theta)} \cdot \frac{d\chi}{dr} \right] \quad (3.207)$$

Now along the cone surface, namely direction s , we have

$$\frac{d\alpha}{ds} = \frac{1}{M_1} \quad (3.208)$$

where M_1 is the shock Mach number of the disturbed shock, which, of course, is a variable, and we have from Fig. 3.13

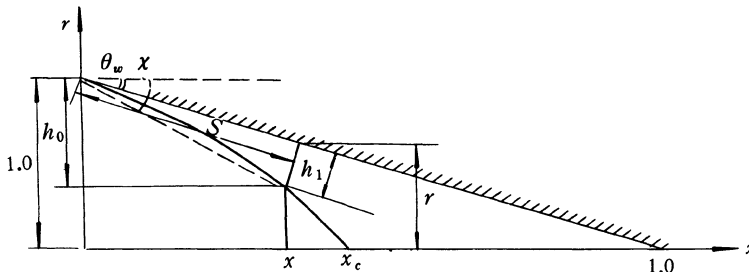


Fig. 3.13 The location of triple point

$$\frac{ds}{dr} = -\frac{1}{\sin\theta} \quad (3.209)$$

Substituting the relations (3.208) and (3.209) into (3.207), and rearranging for $\frac{d\chi}{dr}$, we obtain

$$\frac{d\chi}{dr} = \left[\frac{M_0}{M_1} - \frac{\cos\chi}{\cos(\chi-\theta)} \right] \left[\frac{\cos^2(\chi-\theta)}{(1-r)\sin\theta} \right] \quad (3.210)$$

Finally, the area-shock Mach number relationship is

$$A = A(M)$$

For strong shocks, this becomes

$$\frac{A_1}{A_0} = \left[\frac{M_0}{M_1} \right]^n \quad (3.211)$$

Summarizing the above equations, we obtain a set of shock dynamic equations for internal conical diffraction

$$\begin{cases} \frac{A_1}{A_0} = \frac{\sin(\chi-\theta)}{\sin\chi} \left[\frac{r - \frac{(1-r)\tan(\chi-\theta)}{2}}{1 - \frac{(1-r)}{2} \frac{\sin\theta\cos(\chi-\theta)}{\sin\chi}} \right] \\ \frac{d\chi}{dr} = \left[\frac{M_0}{M_1} - \frac{\cos\chi}{\cos(\chi-\theta)} \right] \left[\frac{\cos^2(\chi-\theta)}{(1-r)\sin\theta} \right] \\ \frac{A_1}{A_0} = \left[\frac{M_0}{M_1} \right]^n \end{cases} \quad (3.212)$$

In the equations (3.212), the area ratio A_1 / A_0 can be canceled if substituting the third expression into the first one. Thus we have two equations with two unknown χ and M_1 , and find the solutions of $\chi = \chi(r)$ and $M_1 = M_1(r)$. It is evident that the shock-shock locus is a curve. We will discuss this further in § 3.10.

§ 3.9 A set of simple, useful equations for external conical diffraction

In order to compare external and internal diffractions by a cone, a similar set of governing equations have been derived using the same assumption that the Mach stem is straight and normal to the surface of the cone (Han, Milton, and Takayama, 1992).

The cross-sectional areas of the ray tube, A_0 and A_1 , can be expressed in a similar manner as the previous one.

$$\begin{cases} A_0 = 2\pi \left[r - \frac{h_0}{2} \right] h_0 = \pi r^2 \\ A_1 = 2\pi \left[r - \frac{h_1 \cos\theta}{2} \right] h_1 \end{cases} \quad (3.213)$$

where r is the radius from the centreline to the triple-point locus and h_1 and h_0 are as shown in Fig. 3.14.

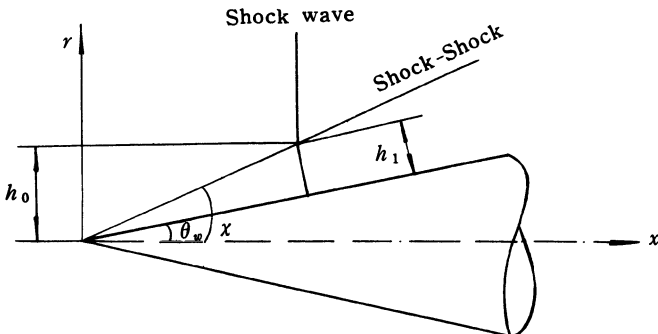


Fig. 3.14 The external diffraction by a cone in a simplified model

It should be noted that the radius of the cone, which is the same as that in § 3.8, may be used instead if preferred, thus making it consistent with the internal case and giving a set of equations more similar to it. However, the designation in Fig. 3.14, is more convenient in this case. From geometrical consideration it can be seen that

$$h_1 = \frac{r \sin(\chi - \theta)}{\sin \chi} \quad (3.214)$$

By substituting the equation (3.214) into the equation (3.213), the area ratio can be found as

$$\frac{A_1}{A_0} = \frac{2 \sin(\chi - \theta) \sin \chi - \sin^2(\chi - \theta) \cos \theta}{\sin^2 \chi} \quad (3.215)$$

or

$$\frac{A_1}{A_0} = \frac{\sin(\chi - \theta)}{\sin \chi} \cdot \left[\frac{2 \sin \chi - \sin(\chi - \theta) \cos \theta}{\sin \chi} \right] \quad (3.216)$$

It can be immediately seen that, unlike the equation (3.205), the area ratio of the equation (3.216) is independent of r .

Next, as in the internal case, the second expression of the equation (3.21) for the undisturbed shock gives

$$\alpha = \frac{x}{M_0} = \frac{r}{M_0 \tan \chi} \quad (3.217)$$

The derivative of α with respect to r is

$$\frac{d\alpha}{dr} = \frac{\sin\chi \cos\chi - r \frac{d\chi}{dr}}{M_0 \sin^2 \chi} \quad (3.218)$$

In a similar manner, for the disturbed shock, we have

$$\frac{d\alpha}{ds} = \frac{1}{M_1} \quad (3.219)$$

Here s is the distance between the Mach stem and the tip of the cone, along the direction coincident with that of the rays. The equation (3.219) can be rewritten as

$$\frac{d\alpha}{dr} = \frac{1}{M_1} \frac{ds}{dr} \quad (3.220)$$

From Fig. 3.14, we have

$$s = \frac{r \cos(\chi - \theta)}{\sin\chi} \quad (3.221)$$

Taking the derivative of s with respect to r , substituting into the equation (3.220) and rearranging give the change in triple-point locus angle with radius

$$\frac{d\chi}{dr} = \frac{\sin\chi \cdot \cos(\chi - \theta) \left[\frac{\cos\chi}{\cos(\chi - \theta)} - \frac{M_0}{M_1} \right]}{r \left[1 - \frac{M_0}{M_1} \cos\theta \right]} \quad (3.222)$$

Summarizing the above equations and considering the $A - M$ relation for strong shocks, a set of shock dynamic equations for external conical diffraction can be obtained

$$\begin{cases} \frac{A_1}{A_0} = \frac{\sin(\chi - \theta)}{\sin\chi} \left[\frac{2\sin\chi - \sin(\chi - \theta)\cos\theta}{\sin\chi} \right] \\ \frac{d\chi}{dr} = \frac{\sin\chi \left[\cos\chi - \frac{M_0}{M_1} \cos(\chi - \theta) \right]}{r \left[1 - \frac{M_0}{M_1} \cos\theta \right]} \\ \frac{A_1}{A_0} = \left[\frac{M_0}{M_1} \right]^n \end{cases} \quad (3.223)$$

The equations (3.223) are similar to the equations (3.212). Next, we will discuss the set of equations(3.223).

Substituting the third expression of (3.223) into the first one, we get

$$\left[\frac{M_0}{M_1} \right] = \left\{ \frac{\sin(\chi - \theta)}{\sin \chi} \left[\frac{2\sin \chi - \sin(\chi - \theta)\cos \theta}{\sin \chi} \right] \right\}^{\frac{1}{n}} = f_1(\chi, \theta) \quad (3.224)$$

Using this in conjunction with the second expression of (3.223) gives

$$\frac{d\chi}{dr} = \frac{\sin \chi [\cos \chi - f_1(\chi, \theta) \cos(\chi - \theta)]}{r \left[1 - \frac{M_0}{M_1} \cos \theta \right]} \quad (3.225)$$

In the equation (3.225), noting that $M_0 < M_1$, it is evident that if $\theta (= \theta_w)$ > 0 , then

$$\left[1 - \frac{M_0}{M_1} \cos \theta \right] > 0 \quad (3.226)$$

Now if θ_w is given and it is assumed that $d\chi / dr = 0$, the following can be obtained for $r \neq 0$

$$\cos \chi - f_1(\chi) \cos(\chi - \theta) = 0 \quad (3.227)$$

Solving the equation (3.227) gives

$$\chi = \text{constant} \quad \text{everywhere} \quad (3.228)$$

There are three possible cases for the condition that $d\chi / dr = 0$, these being that χ is a maximum, minimum or constant. The first two will occur only at particular radial positions.

Therefore, in the present case, χ is independent of r and the triple-point locus must be straight.

For $\chi = \text{constant}$, the second expression of (3.223) can be rewritten as

$$\frac{M_1}{M_0} = \frac{\cos(\chi - \theta)}{\cos \chi} \quad (3.229)$$

The set of equations (3.223) can be simplified to

$$\begin{cases} \frac{A_1}{A_0} = \frac{\sin(\chi - \theta)}{\sin \chi} \cdot \left[\frac{2\sin \chi - \sin(\chi - \theta)\cos \theta}{\sin \chi} \right] \\ \frac{M_1}{M_0} = \frac{\cos(\chi - \theta)}{\cos \chi} \\ \frac{A_1}{A_0} = \left[\frac{M_0}{M_1} \right]^n \end{cases} \quad (3.230)$$

This is a modified set of axisymmetric equations for the external diffraction

by a cone.

The corresponding set of the two-dimensional equations for Mach reflection of a plane shock by a wedge are as follows

$$\begin{cases} \frac{A_1}{A_0} = \frac{\sin(\chi - \theta)}{\sin\chi} \\ \frac{M_1}{M_0} = \frac{\cos(\chi - \theta)}{\cos\chi} \\ \left(\frac{A_1}{A_0} \right)^n = \left[\frac{M_0}{M_1} \right]^n \end{cases} \quad (3.231)$$

It follows from the above two sets of equations that the difference between the wedge and the conical Mach reflection is due only to one factor in the area change relation

$$\left[\frac{2\sin\chi - \sin(\chi - \theta)\cos\theta}{\sin\chi} \right]$$

By using the equations (3.86), (3.87) and (3.88), as an example, taking the half cone angle to be $\theta_w = 28.8^\circ$, Whitham calculated that the triple-point locus angle $\chi = 35.8^\circ$ with the average ratio of shock Mach numbers across the reflection being $M_1 / M_0 = 1.208$.

Using the set of equations (3.230) for the same example, the equivalent values obtained are $\chi = 35.5^\circ$ and $R = M_1 / M_0 = 1.220$. The differences are small with relative differences being $\Delta\chi / \chi = 0.85\%$ and $\Delta R / R = 0.98\%$. If the two-dimensional equations (3.231) are used instead, the values become $\chi = 39.7^\circ$, $R = M_1 / M_0 = 1.28$ with relative errors of $\Delta\chi / \chi = 10.8\%$ and $\Delta R / R = 5.3\%$. This illustrates that the equations (3.230) are a set of simple, accurate equations for calculating the external Mach reflection of a plane shock by a cone.

In the general case, the strong shock relation $\left(\frac{M_0}{M_1} \right)^n = \left(\frac{A_1}{A_0} \right)$ cannot be used, but the derivation is otherwise identical although more complex than that mentioned above and the conclusion that the triple-point locus is straight is still valid. In order to calculate the angle χ and the shock Mach number of Mach stem, M_1 , in the general case, all that is required is the use of a suitable $M-A$ relationship in place of $(M_0 / M_1)^n = (A_1 / A_0)$.

As mentioned already, the equations (3.212) and (3.230) are suitable for the axially-symmetrical internal and external conical diffractions, respectively, but

the relations across the shock-shock surface in the above cases are always the relations (3.231), which just correspond to relations (3.71) and (3.72). We can prove that in the vicinity of the shock-shock surface, the relations (3.212) and (3.230) approach the relation (3.231).

§ 3.10 Different behaviour of the triple-point locus of internal and external conical diffractions

1. External conical diffraction

In order to further analyse the behaviour of the triple-point locus, an examination of the way the area ratio changes when the incident shock moves forward is required.

Consider any two positions of a plane shock as it diffracts around a cone as shown in Fig. 3.15

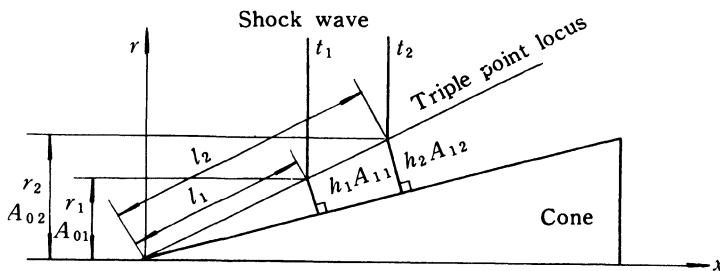


Fig. 3.15 Cross-sectional area of ray tube

At time t_1 ,

$$\frac{A_{01}}{A_{11}} = \frac{r_1^2}{2 \left[r_1 - \frac{h_1 \cos \theta}{2} \right] h_1} \quad (3.232)$$

and at time t_2 ,

$$\frac{A_{02}}{A_{12}} = \frac{r_2^2}{2 \left[r_2 - \frac{h_2 \cos \theta}{2} \right] h_2} \quad (3.233)$$

Since the triple-point locus is a straight, which has been proved in § 3.9, we have the following geometric relation

$$\frac{h_2}{h_1} = \frac{l_2}{l_1} = \frac{r_2}{r_1} = c \quad (3.234)$$

By substituting the equation (3.234) into the equation (3.233) and eliminating c , we have

$$\frac{A_{02}}{A_{12}} = \frac{r_1^2}{2 \left[r_1 - \frac{h_1 \cos \theta}{2} \right] h_1} \quad (3.235)$$

From the equations (3.235) and (3.232), we get

$$\frac{A_{01}}{A_{11}} = \frac{A_{02}}{A_{12}} = \frac{A_{0i}}{A_{1i}} = \text{constant} \quad (3.236)$$

where subscript i represents any position of the shock.

Also at any time, we have the same relation between ratio A and ratio M , that is,

$$\left[\frac{A_{0i}}{A_{1i}} \right]^{\frac{1}{n}} = \frac{M_{1i}}{M_0} \quad (3.237)$$

Hence, if θ_w and χ are given, $M_1 = \text{constant}$ at any position. This is a self-similar flow, but the behaviour of the triple-point locus of the internal conical diffraction is different from that of external conical diffraction.

2. Internal conical diffraction

By using the same method as that in the last section, with the internal set of equation, it can be shown that the triple-point locus in this case is a curve. The Mach number ratio for the reflection is obtained by substituting the third expression into the first one of the equations (3.212).

This gives

$$\frac{M_0}{M_1} = \left\{ \frac{\sin(\chi - \theta)}{\sin \chi} \left[\frac{r - \frac{(1-r) \tan(\chi - \theta)}{2 \tan \theta}}{1 - \frac{(1-r) \sin \chi}{2 \sin \theta \cos(\chi - \theta)}} \right] \right\}^{\frac{1}{n}} = f_2(\chi, \theta, r) \quad (3.238)$$

Substituting the equation (3.238) into the second expression of the equations (3.212), we get

$$\frac{d\chi}{dr} = \left[f_2(\chi, \theta, r) - \frac{\cos \chi}{\cos(\chi - \theta)} \right] \left[\frac{\cos^2(\chi - \theta)}{(1-r)\sin \theta} \right] \quad (3.239)$$

A comparison of the equation (3.239) with the equation (3.225) shows that

in the former, M_1 is a function of χ and r , but in the latter (external conical diffraction), M_1 is independent of r . Hence in the present case (that is, the equation (3.239)), if $\frac{d\chi}{dr} = 0$ and θ is given, the expression obtained is

$$\cos\chi - f_2(\chi, r)\cos(\chi - \theta) = 0 \quad (3.240)$$

From the equation (3.240), it can be seen that

$$\chi = \chi(r) \quad (3.241)$$

The relation (3.241) shows that χ is a continuous function of r . It should be noted that neither the equation (3.240) nor (3.241) is generally valid as a relation between χ and r , but is true only for the condition that $d\chi/dr = 0$. It is impossible for the function $\chi(r)$ to generally satisfy the condition $d\chi/dr = 0$, that is, χ must be a variable and the triple-point locus must be a curve. The shape of the curve and the reasons for the curvature need discussion.

The equation (3.205) provides the starting point for this discussion. In order to obtain the rule for the way the area ratio of the disturbed to undisturbed part of the shock changes with shock position, the angle χ will be assumed to be constant. The tendency for this angle to change will then be examined.

The derivative of the equation (3.205) is

$$\frac{d}{dr} \left[\frac{A_0}{A_1} \right] = - \frac{\sin\chi}{2\sin(\chi - \theta) \left[r - (1-r) \frac{\tan(\chi - \theta)}{2\tan\theta} \right]^2} < 0 \quad (3.242)$$

This means that, as the shock wave moves forward along the conical contraction channel, the ratio A_0/A_1 and hence the ratio M_1/M_0 increase with decreasing r .

To further investigate the change in A_0 and A_1 , their derivatives with respect to r can be considered separately. For A_0 , from the equation (3.203), this derivative is

$$\frac{dA_0}{dr} = - \frac{2\pi\sin\chi}{\sin\theta\cos(\chi - \theta)} \left[1 - (1-r) \frac{\sin\chi}{\sin\theta\cos(\chi - \theta)} \right] \quad (3.243)$$

In the range of $\left[1 - \frac{\sin\theta\cos(\chi - \theta)}{\sin\chi} \right] < r < 1$, that is, the whole triple-point locus, which is regarded as a straight here, we have

$$\frac{dA_0}{dr} < 0 \quad (3.244)$$

The relation (3.244) means that A_0 always increases when r decreases.

Similarly, for A_1 , the derivative is

$$\frac{dA_1}{dr} = 2\pi \left[\frac{(1-2r)}{\sin\theta} \cdot \tan(\chi - \theta) + \frac{(1-r)\tan^2(\chi - \theta)}{\sin\theta\tan\theta} \right] \quad (3.245)$$

It is evident from this that there is a transition point for the change of A_1 with r . Putting $dA_1/dr = 0$ gives

$$r_T = \frac{\tan(\chi - \theta) + \tan\theta}{\tan(\chi - \theta) + 2\tan\theta} \quad (3.246)$$

The radius r_T is designated here as the transition radius. It should be remembered that radius is measured here from the centreline to the Mach stem foot on the wall surface. We have

$$r > r_T, \quad \frac{dA_1}{dr} < 0 \quad (3.247)$$

$$r < r_T, \quad \frac{dA_1}{dr} > 0 \quad (3.248)$$

The second derivatives of A_0 and A_1 respectively with r can also be considered and the following relations can then be obtained and examined for $r > r_T$ and $r < r_T$

$$\frac{d}{dr} \left[\frac{dA_0}{dr} \right] = -2\pi \frac{\sin^2\chi}{\sin^2\theta \cos^2(\chi - \theta)} < 0 \quad (3.249)$$

$$\frac{d}{dr} \left[\frac{dA_1}{dr} \right] = -2\pi \frac{\tan(\chi - \theta)}{\sin\theta} \left[2 + \frac{\tan(\chi - \theta)}{\tan\theta} \right] < 0 \quad (3.250)$$

The relations for A_1 and A_0 , can then be summarised as follows

$$\left. \begin{array}{ll} r > r_T & r < r_T \\ \frac{dA_1}{dr} < 0 & \frac{dA_1}{dr} > 0 \\ \frac{dA_0}{dr} < 0 & \frac{dA_0}{dr} < 0 \\ \frac{d}{dr} \left[\frac{A_0}{A_1} \right] < 0 & \frac{d}{dr} \left[\frac{dA_0}{dr} \right] < 0 \quad \frac{d}{dr} \left[\frac{dA_1}{dr} \right] < 0 \end{array} \right\} \quad (3.251)$$

It follows from relations (3.251) that, if a straight triple-point locus is formed by the movement of a plane shock wave along a conical contraction channel, the ratio of the area A_0/A_1 always increases, when the radius of the cone decreases. A very important phenomenon is that A_0 always increases with the decreasing of r , but A_1 behaves differently, i.e., it increases with the de-

creasing of r when $r > r_T$ and decreases with the decreasing of r when $r < r_T$. According to the relationship (3.250),

$$\frac{d}{dr} \left[\frac{dA_1}{dr} \right] < 0$$

the more r decreases, the greater the decreasing in rate of A_1 will be. Thus, the following results can be obtained. When $r > r_T$, the area ratio A_0 / A_1 increases slowly and from the relation

$$M_1 = M_0 \left[\frac{A_0}{A_1} \right]^{\frac{1}{n}}$$

M_1 also increases slowly. When $r < r_T$, A_0 / A_1 and M_1 both increases rapidly.

Next let us discuss the change in the angle χ . In order to analyse the change in angle χ , it is necessary to use the equation (3.210). It follows from this equation that, for the whole shock-shock locus, $\frac{d\chi}{dr} < 0$, and $\frac{d\chi}{dr} \rightarrow 0$, as $r \rightarrow 1$, so in the region from $r = r_T$ to $r = 1$, the shock-shock locus approaches a straight, and the factor

$$\left[\frac{M_0}{M_1} - \frac{\cos \chi}{\cos(\chi - \theta)} \right]$$

approaches zero, that is,

$$M_1 \approx M_0 \frac{\cos(\chi - \theta)}{\cos \chi} \quad (3.252)$$

Under the condition that $r = 1$, the initial set of equations (3.212) becomes the equations (3.231). These can be used to obtain an initial value of χ_i and the initial Mach number of the disturbed shock, M_{1i} , can be expressed as

$$M_{1i} = M_0 \frac{\cos(\chi_i - \theta)}{\cos \chi_i} \quad (3.253)$$

where subscript i denotes initial values.

When $r > r_T$, M_1 increases only slowly as r reduces. That is, in this region ($1 > r > r_T$), M_1 approaches M_{1i} , χ approaches χ_i . This means that, in the above analysis, the assumption that $\chi = \text{constant}$ approximately is valid in the range from the initial point $r = 1$ to the vicinity of the transition point, T , at radius r_T .

When $r < r_T$, if χ is kept constant at a value of χ_T , which is the triple-point locus angle at transition point T , the equation (3.210) shows that $d\chi / dr < 0$ and $|d\chi / dr|$ increases with the further decrease of r . Take the following example:

$$\begin{aligned}\theta_w &= 20^\circ, & \chi = \chi_T \approx \chi_i = 34.64^\circ, \\ r = r_T &= 0.632, & \frac{d\chi}{dr} = -0.365, \\ r &= 0.600, & \frac{d\chi}{dr} = -0.389, \\ r = r_c &= 0.490, & \frac{d\chi}{dr} = -0.503.\end{aligned}$$

r_c is the radius of the cone at point c , where the triple-point locus intersects with the centreline. Therefore, $d\chi / dr < 0$ acts in such a way that it pushes the triple-point locus down, making χ increase more rapidly with the decreasing of r to form a convex curve as shown in Fig. 3.16.

Summarizing the above analysis gives the following results. In the case of internal diffraction of a plane shock moving along a conical contraction channel, the triple-point locus is a curve and there is a transition point T at radius r_T on it. Before this point when $r > r_T$, the portion of the triple-point locus lying in this region is nearly straight. After the transition point, $r < r_T$ and $x_T < x < x_c$, the portion of the triple-point locus in this region is now markedly curved. The triple-point locus as a whole is also a convex curve. The location of the transition point, x_T , can be determined by the following relation

$$x_T = 1 - [r_T + (1 - r_T)\tan(\chi_T - \theta)\tan\theta] \quad (3.254)$$

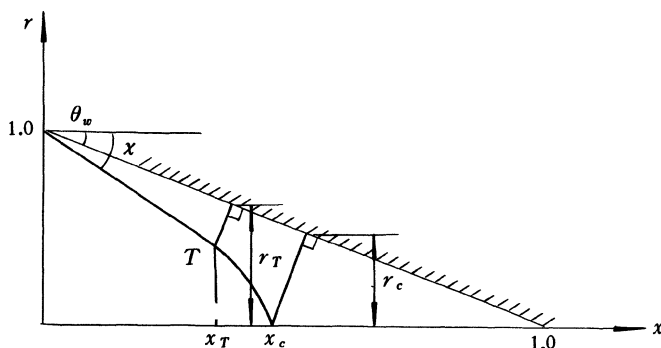


Fig. 3.16 The transition point on the triple point locus

In addition, it is also noted that the region in which the triple-point locus is markedly curved decreases with the decreasing of the half cone angle θ_w by using the equation (3.212), as shown in Table 3.1. The above analysis is also justified by the computational results obtained by Doung (1982) as shown in Table 3.2.

Table 3.1 The transition point and the intersection point of the triple-point locus with the centreline at $M_0 = 6$ ($\gamma = 1.4$)

θ_w	r_T	x_T	r_c	x_c	$(x_c - x_T)$
10 °	0.749	0.236	0.720	0.269	0.033
20 °	0.632	0.333	0.490	0.479	0.146
30 °	0.569	0.386	0.311	0.641	0.255

Table 3.2 The changes in angle χ and M_1 / M_0 ($\gamma = 1.4$)

θ_w	x_c	$\Delta\chi_1$	$\Delta\chi_2$	$\Delta(M_1 / M_0)_1$	$\Delta(M_1 / M_0)_2$
10 °	0.303	1.21 °	7.07 °	0.04	0.09
20 °	0.512	0.74 °	6.97 °	0.05	0.15
30 °	0.676	0.84 °	6.01 °	0.04	0.14

In table 3.2, the subscript 1 denotes the changes in the region of $0 < x < x_T$ and the subscript 2 denotes those in the region of $x_T < x < x_c$. If the ratios representing the relative rate of change per unit length along the x -axis in these two regions for χ and M are called R_χ and R_M , respectively, these can be expressed as

$$R_\chi = \frac{\Delta\chi_2}{(x_c - x_T)} / \frac{\Delta\chi_1}{x_T} \quad (3.255)$$

$$R_M = \frac{\Delta(M_1 / M_0)_2}{(x_c - x_T)} / \frac{\Delta(M_1 / M_0)_1}{x_T} \quad (3.256)$$

These have been evaluated for a range of angles with the results as the follows

θ_w	10 °	20 °	30 °
R_χ	41.8	21.5	10.8
R_M	16.1	6.8	5.3

The results show that the relative changes in χ and M_1 in the region of $x_T < x < x_C$ are much greater than those in the region of $x_0 (= 0) < x < x_T$. The main reason for this is that dA_1 / dr changes signs at the transition point.

The internal diffraction of a plane shock wave moving along a conically contracting channel is a more interesting and important research topic, which includes both single and multiple cones. Many researchers, for example, Russell (1967), Milton (1969, 1971), Setchell, Storm and Sturtevant (1972), Gale (1977), Duong and Milton (1985), Milton, Duong and Takayama (1985), Han, Milton and Takayama (1992) have obtained a lot of results in this research field. Certainly, further studies in the fields including external and internal diffractions will be still needed.

Chapter 4 Equations of Shock Dynamics for a Nonuniform Quiescent Gas Ahead of a Shock Wave

§ 4.1 Area relation along a tube

In this chapter, we will discuss a moving shock propagating into a nonuniform quiescent gas. To solve the kind of problems, similarly, we have to establish a set of equations of shock dynamics which include geometrical relations and area relation along a ray tube. In this section, we will derive the area relation along a tube.

In Chapter 1, we have known that there are three methods that can be used for establishing the area relation along a tube, that is, Chester's method, Chisnell's method and Whitham's method. Among them, Whitham's method is more convenient, so in this section we will extend Whitham's method from uniform quiescent gas ahead of a shock to a nonuniform quiescent gas (Catherasoo and Sturtevant, 1983).

For a uniform quiescent gas, substituting the moving shock relation into the relation of characteristic C^+ , we can obtain so-called CCW relation as

$$-\frac{dA}{A} = \frac{2M}{(M^2 - 1)K(M)} dM$$

For a nonuniform quiescent gas, the strength of a moving shock which propagates through a varying cross-sectional area tube is influenced by not only the change in area, but also the changes in the parameters ahead of the shock.

Next, we will derive the relation among the shock Mach number M , cross-sectional area A and parameters in the region ahead of the shock, such as pressure, speed of sound and ratio of specific heats.

From Chapter 1, we know that the compatible relation along the positive characteristics behind the moving shock can be expressed as

$$dp_2 + \rho_2 a_2 du_2 + \frac{\rho_2 a_2 u_2}{u_2 + a_2} \frac{dA}{A} = 0 \quad (4.1)$$

of course, the relation (4.1) is valid along the characteristic C^+ . Now let relation (4.1) be also valid along the moving shock.

The moving shock relations are given as follows

$$\begin{cases} p_2 = p_1 \left(\frac{2\gamma}{\gamma+1} M^2 - \frac{\gamma-1}{\gamma+1} \right) \\ \rho_2 = \rho_1 \frac{(\gamma+1)M^2}{(\gamma-1)M^2 + 2} \\ u_2 = \frac{2a_1}{\gamma+1} \left(M - \frac{1}{M} \right) \\ a_2 = a_1 \frac{[2\gamma M^2 - (\gamma-1)]^{\frac{1}{2}} [(\gamma-1)M^2 + 2]^{\frac{1}{2}}}{(\gamma+1)M} \end{cases} \quad (4.2)$$

It should be noted that in the case of a nonuniform gas ahead of a shock, p_1 , ρ_1 , and a_1 are variables.

Differentiating relations (4.2), we can obtain

$$\begin{aligned} dp_2 &= p_1 \frac{4\gamma}{\gamma+1} M dM + \left(\frac{2\gamma}{\gamma+1} M^2 - \frac{\gamma-1}{\gamma+1} \right) dp_1 \\ &\quad + \frac{2p_1}{(\gamma+1)^2} (M^2 - 1) d\gamma \end{aligned} \quad (4.3)$$

$$\begin{aligned} du_2 &= \frac{2a_1}{\gamma+1} \left(1 + \frac{1}{M^2} \right) dM + \frac{2}{\gamma+1} \left(M - \frac{1}{M} \right) da_1 \\ &\quad - \frac{2a_1}{(\gamma+1)^2} \left(M - \frac{1}{M} \right) d\gamma \end{aligned} \quad (4.4)$$

From (4.2), also, we have

$$\rho_2 a_2 = \frac{\rho_1 a_1 M}{\mu} \quad (4.5)$$

where

$$\mu = \left[\frac{(\gamma-1)M^2 + 2}{2\gamma M^2 - (\gamma-1)} \right]^{\frac{1}{2}}$$

and

$$\frac{\rho_2 a_2^2 u_2}{u_2 + a_2} = \frac{2\rho_1 a_1^2 \mu (M^2 - 1) [2\gamma M^2 - (\gamma-1)]}{\{2\mu(M^2 - 1) + [(\gamma-1)M^2 + 2]\}(\gamma+1)} \quad (4.6)$$

Substituting (4.3), (4.4), (4.5), (4.6) into (4.2), we can obtain the area relation along a tube with a nonuniform gas ahead of a shock as

$$edM + f d\gamma + g \frac{da_1}{a_1} + h \frac{dp_1}{p_1} = - \frac{dA}{A} \quad (4.7)$$

where

$$\begin{aligned} e &= \frac{2M}{(M^2 - 1)K(M)} \\ f &= \frac{(\mu - \gamma)}{\gamma(\gamma + 1)} \cdot g(M, \gamma) \\ g &= \frac{2\mu(M^2 - 1) + [(\gamma - 1)M^2 + 2]}{[(\gamma - 1)M^2 + 2]} = g(M, \gamma) \\ h &= \frac{1}{2\gamma(M^2 - 1)} \{2(M^2 - 1) + \mu[2\gamma M^2 - (\gamma - 1)]\} \end{aligned}$$

The relation (4.7) applies to a shock propagating through a nonuniform undisturbed medium (quiescent gas) in a solid wall tube. This relation can also be extended to ray tubes in flow field as mentioned in Chapter 2, and thus the relation (4.7) becomes the area relation of shock dynamics for the case of a nonuniform quiescent gas ahead of a shock.

§ 4.2 Two-dimensional equations in the orthogonal curvilinear coordinates

In the case of a uniform quiescent gas ahead of a shock, the shock positions can be represented by the curves

$$\alpha = a_1 t$$

where a_1 is the speed of sound in the uniform region ahead of the shock.

But in the case of a nonuniform quiescent gas ahead of a shock, we cannot use this relation, since $a_1 \neq \text{constant}$ here. The following relation can be used instead

$$\alpha = t \quad (4.8)$$

In the present case, $d\alpha$, $d\beta$ are also called increments,

$$d\alpha = dt \quad (4.9)$$

$W_s d\alpha$ is the distance along a ray between the shock positions given by α and $\alpha + d\alpha$. $Ad\beta$ is the distance along a curved shock between two rays β and $\beta + d\beta$. $W_s d\alpha$ (or $Ma_1 d\alpha$) and $Ad\beta$ are line elements. It should be noted that in the present case, a_1 is a variable, $a_1 = a_1(\alpha, \beta)$.

By using the same method as that in § 2.2, we can obtain

$$\frac{\partial \theta}{\partial \alpha} = -\frac{1}{A} \frac{\partial}{\partial \beta} (Ma_1) \quad (4.10)$$

$$\frac{\partial \theta}{\partial \beta} = \frac{1}{Ma_1} \frac{\partial A}{\partial \alpha} \quad (4.11)$$

Combining (4.10),(4.11) and (4.7), we can obtain the two-dimensional equations for a nonuniform quiescent gas ahead of a shock as follows

$$\begin{cases} \frac{\partial \theta}{\partial \alpha} = -\frac{1}{A} \frac{\partial}{\partial \beta} (M a_1) \\ \frac{\partial \theta}{\partial \beta} = \frac{1}{M a_1} \frac{\partial A}{\partial \alpha} \\ e d M + f d \gamma + g \frac{d a_1}{a_1} + h \frac{d p_1}{p_1} = -\frac{d A}{A} \quad \text{along a ray tube} \end{cases} \quad (4.12)$$

§ 4.3 Three-dimensional equations for a nonuniform quiescent gas

1. The relation between shock Mach number M and function α

In the case of three-dimensional flow, the shock positions can be expressed as

$$\alpha(x, y, z) = t \quad (4.13)$$

This relation can also be written as

$$S(x, y, z, t) = -t + \alpha(x, y, z) = 0 \quad (4.14)$$

Differentiating (4.14) with t , we get the same relation as (3.3)

$$\frac{\partial S}{\partial t} + \nabla S \cdot \vec{W}_s = 0 \quad (4.15)$$

From (4.14), we can obtain

$$\nabla S = \nabla \alpha \quad (4.16)$$

It follows from (4.14), (4.15), and (4.16) that

$$-1 + \nabla \alpha \cdot \vec{W}_s = 0 \quad (4.17)$$

In the case of a shock wave propagating into a nonuniform quiescent gas, the direction of the velocity of the moving shock is the same as the normal to the shock, that is, \vec{W}_s and $\nabla \alpha$ have the same direction, so (4.17) can be written as

$$W_s = \frac{1}{|\nabla \alpha|} \quad (4.18)$$

where

$$W_s = |\vec{W}_s|$$

or

$$Ma_1 = \frac{1}{|\nabla \alpha|} \quad (4.19)$$

Let us stop for a minute and ask ourselves, if we take $\alpha(x, y, z) = a_1(x, y, z) \cdot t$, what relation can be obtained, instead of (4.18)?

2. The unit vector for the ray direction

For a nonuniform quiescent gas ahead of a shock, we also have that rays are orthogonal to the shock surface, and thus we have

$$\vec{i} = \vec{n} = \frac{\nabla \alpha}{|\nabla \alpha|} \quad (4.20)$$

Substituting (4.19) into (4.20), we get

$$\vec{i} = Ma_1 \nabla \alpha \quad (4.21)$$

Expanding (4.21), we get

$$\vec{n} = Ma_1 \frac{\partial \alpha}{\partial x} \vec{e}_x + Ma_1 \frac{\partial \alpha}{\partial y} \vec{e}_y \quad (4.22)$$

Comparing (4.22) with

$$\vec{n} = \cos \theta \vec{e}_x + \sin \theta \vec{e}_y \quad (4.23)$$

we can obtain

$$\frac{\partial \alpha}{\partial x} = \frac{\cos \theta}{Ma_1}, \quad \frac{\partial \alpha}{\partial y} = \frac{\sin \theta}{Ma_1} \quad (4.24)$$

3. The relation between \vec{i} and A

For a nonuniform quiescent gas ahead of a shock, we can also prove that the following relation is valid by using the same method as that in Chapter 3

$$\nabla \cdot \left(\frac{\vec{i}}{A} \right) = 0 \quad (4.25)$$

Substituting (4.21) into (4.25), we get

$$\nabla \cdot \left(\frac{Ma_1}{A} \nabla \alpha \right) = 0 \quad (4.26)$$

Summarizing the equations derived in § 4.1, § 4.2 and § 4.3, we obtain a set of equations of shock dynamics for a nonuniform quiescent gas ahead of a shock in vectorial form as follows

$$\begin{cases} \nabla \cdot \left(\frac{Ma_1}{A} \nabla \alpha \right) = 0 \\ Ma_1 = \frac{1}{|\nabla \alpha|} \\ \frac{dA}{A} + edM + f d\gamma + g \frac{da_1}{a_1} + h \frac{dp_1}{p_1} = 0, \text{ along a ray tube} \end{cases} \quad (4.27)$$

§ 4.4 The various forms of differential equations

1. The equations in plane flow

$$\begin{cases} \frac{\partial}{\partial x} \left(\frac{Ma_1}{A} \frac{\partial \alpha}{\partial x} \right) + \frac{\partial}{\partial y} \left(\frac{Ma_1}{A} \frac{\partial \alpha}{\partial y} \right) = 0 \\ Ma_1 = (\alpha_x^2 + \alpha_y^2)^{-\frac{1}{2}} \\ \frac{dA}{A} + edM + f d\gamma + g \frac{da_1}{a_1} + h \frac{dp_1}{p_1} = 0, \text{ along a ray tube} \end{cases} \quad (4.28)$$

Substituting (4.24) into (4.28), we get

$$\begin{cases} \frac{\partial}{\partial x} \left(\frac{\cos \theta}{A} \right) + \frac{\partial}{\partial y} \left(\frac{\sin \theta}{A} \right) = 0 \\ \frac{\partial}{\partial x} \left(\frac{\sin \theta}{Ma_1} \right) - \frac{\partial}{\partial y} \left(\frac{\cos \theta}{Ma_1} \right) = 0 \\ \frac{dA}{A} + edM + f d\gamma + g \frac{da_1}{a_1} + h \frac{dp_1}{p_1} = 0, \text{ along a ray tube} \end{cases} \quad (4.29)$$

and from (4.12), we have

$$\begin{cases} \frac{\partial \theta}{\partial \alpha} = -\frac{1}{A} \frac{\partial}{\partial \beta} (Ma_1) \\ \frac{\partial \theta}{\partial \beta} = \frac{1}{Ma_1} \frac{\partial A}{\partial \alpha} \\ \frac{dA}{A} + edM + f d\gamma + g \frac{da_1}{a_1} + h \frac{dp_1}{p_1} = 0, \text{ along a ray tube} \end{cases} \quad (4.30)$$

2. Three-dimensional equations

The equations (4.27) can be written in two forms, that is, the equations are denoted either by the function $\alpha(x, y, z)$ or by the shock Mach number, M , and the shock angles, θ_1 , θ_2 , and θ_3 .

$$\begin{cases} \frac{\partial}{\partial x} \left(\frac{Ma_1}{A} \alpha_x \right) + \frac{\partial}{\partial y} \left(\frac{Ma_1}{A} \alpha_y \right) + \frac{\partial}{\partial z} \left(\frac{Ma_1}{A} \alpha_z \right) = 0 \\ Ma_1 = (\alpha_x^2 + \alpha_y^2 + \alpha_z^2)^{-\frac{1}{2}} \\ \frac{dA}{A} + edM + f d\gamma + g \frac{da_1}{a_1} + h \frac{dp_1}{p_1} = 0, \text{ along a ray tube} \end{cases} \quad (4.31)$$

Next, we derive the relation between α , a_1 , M , and θ_i ($i = 1, 2$, and 3).

From (4.21), we have

$$\vec{n} = Ma_1 \left(\frac{\partial \alpha}{\partial x} \vec{e}_x + \frac{\partial \alpha}{\partial y} \vec{e}_y + \frac{\partial \alpha}{\partial z} \vec{e}_z \right) \quad (4.32)$$

The unit vector \vec{n} can also be expressed as

$$\vec{n} = \cos \theta_1 \vec{e}_x + \cos \theta_2 \vec{e}_y + \cos \theta_3 \vec{e}_z \quad (4.33)$$

Comparing (4.32) with (4.33), we get

$$\frac{\partial \alpha}{\partial x} = \frac{\cos \theta_1}{Ma_1}, \quad \frac{\partial \alpha}{\partial y} = \frac{\cos \theta_2}{Ma_1}, \quad \frac{\partial \alpha}{\partial z} = \frac{\cos \theta_3}{Ma_1} \quad (4.34)$$

where θ_1 , θ_2 , and θ_3 are the angles between the normal to the shock surface and x , y , z axes, respectively.

Substituting (4.34) into the first expression of (4.31) and considering

$$\frac{\partial}{\partial x} \left(\frac{\partial}{\partial y} \right) = \frac{\partial}{\partial y} \left(\frac{\partial}{\partial x} \right) \quad \text{and} \quad \frac{\partial}{\partial y} \left(\frac{\partial}{\partial z} \right) = \frac{\partial}{\partial z} \left(\frac{\partial}{\partial y} \right),$$

we can obtain the three-dimensional equations denoted by the shock Mach number M and the angle θ_i ($i = 1, 2, 3$) as

$$\begin{cases} \frac{\partial}{\partial x} \left(\frac{\cos \theta_1}{A} \right) + \frac{\partial}{\partial y} \left(\frac{\cos \theta_2}{A} \right) + \frac{\partial}{\partial z} \left(\frac{\cos \theta_3}{A} \right) = 0 \\ \frac{\partial}{\partial x} \left(\frac{\cos \theta_2}{Ma_1} \right) - \frac{\partial}{\partial y} \left(\frac{\cos \theta_1}{Ma_1} \right) = 0 \\ \frac{\partial}{\partial y} \left(\frac{\cos \theta_3}{Ma_1} \right) - \frac{\partial}{\partial z} \left(\frac{\cos \theta_2}{Ma_1} \right) = 0 \\ \cos^2 \theta_1 + \cos^2 \theta_2 + \cos^2 \theta_3 = 1 \\ \frac{dA}{A} + edM + f d\gamma + g \frac{da_1}{a_1} + h \frac{dp_1}{p_1} = 0, \text{ along a ray tube} \end{cases} \quad (4.35)$$

In all of the above equations in this chapter, the parameters ahead of the shock, such as p_1 , a_1 , γ , are given, so we have five unknown variables, M , θ_1 ,

θ_2 , θ_3 and A .

Substituting the fifth expression into the first one, we can eliminate the cross-sectional area A . Considering the fourth expression, we can obtain three equations with three unknown variables, M , θ_1 , θ_2 (or θ_3).

It should be noted that the area relation

$$\frac{dA}{A} + e dM + f d\gamma + g \frac{da_1}{a_1} + h \frac{dp_1}{p_1} = 0$$

is valid along the characteristic C^+ or along the direction of shock motion, that is, along a ray for a quiescent gas ahead of a shock. dM , dp_1 ... are the changes along the ray tube. So the above relation can be written as

$$-\frac{1}{A} \frac{\partial A}{\partial \alpha} = e \frac{\partial M}{\partial \alpha} + f \frac{\partial \gamma}{\partial \alpha} + g \frac{\partial a_1}{\partial \alpha} + h \frac{\partial p_1}{\partial \alpha} \quad (4.36)$$

§ 4.5 Characteristic relations

1. Characteristic relations in the orthogonal curvilinear coordinates α , β

From the equations (4.30) and (4.36), we get

$$\begin{cases} \frac{\partial \theta}{\partial \alpha} + \frac{a_1}{A} \frac{\partial M}{\partial \beta} = -\frac{M}{A} \frac{\partial a_1}{\partial \beta} \\ \frac{\partial \theta}{\partial \beta} = \frac{1}{Ma_1} \frac{\partial A}{\partial \alpha} \\ -\frac{1}{A} \frac{\partial A}{\partial \alpha} = e \frac{\partial M}{\partial \alpha} + f \frac{\partial \gamma}{\partial \alpha} + g \frac{\partial a_1}{\partial \alpha} + h \frac{\partial p_1}{\partial \alpha} \end{cases} \quad (4.37)$$

In the equation (4.37), substituting the third expression into the second one, we get the following equations

$$\frac{\partial \theta}{\partial \alpha} + \frac{a_1}{A} \frac{\partial M}{\partial \beta} = -\frac{M}{A} \frac{\partial a_1}{\partial \beta} \quad (4.38)$$

$$\frac{\partial \theta}{\partial \beta} + \frac{Ae}{Ma_1} \frac{\partial M}{\partial \alpha} = -\frac{A}{Ma_1} \left(\frac{h}{p_1} \frac{\partial p_1}{\partial \alpha} + \frac{g}{a_1} \frac{\partial a_1}{\partial \alpha} + f \frac{\partial \gamma}{\partial \alpha} \right) \quad (4.39)$$

Multiplying each terms of (4.39) by c_1 , then adding (4.38) to it, we get

$$\begin{aligned} \left(\frac{\partial \theta}{\partial \alpha} + c_1 \frac{\partial \theta}{\partial \beta} \right) + \frac{c_1 Ae}{Ma_1} \frac{\partial M}{\partial \alpha} + \frac{a_1}{A} \frac{\partial M}{\partial \beta} &= -\frac{M}{A} \frac{\partial a_1}{\partial \beta} \\ -\frac{c_1 A}{Ma_1} \left(\frac{h}{p_1} \frac{\partial p_1}{\partial \alpha} + \frac{g}{a_1} \frac{\partial a_1}{\partial \alpha} + f \frac{\partial \gamma}{\partial \alpha} \right) \end{aligned} \quad (4.40)$$

The second and third terms of the left hand side in (4.40) can be written as

$$\frac{c_1 A e}{M a_1} \frac{\partial M}{\partial \alpha} + \frac{a_1}{A} \frac{\partial M}{\partial \beta} = \omega(M) \left(\frac{\partial M}{\partial \alpha} + c_1 \frac{\partial M}{\partial \beta} \right) \quad (4.41)$$

From (4.41), we can obtain

$$\omega(M) = \frac{c_1 A e}{M a_1} \quad (4.42)$$

$$\frac{M a_1^2}{c_1 A^2 e} = c_1 \quad (4.43)$$

(4.43) can be rewritten as

$$c_1 = \frac{a_1}{A} \sqrt{\frac{M}{e}} = \frac{a_1}{A} \left[\frac{(M^2 - 1)K(M)}{2} \right]^{\frac{1}{2}} \quad (4.44)$$

Substituting (4.44) into (4.42), we get

$$\omega(M) = \left[\frac{2}{(M^2 - 1)K(M)} \right]^{\frac{1}{2}} \quad (4.45)$$

Considering (4.41), the equation (4.40) can be rewritten as

$$\begin{aligned} \left(\frac{\partial \theta}{\partial \alpha} + c_1 \frac{\partial \theta}{\partial \beta} \right) + \omega(M) \left(\frac{\partial M}{\partial \alpha} + c_1 \frac{\partial M}{\partial \beta} \right) &= - \frac{M}{A} \frac{\partial a_1}{\partial \beta} \\ - \frac{c_1 A}{M a_1} \left(\frac{h}{p_1} \frac{\partial p_1}{\partial \alpha} + \frac{g}{a_1} \frac{\partial a_1}{\partial \alpha} + f \frac{\partial \gamma}{\partial \alpha} \right) \end{aligned} \quad (4.46)$$

or

$$\left(\frac{d\theta}{d\alpha} \right)_1 + \omega(M) \left(\frac{dM}{d\alpha} \right)_1 = -(F + c_1 G) \quad (4.47)$$

where

$$\begin{aligned} \left(\frac{d}{d\alpha} \right)_1 &= \frac{\partial}{\partial \alpha} + \frac{\partial}{\partial \beta} \frac{d\beta}{d\alpha} = \frac{\partial}{\partial \alpha} + c_1 \frac{\partial}{\partial \beta} \\ F &= \frac{M}{A} \frac{\partial a_1}{\partial \beta} \\ G &= \frac{A}{M a_1} \left(\frac{h}{p_1} \frac{\partial p_1}{\partial \alpha} + \frac{g}{a_1} \frac{\partial a_1}{\partial \alpha} + f \frac{\partial \gamma}{\partial \alpha} \right) \end{aligned}$$

Similarly, after the operation of (4.38) – (4.39) $\times c_1$, we get

$$\left(\frac{d\theta}{d\alpha}\right)_2 - \omega(M) \left(\frac{dM}{d\alpha}\right)_2 = -(F - c_1 G) \quad (4.48)$$

where

$$\left(\frac{d}{d\alpha}\right)_2 = \frac{\partial}{\partial\alpha} + \frac{\partial}{\partial\beta} \frac{d\beta}{d\alpha} = \frac{\partial}{\partial\alpha} - c_1 \frac{\partial}{\partial\beta}$$

Combining (4.47) and (4.48), we get

$$\begin{cases} \left(\frac{d\theta}{d\alpha}\right)_1 + \omega(M) \left(\frac{dM}{d\alpha}\right)_1 = -(F + c_1 G) & \text{along } \frac{d\beta}{d\alpha} = +c_1 \\ \left(\frac{d\theta}{d\alpha}\right)_2 - \omega(M) \left(\frac{dM}{d\alpha}\right)_2 = -(F - c_1 G) & \text{along } \frac{d\beta}{d\alpha} = -c_1 \end{cases} \quad (4.49)$$

The relations (4.49) can be expressed in another form according to the following expressions, that is,

$$\frac{d}{dM} \left[\int_1^M \omega(M') dM' \right] = \omega(M) \quad (4.50)$$

$$\begin{aligned} \left(\frac{d}{d\alpha}\right)_1 \int_1^M \omega(M') dM' &= \frac{d}{dM} \left[\int_1^M \omega(M') dM' \right] \left(\frac{dM}{d\alpha}\right)_1 \\ &= \omega(M) \left(\frac{dM}{d\alpha}\right)_1 \end{aligned} \quad (4.51)$$

$$\left(\frac{d}{d\alpha}\right)_2 \int_1^M \omega(M') dM' = \omega(M) \left(\frac{dM}{d\alpha}\right)_2 \quad (4.52)$$

Substituting (4.51) and (4.52) into (4.49), we get

$$\begin{cases} \left(\frac{\partial}{\partial\alpha} + c_1 \frac{\partial}{\partial\beta}\right) \left[\theta + \int_1^M \omega(M') dM' \right] = -(F + c_1 G) \\ \left(\frac{\partial}{\partial\alpha} - c_1 \frac{\partial}{\partial\beta}\right) \left[\theta - \int_1^M \omega(M') dM' \right] = -(F - c_1 G) \end{cases} \quad (4.53)$$

From (4.44) and (4.45), we have

$$\omega(M) = \frac{a_1}{Ac_1} \quad (4.54)$$

Substituting (4.54) into (4.53), we get

$$\begin{cases} \left(\frac{\partial}{\partial\alpha} + c_1 \frac{\partial}{\partial\beta}\right) \left(\theta + \int_1^M \frac{a_1 dM}{Ac_1} \right) = -(F + c_1 G) \\ \left(\frac{\partial}{\partial\alpha} - c_1 \frac{\partial}{\partial\beta}\right) \left(\theta - \int_1^M \frac{a_1 dM}{Ac_1} \right) = -(F - c_1 G) \end{cases} \quad (4.55)$$

We can make the comparison of (4.55) with (2.20) to see the difference between the cases of the uniform and nonuniform quiescent gases ahead of shocks.

The speed of the disturbance wave propagating along the shock front is expressed as

$$W_d = \frac{Ad\beta}{dt} = \frac{Ad\beta}{d\alpha} = Ac_1 \quad (\text{for upward wave}) \quad (4.56)$$

Substituting (4.44) into (4.56), we get

$$W_d = a_1 \left[\frac{(M^2 - 1)K(M)}{2} \right]^{\frac{1}{2}} \quad (4.57)$$

The relation (4.57) is the same as (2.47) in form, while the difference is that a_1 in (4.57) is a variable, and a_1 in (2.47) is a constant.

2. Characteristic relations in rectangular coordinates x, y

In order to derive the characteristic relations in rectangular coordinates, it is necessary to use coordinates x, y to describe the area relation (4.36).

Along a ray ($\beta = \text{constant}$), we have

$$\begin{cases} x = x(\alpha) \\ y = y(\alpha) \end{cases} \quad (4.58)$$

Expanding (4.36), we have

$$\begin{aligned} & \frac{1}{A} \left(\frac{\partial A}{\partial x} \frac{dx}{d\alpha} + \frac{\partial A}{\partial y} \frac{dy}{d\alpha} \right) + e \left(\frac{\partial M}{\partial x} \frac{dx}{d\alpha} + \frac{\partial M}{\partial y} \frac{dy}{d\alpha} \right) \\ & + f \left(\frac{\partial \gamma}{\partial x} \frac{dx}{d\alpha} + \frac{\partial \gamma}{\partial y} \frac{dy}{d\alpha} \right) + \frac{g}{a_1} \left(\frac{\partial a_1}{\partial x} \frac{dx}{d\alpha} + \frac{\partial a_1}{\partial y} \frac{dy}{d\alpha} \right) \\ & + \frac{h}{p_1} \left(\frac{\partial p_1}{\partial x} \frac{dx}{d\alpha} + \frac{\partial p_1}{\partial y} \frac{dy}{d\alpha} \right) = 0 \end{aligned} \quad (4.59)$$

Rearranging (4.59), we get

$$\begin{aligned} & \left(\frac{1}{A} \frac{\partial A}{\partial x} + e \frac{\partial M}{\partial x} + f \frac{\partial \gamma}{\partial x} + \frac{g}{a_1} \frac{\partial a_1}{\partial x} + \frac{h}{p_1} \frac{\partial p_1}{\partial x} \right) \\ & + \frac{dy}{dx} \left(\frac{1}{A} \frac{\partial A}{\partial y} + e \frac{\partial M}{\partial y} + f \frac{\partial \gamma}{\partial y} + \frac{g}{a_1} \frac{\partial a_1}{\partial y} + \frac{h}{p_1} \frac{\partial p_1}{\partial y} \right) = 0 \end{aligned} \quad (4.60)$$

In (4.60), $\frac{dy}{dx}$ is the slope of the tangent to the ray, so

$$\frac{dy}{dx} = \tan \theta \quad (4.61)$$

Substituting (4.61) into (4.60) and rearranging, we get

$$\begin{aligned}
& \frac{1}{A} \frac{\partial A}{\partial x} + \tan\theta \frac{1}{A} \frac{\partial A}{\partial y} \\
&= - \left(e \frac{\partial M}{\partial x} + f \frac{\partial \gamma}{\partial x} + \frac{g}{a_1} \frac{\partial a_1}{\partial x} + \frac{h}{p_1} \frac{\partial p_1}{\partial x} \right) \\
&\quad - \tan\theta \left(e \frac{\partial M}{\partial y} + f \frac{\partial \gamma}{\partial y} + \frac{g}{a_1} \frac{\partial a_1}{\partial y} + \frac{h}{p_1} \frac{\partial p_1}{\partial y} \right)
\end{aligned} \tag{4.62}$$

Now we can derive the characteristic relations from the following equations

$$\begin{cases}
\frac{\partial}{\partial x} \left(\frac{\cos\theta}{A} \right) + \frac{\partial}{\partial y} \left(\frac{\sin\theta}{A} \right) = 0 \\
\frac{\partial}{\partial x} \left(\frac{\sin\theta}{Ma_1} \right) - \frac{\partial}{\partial y} \left(\frac{\cos\theta}{Ma_1} \right) = 0 \\
-\frac{1}{A} \left(\frac{\partial A}{\partial x} + \tan\theta \frac{\partial A}{\partial y} \right) = \left(e \frac{\partial M}{\partial x} + f \frac{\partial \gamma}{\partial x} + \frac{g}{a_1} \frac{\partial a_1}{\partial x} + \frac{h}{p_1} \frac{\partial p_1}{\partial x} \right) \\
+ \tan\theta \left(e \frac{\partial M}{\partial y} + f \frac{\partial \gamma}{\partial y} + \frac{g}{a_1} \frac{\partial a_1}{\partial y} + \frac{h}{p_1} \frac{\partial p_1}{\partial y} \right)
\end{cases} \tag{4.63}$$

Expanding the first expression of (4.63), we get

$$-\frac{1}{A} \left(\frac{\partial A}{\partial x} + \tan\theta \frac{\partial A}{\partial y} \right) = \tan\theta \frac{\partial \theta}{\partial x} - \frac{\partial \theta}{\partial y} \tag{4.64}$$

Substituting the third expression of (4.63) into (4.64), we get

$$\begin{aligned}
\tan\theta \frac{\partial \theta}{\partial x} - \frac{\partial \theta}{\partial y} &= \left(e \frac{\partial M}{\partial x} + f \frac{\partial \gamma}{\partial x} + \frac{g}{a_1} \frac{\partial a_1}{\partial x} + \frac{h}{p_1} \frac{\partial p_1}{\partial x} \right) \\
&\quad + \tan\theta \left(e \frac{\partial M}{\partial y} + f \frac{\partial \gamma}{\partial y} + \frac{g}{a_1} \frac{\partial a_1}{\partial y} + \frac{h}{p_1} \frac{\partial p_1}{\partial y} \right)
\end{aligned} \tag{4.65}$$

Expanding the second expression of (4.63) and combining (4.65), we have the following equations

$$\cos\theta \frac{\partial \theta}{\partial x} + \sin\theta \frac{\partial \theta}{\partial y} - \frac{\sin\theta}{M} \frac{\partial M}{\partial x} + \frac{\cos\theta}{M} \frac{\partial M}{\partial y} = \frac{\sin\theta}{a_1} \frac{\partial a_1}{\partial x} - \frac{\cos\theta}{a_1} \frac{\partial a_1}{\partial y} \tag{4.66}$$

$$\begin{aligned}
\sin\theta \frac{\partial \theta}{\partial x} - \cos\theta \frac{\partial \theta}{\partial y} - e \cos\theta \frac{\partial M}{\partial x} - e \sin\theta \frac{\partial M}{\partial y} &= \frac{h}{p_1} \left(\cos\theta \frac{\partial p_1}{\partial x} + \sin\theta \frac{\partial p_1}{\partial y} \right) \\
&\quad + \frac{g}{a_1} \left(\cos\theta \frac{\partial a_1}{\partial x} + \sin\theta \frac{\partial a_1}{\partial y} \right) + f \left(\cos\theta \frac{\partial \gamma}{\partial x} + \sin\theta \frac{\partial \gamma}{\partial y} \right)
\end{aligned} \tag{4.67}$$

Multiplying each of terms of (4.66) by R and then adding (4.67) to it, we get

$$\begin{aligned}
& (R \cos \theta + \sin \theta) \frac{\partial \theta}{\partial x} + (R \sin \theta - \cos \theta) \frac{\partial \theta}{\partial y} - \left(\frac{R \sin \theta}{M} + e \cos \theta \right) \frac{\partial M}{\partial x} \\
& + \left(\frac{R \cos \theta}{M} - e \sin \theta \right) \frac{\partial M}{\partial y} = \left(\frac{R \sin \theta}{a_1} + \frac{g \cos \theta}{a_1} \right) \frac{\partial a_1}{\partial x} \\
& + \left(\frac{g \sin \theta}{a_1} - \frac{R \cos \theta}{a_1} \right) \frac{\partial a_1}{\partial y} + \frac{h}{p_1} \left(\cos \theta \frac{\partial p_1}{\partial x} + \sin \theta \frac{\partial p_1}{\partial y} \right) \\
& + f \left(\cos \theta \frac{\partial \gamma}{\partial x} + \sin \theta \frac{\partial \gamma}{\partial y} \right)
\end{aligned} \tag{4.68}$$

The relation (4.68) can be written in the following form

$$\left[\frac{\partial \theta}{\partial x} + \left(\frac{dy}{dx} \right) \frac{\partial \theta}{\partial y} \right] + F_1 \left[\frac{\partial M}{\partial x} + \left(\frac{dy}{dx} \right) \frac{\partial M}{\partial y} \right] = F_2 \tag{4.69}$$

where

$$\frac{dy}{dx} = \frac{R \sin \theta - \cos \theta}{R \cos \theta + \sin \theta} = \frac{\frac{R \cos \theta}{M} - e \sin \theta}{-\frac{R \sin \theta}{M} - e \cos \theta} \tag{4.70}$$

$$F_1 = -\frac{e}{R} \frac{\left(\cos \theta + \frac{R}{Me} \sin \theta \right)}{\left(\cos \theta + \frac{1}{R} \sin \theta \right)} \tag{4.71}$$

$$\begin{aligned}
F_2 &= \left(\frac{R \cos \theta}{R \cos \theta + \sin \theta} \right) \left[\left(\tan \theta + \frac{g}{R} \right) \frac{1}{a_1} \frac{\partial a_1}{\partial x} \right. \\
&\quad + \left(\frac{g}{R} \tan \theta - 1 \right) \frac{1}{a_1} \frac{\partial a_1}{\partial y} + \frac{h}{p_1 R} \left(\frac{\partial p_1}{\partial x} + \tan \theta \frac{\partial p_1}{\partial y} \right) \\
&\quad \left. + \frac{f}{R} \left(\frac{\partial \gamma}{\partial x} + \tan \theta \frac{\partial \gamma}{\partial y} \right) \right]
\end{aligned} \tag{4.72}$$

From equation (4.70), we can find out R , that is,

$$R = \pm \sqrt{Me} \tag{4.73}$$

Substituting $R = -\sqrt{Me}$ into (4.70) and setting $\tan v = \frac{1}{\sqrt{Me}}$, we get

$$\frac{dy}{dx} = \frac{\tan \theta + \tan v}{1 - \tan \theta \tan v} = \tan(\theta + v) \tag{4.74}$$

Substituting $R = +\sqrt{Me}$ into (4.70), we get

$$\frac{dy}{dx} = \tan(\theta - v) \tag{4.75}$$

Substituting $R = \mp \sqrt{Me}$ into (4.71), we get

$$F_1 = \pm \sqrt{\frac{e}{M}} = \pm \left[\frac{2}{(M^2 - 1)K(M)} \right]^{\frac{1}{2}} = \pm \omega(M) \quad (4.76)$$

Substituting $R = \mp \sqrt{Me}$ into (4.72), we get the expression for F_2

$$\begin{aligned} F_{2(1)} &= \left(\frac{1}{1 - \tan\theta\tan\nu} \right) \left[(\tan\theta - g\tan\nu) \frac{1}{a_1} \frac{\partial a_1}{\partial x} \right. \\ &\quad + (-g\tan\theta\tan\nu - 1) \frac{1}{a_1} \frac{\partial a_1}{\partial y} - \tan\nu \frac{h}{p_1} \left(\frac{\partial p_1}{\partial x} + \tan\theta \frac{\partial p_1}{\partial y} \right) \\ &\quad \left. - \tan\nu \cdot f \left(\frac{\partial \gamma}{\partial x} + \tan\theta \frac{\partial \gamma}{\partial y} \right) \right] \end{aligned} \quad (4.77)$$

$$\begin{aligned} F_{2(2)} &= \left(\frac{1}{1 + \tan\theta\tan\nu} \right) \left[(\tan\theta + g\tan\nu) \frac{1}{a_1} \frac{\partial a_1}{\partial x} \right. \\ &\quad + (g\tan\theta\tan\nu - 1) \frac{1}{a_1} \frac{\partial a_1}{\partial y} + \tan\nu \frac{h}{p_1} \left(\frac{\partial p_1}{\partial x} + \tan\theta \frac{\partial p_1}{\partial y} \right) \\ &\quad \left. + \tan\nu \cdot f \left(\frac{\partial \gamma}{\partial x} + \tan\theta \frac{\partial \gamma}{\partial y} \right) \right] \end{aligned} \quad (4.78)$$

where the subscript (1) corresponds to $R = -\sqrt{Me}$, and the subscript (2) to $R = +\sqrt{Me}$.

Finally, we can obtain the characteristic relations in rectangular coordinates

$$\begin{cases} \left(\frac{d\theta}{dx} \right)_1 + \omega(M) \left(\frac{dM}{dx} \right)_1 = F_{2(1)} & \text{along } \left(\frac{dy}{dx} \right)_1 = \tan(\theta + \nu) \\ \left(\frac{d\theta}{dx} \right)_2 - \omega(M) \left(\frac{dM}{dx} \right)_2 = F_{2(2)} & \text{along } \left(\frac{dy}{dx} \right)_2 = \tan(\theta - \nu) \end{cases} \quad (4.79)$$

In the relations (4.79),

$$\left(\frac{d\theta}{dx} \right)_1 = \frac{\partial \theta}{\partial x} + \left(\frac{dy}{dx} \right)_1 \frac{\partial \theta}{\partial y} = \frac{\partial \theta}{\partial x} + \tan(\theta + \nu) \frac{\partial \theta}{\partial y} \quad (4.80)$$

$$\left(\frac{d\theta}{dx} \right)_2 = \frac{\partial \theta}{\partial x} + \left(\frac{dy}{dx} \right)_2 \frac{\partial \theta}{\partial y} = \frac{\partial \theta}{\partial x} + \tan(\theta - \nu) \frac{\partial \theta}{\partial y} \quad (4.81)$$

The relations (4.79) can be rewritten as

$$\begin{cases} d\theta + \omega(M)dM = F_{2(1)}dx & \text{along } \frac{dy}{dx} = \tan(\theta + \nu) \\ d\theta - \omega(M)dM = F_{2(2)}dx & \text{along } \frac{dy}{dx} = \tan(\theta - \nu) \end{cases} \quad (4.82)$$

The relations (4.49) can be rewritten as

$$\begin{cases} d\theta + \omega(M)dM = -(F + c_1 G)d\alpha & \text{along } \frac{d\beta}{d\alpha} = +c_1 \\ d\theta - \omega(M)dM = -(F - c_1 G)d\alpha & \text{along } \frac{d\beta}{d\alpha} = -c_1 \end{cases} \quad (4.83)$$

Up to now, we have explained shock dynamics for a quiescent gas of a shock wave including uniform and nonuniform cases. Starting from the next Chapter, we will discuss a shock wave propagating into a uniform flow (Chapter 5) and a nonuniform flow (Chapters 6 and 7).

Part 2 Shock Dynamics for a Moving Gas Ahead of a Shock Wave

Chapter 5 Two-Dimensional Equations For a Uniform Moving Gas Ahead of a Shock Wave

A kind of problems on shock waves propagating into moving gases is a new research area for the shock dynamics. So in the part 2 of this book, we will pay great attention to introducing and discussing the kind of problems on shock dynamics for a moving gas ahead of a shock wave, including uniform and nonuniform flows, one-dimensional case to the three-dimensional case.

Chapter 5 explains the case of a uniform flow ahead of a shock wave. Firstly the transformation of coordinates and the two-dimensional equations denoted by $\alpha(x, y)$ (Whitham, 1968), then the two-dimensional equations denoted by $M(x, y)$ and $\theta(x, y)$ (Han and Yin, 1989A), and the corresponding disturbance relations, finally, an application of regular reflection on a wedge (Han, 1991) are discussed.

Chapter 6 explains the one- and two-dimensional cases of nonuniform flows ahead of shock waves. Firstly, the one-dimensional area equation (Chestner, 1960), then the transformation of coordinates in an infinitesimal element and two-dimensional equations (Han and Yin, 1989A), finally, shock wave-vortex interaction (Han and Chow, 1991) are discussed.

Chapter 7 explains the three-dimensional case of a nonuniform flow ahead of a shock wave. Firstly, the three-dimensional equations (Han and Yin, 1989B), then the shock-shock relations (Han and Yin, 1992), finally, an interaction of a moving shock with a bow shock are discussed.

§ 5.1 Two frames of reference

In the case of a shock wave propagating into a uniform moving gas, in general, the rays are not orthogonal to the shock surfaces. In the present case, how to establish the geometrical relations and area relation is an important issue, and we will explain and derive these relations in this chapter.

In this section, we first introduce two types of frames of reference, then derive the relations of transformation between the two frames of reference.

As shown in Fig. 5.1, there are two frames of reference. One is a stationary frame of reference, which is attached to the body diffracted by the shock. In this frame of reference, the rays are not coincident with the normal to the shock, namely $\vec{i} \neq \vec{n}$ in general. The other is a moving frame of reference, which is at-

tached to the uniform moving gas ahead of the shock. In this frame of reference, the rays are orthogonal to the shock surfaces (the gas ahead of the shock is at rest), the direction of rays is consistent with that of the normal to the shock.

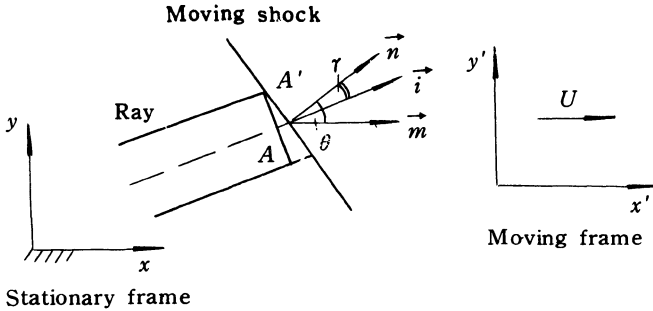


Fig. 5.1 Transformation of coordinates from moving frame into stationary frame

Let the stationary frame have coordinates x , y , t , in which the gas ahead of the shock is in motion. Let the moving frame have coordinates x' , y' , t' , in which the gas ahead of the shock is at rest.

m , U and a_1 are the flow Mach number, flow velocity, and the speed of sound in the flow field ahead of the shock, respectively. A is the cross-sectional area along a ray tube in the stationary frame, and A' is the area of shock cut out by the ray tube.

Letting the direction of the flow ahead of shock coincide with x -axis for the convenience of derivation, we have the following relations between the two kinds of frames of reference as

$$\begin{cases} x = x' + Ut' \\ y = y' \\ t = t' \end{cases} \quad (5.1)$$

The function of shock surface, $\alpha(x, y)$, can be used for describing the shock positions at any time.

In the moving frame of reference, the equation of the shock surface can be written as

$$\alpha'(x', y') = a_1 t' \quad (5.2)$$

where α' is the function of the shock surface in the moving frame.

In the stationary frame of reference, the equation of shock surface can be expressed as

$$\alpha(x,y) = a_1 t \quad (5.3)$$

From the third expression of (5.1), we get

$$\alpha'(x',y') = \alpha(x,y) \quad (5.4)$$

Substituting (5.3) into (5.1), we get

$$\begin{cases} x = x' + m\alpha(x,y) \\ y = y' \\ t = t' \end{cases} \quad (5.5)$$

We now begin to derive the differential relations between the two coordinates.

According to functional relations, we have

$$\frac{\partial}{\partial x'} = \frac{\partial}{\partial x} \frac{\partial x}{\partial x'} + \frac{\partial}{\partial y} \frac{\partial y}{\partial x'} \quad (5.6)$$

$$\frac{\partial}{\partial y'} = \frac{\partial}{\partial x} \frac{\partial x}{\partial y'} + \frac{\partial}{\partial y} \frac{\partial y}{\partial y'} \quad (5.7)$$

In order to find out $\frac{\partial x}{\partial x'}$, $\frac{\partial y}{\partial x'}$, $\frac{\partial x}{\partial y'}$ and $\frac{\partial y}{\partial y'}$, we take the derivatives of the first and second expressions of (5.5) with respect to x' , y' , respectively, and consider the flow Mach number m being constant, that is,

$$\begin{cases} \frac{\partial x}{\partial x'} = \frac{\partial x'}{\partial x'} + m\alpha_x \frac{\partial x}{\partial x'} + m\alpha_y \frac{\partial y}{\partial x'} \\ \frac{\partial y}{\partial x'} = \frac{\partial y'}{\partial x'} \\ \frac{\partial x}{\partial y'} = \frac{\partial x'}{\partial y'} + m\alpha_x \frac{\partial x}{\partial y'} + m\alpha_y \frac{\partial y}{\partial y'} \\ \frac{\partial y}{\partial y'} = \frac{\partial y'}{\partial y'} \end{cases} \quad (5.8)$$

In the moving frame of reference, x' and y' are independent variables, so $\frac{\partial y'}{\partial x'} = 0$, $\frac{\partial x'}{\partial y'} = 0$, $\frac{\partial x'}{\partial x'} = 1$, $\frac{\partial y'}{\partial y'} = 1$, and thus (5.8) can be simplified to

$$\begin{cases} \frac{\partial x}{\partial x'} = 1 + m\alpha_x \frac{\partial x}{\partial x'} \\ \frac{\partial x}{\partial y'} = m\alpha_x \frac{\partial x}{\partial y'} + m\alpha_y \\ \frac{\partial y}{\partial x'} = 0 \\ \frac{\partial y}{\partial y'} = 1 \end{cases} \quad (5.9)$$

From (5.9), we get

$$\frac{\partial x}{\partial x'} = \frac{1}{1 - m\alpha_x} \quad (5.10)$$

$$\frac{\partial x}{\partial y'} = \frac{m\alpha_y}{1 - m\alpha_x} \quad (5.11)$$

Substituting (5.9), (5.10) and (5.11) into (5.6) and (5.7), we get

$$\frac{\partial}{\partial x'} = \frac{1}{1 - m\alpha_x} \frac{\partial}{\partial x} \quad (5.12)$$

$$\frac{\partial}{\partial y'} = \frac{m\alpha_y}{1 - m\alpha_x} \frac{\partial}{\partial x} + \frac{\partial}{\partial y} \quad (5.13)$$

Substituting (5.4) into (5.12) and (5.13), we obtain

$$\frac{\partial \alpha'}{\partial x'} = \frac{\partial \dot{\alpha}}{\partial x'} = \frac{\alpha_x}{1 - m\alpha_x} \quad (5.14)$$

$$\frac{\partial \alpha'}{\partial y'} = \frac{\partial \alpha}{\partial y'} = \frac{\alpha_y}{1 - m\alpha_x} \quad (5.15)$$

Next, we are going to derive the equations of shock dynamics denoted by the function $\alpha(x, y)$.

§ 5.2 Two-dimensional equations denoted by the function $\alpha(x, y)$

In 1968, Whitham derived the two-dimensional equations denoted by the function $\alpha(x, y)$ by means of the transformation of coordinates from the moving frame into the stationary one.

1. The equations in the moving frame

In the moving frame, the gas ahead of the shock is at rest, and the rays are normal to the shock surfaces, so the equations for a uniform quiescent gas ahead of a shock which have been derived in Chapter 3 can be used in the present case, that is,

$$\begin{cases} \nabla \cdot \left(\frac{M'}{A'} \nabla' \alpha' \right) = 0 \\ M' = \frac{1}{|\nabla' \alpha'|} \\ A' = A'(M') \end{cases} \quad (5.16)$$

In two-dimensional flow, (5.16) can be written as

$$\begin{cases} \frac{\partial}{\partial x'} \left(\frac{M'}{A'} \frac{\partial \alpha'}{\partial x'} \right) + \frac{\partial}{\partial y'} \left(\frac{M'}{A'} \frac{\partial \alpha'}{\partial y'} \right) = 0 \\ M' = (\alpha_{x'}^2 + \alpha_{y'}^2)^{-\frac{1}{2}} \\ A' = A'(M') \end{cases} \quad (5.17)$$

2. The equations in the stationary frame

Substituting (5.12), (5.13), (5.14) and (5.15) into (5.17), we can obtain a set of two-dimensional equations of shock dynamics denoted by $\alpha(x, y)$ in the stationary frame as follows

$$\begin{cases} \frac{\partial}{\partial x} \left[\frac{\alpha_x + m\alpha_y^2}{A'(\alpha_x^2 + \alpha_y^2)^{\frac{1}{2}}} \right] + \frac{\partial}{\partial y} \left[\frac{\alpha_y - m\alpha_x \alpha_y}{A'(\alpha_x^2 + \alpha_y^2)^{\frac{1}{2}}} \right] = 0 \\ M' = \frac{1 - m\alpha_x}{(\alpha_x^2 + \alpha_y^2)^{\frac{1}{2}}} \\ A' = A'(M') \end{cases} \quad (5.18)$$

Comparing (5.18) with (5.17), one may ask such questions as

Can the first expression of (5.18) be written as the form of $\nabla \cdot \left(\frac{\vec{i}}{A} \right) = 0$?

What is the expression for unit vector \vec{i} ?

What is the relation between unit vectors \vec{i} and \vec{n} ?

These questions are very important for the analysis of a shock wave moving into a uniform flow ahead of it.

3. Relation $\nabla \cdot \left(\frac{\vec{i}}{A} \right) = 0$ for the case of a uniform flow ahead of a shock

In the case of a quiescent gas ahead of a shock, we have proved the relation $\nabla \cdot \left(\frac{\vec{i}}{A} \right) = 0$. But in the case of a uniform moving gas ahead of a shock, particularly, the direction of flow ahead of a shock being not consistent with the normal to the shock, we should ask: 'Is the relation $\nabla \cdot \left(\frac{\vec{i}}{A} \right) = 0$ valid?'

Now we are going to prove that this relation also applies to the case of a uniform flow ahead of a shock. We choose the volume along any ray in the flow field, which is surrounded with the surface of a ray tube and the two successive shock positions as shown in Fig. 5.2.

In Fig. 5.2, \vec{n}_1 , \vec{n}_2 , and \vec{n} are the outward normals to the shock surfaces and the surface of the ray tube, respectively. A_1 and A_2 are the cross-sectional areas at the position 1 and position 2 of the shock, respectively, S_1 and S_2 are

the areas of the shock cut out by the ray tube, respectively, S is the surface of the ray tube, and γ_1 and γ_2 are the angles between the direction of the ray and the outward normals to the shock at the positions 1 and 2, respectively.

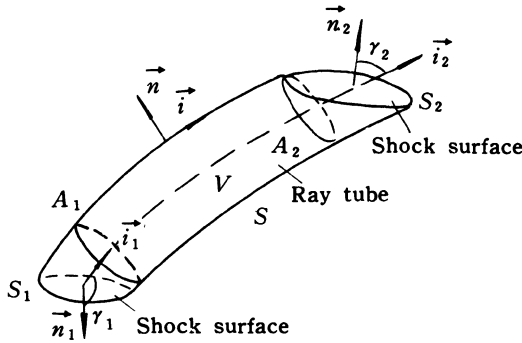


Fig. 5.2 The volume surrounded with the surface of the ray tube and the two successive shock positions

By applying the divergence theorem to the volume, we have

$$\int_V \nabla \cdot \left(\frac{\vec{i}}{A} \right) dV = \int_{S_1 + S + S_2} \frac{\vec{i} \cdot \vec{n}}{A} dS \quad (5.19)$$

where

$$\begin{aligned} \text{on } S_1, \quad & \vec{i}_1 \cdot \vec{n}_1 = \cos\gamma_1, \\ \text{on } S_2, \quad & \vec{i}_2 \cdot \vec{n}_2 = \cos\gamma_2, \\ \text{on } S, \quad & \vec{i} \cdot \vec{n} = 0. \end{aligned}$$

The relation (5.19) can be rewritten as

$$\int_V \nabla \cdot \left(\frac{\vec{i}}{A} \right) dV = \int_{S_1} \frac{\cos\gamma_1}{A} dS + \int_{S_2} \frac{\cos\gamma_2}{A} dS \quad (5.20)$$

As the diameter of the ray tube diminishes to zero, we have

$$\int_V \nabla \cdot \left(\frac{\vec{i}}{A} \right) dV = \frac{\cos\gamma_1}{A_1} S_1 + \frac{\cos\gamma_2}{A_2} S_2 \quad (5.21)$$

In Fig. 5.2, we can obtain

$$\begin{cases} A_1 = S_1 \cos(\pi - \gamma_1) \\ A_2 = S_2 \cos\gamma_2 \end{cases} \quad (5.22)$$

Substituting (5.22) into (5.21), we get

$$\int_V \nabla \cdot \left(\frac{\vec{i}}{A} \right) dV = 0 \quad (5.23)$$

Since the volume of the ray tube is taken arbitrarily, we get

$$\nabla \cdot \left(\frac{\vec{i}}{A} \right) = 0 \quad (5.24)$$

The relation (5.24) can also be written as

$$\nabla \cdot \vec{i} = \frac{1}{A} \frac{dA}{dS_r} \quad (5.25)$$

The meaning of $\nabla \cdot \vec{i}$ is the same as the explanation in Chapter 3. So in the case of a uniform moving gas ahead of a shock, similarly, (5.24) is the kinematic relation of shock dynamics.

4. The expression for unit vector \vec{i} and the relation between \vec{i} and \vec{n}

Our purpose is to find out the expression for the unit vector \vec{i} from relation (5.24). We can write the unit vector \vec{i} in the following form

$$\vec{i} = f_1(x, y) \vec{e}_x + f_2(x, y) \vec{e}_y \quad (5.26)$$

Substituting (5.26) into (5.24), we get

$$\frac{\partial}{\partial x} \left[\frac{f_1(x, y)}{A} \right] + \frac{\partial}{\partial y} \left[\frac{f_2(x, y)}{A} \right] = 0 \quad (5.27)$$

We now make the comparison of (5.27) with the first expression of (5.18) for finding the expression for \vec{i} .

The first expression of (5.18) can be rewritten as

$$\frac{\partial}{\partial x} \left[\frac{B_0}{A'} \cdot \frac{(\alpha_x + m\alpha_y^2)}{B_0(\alpha_x^2 + \alpha_y^2)^{\frac{1}{2}}} \right] + \frac{\partial}{\partial y} \left[\frac{B_0}{A'} \cdot \frac{(\alpha_y - m\alpha_x \alpha_y)}{B_0(\alpha_x^2 + \alpha_y^2)^{\frac{1}{2}}} \right] = 0 \quad (5.28)$$

Let $\frac{B_0}{A'} = \frac{1}{A}$, that is,

$$A' = AB_0 \quad (5.29)$$

Thus we can obtain

$$f_1(x, y) = \frac{\alpha_x + m\alpha_y^2}{B_0(\alpha_x^2 + \alpha_y^2)^{\frac{1}{2}}} \quad (5.30)$$

$$f_2(x, y) = \frac{\alpha_y - m\alpha_x \alpha_y}{B_0(\alpha_x^2 + \alpha_y^2)^{\frac{1}{2}}} \quad (5.31)$$

If $f_1(x, y)$ and $f_2(x, y)$ are the components of the unit vector \vec{i} in x, y directions, respectively, we must have

$$\left\{ \left[\frac{\alpha_x + m\alpha_y^2}{B_0(\alpha_x^2 + \alpha_y^2)^{\frac{1}{2}}} \right]^2 + \left[\frac{\alpha_y - m\alpha_x\alpha_y}{B_0(\alpha_x^2 + \alpha_y^2)^{\frac{1}{2}}} \right]^2 \right\}^{\frac{1}{2}} = 1 \quad (5.32)$$

From (5.32), we can obtain

$$B_0 = (1 + m^2 \alpha_y^2)^{\frac{1}{2}} \quad (5.33)$$

Substituting (5.33) into (5.30), (5.31), (5.26) and (5.29), we get

$$\vec{i} = \frac{(\alpha_x + m\alpha_y^2)\vec{e}_x + (\alpha_y - m\alpha_x\alpha_y)\vec{e}_y}{\left[(\alpha_x^2 + \alpha_y^2)(1 + m^2 \alpha_y^2) \right]^{\frac{1}{2}}} \quad (5.34)$$

$$A' = A(1 + m^2 \alpha_y^2)^{\frac{1}{2}} \quad (5.35)$$

From Fig. 5.1, we have

$$A' \cos \gamma = A \quad (5.36)$$

Next we derive the relation between \vec{i} and \vec{n} .

The unit vector of the normal to the shock can be written as

$$\vec{n} = \frac{\nabla \alpha}{|\nabla \alpha|} = \frac{\alpha_x \vec{e}_x + \alpha_y \vec{e}_y}{(\alpha_x^2 + \alpha_y^2)^{\frac{1}{2}}} \quad (5.37)$$

From (5.34) and (5.37), we have

$$\vec{i} \cdot \vec{n} = \frac{1}{(1 + m^2 \alpha_y^2)^{\frac{1}{2}}} \quad (5.38)$$

From Fig. 5.1, we have

$$\cos \gamma = \frac{1}{(1 + m^2 \alpha_y^2)^{\frac{1}{2}}} \quad (5.39)$$

§ 5.3 Two-dimensional equations denoted by shock Mach number M and shock angle θ (Han and Yin, 1989A)

1. The relations between M , θ , and α

In order to derive the two-dimensional equations directly denoted by M and θ , it is necessary to find out the relations between M , θ , and α .

We know that in the transformation of coordinates from the moving frame into the stationary one, M and θ are unchanged, that is,

$$M' = M, \quad \theta = \theta' \quad (5.40)$$

Therefore, the unit vector of the normal to the shock can be expressed as

$$\vec{n} = \cos\theta \vec{e}_x + \sin\theta \vec{e}_y \quad (5.41)$$

From the second expression of (5.18), we have

$$\vec{n} = \frac{M}{1 - m\alpha_x} \nabla \alpha = \frac{M(\alpha_x \vec{e}_x + \alpha_y \vec{e}_y)}{1 - m\alpha_x} \quad (5.42)$$

From (5.41) and (5.42), we can obtain

$$\begin{cases} \frac{\partial \alpha}{\partial x} = \frac{\cos\theta}{M + m\cos\theta} \\ \frac{\partial \alpha}{\partial y} = \frac{\sin\theta}{M + m\cos\theta} \end{cases} \quad (5.43)$$

2. The equations denoted by M and θ

Substituting (5.43) into the first expression of (5.18) and noting that $\frac{\partial}{\partial x} \left(\frac{\partial \alpha}{\partial y} \right) = \frac{\partial}{\partial y} \left(\frac{\partial \alpha}{\partial x} \right)$, we get

$$\begin{cases} \frac{\partial}{\partial x} \left[\frac{M\cos\theta + m}{(M + m\cos\theta)A'} \right] + \frac{\partial}{\partial y} \left[\frac{M\sin\theta}{(M + m\cos\theta)A'} \right] = 0 \\ \frac{\partial}{\partial x} \left[\frac{\sin\theta}{(M + m\cos\theta)} \right] - \frac{\partial}{\partial y} \left[\frac{\cos\theta}{(M + m\cos\theta)} \right] = 0 \end{cases} \quad (5.44)$$

$A' = A'(M)$

(5.44) is a set of two-dimensional equations of shock dynamics denoted by M and θ for a uniform flow ahead of a shock.

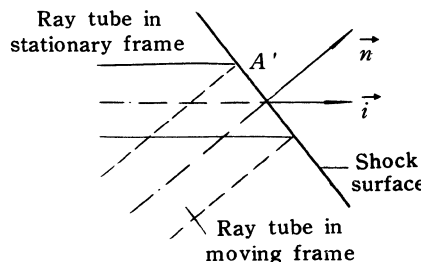


Fig. 5.3 The ray tube in the stationary frame and the moving frame

The full line refers to the ray tube in the stationary frame,
the broken line refers to the ray tube in the moving frame

It should be noted that in the third expression of (5.44), M can be used instead of M' ; A' is the area of the shock cut out by the ray tube in the stationary frame of reference, and at the same time, A' is the cross-sectional area along the ray tube in the moving frame of reference (as shown in Fig. 5.3).

3. The expression for unit vector \vec{i} and relation between \vec{i} and \vec{n}

Substituting (5.43) into (5.34), we can obtain the expression for \vec{i} denoted by M and θ as follows

$$\vec{i} = \frac{(M\cos\theta + m)\vec{e}_x + (M\sin\theta)\vec{e}_y}{(M^2 + 2Mm\cos\theta + m^2)^{\frac{1}{2}}} \quad (5.45)$$

Substituting (5.43) into (5.38), we get

$$\vec{i} \cdot \vec{n} = \frac{(M + m\cos\theta)}{(M^2 + 2Mm\cos\theta + m^2)^{\frac{1}{2}}} \quad (5.46)$$

Starting with Fig. 5.1, we can obtain the same expression for \vec{i} as (5.45) by means of another way. In Fig. 5.1, we have

$$\vec{i} = \cos(\theta - \gamma)\vec{e}_x + \sin(\theta - \gamma)\vec{e}_y \quad (5.47)$$

From (5.46), we get

$$\cos\gamma = \frac{M + m\cos\theta}{(M^2 + 2Mm\cos\theta + m^2)^{\frac{1}{2}}} \quad (5.48)$$

and

$$\sin\gamma = (1 - \cos^2\gamma)^{\frac{1}{2}} = \frac{m\sin\theta}{(M^2 + 2Mm\cos\theta + m^2)^{\frac{1}{2}}} \quad (5.49)$$

From (5.48) and (5.49), we can derive

$$\cos(\theta - \gamma) = \frac{M\cos\theta + m}{(M^2 + 2Mm\cos\theta + m^2)^{\frac{1}{2}}} \quad (5.50)$$

$$\sin(\theta - \gamma) = \frac{M\sin\theta}{(M^2 + 2Mm\cos\theta + m^2)^{\frac{1}{2}}} \quad (5.51)$$

Substituting (5.50) and (5.51) into (5.47), we can obtain the expression (5.45).

§ 5.4 The behavior of shock propagating into the uniform flow

The expression for \vec{i} , (5.45), can also be written in the following form

$$\vec{i} = \frac{\vec{M} + \vec{m}}{|\vec{M} + \vec{m}|} \quad (5.52)$$

where $\vec{M} = M\vec{n}$, $\vec{m} = m\vec{n}_f$, $M = W_s/a_1$, $\vec{n} = \cos\theta\vec{e}_x + \sin\theta\vec{e}_y$, and $\vec{n}_f = \vec{e}_x$, the unit vector of the flow ahead of the shock.

It follows from (5.52) that the direction of the ray \vec{i} is consistent with that of the resultant vector of the shock velocity relative to the uniform flow and the flow velocity in the uniform region ahead of the shock, that is,

$$\vec{i} \parallel (\vec{W}_s + \vec{V}_1) \quad (5.53)$$

$(\vec{W}_s + \vec{V}_1)$ can be expressed by their tangential and normal components as

$$\vec{W}_s + \vec{V}_1 = W_s \vec{n} + V_{1\tau} \vec{\tau} + V_{1n} \vec{n} \quad (5.54)$$

where $\vec{\tau}$ and \vec{n} are the unit vectors in the tangential and normal directions of the shock, respectively; $V_{1\tau}$ and V_{1n} are the tangential and normal components of the flow velocity ahead of the shock.

Now we make the comparison of the direction of the ray with the direction of the flow behind the shock.

The flow velocity behind the shock can be expressed as

$$\vec{V}_2 = V_{2\tau} \vec{\tau} + V_{2n} \vec{n} \quad (5.55)$$

where $V_{2\tau}$ and V_{2n} are the tangential and normal components of the flow velocity behind the shock.

We know that the tangential components of the flow velocities across the shock are equal, that is,

$$V_{2\tau} = V_{1\tau} \quad (5.56)$$

According to the moving shock relation, the normal component of the flow velocity behind the shock is expressed as

$$V_{2n} = V_{1n} + \frac{2a_1}{\gamma + 1} \left(\frac{W_s}{a_1} - \frac{a_1}{W_s} \right) \quad (5.57)$$

Substituting (5.56) and (5.57) into (5.55), we get

$$\vec{V}_2 = V_{1\tau} \vec{\tau} + V_{1n} \vec{n} + \frac{2a_1}{\gamma + 1} \left(\frac{W_s}{a_1} - \frac{a_1}{W_s} \right) \vec{n} \quad (5.58)$$

By comparing (5.58) with (5.54), it is evident that the direction of the vector $(\vec{W}_s + \vec{V}_1)$, namely, the direction of the ray is different from that of the flow velocity behind the shock, that is, the rays are not coincident with the particle paths behind the shock in the stationary frame of reference.

It follows from (5.54) and (5.58) that there are two special cases in which the direction of the ray is consistent with that of the particle path.

[case 1]: $V_{1r} = 0$, the direction of the ray is consistent with that of the flow velocity behind the shock, that is,

$$\vec{W}_s + \vec{V}_1 = (W_s + V_{1n})\vec{n} \quad (5.59)$$

$$\vec{V}_2 = \left[V_{1n} + \frac{2a_1}{\gamma + 1} \left(\frac{W_s}{a_1} - \frac{a_1}{W_s} \right) \right] \vec{n} \quad (5.60)$$

[case 2]: $\vec{V}_1 = 0$, the case corresponds to that of the quiescent gas ahead of the shock or the moving frame of reference attached to the uniform flow ahead of the shock, that is,

$$\vec{W}_s = W_s \vec{n} \quad (5.61)$$

$$\vec{V}_2 = \frac{2a_1}{\gamma + 1} \left(\frac{W_s}{a_1} - \frac{a_1}{W_s} \right) \vec{n} \quad (5.62)$$

Only in the above two cases, the ray tube can be regarded as a solid wall tube, and the area relation derived in Chapter 1 can be used to the ray tubes in the entire flow field.

Next, we will discuss another important problem in detail, that is, the shock Mach number M and shock angle θ cannot be influenced by the transformation of coordinates as mentioned already in § 5.3.

We can see that when a supersonic flow passes through a wedge, an oblique shock is attached to the wedge (as shown in Fig. 5.4). In the figure, \vec{V}_1 is the velocity of the flow ahead of the shock and \vec{V}_2 is the velocity of the flow behind the shock.

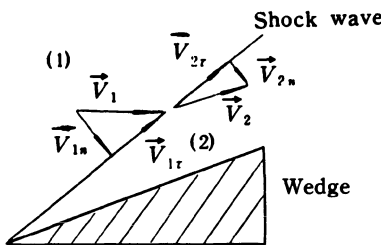


Fig. 5.4 An oblique shock is attached to the wedge

Now we make a transformation of coordinates, that is, a moving frame of reference is attached to the uniform supersonic flow ahead of the shock, which corresponds to that the entire flow field is superposed a velocity $-\vec{V}_1$, and then we have the following flow as shown in Fig. 5.5.

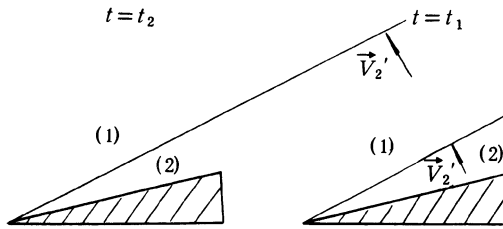


Fig. 5.5 The flow field in moving frame

In the moving frame of reference, the velocity in region (1), $\vec{V}'_1 = 0$, the velocity in region (2), \vec{V}'_2 , can be written as

$$\vec{V}'_2 = (V_{2n} - V_{1n})\vec{n} + (V_{2\tau} - V_{1\tau})\vec{\tau} \quad (5.63)$$

Since the tangential velocity is continuous, namely, $V_{1\tau} = V_{2\tau}$, we get

$$\vec{V}'_2 = (V_{2n} - V_{1n})\vec{n} \quad (5.64)$$

It follows from (5.64) that in the moving frame, the the flow behind the shock is normal to the shock front. At the same time, the wedge moves forward with the velocity $-\vec{V}_1$, and the oblique shock also moves forward.

Now we want to ask a question: Do the shock strength M and shock angle θ remain unchanged in the two cases shown in Fig. 5.4 and Fig. 5.5?

The shock which is superposed a uniform velocity $-\vec{V}_1$ does not rotate, that is, shock angle θ is unchanged.

In Fig. 5.4, the relation between the shock strength and the flow velocities can be expressed as

$$\frac{V_{2n} - V_{1n}}{a_1} = \frac{2}{\gamma + 1} \left(M - \frac{1}{M} \right) \quad (5.65)$$

It is evident that the shock cannot influence the tangential velocities so there is no tangential velocity in (5.65).

In Fig. 5.5, that is, in the moving frame of reference, we have

$$\frac{V'_2 - V'_1}{a_1} = \frac{2}{\gamma + 1} \left(M - \frac{1}{M} \right) \quad (5.66)$$

We know that $V'_1 = 0$, $V'_2 = V_{2n} - V_{1n}$, and thus (5.66) can be rewritten as

$$\frac{V_{2n} - V_{1n}}{a_1} = \frac{2}{\gamma + 1} (M - \frac{1}{M}) \quad (5.67)$$

It follows from (5.65) and (5.67) that in the two cases, the shock strengths are equal, that is, the shock speed relative to the flow field ahead of the shock remain unchanged and the shock propagates along the direction of its normal relative to the flow field ahead of it, which can be expressed as follows

$$(M)_M = (M)_s \quad (5.68)$$

$$(\vec{W})_M = (\vec{W})_s \quad (5.69)$$

where subscript M refers to the moving frame of the reference, subscript s refers to the stationary frame of reference.

In fact, the above discussion concludes that the shock wave is a normal discontinuity and it propagates always along its normal direction.

§ 5.5 Characteristic relations in the rectangular coordinates

1. The expanded two-dimensional equations of shock dynamics

Expanding the equations (5.44), we get

$$\begin{cases} C_c \frac{\partial \theta}{\partial x} + C_s \frac{\partial \theta}{\partial y} - \sin \theta \frac{\partial M}{\partial x} + \cos \theta \frac{\partial M}{\partial y} = 0 \\ (M^2 - m^2) \sin \theta \frac{\partial \theta}{\partial x} - MC_c \frac{\partial \theta}{\partial y} + (m \sin^2 \theta - BC_c e) \frac{\partial M}{\partial y} \\ \quad - (m \cos \theta \sin \theta + BC_s e) \frac{\partial M}{\partial y} = 0 \end{cases} \quad (5.70)$$

where

$$B = M + m \cos \theta, \quad C_c = M \cos \theta + m,$$

$$C_s = M \sin \theta, \quad e = \frac{2M}{(M^2 - 1)K(M)}$$

In (5.70), A' is eliminated, so there are two unknown functions M and θ in it.

2. Characteristic relations

By using the same method as that in § 4.5, we can derive the characteristic relations for the moving gas ahead of a shock.

Multiplying each of the terms of the first expression of (5.70) by Z and adding the second expression to it, we get

$$\left[ZC_c + (M^2 - m^2) \sin \theta \right] \frac{\partial \theta}{\partial x} + [ZC_s - MC_c] \frac{\partial \theta}{\partial y}$$

$$\begin{aligned}
& + \left[(m \sin^2 \theta - BC_c e) - Z \sin \theta \right] \frac{\partial M}{\partial x} \\
& + [Z \cos \theta - (m \cos \theta \cdot \sin \theta + BC_s e)] \frac{\partial M}{\partial y} = 0
\end{aligned} \tag{5.71}$$

The relation of (5.71) can be written in the following form

$$\left[\frac{\partial \theta}{\partial x} + \left(\frac{dy}{dx} \right) \frac{\partial \theta}{\partial y} \right] + F_1 \left[\frac{\partial M}{\partial x} + \left(\frac{dy}{dx} \right) \frac{\partial M}{\partial y} \right] = F_2 \tag{5.72}$$

By comparing (5.72) with (5.71), we get

$$\begin{aligned}
\frac{dy}{dx} &= \frac{Z C_s - M C_c}{Z C_c + (M^2 - m^2) \sin \theta} \\
&= \frac{Z \cos \theta - m \cos \theta \cdot \sin \theta - BC_s e}{m \sin^2 \theta - Z \sin \theta - BC_c e}
\end{aligned} \tag{5.73}$$

$$F_1 = \frac{m \sin^2 \theta - Z \sin \theta - BC_c e}{Z C_c + (M^2 - m^2) \sin \theta} \tag{5.74}$$

$$F_2 = 0 \tag{5.75}$$

From (5.73), we have

$$\begin{aligned}
& (C_s \sin \theta + C_c \cos \theta) Z^2 + [(M^2 - m^2) \cos \theta - M C_c] \sin \theta \cdot Z \\
& - m \sin \theta (C_s \sin \theta + C_c \cos \theta) Z \\
& - (BC_s e + m \cos \theta \cdot \sin \theta) (M^2 - m^2) \sin \theta \\
& + M C_c (m \sin^2 \theta - BC_c e) = 0
\end{aligned} \tag{5.76}$$

We can prove that

$$\begin{cases} C_s \sin \theta + C_c \cos \theta = B \\ (M^2 - m^2) \cos \theta - M C_c = -mB \\ C_c^2 + (M^2 - m^2) \sin^2 \theta = B^2 \end{cases} \tag{5.77}$$

Substituting (5.77) into (5.76), we get

$$Z^2 - 2m \sin \theta \cdot Z + (m^2 \sin^2 \theta - B^2 M e) = 0 \tag{5.78}$$

From (5.78), we can find out Z , as

$$Z = m \sin \theta \mp B \sqrt{M e} \tag{5.79}$$

Substituting $Z = m \sin \theta - B \sqrt{M e}$ into (5.73), we get

$$\frac{dy}{dx} = \frac{M \sin \theta \sqrt{Me} + M \cos \theta}{(M \cos \theta + m) \sqrt{Me} - M \sin \theta} \quad (5.80)$$

(5.80) can be rewritten as

$$\frac{dy}{dx} = \tan(\theta + v_1) \quad (5.81)$$

where

$$\tan v_1 = \frac{\left[\frac{1}{2}(M^2 - 1)K(M) \right]^{\frac{1}{2}} - m \sin \theta}{M + m \cos \theta}$$

Substituting $Z = m \sin \theta + B \sqrt{Me}$ into (5.73), we get

$$\frac{dy}{dx} = \tan(\theta - v_2) \quad (5.82)$$

where

$$\tan v_2 = \frac{\left[\frac{1}{2}(M^2 - 1)K(M) \right]^{\frac{1}{2}} + m \sin \theta}{M + m \cos \theta}$$

Substituting (5.79) into (5.74), we get

$$F_1 = \pm \left[\frac{2}{(M^2 - 1)K(M)} \right]^{\frac{1}{2}} = \pm \omega(M) \quad (5.83)$$

The sign “+” in (5.83) corresponds to “−” in (5.79). Thus we can obtain the characteristic relations in the two-dimensional case as follows

$$\begin{cases} \left(\frac{d\theta}{dx} \right)_1 + \omega(M) \left(\frac{dM}{dx} \right)_1 = 0 & \text{along } \left(\frac{dy}{dx} \right)_1 = \tan(\theta + v_1) \\ \left(\frac{d\theta}{dx} \right)_2 - \omega(M) \left(\frac{dM}{dx} \right)_2 = 0 & \text{along } \left(\frac{dy}{dx} \right)_2 = \tan(\theta - v_2) \end{cases} \quad (5.84)$$

From (4.50), we have

$$\frac{d}{dx} \int_1^M \omega(M') dM' = \frac{d}{dM} \left[\int_1^M \omega(M') dM' \right] \frac{dM}{dx} = \omega(M) \frac{dM}{dx} \quad (5.85)$$

$\left(\frac{d\theta}{dx} \right)_1$ and $\left(\frac{d\theta}{dx} \right)_2$ in (5.84) can be written as

$$\left(\frac{d\theta}{dx} \right)_1 = \frac{\partial \theta}{\partial x} + \left(\frac{dy}{dx} \right)_1 \frac{\partial \theta}{\partial y} \quad (5.86)$$

$$\left(\frac{d\theta}{dx} \right)_2 = \frac{\partial \theta}{\partial x} + \left(\frac{dy}{dx} \right)_2 \frac{\partial \theta}{\partial y} \quad (5.87)$$

Substituting (5.85), (5.86), (5.87), into (5.84) and noting (5.83), we get

$$\begin{cases} \left[\frac{\partial}{\partial x} + \left(\frac{dy}{dx} \right)_1 \frac{\partial}{\partial y} \right] \left[\theta + \int_1^M \omega(M) dM \right] = 0 \\ \left[\frac{\partial}{\partial x} + \left(\frac{dy}{dx} \right)_2 \frac{\partial}{\partial y} \right] \left[\theta - \int_1^M \omega(M) dM \right] = 0 \end{cases} \quad (5.88)$$

or

$$\begin{cases} \left[\frac{\partial}{\partial x} + \left(\frac{dy}{dx} \right)_1 \frac{\partial}{\partial y} \right] \left\{ \theta + \int_1^M \left[\frac{2}{(M^2 - 1)K(M)} \right]^{\frac{1}{2}} dM \right\} = 0 \\ \left[\frac{\partial}{\partial x} + \left(\frac{dy}{dx} \right)_2 \frac{\partial}{\partial y} \right] \left\{ \theta - \int_1^M \left[\frac{2}{(M^2 - 1)K(M)} \right]^{\frac{1}{2}} dM \right\} = 0 \end{cases} \quad (5.89)$$

or

$$\begin{cases} \theta + \int_1^M \omega(M) dM = \text{constant} & \text{along } \frac{dy}{dx} = \tan(\theta + v_1) \\ \theta - \int_1^M \omega(M) dM = \text{constant} & \text{along } \frac{dy}{dx} = \tan(\theta - v_2) \end{cases} \quad (5.90)$$

By comparing (5.90) with (2.44) and (2.45), we find out that the compatible relations along the characteristic curves are the same in a uniform quiescent gas and a moving gas ahead of a shock, the difference between the two cases is the expressions for characteristic curves.

Letting $m = 0$ in (5.81) and (5.82), we can obtain (2.42) and (2.43). Also, making comparison of (5.90) with (4.79), we find out that the nonuniformity of the gas ahead of a shock makes F_2 , the right hand side term of (4.79), not equal to zero, while for the uniform moving gas ahead of a shock, we have $F_2 = 0$.

Next, we will apply the above relations to make an analysis and a calculation of a reflected shock in the case of the regular reflection of a moving plane shock over a wedge.

§ 5.6 Application of theory of sound to regular reflection over a wedge

In this section we will discuss the first disturbance point on a reflected shock wave in the case of regular reflection over a wedge by using the theory of sound (Han 1991). The reflected wave is disturbed by a series of sound waves in the region behind it as shown in Fig. 5.6. The first sound wave which propagates in the uniform region 3 overtakes the reflected shock to form the first disturbance point F . The part of the reflected shock in front of this point is a plane shock, after the point, the reflected shock is getting curved. The theory of sound

can only be used to calculate the first disturbance point.

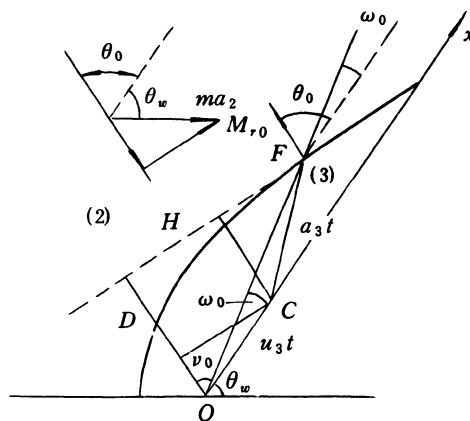


Fig. 5.6 The first disturbance point on the reflected shock

Since the first sound wave propagates in the uniform region 3, the radius of the sonic circle can be expressed as $a_3 t$, where a_3 is the speed of sound in the region 3; the distance between the origin O and C , the center of the first sonic circle, is equal to $u_3 t$, where u_3 is flow velocity in the region 3, which is in parallel with the surface of wedge.

If the incident shock Mach number M_s and the wedge angle θ_w are given, it is easy for us to find the initial reflected shock Mach number M_{r0} and the shock angle θ_0 , where θ_0 is the angle between the normal to the reflected shock and x -axis, by using the two-shock theory.

In order to determine the location of the first disturbance point F , namely, ω_0 , the angle between the line from first disturbance point to the origin O and x -axis, we first need to find the angle v_0 , which is the angle between the normal to the plane part of the reflected shock and the line FO . The angle v_0 can be expressed as

$$\tan v_0 = \frac{H}{D} \quad (5.91)$$

where

$$H = [(a_3 t)^2 - (D - u_3 t \cos \theta_0)^2]^{1/2} + u_3 t \sin \theta_0$$

$$D = [(M_{r0} + m \cos(\theta_0 + \theta_w)) a_2 t]$$

It follows from relation (5.91) that D is the distance that the first disturbance point travels along the direction normal to the plane part of the reflected shock. H is the distance in the tangential direction of the plane part of the re-

flected shock which the first disturbance point travels through.

By substituting the following moving shock relations

$$\left(\frac{a_3}{a_2}\right)^2 = \frac{[2\gamma M_{r0}^2 - (\gamma - 1)][(\gamma - 1)M_{r0}^2 + 2]}{(\gamma + 1)^2 M_{r0}^2} \quad (5.92)$$

$$\left(\frac{u_3}{a_2}\right) = \frac{m \cos(\theta_0 + \theta_w)}{\cos \theta_0} + \frac{2}{\gamma + 1} \left(M_{r0} - \frac{1}{M_{r0}}\right) \frac{1}{\cos \theta_0} \quad (5.93)$$

into relation (5.91), we can obtain

$$\tan v_0 = \frac{W_{ds} + W_\tau}{[M_{r0} + m \cos(\theta_0 + \theta_w)]a_2} \quad (5.94)$$

where $W_{ds} = a_2 \left[\frac{[(\gamma - 1)M_{r0}^2 + 2](M_{r0}^2 - 1)}{(\gamma + 1)M_{r0}^2} \right]^{\frac{1}{2}},$

$$W_\tau = a_2 \left[m \cos(\theta_0 + \theta_w) + \frac{2(M_{r0}^2 - 1)}{(\gamma + 1)M_{r0}} \right] \tan \theta_0.$$

It follows from relation (5.94) that W_{ds} is the relative speed of the first disturbance point propagating along the direction of the plane part of the reflected shock, which is just equal to Skews' results (see relation (2.99)) and W_τ is the tangential flow velocity behind the plane reflected shock (in region 3), which is equal to that ahead of the reflected shock according to the behaviour of shock. Thus we have

$$W_\tau = m a_2 \sin(\theta_0 + \theta_w) \quad (5.95)$$

Now we can determine the location of the first disturbance point, that is, the angle ω_0 by using the following relation

$$\omega_0 = \theta_0 - v_0 \quad (5.96)$$

According to the above discussion, we can obtain that in the case of the uniform flow ahead of a shock, the relative speed of the first disturbance point along the shock surface is independent of the uniform flow ahead of the shock.

§ 5.7 Formation of a reflected shock wave

As an application of the shock dynamic equations for a moving gas ahead of a shock wave, we here make a description of the reflected shock in the case of regular reflection over a wedge by using the viewpoint of shock dynamics.

The purpose is to answer the following questions:

Why is a plane reflected shock not formed? What is the law that the strength and direction of the reflected shock change? How to find the shape of the reflected shock? These questions will be answered in this section and the following sections (Han, 1991).

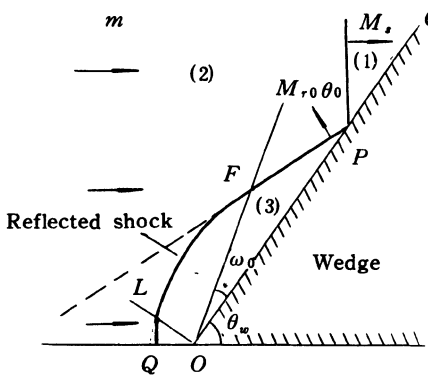


Fig. 5.7 Regular reflection of a moving shock over a wedge

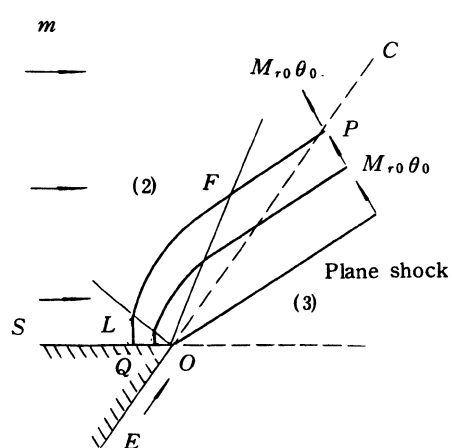


Fig. 5.8 Formation of a reflected shock

If the incident shock Mach number M_s and wedge angle θ_w are given, we can find reflected shock Mach number M_{r0} and angle θ_0 by using the oblique shock relation. The wave pattern is shown in Fig. 5.7.

The reason for the formation of such a curved reflected shock is that the reflected shock is disturbed by a sharp corner. We imagine that the formation of the curved reflected shock can be regarded as a result of the diffraction of a plane shock (as shown in Fig. 5.8), whose Mach number is M_{r0} , over a sharp corner $\angle SOE$. Extending the line CO , we can obtain the sharp corner. When the shock wave has not passed through the point O , it satisfies the boundary condition on the surface of the wall OE and is not disturbed by the sharp corner, that is, the flow behind the plane shock is in parallel with the wall OE , but when the shock wave has passed through the point O , it is disturbed and a curved reflected shock is formed, because a shock-expansion simple wave propagates on it from the point Q to the point P , such a simple wave makes the strength of the reflected shock decrease from the point P to the point Q . In the case of the regular reflection, the part of the reflected shock from the first disturbance point F to point P is straight. L is the last disturbance point, so QL is

a plane shock too. But experimental results show that QL is not a plane shock and we will discuss this problem later in section 5.9.

Summarizing the above discussion, the basic idea for the formation of the reflected shock is presented as follows:

For the regular reflection of a plane shock over a straight wedge, a curved reflected shock is formed as a result of the diffraction of a plane reflected shock around a sharp corner whose angle is constructed by both flow directions behind and ahead of the plane reflected shock.

According to this idea, the initial shock Mach number M_{r0} and the angle θ_0 of the reflected shock can be determined by means of the incident shock Mach number M_s , the angle of the wedge θ_w and the oblique shock wave relations.

§ 5.8 Basic relations for the calculation of reflected shock

In order to calculate the strength, orientation and shape of the reflected shock and analyse the disturbance wave propagating on the reflected shock in the case of the regular reflection, it is necessary for us to establish a set of governing equations, that is, two-dimensional shock dynamic equations for a uniform flow ahead of a shock. Han and Yin (1989A) derived the two-dimensional shock dynamic equations for a moving gas including a uniform flow and a nonuniform flow ahead of a shock.

If a coordinate system as shown in Fig. 5.9 (Han, 1991) is chosen, for the reflected shock wave, we have

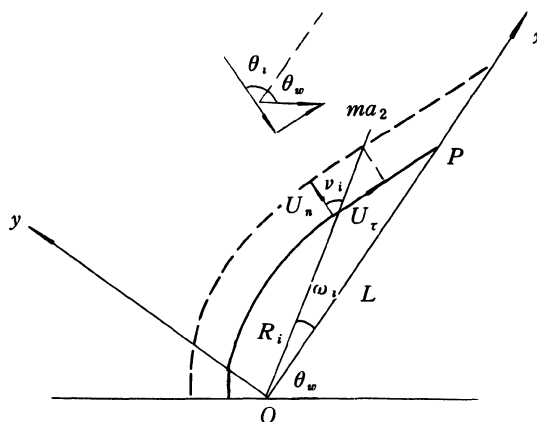


Fig. 5.9 The shape of reflected shock and the disturbance wave propagating on it

$$\begin{cases} \frac{\partial}{\partial x} \left[\frac{M_r \cos\theta + m \cos\varepsilon}{(M_r + m \cos(\theta - \varepsilon)) A'} \right] + \frac{\partial}{\partial y} \left[\frac{M_r \sin\theta + m \sin\varepsilon}{(M_r + m \cos(\theta - \varepsilon)) A'} \right] = 0 \\ \frac{\partial}{\partial x} \left[\frac{\sin\theta}{a_2(M_r + m \cos(\theta - \varepsilon))} \right] - \frac{\partial}{\partial y} \left[\frac{\cos\theta}{a_2(M_r + m \cos(\theta - \varepsilon))} \right] = 0 \\ \frac{dA'}{A'} = \frac{2M_r dM_r}{(M_r - 1)K(M_r)} \end{cases} \quad (5.97)$$

where M_r is the shock Mach number along the reflected shock, m is the flow Mach number in the uniform region which is induced by the incident shock (whose Mach number is M_s) and is in front of the reflected shock; θ and ε are the reflected shock angle and the flow angle in the uniform region with respect to x axis; a_2 is the speed of sound in the uniform region, namely, in region 2; A' is the cross-sectional area of the ray tube in a moving frame which is attached to the region 2.

From the equation (5.97), we can obtain two families of characteristics. One corresponds to the upward waves and the other corresponds to the downward waves. In the present case, as shown in Figs. 5.8 and 5.9, the disturbance wave propagating on the reflected shock is a downward simple wave. The characteristic relations can be expressed as follows

$$\begin{cases} \theta + \int_1^{M_r} \left[\frac{2}{(M_r^2 - 1)K(M_r)} \right]^{\frac{1}{2}} dM = \text{constant everywhere} \\ \theta - \int_1^{M_r} \left[\frac{2}{(M_r^2 - 1)K(M_r)} \right]^{\frac{1}{2}} dM = \text{constant along } \frac{dy}{dx} = \tan\omega \end{cases} \quad (5.98)$$

where $\omega = \theta - v$,

$$\tan v = \frac{\left[\frac{1}{2}(M_r^2 - 1)K(M_r) \right]^{\frac{1}{2}} + m \sin(\theta - \varepsilon)}{M_r + m \cos(\theta - \varepsilon)}$$

It should be noted that the maximum reflected shock Mach number is about 2.5, even if the incident shock is very strong. So the change in the shock strength is in a narrow region, and K can be regarded as a constant, or an average value of K over the range from the initial shock Mach number to the final shock Mach number can be taken. In the coordinate system as shown in Fig. 5.9, $\varepsilon = -\theta_w$, the equations (5.98) can be simplified to

$$\begin{cases} M_{ri} = \operatorname{ch}[\operatorname{ch}^{-1} M_{r0} - (\theta_i - \theta_0)(K/2)^{\frac{1}{2}}(180/\pi)], \\ \omega_i = \theta_i - v_i \\ \tan v_i = \frac{[K(M_{ri}^2 - 1)/2]^{\frac{1}{2}} + m \sin(\theta_i + \theta_w)}{M_{ri} + m \cos(\theta_i + \theta_w)} \end{cases} \quad (5.99)$$

Next we will analyse the propagation of the disturbance wave on the reflected shock surface in the case of the uniform flow ahead of it. We know that in the case of a moving shock propagating into a quiescent gas, Whitham (1957) has obtained the rate of the disturbance wave propagating on the shock surface as

$$W_d = a_0 [(M^2 - 1)K(M)/2]^{\frac{1}{2}} \quad (5.100)$$

In the present case, the tangential and normal components of the velocity of the disturbance point propagating on the reflected shock surface can be written, respectively, as

$$\begin{cases} U_t = W_{dr} + ma_2 \sin(\theta_i + \theta_w) \\ U_n = M_{ri} a_2 + ma_2 \cos(\theta_i + \theta_w) \end{cases} \quad (5.101)$$

where W_{dr} is the relative rate of the disturbance wave propagating on the reflected shock. $ma_2 \sin(\theta_i + \theta_w)$ and $ma_2 \cos(\theta_i + \theta_w)$ are the tangential and normal components of the flow velocity ahead of the reflected shock.

The ratio of the components can be expressed as

$$\tan v_i = \frac{U_t}{U_n} = \frac{W_{dr} + ma_2 \sin(\theta_i + \theta_w)}{M_{ri} a_2 + ma_2 \cos(\theta_i + \theta_w)} \quad (5.102)$$

By comparison of (5.102) with (5.99), we find that the relative rate of disturbance wave propagating on the shock surface has the following expression

$$W_{dr} = a_2 \left[(M_r^2 - 1)K(M_r)/2 \right]^{\frac{1}{2}} \quad (5.103)$$

which remains the same form as the expression (5.100).

In order to find the shape of the reflected shock, we need to find the expression of the distance from the reflected shock surface to the origin O .

The time interval that the incident shock moves from the origin O to the point P , t_i , can be expressed as

$$t_i = \frac{L \cos \theta_w}{M_s a_1} \quad (5.104)$$

where a_1 is the speed of sound in region (1), L is the distance between the reflected point P and the origin O .

The velocity of the disturbance point in this coordinate system is obtained as

$$U = [M_{ri} + m\cos(\theta_i + \theta_w)]a_2 / \cos v_i \quad (5.105)$$

where $v_i = \theta_i - \omega_i$.

So the distance from the origin O to the shock surface, R_i , can be written as

$$R_i = Ut_i \quad (5.106)$$

Since the same time interval from the origin O to any point on the shock surface at any given time is kept, and from (5.104), (5.105) and (5.106), we obtain

$$R_i = \frac{[M_{ri} + m\cos(\theta_i + \theta_w)]a_{21} \cdot L \cos \theta_w}{M_s \cos(\theta_i - \omega_i)} \quad (5.107)$$

where $a_{21} = a_2 / a_1$.

It is easy for us to find the shape of the reflected shock by using relations (5.99) and (5.107) or to calculate the strengths of the reflected shock according to the shape of the reflected shock, which may be given by experiments or numerical calculations.

§ 5.9 First disturbance point and last disturbance point

In this section (Han, 1991), we first discuss the first disturbance point, and then the last disturbance point.

According to the two-shock theory and the equation (5.99), we find that when θ_w decreases, ω_0 decreases, and the first disturbance point F approaches point P . Of course, when $\omega_0=0$, the transition from RR to MR occurs. This is a criterion of transition from RR to MR in the shock dynamic theory.

In order to make a comparison of this transition criterion with the sonic criterion, ω_{or} denotes the angle between the line from the origin O to the first disturbance point and x -axis in this theory; ω_{os} denotes the angle in the theory of sound.

Under the condition of transition in the detachment criterion, we can obtain the critical wedge angle θ_{wT} at different shock Mach number M_s . Our purpose is to see the changes in ω_{or} and ω_{os} at different wedge angle θ_{wT} . By using relations (5.94), (5.95) and (5.99), we have

$$\tan v_{os} = \frac{(W_{dso} / a_2) + m \sin(\theta_0 + \theta_{wT})}{M_{ro} + m \cos(\theta_0 + \theta_{wT})} \quad (5.108)$$

$$\tan v_{or} = \frac{(W_{dro} / a_2) + m \sin(\theta_0 + \theta_{wT})}{M_{ro} + m \cos(\theta_0 + \theta_{wT})} \quad (5.109)$$

and

$$\omega_{os} = \theta_0 - v_{os} \quad (5.110)$$

$$\omega_{or} = \theta_0 - v_{or} \quad (5.111)$$

In the above relations (5.108), (5.109), (5.110), and (5.111), the subscript "o" represents the first disturbance point; the subscript "s" and subscript "r" represent the results from the theory of sound and from the shock dynamics, respectively.

The results are given in Table 5.1, which shows that this transition boundary is located under that of the detachment criterion, but the transition boundary of the sonic criterion is located over that of the detachment criterion. We will discuss the transition criteria systematically in Chapter 8.

Table 5.1 A comparison of this criterion with the sonic criterion

M_s	θ_{wT}	ω_{or}	ω_{os}
1.05	29.9 °	4.46 °	-4.07 °
1.50	49.0 °	4.22 °	-2.36 °
2.00	50.6 °	3.14 °	-1.47 °
3.00	50.7 °	1.96 °	-1.15 °
5.00	50.4 °	1.42 °	-0.91 °
8.00	50.2 °	1.39 °	-0.68 °

where θ_{wT} is the critical wedge angle in the detachment criterion.

Next we will discuss the last disturbance point. There are some problems for us to calculate the last disturbance point if the equations (5.98), or (5.99), or Whitham's method (Whitham, 1957) is used. The first is that the portion of the reflected shock from the last disturbance point to the wall surface, LQ , is a straight line, particularly, when the incident shock is strong, the length of LQ increases quickly with the increase of M_s , but experimental results show that LQ is not a straight line (as shown in Fig. 5.10). The reason would be that, after the last disturbance wave moves over, the portion of the reflected shock propagates forward without the disturbance of the wall OS and the rate of the last disturbance wave, W_{dL} , is not equal to zero, so a straight line LQ is

formed. In fact, according to the viewpoint of gasdynamics, the last disturbance sound wave generated at the corner O overtakes the reflected shock, which must make the shock curved. It means that LQ is not a straight line and the rate of the last disturbance point on the wall surface OS , W_{dL} , must be equal to zero.

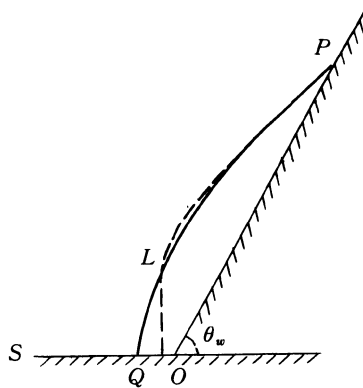


Fig. 5.10 Comparison of experimental results with relations (5.98) (or Whitham's results (1957)), solid line is experimental results, dashed line is the results of relations (5.98) at strong incident Mach number M_s

So, some improvement on the relation of the rate of the disturbance wave is needed, that is, the following conditions should be satisfied.

$$M_{ri} = M_{ro}, W_{dr} = a_2 [(M_{ro}^2 - 1)K / 2]^{1/2} \quad (5.112)$$

$$M_{ri} = M_{rL}, W_{dL} = 0 \quad (5.113)$$

where subscript "L" denotes the last disturbance point, subscript "o" denotes the first disturbance point.

Substituting (5.112) and (5.113) into the following relation

$$W_{dr} = a_2 [f_1 (M_{ri}^2 - 1)K / 2 + f_2] \quad (5.114)$$

Solving for f_1 and f_2 , and substituting them into (5.114), we can obtain

$$W_{dr} = a_2 [(K / 2)(M_{ri}^2 - M_{rL}^2) \cdot (M_{ro}^2 - 1) / (M_{ro}^2 - M_{rL}^2)]^{1/2} \quad (5.115)$$

This is an improved relation for calculating the rate of the disturbance wave propagating on the shock surface.

The second problem for calculating the reflected shock is that the shock

Mach number M_{ri} decreases too quickly with increasing θ_i , so we need to improve the first expression of (5.99). The results are given as follows

$$M_{ri} = \text{ch}[\text{ch}^{-1} M_{ro} - N \cdot (\theta_i - \theta_0)(K/2)^{\frac{1}{2}}(180/\pi)] \quad (5.116)$$

where N is a coefficient.

By means of the above improvements, the calculations have been made under the conditions of $M_s = 2.05$ and $M_s = 4.68$, respectively. The shapes of the reflected shocks are shown in agreement with the experimental results (Deschambault and Glass, 1983) and the numerical calculations (Kutler and Shankar, 1977).

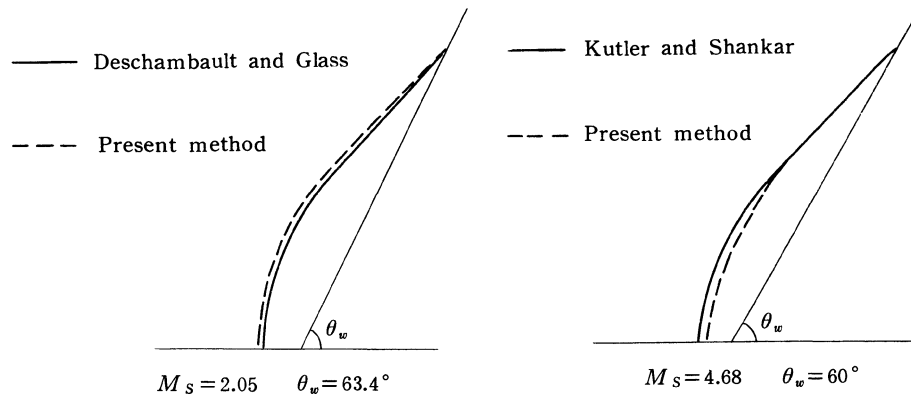


Fig. 5.11 Comparison with the experimental results (Deschambault and Glass, 1983)

Fig. 5.12 Comparison with the numerical calculations (Kutler and Shankar, 1977)

According to the above application of shock dynamic equations for a uniform flow ahead of a shock to the regular reflection of a plane moving shock on a wedge, we find that shock dynamics is a useful and fast method to calculate and analyse the variations in the strength and orientation of a shock wave, but further improvements are still needed.

§ 5.10 The equations for axially-symmetrical flow

In the case of the axially-symmetrical flow, the unit vector for the ray direction can be expressed as

$$\vec{i} = \frac{(M\cos\theta + m)\vec{e}_x + M\sin\theta\vec{e}_r}{(M^2 + 2Mm\cos\theta + m^2)^{\frac{1}{2}}} \quad (5.117)$$

where \vec{e}_x and \vec{e}_r are the unit vectors in x and r directions, respectively.

Substituting (5.117) into (5.24), we get

$$\frac{\partial}{\partial x} \left[\frac{r(M\cos\theta + m)}{A \cdot N} \right] + \frac{\partial}{\partial r} \left[\frac{r(M\sin\theta)}{A \cdot N} \right] = 0 \quad (5.118)$$

where $N = (M^2 + 2Mm\cos\theta + m^2)^{\frac{1}{2}}$

In the axially-symmetrical flow, similarly, we have

$$\vec{n} = \cos\theta \cdot \vec{e}_x + \sin\theta \cdot \vec{e}_r, \quad (5.119)$$

From (5.117) and (5.119), we have

$$\vec{i} \cdot \vec{n} = \frac{M + m\cos\theta}{N} \quad (5.120)$$

and

$$A'(\vec{i} \cdot \vec{n}) = A \quad (5.121)$$

or

$$A'(M + m\cos\theta) = A \cdot N \quad (5.122)$$

Substituting (5.122) into (5.118), we get

$$\frac{\partial}{\partial x} \left[\frac{r(M\cos\theta + m)}{(M + m\cos\theta)A'} \right] + \frac{\partial}{\partial r} \left[\frac{r(M\sin\theta)}{(M + m\cos\theta)A'} \right] = 0 \quad (5.123)$$

According to the following relation

$$M + m\cos\theta = \frac{1}{|\nabla \alpha|} \quad (5.124)$$

we can obtain

$$\frac{\partial}{\partial x} \left(\frac{\sin\theta}{M + m\cos\theta} \right) - \frac{\partial}{\partial r} \left(\frac{\cos\theta}{M + m\cos\theta} \right) = 0 \quad (5.125)$$

Summarizing the above relations and considering the area relation, we get

$$\begin{cases} \frac{\partial}{\partial x} \left[\frac{r(M\cos\theta + m)}{(M + m\cos\theta)A'} \right] + \frac{\partial}{\partial r} \left[\frac{r(M\sin\theta)}{(M + m\cos\theta)A'} \right] = 0 \\ \frac{\partial}{\partial x} \left[\frac{\sin\theta}{M + m\cos\theta} \right] - \frac{\partial}{\partial r} \left[\frac{\cos\theta}{M + m\cos\theta} \right] = 0 \\ A' = A'(M) \end{cases} \quad (5.126)$$

Expanding the equations (5.126), we get

$$\begin{cases} C_c \frac{\partial \theta}{\partial r} + C_s \frac{\partial \theta}{\partial r} - \sin \theta \frac{\partial M}{\partial x} + \cos \theta \frac{\partial M}{\partial r} = 0 \\ (M^2 - m^2) \sin \theta \frac{\partial \theta}{\partial x} - MC_c \frac{\partial \theta}{\partial r} + (m \sin^2 \theta - BC_c e) \frac{\partial M}{\partial x} \\ \quad - (m \cos \theta \cdot \sin \theta + BC_s e) \frac{\partial M}{\partial r} = \frac{BC_s}{r} \end{cases} \quad (5.127)$$

The difference between (5.127) and (5.70) is that there is the term of BC_s / r in the second expression of (5.127).

By using the same method as that in § 5.5, we can obtain the following characteristic relations in the axially-symmetrical flow

$$\begin{cases} \left(\frac{d\theta}{dx} \right)_1 + \omega(M) \left(\frac{dM}{dx} \right)_1 = \frac{C_s}{r(M \sin \theta - C_c \sqrt{Me})} \\ \text{along } \left(\frac{dr}{dx} \right)_1 = \tan(\theta + v_1) \\ \left(\frac{d\theta}{dx} \right)_2 - \omega(M) \left(\frac{dM}{dx} \right)_2 = \frac{C_s}{r(M \sin \theta + C_c \sqrt{Me})} \\ \text{along } \left(\frac{dr}{dx} \right)_2 = \tan(\theta - v_2) \end{cases} \quad (5.128)$$

where

$$\begin{aligned} \left(\frac{d\theta}{dx} \right)_1 &= \frac{\partial \theta}{\partial x} + \left(\frac{dr}{dx} \right)_1 \frac{\partial \theta}{\partial r}, \\ \left(\frac{d\theta}{dx} \right)_2 &= \frac{\partial \theta}{\partial x} + \left(\frac{dr}{dx} \right)_2 \frac{\partial \theta}{\partial r}. \end{aligned}$$

or

$$\begin{cases} \left[\frac{\partial}{\partial x} + \left(\frac{dr}{dx} \right)_1 \frac{\partial}{\partial r} \right] \left[\theta + \int_1^M \omega(M) dM \right] = \frac{C_s}{r(M \sin \theta - C_c \sqrt{Me})} \\ \left[\frac{\partial}{\partial x} + \left(\frac{dr}{dx} \right)_2 \frac{\partial}{\partial r} \right] \left[\theta - \int_1^M \omega(M) dM \right] = \frac{C_s}{r(M \sin \theta + C_c \sqrt{Me})} \end{cases} \quad (5.129)$$

It should be noted that in the case of the axially-symmetrical flow, the term in the right-hand side of (5.128) and (5.129) is not equal to zero, even in a uniform quiescent gas ahead of a shock.

If the flow Mach number ahead of the shock, m , is equal to zero, the relations (5.129) can be simplified to

$$\left\{ \left[\frac{\partial}{\partial x} + \left(\frac{dr}{dx} \right)_1 \frac{\partial}{\partial r} \right] \left[\theta + \int_1^M \omega(M) dM \right] \right. = \frac{1}{r(1 - \cot\theta \cdot \sqrt{Me})} \quad (5.130)$$

$$\left. \left[\frac{\partial}{\partial x} + \left(\frac{dr}{dx} \right)_2 \frac{\partial}{\partial r} \right] \left[\theta - \int_1^M \omega(M) dM \right] \right. = \frac{1}{r(1 + \cot\theta \cdot \sqrt{Me})}$$

Up to now, we have already derived two-dimensional equations for a uniform moving gas ahead of a shock and the corresponding characteristic relations.

Chapter 6 One- and Two-Dimensional Equations for a Nonuniform Moving Gas Ahead of a Shock Wave

In this chapter, We will discuss the one-dimensional area relation and two-dimensional equations of shock dynamics for a nonuniform, steady flow ahead of a shock.

§ 6.1 One-dimensional area relation for a nonuniform, steady flow ahead of a shock

One-dimensional area relation for a nonuniform, steady flow ahead of a shock is to describe a moving shock propagating through a varying cross-sectional area tube (or channel) in which there is a steady flow (supersonic or subsonic flow) originally.

For the shock moving into such a tube with a nonuniform, steady flow ahead of it, the strength of the moving shock is influenced by not only the change in the area, but also the changes in the parameters ahead of the shock. Chester(1960) extend Whitham's method which had been used for deriving the area relation for a uniform quiescent gas ahead of a shock to the case of nonuniform moving gas.

From Chapter 1, we know that the compatible relation along the positive characteristics behind the moving shock, C^+ can be written as

$$dp_2 + \rho_2 a_2 du_2 + \frac{\rho_2 a_2^2 u_2}{u_2 + a_2} \frac{dA}{A} = 0 \quad (6.1)$$

(6.1) can be rewritten as

$$\frac{dp_2}{\gamma p_2} + m_2 \frac{du_2}{u_2} + \frac{m_2}{m_2 + 1} \frac{dA}{A} = 0 \quad (6.2)$$

where subscript "2" represents the state behind the moving shock, m_2 is the flow Mach number behind the moving shock.

The moving shock relations in the case of shock propagating into a moving gas are given as follows

$$\begin{cases} \frac{p_2 - p_1}{p_1} = \frac{2\gamma}{\gamma + 1} (M^2 - 1) \\ \frac{u_2 - u_1}{u_1} = \frac{2}{\gamma + 1} \frac{1}{m_1} (M - \frac{1}{M}) \\ m_2 = \frac{(\gamma + 1)m_1 M + 2(M^2 - 1)}{[2\gamma M^2 - (\gamma - 1)]^{\frac{1}{2}}[(\gamma - 1)M^2 + 2]^{\frac{1}{2}}} \end{cases} \quad (6.3)$$

The relations of homoentropic, steady flow ahead of the shock are expressed as

$$\begin{cases} \frac{p_1}{p_T} = (1 + \frac{\gamma - 1}{2} m_1^2)^{-\frac{\gamma}{\gamma - 1}} \\ \frac{u_1}{a_T} = \frac{u_1}{a_1} \cdot \frac{a_1}{a_T} = m_1 \left(1 + \frac{\gamma - 1}{2} m_1^2 \right)^{-\frac{1}{2}} \\ \frac{dA}{A} = \frac{m_1^2 - 1}{1 + \frac{\gamma - 1}{2} m_1^2} \frac{dm_1}{m_1} \end{cases} \quad (6.4)$$

where p_T and a_T are stagnation parameters, m_1 is the flow Mach number in the region ahead of the shock.

From the first expressions of (6.3) and (6.4), we have

$$p_2 = p_T T(m_1)^{-\frac{\gamma}{\gamma - 1}} \left(\frac{2\gamma}{\gamma + 1} M^2 - \frac{\gamma - 1}{\gamma + 1} \right) \quad (6.5)$$

where $T(m_1) = 1 + \frac{\gamma - 1}{2} m_1^2$

Differentiating (6.5), we get

$$\begin{aligned} dp_2 = & -\gamma p_T \left(\frac{2\gamma}{\gamma + 1} M^2 - \frac{\gamma - 1}{\gamma + 1} \right) T(m_1)^{-\frac{2\gamma}{\gamma - 1}} \cdot m_1 dm_1 \\ & + \frac{4\gamma}{\gamma + 1} p_T T(m_1)^{-\frac{\gamma}{\gamma - 1}} \cdot M dM \end{aligned} \quad (6.6)$$

The first term of (6.2) can be written as

$$\frac{dp_2}{\gamma p_2} = \frac{4M dM}{[2\gamma M^2 - (\gamma - 1)]} - \frac{m_1 dm_1}{T(m_1)} \quad (6.7)$$

From the second expressions of (6.3) and (6.4), we have

$$u_2 = a_T T(m_1)^{-\frac{1}{2}} \left[\frac{2(M^2 - 1)}{(\gamma + 1)M} + m_1 \right] \quad (6.8)$$

Differentiating (6.8), we get

$$du_2 = a_T T(m_1)^{-\frac{1}{2}} \left[1 - \frac{\gamma-1}{\gamma+1} m_1 \left(\frac{M^2 - 1}{M} \right) T(m_1)^{-1} - \frac{\gamma-1}{2} m_1^2 T(m_1)^{-1} \right] dm_1 + \frac{2a_T T(m_1)^{-\frac{1}{2}}}{\gamma+1} \left(1 + \frac{1}{M^2} \right) dM \quad (6.9)$$

Thus we can obtain the second term of (6.2) as

$$m_2 \frac{du_2}{u_2} = \frac{m_2}{S} \left[1 - \frac{\gamma-1}{\gamma+1} m_1 \left(\frac{M^2 - 1}{M} \right) T(m_1)^{-1} - \frac{\gamma-1}{2} m_1^2 T(m_1)^{-1} \right] dm_1 + \frac{m_2}{S} \frac{2}{\gamma+1} \left(1 + \frac{1}{M^2} \right) dM \quad (6.10)$$

$$\text{where } S = S(M, m_1) = \frac{2(M^2 - 1)}{(\gamma + 1)M} + m_1$$

The third term of (6.2) is written as

$$\frac{m_2}{m_2 + 1} \frac{dA}{A} = \frac{m_1^2 - 1}{T(m_1)} \cdot \left(\frac{m_2}{m_2 + 1} \right) dm_1 \quad (6.11)$$

Substituting (6.7), (6.10), and (6.11) into (6.2), and combining the third expression of (6.4), we can obtain the relations for one-dimensional shock moving through a tube with a nonuniform flow in it as follows

$$\begin{cases} dM = G dm_1 \\ \frac{dA}{A} = \frac{m_1^2 - 1}{1 + \frac{\gamma-1}{2} m_1^2} \cdot \frac{dm_1}{m_1} \end{cases} \quad (6.12)$$

where

$$G = \left[\frac{\frac{m_1}{T} + \left(\frac{\gamma-1}{2} \right) m_1 \frac{m_2}{T} - \frac{m_2}{S} - \frac{(m_1^2 - 1)}{m_1 T} \left(\frac{m_2}{m_2 + 1} \right)}{\frac{2m_2}{(\gamma + 1)S} \cdot \left(1 + \frac{1}{M^2} \right) + \frac{4M}{2\gamma M^2 - (\gamma - 1)}} \right]$$

In the case of the direction of the shock motion being the same as that of the gas flow ahead of the shock, $G > 0$.

It follows from (6.12) that for supersonic flow ahead of the shock in the varying cross-sectional area tube

$$\begin{cases} dA > 0, & dm_1 > 0, & dM > 0 \\ dA < 0, & dm_1 < 0, & dM < 0 \end{cases} \quad (6.13)$$

for subsonic flow in the tube

$$\begin{cases} dA > 0, & dm_1 < 0, & dM < 0 \\ dA < 0, & dm_1 > 0, & dM > 0 \end{cases} \quad (6.14)$$

The relations (6.12) give us a new concept that when a moving shock propagating through a tube with a steady, nonuniform flow in it, the shock strength changes in different ways, depending on whether supersonic flow or subsonic flow is in the tube.

It should be noted that the above conclusion is valid only under the condition that the shock wave and the flow ahead of it have the same direction. If the directions are different, the conclusion would be complicated.

In addition, as mentioned already in § 5.4, it is hardly possible to use relations (6.12) in the ray tubes for a moving shock propagating into a nonuniform, two- or three-dimensional flow fields, because the directions of the shock wave and of the gas flow ahead of it are different.

§ 6.2 Basic idea for establishing the two-dimensional equations of shock dynamics

In Chapter 5, by means of transformation of coordinates from the moving frame of reference into the stationary one, the equations of shock dynamics for a uniform flow ahead of a shock have been derived. In this chapter, we will confront a nonuniform flow field ahead of a shock. How to make the transformation of coordinates in such a nonuniform flow field? How to establish an area relation in the case of the directions of the shock and the flow ahead of it being different? The basic idea was presented by Han and Yin (1989A).

1. The geometrical relations

In order to establish the geometrical relations, we may divide the nonuniform flow field immediately ahead of the shock surface into a lot of small regions (fluid elements). Firstly, each region can be regarded as a uniform flow field, the flow Mach number m and the flow angle ε in each region are constant, but m and ε change from one region into another. A transient moving frame of reference attached to a small uniform region can be used and then the transformation of coordinates from the moving frame of reference into a stationary one is made. Thus we can obtain the geometrical equations of shock dynamics for the small region. It should be noted that there are lots of moving frames, but only one stationary frame which is attached to the body diffracted

by the shock.

The same method can be used for every region, and we will obtain a series of equations all with the same form. Now, if the m and ε in the equations are regarded as variables, we can extend the geometrical relations (equations) of shock dynamics for small region to the entire flow field.

2. The area relation

For the establishment of the area relation for a nonuniform flow field ahead of a shock, we cannot use the relation (6.12) which only applies to the case of the directions of the normal to the shock and the flow ahead of the shock being the same, this is because in the present case, the direction of the normal to shock surface is different from the direction of flow ahead of the shock in general. On the other hand, we can not try to derive the area relation along a ray tube under the condition of the stationary coordinate system either, this is because the rays are not consistent with the particle paths behind the shock in this case, such a ray tube in the stationary frame of reference will lose its physical significance, that is, in this case, the ray tube cannot be regarded as a solid wall tube. So in this chapter, the concept of the ray tube in the moving frame of reference will be introduced, then by means of the transformation of coordinates from the moving frame into the stationary one for an infinitesimal fluid element, we will obtain the area relation for a nonuniform flow ahead of a shock.

§ 6.3 Transformation of coordinates in any small region

Every small uniform region has own individual moving coordinate system, so we cannot use the following relation

$$\alpha(x, y) = a_1 t$$

This relation only applies to the uniform flow ahead of the shock.

For a small uniform region in the nonuniform flow field, the following relations can be used:

in the moving frame of reference, the equation of the shock surface can be written as

$$\alpha'(x', y') = t' \quad (6.15)$$

in the stationary frame of reference, the equation of the shock surface can be written as

$$\alpha(x, y) = t \quad (6.16)$$

The relations between the two coordinates are expressed as

$$\begin{cases} x = x' + U \cos \varepsilon \cdot t' + a = x' + ma \cdot \cos \varepsilon \cdot \alpha(x,y) + a \\ y = y' + U \sin \varepsilon \cdot t' + b = y' + ma \cdot \sin \varepsilon \cdot \alpha(x,y) + b \\ t = t' \end{cases} \quad (6.17)$$

where

x', y', t' are the coordinates in the moving frame;

x, y, t are the coordinates in the stationary frame.

a and b are constant for each small region, but they are of different value for the different region.

Next, we begin to derive the differential relations between the two coordinates.

According to the above functional relations, we have

$$\frac{\partial}{\partial x'} = \frac{\partial}{\partial x} \frac{\partial x}{\partial x'} + \frac{\partial}{\partial y} \frac{\partial y}{\partial x'} \quad (6.18)$$

$$\frac{\partial}{\partial y'} = \frac{\partial}{\partial x} \frac{\partial x}{\partial y'} + \frac{\partial}{\partial y} \frac{\partial y}{\partial y'} \quad (6.19)$$

In order to find out $\frac{\partial x}{\partial x'}, \frac{\partial y}{\partial x'}, \frac{\partial x}{\partial y'}, \frac{\partial y}{\partial y'}$, we take the derivatives of the first and second expressions of (6.17) with respect to x', y' , respectively, and consider that m, a and ε in the small region are constant, thus obtaining

$$\begin{cases} \frac{\partial x}{\partial x'} = \frac{\partial x'}{\partial x'} + ma \cdot \cos \varepsilon \cdot \alpha_x \frac{\partial x}{\partial x'} + ma \cdot \cos \varepsilon \cdot \alpha_y \frac{\partial y}{\partial x'} \\ \frac{\partial y}{\partial x'} = \frac{\partial y'}{\partial x'} + ma \cdot \sin \varepsilon \cdot \alpha_x \frac{\partial x}{\partial x'} + ma \cdot \sin \varepsilon \cdot \alpha_y \frac{\partial y}{\partial x'} \\ \frac{\partial x}{\partial y'} = \frac{\partial x'}{\partial y'} + ma \cdot \cos \varepsilon \cdot \alpha_x \frac{\partial x}{\partial y'} + ma \cdot \cos \varepsilon \cdot \alpha_y \frac{\partial y}{\partial y'} \\ \frac{\partial y}{\partial y'} = \frac{\partial y'}{\partial y'} + ma \cdot \sin \varepsilon \cdot \alpha_x \frac{\partial x}{\partial y'} + ma \cdot \sin \varepsilon \cdot \alpha_y \frac{\partial y}{\partial y'} \end{cases} \quad (6.20)$$

In the moving frame of reference, x' and y' are independent variables, so $\frac{\partial y'}{\partial x'} = 0$, $\frac{\partial x'}{\partial y'} = 0$, $\frac{\partial x'}{\partial x'} = 1$, and $\frac{\partial y'}{\partial y'} = 1$.

Thus the relations (6.20) can be simplified to

$$\begin{cases} (1 - ma \cdot \cos\epsilon \cdot \alpha_x) \frac{\partial x}{\partial x'} = 1 + ma \cdot \cos\epsilon \cdot \alpha_y \frac{\partial y}{\partial x'} \\ ma \cdot \sin\epsilon \cdot \alpha_x \frac{\partial x}{\partial x'} = (1 - ma \cdot \sin\epsilon \cdot \alpha_y) \frac{\partial y}{\partial x'} \\ (1 - ma \cdot \cos\epsilon \cdot \alpha_x) \frac{\partial x}{\partial y'} = ma \cdot \cos\epsilon \cdot \alpha_y \frac{\partial y}{\partial y'} \\ 1 + ma \cdot \sin\epsilon \cdot \alpha_x \frac{\partial x}{\partial y'} = (1 - ma \cdot \sin\epsilon \cdot \alpha_y) \frac{\partial y}{\partial y'} \end{cases} \quad (6.21)$$

From (6.21), we get

$$\begin{cases} \frac{\partial x}{\partial x'} = \frac{1 - ma \cdot \sin\epsilon \cdot \alpha_y}{1 - ma \cdot \cos\epsilon \cdot \alpha_x - ma \cdot \sin\epsilon \cdot \alpha_y} \\ \frac{\partial y}{\partial x'} = \frac{ma \cdot \sin\epsilon \cdot \alpha_x}{1 - ma \cdot \cos\epsilon \cdot \alpha_x - ma \cdot \sin\epsilon \cdot \alpha_y} \\ \frac{\partial x}{\partial y'} = \frac{ma \cdot \cos\epsilon \cdot \alpha_y}{1 - ma \cdot \cos\epsilon \cdot \alpha_x - ma \cdot \sin\epsilon \cdot \alpha_y} \\ \frac{\partial y}{\partial y'} = \frac{1 - ma \cdot \cos\epsilon \cdot \alpha_x}{1 - ma \cdot \cos\epsilon \cdot \alpha_x - ma \cdot \sin\epsilon \cdot \alpha_y} \end{cases} \quad (6.22)$$

Substituting (6.22) into (6.18) and (6.19), we get

$$\begin{cases} \frac{\partial}{\partial x'} = \frac{(1 - ma \cdot \sin\epsilon \cdot \alpha_y) \frac{\partial}{\partial x} + ma \cdot \sin\epsilon \cdot \alpha_x \frac{\partial}{\partial y}}{1 - ma \cdot \cos\epsilon \cdot \alpha_x - ma \cdot \sin\epsilon \cdot \alpha_y} \\ \frac{\partial}{\partial y'} = \frac{ma \cdot \cos\epsilon \cdot \alpha_y \frac{\partial}{\partial x} + (1 - ma \cdot \cos\epsilon \cdot \alpha_x) \frac{\partial}{\partial y}}{1 - ma \cdot \cos\epsilon \cdot \alpha_x - ma \cdot \sin\epsilon \cdot \alpha_y} \end{cases} \quad (6.23)$$

From (6.15) and (6.16), we have

$$\alpha'(x', y') = \alpha(x, y) \quad (6.24)$$

Substituting (6.24) into (6.23), we get

$$\begin{cases} \frac{\partial \alpha'}{\partial x'} = \frac{\alpha_x}{1 - ma \cdot \cos\epsilon \cdot \alpha_x - ma \cdot \sin\epsilon \cdot \alpha_y} \\ \frac{\partial \alpha'}{\partial y'} = \frac{\alpha_y}{1 - ma \cdot \cos\epsilon \cdot \alpha_x - ma \cdot \sin\epsilon \cdot \alpha_y} \end{cases} \quad (6.25)$$

where U and a are the flow velocity and speed of sound in the small region ahead of the shock, respectively; ϵ is the angle between the direction of flow ahead of the shock and x -axis; m is flow Mach number in the small region ahead of shock.

The transient transformation of coordinates in a small uniform region is shown in Fig. 6.1.

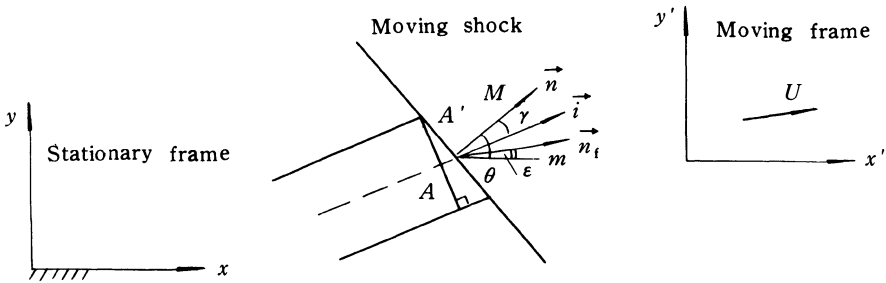


Fig. 6.1 Transient transformation of coordinates in small uniform region

§ 6.4 Two-dimensional equations denoted by the function $\alpha(x, y)$ for a small region

1. The equations in the moving frame of reference for small uniform region

For any small uniform region, if the moving frame is attached to the flow field ahead of a shock, the rays are orthogonal to the shock surface, we can obtain

$$\begin{cases} \nabla' \cdot \left(\frac{Ma}{A'} \nabla' \alpha' \right) = 0 \\ Ma = \frac{1}{|\nabla' \alpha'|} \\ A' = A'(M, P, a) \end{cases} \quad \text{along a ray tube in the moving frame.} \quad (6.26)$$

The equations (6.26) are the same as (4.27).

There are two differences between the equations (6.26) and (5.16). One is that in (6.26), the expression $\alpha'(x', y') = t'$ is used, while in the equations (5.16), the expression $\alpha'(x', y') = a_1 t$ is used. The other is that in (6.26), relation $A' = A'(M, P, a)$ along ray tube in the moving frame (we will make detailed derivation in § 6.6) is used, while in (5.16), relation $A' = A'(M)$ is used. Why do the two equations have such differences? This is because although the small region is uniform, the entire flow field is nonuniform. Our purpose is to find out the equations which applies to the entire flow field. If the equations (5.16) which only applies to uniform flow were used, we would lose the terms of first

order partial derivatives of the flow parameters in the nonuniform region ahead of the shock. This is an important idea for establishing the equations for a nonuniform flow ahead of a shock.

2. The equations in stationary frame of reference for a small uniform region

Substituting (6.23) and (6.25) into the following equations derived from (6.26)

$$\begin{cases} \frac{\partial}{\partial x'} \left(\frac{Ma}{A'} \frac{\partial \alpha'}{\partial x'} \right) + \frac{\partial}{\partial y'} \left(\frac{Ma}{A'} \frac{\partial \alpha'}{\partial y'} \right) = 0 \\ Ma = \left[\left(\frac{\partial \alpha'}{\partial x'} \right)^2 + \left(\frac{\partial \alpha'}{\partial y'} \right)^2 \right]^{-\frac{1}{2}} \\ A' = A'(M, p, a), \quad \text{along a ray tube in the moving frame} \end{cases} \quad (6.27)$$

we get

$$\begin{cases} \frac{\partial}{\partial x} \left[\frac{\alpha_x + ma\alpha_y J}{A'(\alpha_x^2 + \alpha_y^2)^{\frac{1}{2}}} \right] + \frac{\partial}{\partial y} \left[\frac{\alpha_y - ma\alpha_x J}{A'(\alpha_x^2 + \alpha_y^2)^{\frac{1}{2}}} \right] = 0 \\ Ma = \frac{1 - ma \cdot \cos\epsilon \cdot \alpha_x - ma \cdot \sin\epsilon \cdot \alpha_y}{(\alpha_x^2 + \alpha_y^2)^{\frac{1}{2}}} \\ A' = A'(M, p, a), \quad \text{along a ray tube in the moving frame} \end{cases} \quad (6.28)$$

where $J = \alpha_y \cdot \cos\epsilon - \alpha_x \cdot \sin\epsilon$.

The equations (6.28) are the equations of shock dynamics for any small region in the stationary frame of reference, which are denoted by function $\alpha(x, y)$.

3. The expression for unit vector \vec{i} and the relation between \vec{i} and \vec{n}

For the uniform flow ahead of the shock, from (5.28), we have the following relation, which also applies to any small region,

$$\nabla \cdot \left(\frac{\vec{i}}{A} \right) = 0 \quad (6.29)$$

By using the same method as in Chapter 5, the unit vector \vec{i} can be expressed as

$$\vec{i} = f_1(x, y) \vec{e}_x + f_2(x, y) \vec{e}_y. \quad (6.30)$$

Thus (6.29) can be written as

$$\frac{\partial}{\partial x} \left[\frac{f_1(x, y)}{A} \right] + \frac{\partial}{\partial y} \left[\frac{f_2(x, y)}{A} \right] = 0 \quad (6.31)$$

The first expression of (6.28) can be written as

$$\frac{\partial}{\partial x} \left[\frac{B_1}{A'} \cdot \frac{(\alpha_x + ma\alpha_y J)}{B_1(\alpha_x^2 + \alpha_y^2)^{\frac{1}{2}}} \right] + \frac{\partial}{\partial y} \left[\frac{B_1}{A'} \cdot \frac{(\alpha_y - ma\alpha_x J)}{B_1(\alpha_x^2 + \alpha_y^2)^{\frac{1}{2}}} \right] = 0 \quad (6.32)$$

By comparing (6.32) with (6.31), we get

$$A' = AB_1 \quad (6.33)$$

$$f_1(x, y) = \frac{\alpha_x + ma\alpha_y J}{B_1(\alpha_x^2 + \alpha_y^2)^{\frac{1}{2}}} \quad (6.34)$$

$$f_2(x, y) = \frac{\alpha_y - ma\alpha_x J}{B_1(\alpha_x^2 + \alpha_y^2)^{\frac{1}{2}}} \quad (6.35)$$

Since \vec{i} is a unit vector, we have

$$\left\{ \left[\frac{\alpha_x + ma\alpha_y J}{B_1(\alpha_x^2 + \alpha_y^2)^{\frac{1}{2}}} \right]^2 + \left[\frac{\alpha_y - ma\alpha_x J}{B_1(\alpha_x^2 + \alpha_y^2)^{\frac{1}{2}}} \right]^2 \right\}^{\frac{1}{2}} = 1 \quad (6.36)$$

From (6.36), we have

$$B_1 = (1 + m^2 a^2 J^2)^{\frac{1}{2}} \quad (6.37)$$

From (6.37), (6.35), (6.34), (6.33), and (6.30), we get

$$\vec{i} = \frac{(\alpha_x + ma\alpha_y J)\vec{e}_x + (\alpha_y - ma\alpha_x J)\vec{e}_y}{\left[(\alpha_x^2 + \alpha_y^2)(1 + m^2 a^2 J^2)^{\frac{1}{2}} \right]} \quad (6.38)$$

$$A' = (1 + m^2 a^2 J^2)^{\frac{1}{2}} A \quad (6.39)$$

Next, we derive the relation between \vec{i} and \vec{n} .

We know that the unit vector of the normal to the shock can be written as

$$\vec{n} = \frac{\nabla \alpha}{|\nabla \alpha|} = \frac{\alpha_x \vec{e}_x + \alpha_y \vec{e}_y}{(\alpha_x^2 + \alpha_y^2)^{\frac{1}{2}}} \quad (6.40)$$

From (6.38) and (6.40), we get

$$\vec{i} \cdot \vec{n} = \frac{1}{(1 + m^2 a^2 J^2)^{\frac{1}{2}}} \quad (6.41)$$

From Fig. 6.1,

$$\vec{i} \cdot \vec{n} = \cos \gamma$$

thus we get

$$\cos\gamma = \frac{1}{(1 + m^2 a^2 J^2)^{\frac{1}{2}}} \quad (6.42)$$

$$A' \cos\gamma = A \quad (6.43)$$

§ 6.5 Two-dimensional equations denoted by shock Mach number M and shock angle θ for a small region

1. The relations between M, θ and α

In order to derive the two-dimensional equations directly denoted by M and θ , it is necessary to find out the relations between M, θ and α .

By using the same method as adopted in Chapter 5, and from the second expression of (6.28), we have

$$\vec{n} = \frac{Ma(\alpha_x \vec{e}_x + \alpha_y \vec{e}_y)}{1 - ma \cdot \cos\epsilon \cdot \alpha_x - ma \cdot \sin\epsilon \cdot \alpha_y} \quad (6.44)$$

and

$$\vec{n} = \cos\theta \vec{e}_x + \sin\theta \vec{e}_y \quad (6.45)$$

From (6.44) and (6.45), we can obtain two important relations

$$\alpha_x = \frac{\cos\theta}{a[M + m\cos(\theta - \epsilon)]} \quad (6.46)$$

$$\alpha_y = \frac{\sin\theta}{a[M + m\cos(\theta - \epsilon)]} \quad (6.47)$$

2. The two-dimensional equations

Substituting (6.46) and (6.47) into the first expression of (6.28) and noting that $\frac{\partial}{\partial x} \left(\frac{\partial \alpha}{\partial y} \right) = \frac{\partial}{\partial y} \left(\frac{\partial \alpha}{\partial x} \right)$, we get

$$\begin{cases} \frac{\partial}{\partial x} \left[\frac{M\cos\theta + m\cos\epsilon}{(M + m\cos(\theta - \epsilon))A'} \right] + \frac{\partial}{\partial y} \left[\frac{M\sin\theta + m\sin\epsilon}{(M + m\cos(\theta - \epsilon))A'} \right] = 0 \\ \frac{\partial}{\partial x} \left[\frac{\sin\theta}{a(M + m\cos(\theta - \epsilon))} \right] - \frac{\partial}{\partial y} \left[\frac{\cos\theta}{a(M + m\cos(\theta - \epsilon))} \right] = 0 \end{cases} \quad (6.48)$$

$A' = A'(M, p, a)$, along the ray tube in the moving frame.

(6.48) is two-dimensional equations of shock dynamics for a small region denoted by M and θ .

3. The expression for unit vector \vec{i}

Substituting (6.46) and (6.47) into (6.38), we get

$$\vec{i} = \frac{(M\cos\theta + m\cos\epsilon)\vec{e}_x + (M\sin\theta + m\sin\epsilon)\vec{e}_y}{[M^2 + 2Mm\cos(\theta - \epsilon) + m^2]^{\frac{1}{2}}} \quad (6.49)$$

or

$$\vec{i} = \frac{M(\cos\theta\vec{e}_x + \sin\theta\vec{e}_y) + m(\cos\epsilon\vec{e}_x + \sin\epsilon\vec{e}_y)}{[M^2 + 2Mm\cos(\theta - \epsilon) + m^2]^{\frac{1}{2}}} \quad (6.50)$$

(6.50) can be rewritten as

$$\vec{i} = \frac{\vec{M} + \vec{m}}{|\vec{M} + \vec{m}|} \quad (6.51)$$

where $\vec{M} = M\vec{n}$, $\vec{m} = m\vec{n}_f$,

$\vec{n} = \cos\theta\vec{e}_x + \sin\theta\vec{e}_y$, the unit vector of the normal to the shock.

$\vec{n}_f = \cos\epsilon\vec{e}_x + \sin\epsilon\vec{e}_y$, the unit vector of the flow ahead of the shock.

It follows from (6.51) and Fig. 6.2 that the direction of the unit vector \vec{i} is the same as that of the resultant vector of the vector \vec{M} and the vector \vec{m} .

As mentioned already in § 5.4, the rays are not consistent with the particle path immediately behind the shock.

By using the same method as in § 5.3, and from Fig. 6.2, we have

$$\vec{i} = \cos(\theta - \gamma)\vec{e}_x + \sin(\theta - \gamma)\vec{e}_y \quad (6.52)$$

The same expression as (6.49) or (6.50) can be obtained.

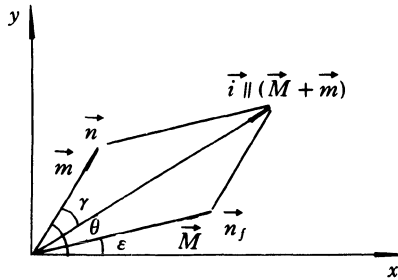


Fig. 6.2 The direction of unit vector along the ray, \vec{i}

§ 6.6 The area relation along ray tube in moving frame

In this section, we will derive the area expression along ray tube in moving frame.

In the case of a nonuniform quiescent gas ahead of a shock, from Chapter 4, we have obtained the following area relation along a ray tube (where the ratio of specific heats, γ , is assumed as a constant.)

$$edM + h\frac{dp}{p} + g\frac{da}{a} + \frac{dA}{A} = 0 \quad (6.53)$$

where the expressions for e , h , g have been given in relation (4.7).

The premise under which relation (6.53) is valid is that the rays are orthogonal to shock surfaces, that is, the gas ahead of the shock is at rest.

For each small uniform region, if the moving frame is attached to the flow field ahead of the shock, the rays must be orthogonal to shock surfaces. (6.53) can be used along a ray tube in the moving frame as follows

$$e\frac{dM}{d\alpha'} + h\frac{dp}{p d\alpha'} + g\frac{da}{a d\alpha'} + \frac{1}{A'}\frac{dA'}{d\alpha'} = 0 \quad (6.54)$$

where α' is curvilinear coordinate along a ray in the moving frame (that is, along the $\beta' = \text{constant}$).

In this moving frame, along a ray tube, we have

$$\begin{cases} x' = x'(\alpha') \\ y' = y'(\alpha') \end{cases} \quad (6.55)$$

Expanding the expression (6.54) by using relations (6.55), we obtain

$$\begin{aligned} & e\left(\frac{\partial M}{\partial x'}\frac{dx'}{d\alpha'} + \frac{\partial M}{\partial y'}\frac{dy'}{d\alpha'}\right) + \frac{g}{a}\left(\frac{\partial a}{\partial x'}\frac{dx'}{d\alpha'} + \frac{\partial a}{\partial y'}\frac{dy'}{d\alpha'}\right) \\ & + \frac{h}{p}\left(\frac{\partial p}{\partial x'}\frac{dx'}{d\alpha'} + \frac{\partial p}{\partial y'}\frac{dy'}{d\alpha'}\right) + \frac{1}{A'}\left(\frac{\partial A'}{\partial x'}\frac{dx'}{d\alpha'} + \frac{\partial A'}{\partial y'}\frac{dy'}{d\alpha'}\right) = 0 \end{aligned} \quad (6.56)$$

Rearranging (6.56), we get

$$\begin{aligned} & \left(e\frac{\partial M}{\partial x'} + \frac{h}{p}\frac{\partial p}{\partial x'} + \frac{g}{a}\frac{\partial a}{\partial x'} + \frac{1}{A'}\frac{\partial A'}{\partial x'}\right) \\ & + \frac{dy'}{dx'}\left(e\frac{\partial M}{\partial y'} + \frac{h}{p}\frac{\partial p}{\partial y'} + \frac{g}{a}\frac{\partial a}{\partial y'} + \frac{1}{A'}\frac{\partial A'}{\partial y'}\right) = 0 \end{aligned} \quad (6.57)$$

$\frac{dy'}{dx'}$ in (6.57) is the slope of the tangent to the ray in the moving frame. The direction of the tangent to the ray is the same as that of direction of \vec{n} , so

$$\frac{dy'}{dx'} = \tan\theta \quad (6.58)$$

Substituting (6.58) into (6.57), we get

$$\frac{1}{A'}\frac{\partial A'}{\partial x'} + \tan\theta \cdot \frac{1}{A'}\frac{\partial A'}{\partial y'} = -\left(e\frac{\partial M}{\partial x'} + \frac{h}{p}\frac{\partial p}{\partial x'} + \frac{g}{a}\frac{\partial a}{\partial x'}\right)$$

$$-\tan\theta \cdot \left(e \frac{\partial M}{\partial y'} + h \frac{\partial p}{\partial y'} + g \frac{\partial a}{\partial y'} \right) \quad (6.59)$$

We now make the transformation of coordinates for relation (6.59) from the moving frame into the stationary one, that is, substitute (6.23) into (6.59), and thus we can obtain the area relation along a ray tube in the moving frame which is expressed by the stationary coordinates as follows

$$\begin{aligned} \frac{1}{A'} \frac{\partial A'}{\partial x} + G \frac{1}{A'} \frac{\partial A'}{\partial y} &= - \left[\left(e \frac{\partial M}{\partial x} + h \frac{\partial p}{\partial x} + g \frac{\partial a}{\partial x} \right) \right. \\ &\quad \left. + G \left(e \frac{\partial M}{\partial y} + h \frac{\partial p}{\partial y} + g \frac{\partial a}{\partial y} \right) \right] \end{aligned} \quad (6.60)$$

where

$$G = \frac{M \sin\theta + m \sin\epsilon}{M \cos\theta + m \cos\epsilon}$$

If the flow field ahead of the shock is steady and homoentropic, p and a can be expressed by the flow Mach number m , and we get

$$\begin{cases} \frac{da}{a} = -\frac{\gamma-1}{2} \cdot \frac{mdm}{(1+\frac{\gamma-1}{2}m^2)} \\ \frac{dp}{p} = -\frac{\gamma mdm}{(1+\frac{\gamma-1}{2}m^2)} \end{cases} \quad (6.61)$$

Substituting (6.61) into (6.60), we get

$$\frac{1}{A'} \frac{\partial A'}{\partial x} + G \frac{1}{A'} \frac{\partial A'}{\partial y} = - \left[\left(e \frac{\partial M}{\partial x} - f \frac{\partial m}{\partial x} \right) + G \left(e \frac{\partial M}{\partial y} - f \frac{\partial m}{\partial y} \right) \right] \quad (6.62)$$

where

$$f = \frac{m(\frac{\gamma-1}{2}g + \gamma h)}{(1+\frac{\gamma-1}{2}m^2)}$$

§ 6.7 The equations in stationary frame of reference for entire flow field

The equations of shock dynamics for entire flow field is all the same as the equations (6.48) in form. (6.48) applies to any small regions, so the only thing we have to do is that in the equations for entire flow field, the parameters ahead of the shock, such as m (or p , a) and ϵ , are regarded as variables. If the equations with the variables m , p , a , and ϵ are expanded, the terms of the partial

derivatives of m (or p , a) and ε , will occur. In addition, the expression (6.60) or (6.62) is used instead of $A' = A'(M, p, a)$, we can obtain the equations which apply to entire flow field as follows

$$\left\{ \begin{array}{l} \frac{\partial}{\partial x} \left[\frac{M \cos \theta + m \cos \varepsilon}{(M + m \cos(\theta - \varepsilon)) A'} \right] + \frac{\partial}{\partial y} \left[\frac{M \sin \theta + m \sin \varepsilon}{(M + m \cos(\theta - \varepsilon)) A'} \right] = 0 \\ \frac{\partial}{\partial x} \left[\frac{\sin \theta}{a(M + m \cos(\theta - \varepsilon))} \right] - \frac{\partial}{\partial y} \left[\frac{\cos \theta}{a(M + m \cos(\theta - \varepsilon))} \right] = 0 \\ \frac{1}{A'} \frac{\partial A'}{\partial x} + G \frac{1}{A'} \frac{\partial A'}{\partial y} = - \left[\left(e \frac{\partial M}{\partial x} + \frac{h}{p} \frac{\partial p}{\partial x} + \frac{g}{a} \frac{\partial a}{\partial x} \right) \right. \\ \quad \left. + G \left(e \frac{\partial M}{\partial y} + \frac{h}{p} \frac{\partial p}{\partial y} + \frac{g}{a} \frac{\partial a}{\partial y} \right) \right] \end{array} \right. \quad (6.63)$$

By expanding the first expression of (6.63), and substituting the third expression into the first one, the terms of partial derivative of A' can be eliminated, and thus we can obtain the partial differential equations only with unknown quantities M and θ . The parameters ahead of the shock, such as m , ε , p , and a , are given.

The equations (6.63) are the two-dimensional equations of shock dynamics for the case of a nonuniform flow ahead of a shock.

It is evident that if the flow field is homoentropic, relation (6.62) can be used instead of the third expression of (6.63).

Next, we will derive the equations of shock dynamics in axially-symmetrical form.

In the case of nonuniform flow ahead of the shock, along any ray tube in the stationary frame of reference, the following relation is also valid

$$\nabla \cdot \left(\frac{\vec{i}}{A} \right) = 0 \quad (6.64)$$

The unit vector along a ray, \vec{i} , may be written as

$$\vec{i} = \frac{(M \cos \theta + m \cos \varepsilon) \vec{e}_x + (M \sin \theta + m \sin \varepsilon) \vec{e}_r}{[M^2 + 2Mm \cos(\theta - \varepsilon) + m^2]^{\frac{1}{2}}} \quad (6.65)$$

where θ and ε are the angles of the normal to the shock and the velocity of the flow ahead of the shock with x -axis, respectively, \vec{e}_x and \vec{e}_r are the unit vectors in x , r directions, respectively. Substituting (6.65) into (6.64), we get

$$\begin{aligned} & \frac{\partial}{\partial x} \left[\frac{r(M \cos \theta + m \cos \varepsilon)}{A(M^2 + 2Mm \cos(\theta - \varepsilon) + m^2)^{\frac{1}{2}}} \right] \\ & + \frac{\partial}{\partial r} \left[\frac{r(M \sin \theta + m \sin \varepsilon)}{A(M^2 + 2Mm \cos(\theta - \varepsilon) + m^2)^{\frac{1}{2}}} \right] = 0 \end{aligned} \quad (6.66)$$

The same method can be used for finding the relation between A and A' , that is,

$$A' \vec{n} \cdot \vec{i} = A \quad (6.67)$$

where

$$\vec{n} = \cos\theta \vec{e}_x + \sin\theta \vec{e}_r.$$

Substituting (6.65) into (6.67), we get

$$\frac{A}{A'} = \frac{M + m\cos(\theta - \varepsilon)}{[M^2 + 2Mm\cos(\theta - \varepsilon) + m^2]^{\frac{1}{2}}} \quad (6.68)$$

Substituting (6.68) into (6.66), we get

$$\frac{\partial}{\partial x} \left[\frac{r(M\cos\theta + m\cos\varepsilon)}{(M + m\cos(\theta - \varepsilon))A'} \right] + \frac{\partial}{\partial r} \left[\frac{r(M\sin\theta + m\sin\varepsilon)}{(M + m\cos(\theta - \varepsilon))A'} \right] = 0 \quad (6.69)$$

Next, we derive another geometrical relation as follows.

The function of shock surface, α , may be expressed in the cylindrical coordinates as

$$\alpha(x, \varphi, r) = t \quad (6.70)$$

or

$$S(x, \varphi, r, t) = \alpha(x, \varphi, r) - t = 0 \quad (6.71)$$

From (6.71), we can obtain

$$U_s = \frac{1}{|\nabla \alpha|} \quad (6.72)$$

where U_s is the absolute velocity of the shock wave in the stationary frame and

$$U_s = [M + m\cos(\theta - \varepsilon)]a \quad (6.73)$$

From (6.72) and (6.73), we have

$$[M + m\cos(\theta - \varepsilon)]a = \frac{1}{|\nabla \alpha|} \quad (6.74)$$

We now derive the relation among M , θ and α in axially-symmetrical flow. The unit vector \vec{n} may be written as

$$\vec{n} = \frac{\nabla \alpha}{|\nabla \alpha|} = [M + m\cos(\theta - \varepsilon)]a(\alpha_x \vec{e}_x + \alpha_r \vec{e}_r) \quad (6.75)$$

and

$$\vec{n} = \cos\theta \vec{e}_x + \sin\theta \vec{e}_r, \quad (6.76)$$

From (6.75) and (6.76), we get

$$\begin{cases} \frac{\partial \alpha}{\partial x} = \frac{\cos \theta}{[M + m \cos(\theta - \varepsilon)]a} \\ \frac{\partial \alpha}{\partial r} = \frac{\sin \theta}{[M + m \cos(\theta - \varepsilon)]a} \end{cases} \quad (6.77)$$

From (6.77), we have

$$\frac{\partial}{\partial x} \left[\frac{\sin \theta}{(M + m \cos(\theta - \varepsilon))a} \right] - \frac{\partial}{\partial r} \left[\frac{\cos \theta}{(M + m \cos(\theta - \varepsilon))a} \right] = 0 \quad (6.78)$$

The area relation may be written as

$$\begin{aligned} -\frac{1}{A'} \left(\frac{\partial A'}{\partial x} + G \frac{\partial A'}{\partial r} \right) &= \left(e \frac{\partial M}{\partial x} + \frac{h}{p} \frac{\partial p}{\partial x} + \frac{g}{a} \frac{\partial a}{\partial x} \right) \\ &\quad + G \left(e \frac{\partial M}{\partial r} + \frac{h}{p} \frac{\partial p}{\partial r} + \frac{g}{a} \frac{\partial a}{\partial r} \right) \end{aligned} \quad (6.79)$$

where

$$G = \frac{M \sin \theta + m \sin \varepsilon}{M \cos \theta + m \cos \varepsilon}$$

Summarizing the above equations, (6.69), (6.78) and (6.79), we can obtain a set of equations for axially-symmetrical flow as follows

$$\begin{cases} \frac{\partial}{\partial x} \left[\frac{r(M \cos \theta + m \cos \varepsilon)}{(M + m \cos(\theta - \varepsilon))A'} \right] + \frac{\partial}{\partial r} \left[\frac{r(M \sin \theta + m \sin \varepsilon)}{(M + m \cos(\theta - \varepsilon))A'} \right] = 0 \\ \frac{\partial}{\partial x} \left[\frac{\sin \theta}{(M + m \cos(\theta - \varepsilon))a} \right] - \frac{\partial}{\partial r} \left[\frac{\cos \theta}{(M + m \cos(\theta - \varepsilon))a} \right] = 0 \\ -\frac{1}{A'} \left(\frac{\partial A'}{\partial x} + G \frac{\partial A'}{\partial r} \right) = \left(e \frac{\partial M}{\partial x} + \frac{h}{p} \frac{\partial p}{\partial x} + \frac{g}{a} \frac{\partial a}{\partial x} \right) \\ \quad + G \left(e \frac{\partial M}{\partial r} + \frac{h}{p} \frac{\partial p}{\partial r} + \frac{g}{a} \frac{\partial a}{\partial r} \right) \end{cases} \quad (6.80)$$

Expanding the first expression of (6.80), we get

$$\begin{aligned} G_s \frac{\partial \theta}{\partial x} - G_c \frac{\partial \theta}{\partial r} - m D_c \frac{\partial M}{\partial x} - m D_s \frac{\partial M}{\partial r} + BC_c \frac{1}{A'} \left(\frac{\partial A'}{\partial x} + G \frac{\partial A'}{\partial r} \right) \\ = \frac{BC_s}{r} - MD_c \frac{\partial m}{\partial x} - MD_s \frac{\partial m}{\partial r} - E_s \frac{\partial \varepsilon}{\partial x} + E_c \frac{\partial \varepsilon}{\partial r} \end{aligned} \quad (6.81)$$

where

$$B = M + m \cos(\theta - \varepsilon),$$

$$C_c = M \cos \theta + m \cos \varepsilon,$$

$$C_s = M \sin \theta + m \sin \varepsilon,$$

$$D_c = \cos(\theta - \varepsilon) \cos \theta - \cos \varepsilon,$$

$$D_s = \cos(\theta - \varepsilon) \sin \theta - \sin \varepsilon,$$

$$E_c = [Mm\cos\epsilon - Mm\sin\theta\sin(\theta - \epsilon) + m^2\cos\theta],$$

$$E_s = [Mm\sin\epsilon + Mm\cos\theta\sin(\theta - \epsilon) + m^2\sin\theta],$$

$$G_c = [M^2\cos\theta + Mm\cos\epsilon + m^2\sin\theta\sin(\theta - \epsilon)],$$

$$G_s = [M^2\sin\theta + Mm\sin\epsilon - m^2\cos\theta\sin(\theta - \epsilon)].$$

Under the condition of homoentropic, steady flow ahead of the shock, the third expression of (6.80) can be expressed as

$$\frac{1}{A'} \left(\frac{\partial A'}{\partial x} + G \frac{\partial A'}{\partial r} \right) = - \left[\left(e \frac{\partial M}{\partial x} - f \frac{\partial m}{\partial x} \right) + G \left(e \frac{\partial M}{\partial r} - f \frac{\partial m}{\partial r} \right) \right] \quad (6.82)$$

where e and f have the same meaning as (6.62).

Substituting (6.82) into (6.81), we can eliminate $\frac{1}{A'} \left(\frac{\partial A'}{\partial x} + G \frac{\partial A'}{\partial r} \right)$ and obtain the following relation

$$\begin{aligned} & G_s \frac{\partial \theta}{\partial x} - G_c \frac{\partial \theta}{\partial r} - (mD_c + BC_c e) \frac{\partial M}{\partial x} - (mD_s + BC_s e) \frac{\partial M}{\partial r} \\ &= \frac{BC_s}{r} - (MD_c + BC_c f) \frac{\partial m}{\partial x} - (MD_s + BC_s f) \frac{\partial m}{\partial r} - E_s \frac{\partial \epsilon}{\partial x} + E_c \frac{\partial \epsilon}{\partial r} \end{aligned} \quad (6.83)$$

Expanding the second expression of (6.80), we get

$$\begin{aligned} & C_c \frac{\partial \theta}{\partial x} + C_s \frac{\partial \theta}{\partial r} - \sin\theta \frac{\partial M}{\partial x} + \cos\theta \frac{\partial M}{\partial r} \\ &= \cos(\theta - \epsilon) \left(\sin\theta \frac{\partial m}{\partial x} - \cos\theta \frac{\partial m}{\partial r} \right) + m\sin(\theta - \epsilon) \left(\sin\theta \frac{\partial \epsilon}{\partial x} - \cos\theta \frac{\partial \epsilon}{\partial r} \right) \\ &+ \left(\frac{B}{a} \right) \left(\sin\theta \frac{\partial a}{\partial x} - \cos\theta \frac{\partial a}{\partial r} \right) \end{aligned} \quad (6.84)$$

From (6.61), we have

$$\begin{cases} \frac{1}{a} \frac{\partial a}{\partial x} = - \frac{(\gamma - 1)m}{2T} \frac{\partial m}{\partial x} \\ \frac{1}{a} \frac{\partial a}{\partial r} = - \frac{(\gamma - 1)m}{2T} \frac{\partial m}{\partial r} \end{cases} \quad (6.85)$$

$$\text{where } T = 1 + \frac{\gamma - 1}{2} m^2.$$

Substituting (6.85) into (6.84), and combining (6.83), we get the expanded equations for a nonuniform, steady, and homoentropic flow ahead of a shock as follows

$$\left\{ \begin{array}{l} C_c \frac{\partial \theta}{\partial x} + C_s \frac{\partial \theta}{\partial r} - \sin \theta \frac{\partial M}{\partial x} + \cos \theta \frac{\partial M}{\partial r} \\ = \left[\cos(\theta - \varepsilon) - \frac{(\gamma - 1)mB}{2T} \right] \left(\sin \theta \frac{\partial m}{\partial x} - \cos \theta \frac{\partial m}{\partial r} \right) \\ + \sin(\theta - \varepsilon) \cdot m \left(\sin \theta \frac{\partial \varepsilon}{\partial x} - \cos \theta \frac{\partial \varepsilon}{\partial r} \right) \\ G_s \frac{\partial \theta}{\partial x} - G_c \frac{\partial \theta}{\partial r} - (mD_c + BC_c e) \frac{\partial M}{\partial x} - (mD_s + BC_s e) \frac{\partial M}{\partial r} \\ = \frac{BC_s}{r} - (MD_c + BC_c f) \frac{\partial m}{\partial x} - (MD_s + BC_s f) \frac{\partial m}{\partial r} \\ - E_s \frac{\partial \varepsilon}{\partial x} + E_c \frac{\partial \varepsilon}{\partial r} \end{array} \right. \quad (6.86)$$

If the term $\frac{BC_s}{r}$ is deleted and the coordinate y is used instead of r , we can obtain the equations for plane flow.

If the flow Mach number m and flow angle ε in the region ahead of the shock remain constant, the two-dimensional equations can be written as

$$\left\{ \begin{array}{l} C_c \frac{\partial \theta}{\partial x} + C_s \frac{\partial \theta}{\partial y} - \sin \theta \frac{\partial M}{\partial x} + \cos \theta \frac{\partial M}{\partial y} = 0 \\ G_s \frac{\partial \theta}{\partial x} - G_c \frac{\partial \theta}{\partial y} - (mD_c + BC_c e) \frac{\partial M}{\partial x} - (mD_s + BC_s e) \frac{\partial M}{\partial y} = 0 \end{array} \right. \quad (6.87)$$

If the flow direction ahead of the shock is the same as x -axis, that is, $\varepsilon = 0$, we can obtain the following equations, which are the same as (5.70),

$$\left\{ \begin{array}{l} C_c \frac{\partial \theta}{\partial x} + C_s \frac{\partial \theta}{\partial y} - \sin \theta \frac{\partial M}{\partial x} + \cos \theta \frac{\partial M}{\partial y} = 0 \\ (M^2 - m^2) \sin \theta \frac{\partial \theta}{\partial x} - M(M \cos \theta + m) \frac{\partial \theta}{\partial y} \\ + (m \sin^2 \theta - BC_c e) \frac{\partial M}{\partial x} - (m \sin \theta \cos \theta + BC_s e) \frac{\partial M}{\partial y} = 0 \end{array} \right. \quad (6.88)$$

By comparing (6.87) with (6.86), we find out that in the case of nonuniform flow ahead of the shock, the equations have not only the variables $m(x, r)$, $\varepsilon(x, r)$, but also the terms $\frac{\partial m}{\partial x}$, $\frac{\partial m}{\partial r}$, $\frac{\partial \varepsilon}{\partial x}$ and $\frac{\partial \varepsilon}{\partial r}$.

In the case of a quiescent gas ahead of a shock, the equations (6.63) and (6.86) may be further simplified, and the same equations as (4.66), (4.67) and (3.35) can be obtained.

Now we will derive the two-dimensional characteristic relations.

The two-dimensional equations of shock dynamics may be written as

$$\left\{ \begin{array}{l} C_c \frac{\partial \theta}{\partial x} + C_s \frac{\partial \theta}{\partial y} - \sin \theta \frac{\partial M}{\partial x} + \cos \theta \frac{\partial M}{\partial y} = L \\ G_s \frac{\partial \theta}{\partial x} - G_c \frac{\partial \theta}{\partial y} - (mD_c + BC_c e) \frac{\partial M}{\partial x} \end{array} \right. \quad (6.89)$$

$$\left. \begin{array}{l} - (mD_s + BC_s e) \frac{\partial M}{\partial y} = N \end{array} \right. \quad (6.90)$$

where

$$L = L_1 \frac{\partial m}{\partial x} - L_2 \frac{\partial m}{\partial y} + L_3 \frac{\partial \varepsilon}{\partial x} - L_4 \frac{\partial \varepsilon}{\partial y}$$

$$\left\{ \begin{array}{l} L_1 = \left[\cos(\theta - \varepsilon) - \frac{(\gamma - 1)mB}{2T} \right] \sin \theta \\ L_2 = \left[\cos(\theta - \varepsilon) - \frac{(\gamma - 1)mB}{2T} \right] \cos \theta \end{array} \right.$$

$$L_3 = m \sin(\theta - \varepsilon) \sin \theta$$

$$L_4 = m \sin(\theta - \varepsilon) \cos \theta$$

$$N = -N_1 \frac{\partial m}{\partial x} - N_2 \frac{\partial m}{\partial y} - N_3 \frac{\partial \varepsilon}{\partial x} + N_4 \frac{\partial \varepsilon}{\partial y}$$

$$\left\{ \begin{array}{l} N_1 = (mD_c + BC_c f) \\ N_2 = (mD_s + BC_s f) \end{array} \right.$$

$$N_3 = E_s$$

$$N_4 = E_c$$

Multiplying (6.89) by Z , adding (6.90) to it, we get

$$\begin{aligned} & (ZC_c + G_s) \frac{\partial \theta}{\partial x} + (ZC_s - G_c) \frac{\partial \theta}{\partial y} - [(BC_c e + mD_c) + Z \sin \theta] \frac{\partial M}{\partial x} \\ & + [Z \cos \theta - (mD_s + BC_s e)] \frac{\partial M}{\partial y} = ZL + N \end{aligned} \quad (6.91)$$

The same method as adopted in Chapter 5 can be used for finding Z , that is, (6.91) may be written as

$$\left[\frac{\partial \theta}{\partial x} + \left(\frac{dy}{dx} \right) \frac{\partial \theta}{\partial y} \right] + F_1 \left[\frac{\partial M}{\partial x} + \left(\frac{dy}{dx} \right) \frac{\partial M}{\partial y} \right] = F_2 \quad (6.92)$$

By comparing (6.92) with (6.91), we get

$$\frac{dy}{dx} = \frac{ZC_s - G_c}{ZC_c + G_s} = \frac{Z \cos \theta - (mD_s + BC_s e)}{-(BC_c e + mD_c) - Z \sin \theta} \quad (6.93)$$

$$F_1 = \frac{-(BC_c e + mD_c) - Z \sin \theta}{ZC_c + G_s} \quad (6.94)$$

$$F_2 = \frac{ZL + N}{ZC_c + G_s} = R_1 \frac{\partial m}{\partial x} + R_2 \frac{\partial m}{\partial y} + R_3 \frac{\partial \varepsilon}{\partial x} + R_4 \frac{\partial \varepsilon}{\partial y} \quad (6.95)$$

where

$$\begin{aligned} R_1 &= \frac{ZL_1 - N_1}{ZC_c + G_s}, & R_2 &= -\frac{ZL_2 + N_2}{ZC_c + G_s} \\ R_3 &= \frac{ZL_3 - N_3}{ZC_c + G_s}, & R_4 &= -\frac{ZL_4 + N_4}{ZC_c + G_s} \end{aligned}$$

From (6.93), solving for Z , we get

$$Z = m\sin(\theta - \varepsilon) \mp B\sqrt{Me} \quad (6.96)$$

Substituting $Z = m\sin(\theta - \varepsilon) - B\sqrt{Me}$ into (9.63) and (9.64), we get

$$\frac{dy}{dx} = \tan(\theta + v_1) \quad (6.97)$$

where

$$\begin{aligned} \tan v_1 &= \frac{\left[\frac{1}{2}(M^2 - 1)K(M) \right]^{\frac{1}{2}} - m\sin(\theta - \varepsilon)}{M + m\cos(\theta - \varepsilon)} \\ F_1 &= \sqrt{\frac{e}{M}} = \left[\frac{2}{(M^2 - 1)K(M)} \right]^{\frac{1}{2}} = \omega(M) \end{aligned} \quad (6.98)$$

Substituting $Z = m\sin(\theta - \varepsilon) + B\sqrt{Me}$ into (9.63) and (9.64), we get

$$\frac{dy}{dx} = \tan(\theta - v_2) \quad (6.99)$$

where

$$\begin{aligned} \tan v_2 &= \frac{\left[\frac{1}{2}(M^2 - 1)K(M) \right]^{\frac{1}{2}} + m\sin(\theta - \varepsilon)}{M + m\cos(\theta - \varepsilon)} \\ F_1 &= -\sqrt{\frac{e}{M}} = -\left[\frac{2}{(M^2 - 1)K(M)} \right]^{\frac{1}{2}} = -\omega(M) \end{aligned} \quad (6.100)$$

Substituting (6.96) into (6.95), we get

$$F_{2i} = R_{1i} \frac{\partial m}{\partial x} + R_{2i} \frac{\partial m}{\partial y} + R_{3i} \frac{\partial \varepsilon}{\partial x} + R_{4i} \frac{\partial \varepsilon}{\partial y} \quad (6.101)$$

where

$$\begin{aligned}
R_{1i} &= \frac{1}{R_i} \left\{ [m \sin(\theta - \varepsilon) \mp B \sqrt{M e}] \left[\cos(\theta - \varepsilon) - \frac{(\gamma - 1)mB}{2T} \right] \sin\theta \right. \\
&\quad \left. - (MD_c + BC_c f) \right\} \\
R_{2i} &= -\frac{1}{R_i} \left\{ [m \sin(\theta - \varepsilon) \mp B \sqrt{M e}] \left[\cos(\theta - \varepsilon) - \frac{(\gamma - 1)mB}{2T} \right] \cos\theta \right. \\
&\quad \left. + (MD_s + BC_s f) \right\} \\
R_{3i} &= \frac{1}{R_i} \{ [m \sin(\theta - \varepsilon) \mp B \sqrt{M e}] m \sin(\theta - \varepsilon) \sin\theta - E_s \} \\
R_{4i} &= -\frac{1}{R_i} \{ [m \sin(\theta - \varepsilon) \mp B \sqrt{M e}] m \sin(\theta - \varepsilon) \cos\theta - E_c \} \\
R_i &= B(M \sin\theta \mp C_c \sqrt{M e})
\end{aligned}$$

In the above expressions, the subscript $i = 1$ corresponds to the symbol “-”; $i = 2$ corresponds to the symbol “+”.

Now, we can write the characteristic relations as follows

$$\left\{
\begin{array}{l}
\left(\frac{d\theta}{dx} \right)_1 + \omega(M) \left(\frac{dM}{dx} \right)_1 = R_{11} \frac{\partial m}{\partial x} + R_{21} \frac{\partial m}{\partial y} + R_{31} \frac{\partial \varepsilon}{\partial x} + R_{41} \frac{\partial \varepsilon}{\partial y} \\
\text{along } \left(\frac{dy}{dx} \right)_1 = \tan(\theta + v_1) \\
\left(\frac{d\theta}{dx} \right)_2 - \omega(M) \left(\frac{dM}{dx} \right)_2 = R_{12} \frac{\partial m}{\partial x} + R_{22} \frac{\partial m}{\partial y} + R_{32} \frac{\partial \varepsilon}{\partial x} + R_{42} \frac{\partial \varepsilon}{\partial y} \\
\text{along } \left(\frac{dy}{dx} \right)_2 = \tan(\theta - v_2)
\end{array} \right. \quad (6.102)$$

It follows from (6.102) that the difference of the equations of the characteristics between uniform and nonuniform flows ahead of shocks is the terms on the right-hand side of the equations. For the uniform flow, the terms on the right-hand side of the equations are equal to zero; for the nonuniform flow, the terms on the right-hand side are not equal to zero.

In this chapter, the transient transformation of coordinates in the infinitesimal fluid element may be used for establishing the geometrical relations and the area relation.

In next chapter, for three-dimensional equations of shock dynamics, another method can be used for establishing the geometrical equations, the same method as adopted in this chapter will be used for deriving the area relation.

§ 6.8 Shock wave-vortex interaction

Shock wave-vortex interaction is an important topic. In this section, we will use shock dynamics to study the shock wave-vortex interaction. Han and Chow (1991) presented the basic idea and method for the two-dimensional interaction.

We know that the equations (6.63) or their expanded expressions are two-dimensional shock dynamics equations, which are suitable for the nonuniform flow ahead of the shock wave. The parameters in the flow field ahead of the shock are flow Mach number $m = m(x, y)$, flow angle $\varepsilon = \varepsilon(x, y)$, pressure $p = p(x, y)$, and speed of sound $a = a(x, y)$.

Now what we want to study is that a moving shock propagates through the flow field of a vortex which is originally located at somewhere ahead of the shock. Therefore the flow field ahead of the shock is nonuniform and non-isentropic (inside the core of the vortex).

1. Vortex flow field ahead of the moving shock wave

If a vortex, whose strength is given as K , is placed at the origin (0,0). The distribution of velocity in the flow field outside and inside the core of the vortex can be expressed as follows

$$\begin{cases} V_r = 0 \\ V_\varphi = \begin{cases} \frac{K}{r} & r > r_1 \\ \omega r & r < r_1 \end{cases} \end{cases} \quad (6.103)$$

where ω is the angular velocity, and r_1 is the radius of the vortex core.

The flow field inside the core is regarded as solid-body rotation; the flow field outside the core is an irrotational one, as shown in Fig. 6.3

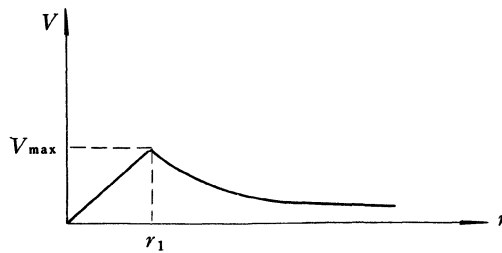


Fig. 6.3 The velocity distribution in the vortex flow

If the radius of core, r_1 , is given, we have

$$\omega = \frac{K}{r_1^2} \quad (6.104)$$

In order to obtain the expressions for V , ε and their derivatives in rectangular coordinate system, if the rotation of vortex, for example, is counter-clockwise, the distribution of velocity can be written as

$$V = \frac{K}{\sqrt{x^2 + y^2}} \quad r > r_1 \quad (6.105)$$

$$V = \omega \sqrt{x^2 + y^2} \quad r < r_1 \quad (6.106)$$

and the flow angle ε can be expressed as

$$\varepsilon = \frac{\pi}{2} + \tan^{-1} \frac{y}{x} \quad (6.107)$$

If the velocity of vortex flow, V , is very low, for example, the flow Mach number, m , is less than the order of $0.2 \sim 0.3$, the speed of sound may be considered as a constant. The expressions for the flow Mach number can be written from relations (6.105) and (6.106) as follows

$$m = \frac{Q}{\sqrt{x^2 + y^2}} \quad r > r_1 \quad (6.108)$$

$$m = Q_1 \sqrt{x^2 + y^2} \quad r < r_1 \quad (6.109)$$

where $Q = \frac{K}{a}$, $Q_1 = \frac{\omega}{a}$, a is the speed of sound, which is a constant.

The derivatives for m and ε are taken with respect to x and y , respectively

$$\begin{cases} \frac{\partial m}{\partial x} = - \frac{Qx}{\sqrt{(x^2 + y^2)^3}} \\ \frac{\partial m}{\partial y} = - \frac{Qy}{\sqrt{(x^2 + y^2)^3}} \end{cases} \quad (r > r_1) \quad (6.110)$$

$$\begin{cases} \frac{\partial m}{\partial x} = \frac{Q_1 x}{\sqrt{x^2 + y^2}} \\ \frac{\partial m}{\partial y} = \frac{Q_1 y}{\sqrt{x^2 + y^2}} \end{cases} \quad (r < r_1) \quad (6.111)$$

$$\frac{\partial \varepsilon}{\partial x} = - \frac{y}{x^2 + y^2}, \quad \frac{\partial \varepsilon}{\partial y} = \frac{x}{x^2 + y^2} \quad (6.112)$$

As mentioned already, $\frac{\partial a}{\partial x}$ and $\frac{\partial a}{\partial y}$ are equal to zero. $\frac{\partial p}{\partial x}$ and $\frac{\partial p}{\partial y}$ can be

obtained by means of the relation between p and V . Of course, the relations inside and outside the vortex core are different.

2. The governing equations for a shock wave moving into a vortex flow

By substituting the relations for the given flow field ahead of the moving shock into the two-dimensional, shock dynamic equations, we can obtain the governing equations, that is, substituting the relations (6.108) through (6.112) and the expressions for $\frac{\partial p}{\partial x}$ and $\frac{\partial p}{\partial y}$ into the equations (6.63), we can obtain the following equations

$$\begin{cases} A_1 \frac{\partial \theta}{\partial x} + A_2 \frac{\partial \theta}{\partial y} + A_3 \frac{\partial M}{\partial x} + A_4 \frac{\partial M}{\partial y} = A_5 \\ B_1 \frac{\partial \theta}{\partial x} + B_2 \frac{\partial \theta}{\partial y} + B_3 \frac{\partial M}{\partial x} + B_4 \frac{\partial M}{\partial y} = B_5 \end{cases} \quad (6.113)$$

where A_i , B_i ($i = 1, 2, 3, 4, 5$) are the function of x , y , M and θ . Obviously, these coefficients of functions inside and outside the core are different.

By using the equations (6.113) and the corresponding characteristic relations like (6.102), and considering the boundary conditions on the upper, lower and left hand sides, where $M = M_0$, $\theta = \theta_0$, $m = 0$, if r is large enough, we can find the distribution of $M = M(x, y)$ and $\theta = \theta(x, y)$. But our purpose is to find the shape of the moving shock as it moves rightward, so the following is needed.

3. Shape of shock surface

We know that the equation of shock surface may be expressed as $\alpha(x, y) = t$ (6.16), where $\alpha = \alpha(x, y)$ is the function of shock surface. $\alpha(x, y) = \text{constant}$ represents the shape of shock surface at a certain time.

By integrating the differential equations of (6.47) and (6.48), we can obtain the function $\alpha(x, y)$ and the equation of shock surface, but this is complicated.

Next we take another way to do this.

If the expression for $\alpha(x, y)$ is given

$$\alpha = \alpha(x, y) \quad (6.114)$$

the isoline for $\alpha(x, y)$ must satisfy the following relation

$$\frac{d\alpha}{ds} = 0 \quad (6.115)$$

where the curve s is an isoline for α . The relation (6.115) can be rewritten as

$$\vec{\tau} \cdot \text{grad}\alpha = 0 \quad (6.116)$$

where $\vec{\tau}$ is the unit vector of the tangent to the isoline, and $\vec{\tau}$ can be expressed, in two-dimensional case, as

$$\vec{n} = \cos\gamma \vec{i} + \sin\gamma \vec{j}$$

where γ is the angle between the tangent to the curves and x -axis.

From relation (6.116), we obtain

$$\frac{dy}{dx} = \tan \gamma = -\frac{\frac{\partial \alpha}{\partial x}}{\frac{\partial \alpha}{\partial y}} \quad (6.117)$$

Substituting the expressions (6.46) and (6.47) for $\frac{\partial \alpha}{\partial x}$ and $\frac{\partial \alpha}{\partial y}$ into (6.117),

the isoline for α can be obtained in the following form

$$\frac{dy}{dx} = -\cot\theta(x, y) \quad (6.118)$$

where θ is the shock angle, which is the function of x, y .

Now the problem for finding the shape of shock surface is transferred to solve an initial value problem. If $\theta = \theta(x, y)$ is obtained from the equations (6.113), by using the value of θ at any particular point, we can find out an isoline for α at the given time.

It should be noted that by using the shock dynamic method, we can only find the shape of shock surface, shock strength and orientation along the shock surface at any given time. If we want to find the flow field behind the shock wave, the combination of shock dynamics with the equations of gasdynamics is necessary.

Chapter 7 Three-Dimensional Equations for a Nonuniform Moving Gas Ahead of a Shock Wave

In Chapter 6, by means of the transient transformation of coordinates in infinitesimal fluid element ahead of the shock, we have derived the geometric relations; by using the concept of ray tube in moving frame of reference, we have obtained the area relation. In this chapter, we will derive three-dimensional geometric relations by using the expression for \vec{i} derived in Chapter 6, the area relation will be derived by using the same method as § 6.6.

§ 7.1 Three-dimensional shock propagating into a nonuniform flow field

A three-dimensional shock propagating into a nonuniform flow field is illustrated in Fig. 7.1.

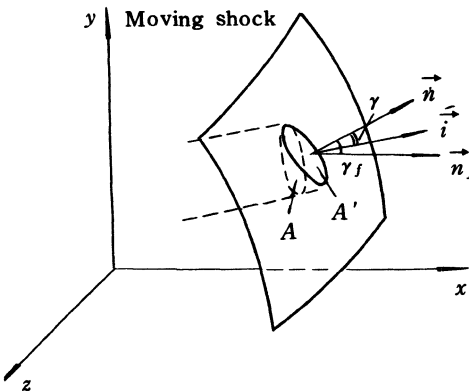


Fig. 7.1 Three-dimensional shock propagating into nonuniform flow field

In Chapter 6, we have obtained the expression for \vec{i} in two-dimensional flows as

$$\vec{i} = \frac{\vec{M} + \vec{m}}{|\vec{M} + \vec{m}|} \quad (7.1)$$

Now we want to extend this result to three-dimensional flows, that is,

$$\vec{M} = M \vec{n}, \vec{m} = m \vec{n}_f \quad (7.2)$$

In three-dimensional flows, \vec{n} and \vec{n}_f can be expressed as

$$\vec{n} = \cos \theta_1 \vec{e}_x + \cos \theta_2 \vec{e}_y + \cos \theta_3 \vec{e}_z \quad (7.3)$$

$$\vec{n}_f = \cos \varepsilon_1 \vec{e}_x + \cos \varepsilon_2 \vec{e}_y + \cos \varepsilon_3 \vec{e}_z \quad (7.4)$$

where θ_1, θ_2 and θ_3 are the angles between the unit vector \vec{i} and x, y, z directions, respectively; $\varepsilon_1, \varepsilon_2$ and ε_3 are the angles between the direction of the flow ahead of the shock and x, y, z directions, respectively.

It is evident that

$$\cos^2 \theta_1 + \cos^2 \theta_2 + \cos^2 \theta_3 = 1 \quad (7.5)$$

$$\cos^2 \varepsilon_1 + \cos^2 \varepsilon_2 + \cos^2 \varepsilon_3 = 1 \quad (7.6)$$

From (7.2), (7.3), and (7.4), we have

$$\begin{aligned} \vec{M} + \vec{m} &= (M \cos \theta_1 + m \cos \varepsilon_1) \vec{e}_x + (M \cos \theta_2 + m \cos \varepsilon_2) \vec{e}_y + (M \cos \theta_3 \\ &\quad + m \cos \varepsilon_3) \vec{e}_z \end{aligned} \quad (7.7)$$

From (7.7), we have

$$\begin{aligned} N &= |\vec{M} + \vec{m}| \\ &= [M^2 + m^2 + 2Mm(\cos \theta_1 \cos \varepsilon_1 + \cos \theta_2 \cos \varepsilon_2 + \cos \theta_3 \cos \varepsilon_3)]^{1/2} \end{aligned} \quad (7.8)$$

$$\begin{aligned} \vec{i} &= \frac{1}{N} [(M \cos \theta_1 + m \cos \varepsilon_1) \vec{e}_x + (M \cos \theta_2 + m \cos \varepsilon_2) \vec{e}_y \\ &\quad + (M \cos \theta_3 + m \cos \varepsilon_3) \vec{e}_z] \end{aligned} \quad (7.9)$$

From (7.3) and (7.9), we get

$$\vec{n} \cdot \vec{i} = \frac{L}{N} = \cos \gamma \quad (7.10)$$

where

$$L = M + m(\cos \theta_1 \cos \varepsilon_1 + \cos \theta_2 \cos \varepsilon_2 + \cos \theta_3 \cos \varepsilon_3)$$

In Fig. 7.1, A' is the area of shock surface cut out by the ray tube in a stationary frame of reference. A is the cross-sectional area along the ray tube. We have the following relation

$$A = A' \cos \gamma = A' \vec{n} \cdot \vec{i} \quad (7.11)$$

$$AN = A'L \quad (7.12)$$

§ 7.2 Transient transformation of coordinates in three-dimensional flow

In the case of three-dimensional flow, the nonuniform flow field immediately ahead of the shock surface can be divided into a lot of small regions. In each region, transient transformation of coordinates can be made for establishing the equations of shock dynamics.

In the moving frame of reference, which attached to any small region, the equation of shock surface can be written as

$$\alpha'(x', y', z') = t' \quad (7.13)$$

In the stationary frame of reference, the equation of shock surface can be written as

$$\alpha(x, y, z) = t \quad (7.14)$$

The relation between the two coordinates is expressed as

$$\begin{cases} x = x' + U \cos \varepsilon_1 \cdot t' \\ y = y' + U \cos \varepsilon_2 \cdot t' \\ z = z' + U \cos \varepsilon_3 \cdot t' \\ t = t' \end{cases} \quad (7.15)$$

From (7.13), (7.14) and (7.15), we have

$$\alpha'(x', y', z') = \alpha(x, y, z) \quad (7.16)$$

Substituting (7.14) into (7.15), we have

$$\begin{cases} x = x' + m \cos \varepsilon_1 \cdot \alpha(x, y, z) = x' + Q_1 \cdot \alpha(x, y, z) \\ y = y' + m \cos \varepsilon_2 \cdot \alpha(x, y, z) = y' + Q_2 \cdot \alpha(x, y, z) \\ z = z' + m \cos \varepsilon_3 \cdot \alpha(x, y, z) = z' + Q_3 \cdot \alpha(x, y, z) \end{cases} \quad (7.17)$$

According to the above functional relations between the two coordinates, we can written

$$\begin{cases} \frac{\partial}{\partial x'} = \frac{\partial}{\partial x} \cdot \frac{\partial x}{\partial x'} + \frac{\partial}{\partial y} \cdot \frac{\partial y}{\partial x'} + \frac{\partial}{\partial z} \cdot \frac{\partial z}{\partial x'} \\ \frac{\partial}{\partial y'} = \frac{\partial}{\partial x} \cdot \frac{\partial x}{\partial y'} + \frac{\partial}{\partial y} \cdot \frac{\partial y}{\partial y'} + \frac{\partial}{\partial z} \cdot \frac{\partial z}{\partial y'} \\ \frac{\partial}{\partial z'} = \frac{\partial}{\partial x} \cdot \frac{\partial x}{\partial z'} + \frac{\partial}{\partial y} \cdot \frac{\partial y}{\partial z'} + \frac{\partial}{\partial z} \cdot \frac{\partial z}{\partial z'} \end{cases} \quad (7.18)$$

In order to obtain $\frac{\partial x}{\partial x'}, \frac{\partial x}{\partial y'}, \frac{\partial x}{\partial z'}, \frac{\partial y}{\partial x'}, \frac{\partial y}{\partial y'}, \frac{\partial y}{\partial z'}, \frac{\partial z}{\partial x'}, \frac{\partial z}{\partial y'}, \frac{\partial z}{\partial z'}$, we take the derivatives of (7.17) with respect to x', y', z' , respectively, and consider that Q_1 , Q_2 , and Q_3 in each small region are constant. The following relations refer to the derivatives of (7.17) with respect to x' .

$$\begin{cases} \frac{\partial x}{\partial x'} = \frac{\partial x'}{\partial x'} + Q_1(\alpha_x \cdot \frac{\partial x}{\partial x'} + \alpha_y \cdot \frac{\partial y}{\partial x'} + \alpha_z \cdot \frac{\partial z}{\partial x'}) \\ \frac{\partial y}{\partial x'} = \frac{\partial y'}{\partial x'} + Q_2(\alpha_x \cdot \frac{\partial x}{\partial x'} + \alpha_y \cdot \frac{\partial y}{\partial x'} + \alpha_z \cdot \frac{\partial z}{\partial x'}) \\ \frac{\partial z}{\partial x'} = \frac{\partial z'}{\partial x'} + Q_3(\alpha_x \cdot \frac{\partial x}{\partial x'} + \alpha_y \cdot \frac{\partial y}{\partial x'} + \alpha_z \cdot \frac{\partial z}{\partial x'}) \end{cases} \quad (7.19)$$

Letting $X_1 = \frac{\partial x}{\partial x'}$, $Y_1 = \frac{\partial y}{\partial x'}$, $Z_1 = \frac{\partial z}{\partial x'}$ and noting $\frac{\partial x'}{\partial x'} = 1$, $\frac{\partial y'}{\partial x'} = 0$,

$\frac{\partial z'}{\partial x'} = 0$, we may rewrite (7.19) in the following form

$$\begin{cases} (1 - Q_1 \alpha_x) X_1 - Q_1 \alpha_y Y_1 - Q_1 \alpha_z Z_1 = 1 \\ Q_2 \alpha_x X_1 + (Q_2 \alpha_y - 1) Y_1 + Q_2 \alpha_z Z_1 = 0 \\ Q_3 \alpha_x X_1 + Q_3 \alpha_y Y_1 + (Q_3 \alpha_z - 1) Z_1 = 0 \end{cases} \quad (7.20)$$

From equations (7.20), we get

$$\begin{cases} X_1 = \frac{D_{x1}}{D} \\ Y_1 = \frac{D_{y1}}{D} \\ Z_1 = \frac{D_{z1}}{D} \end{cases} \quad (7.21)$$

where

$$D = \begin{vmatrix} (1 - Q_1 \alpha_x) & -Q_1 \alpha_y & -Q_1 \alpha_z \\ Q_2 \alpha_x & (Q_2 \alpha_y - 1) & Q_2 \alpha_z \\ Q_3 \alpha_x & Q_3 \alpha_y & (Q_3 \alpha_z - 1) \end{vmatrix} = 1 - Q_1 \alpha_x - Q_2 \alpha_y - Q_3 \alpha_z$$

$$D_{x1} = \begin{vmatrix} 1 & -Q_1 \alpha_y & -Q_1 \alpha_z \\ 0 & (Q_2 \alpha_y - 1) & Q_2 \alpha_z \\ 0 & Q_3 \alpha_y & (Q_3 \alpha_z - 1) \end{vmatrix} = 1 - Q_2 \alpha_y - Q_3 \alpha_z$$

$$D_{y1} = Q_2 \alpha_x$$

$$D_{z1} = Q_3 \alpha_x$$

or, we have

$$\begin{cases} \frac{\partial x}{\partial x'} = X_1 = \frac{1 - Q_2 \alpha_y - Q_3 \alpha_z}{1 - Q_1 \alpha_x - Q_2 \alpha_y - Q_3 \alpha_z} \\ \frac{\partial y}{\partial x'} = Y_1 = \frac{Q_2 \alpha_x}{1 - Q_1 \alpha_x - Q_2 \alpha_y - Q_3 \alpha_z} \\ \frac{\partial z}{\partial x'} = Z_1 = \frac{Q_3 \alpha_x}{1 - Q_1 \alpha_x - Q_2 \alpha_y - Q_3 \alpha_z} \end{cases} \quad (7.22)$$

The same method can be used for taking derivatives of (7.17) with respect to y' and z' , respectively. Letting $X_2 = \frac{\partial x}{\partial y'}$, $Y_2 = \frac{\partial y}{\partial y'}$, $Z_2 = \frac{\partial z}{\partial y'}$, $X_3 = \frac{\partial x}{\partial z'}$, $Y_3 = \frac{\partial y}{\partial z'}$, $Z_3 = \frac{\partial z}{\partial z'}$ and noting $\frac{\partial x'}{\partial y'} = 0$, $\frac{\partial y'}{\partial y'} = 1$, $\frac{\partial z'}{\partial y'} = 0$, $\frac{\partial x'}{\partial z'} = 0$, $\frac{\partial y'}{\partial z'} = 1$, we get

$$\begin{cases} (Q_1 \alpha_x - 1)X_2 + Q_1 \alpha_y Y_2 + Q_1 \alpha_z Z_2 = 0 \\ -Q_2 \alpha_x X_2 + (1 - Q_2 \alpha_y)Y_2 - Q_2 \alpha_z Z_2 = 1 \\ Q_3 \alpha_x X_2 + Q_3 \alpha_y Y_2 + (Q_3 \alpha_z - 1)Z_2 = 0 \end{cases} \quad (7.23)$$

$$\begin{cases} X_2 = \frac{D_{x2}}{D} \\ Y_2 = \frac{D_{y2}}{D} \\ Z_2 = \frac{D_{z2}}{D} \end{cases} \quad (7.24)$$

where D is the same as (7.21)

$$\begin{aligned} D_{x2} &= Q_1 \alpha_y \\ D_{y2} &= 1 - Q_1 \alpha_x - Q_3 \alpha_z \\ D_{z2} &= Q_3 \alpha_y \end{aligned}$$

and

$$\begin{cases} (Q_1 \alpha_x - 1)X_3 + Q_1 \alpha_y Y_3 + Q_1 \alpha_z Z_3 = 0 \\ Q_2 \alpha_x X_3 + (Q_2 \alpha_y - 1)Y_3 + Q_2 \alpha_z Z_3 = 0 \\ -Q_3 \alpha_x X_3 - Q_3 \alpha_y Y_3 + (1 - Q_3 \alpha_z)Z_3 = 1 \end{cases} \quad (7.25)$$

$$\begin{cases} X_3 = D_{x3} / D \\ Y_3 = D_{y3} / D \\ Z_3 = D_{z3} / D \end{cases} \quad (7.26)$$

where D is the same as (7.21)

$$D_{x3} = Q_1 \alpha_z$$

$$D_{y3} = Q_2 \alpha_z$$

$$D_{z3} = 1 - Q_1 \alpha_x - Q_2 \alpha_y$$

Substituting (7.21), (7.24), (7.26) into (7.18), we obtain following relations

$$\begin{cases} \frac{\partial}{\partial x'} = \frac{1}{D} \cdot (D_{x_1} \cdot \frac{\partial}{\partial x} + D_{y_1} \cdot \frac{\partial}{\partial y} + D_{z_1} \cdot \frac{\partial}{\partial z}) \\ \frac{\partial}{\partial y'} = \frac{1}{D} \cdot (D_{x_2} \cdot \frac{\partial}{\partial x} + D_{y_2} \cdot \frac{\partial}{\partial y} + D_{z_2} \cdot \frac{\partial}{\partial z}) \\ \frac{\partial}{\partial z'} = \frac{1}{D} \cdot (D_{x_3} \cdot \frac{\partial}{\partial x} + D_{y_3} \cdot \frac{\partial}{\partial y} + D_{z_3} \cdot \frac{\partial}{\partial z}) \end{cases} \quad (7.27)$$

The above results apply to rectangular coordinate system.

Next, we will discuss a very important problem, that is, we want to know whether the above derivation on the transformation of coordinates from moving frame to stationary one in rectangular coordinate system can be extended to orthogonal curvilinear coordinate system. Let $\vec{e}_1, \vec{e}_2, \vec{e}_3$ be the unit vectors of orthogonal curvilinear coordinates system in a stationary frame and $\vec{e}'_1, \vec{e}'_2, \vec{e}'_3$ be the unit vectors in a moving frame. We can see one of the orthogonal curvilinear coordinates, for example, spherical coordinates as shown in Fig. 7.2.

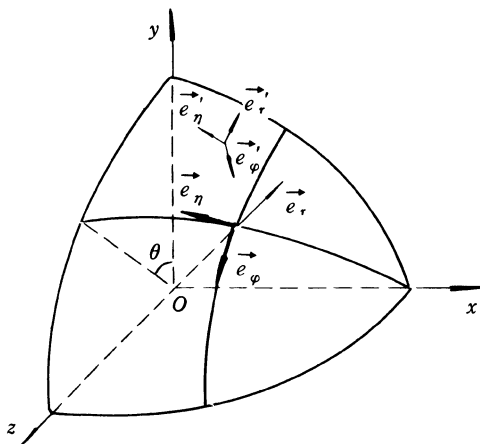


Fig. 7.2 The unit vectors in stationary coordinates system, $\vec{e}_r, \vec{e}_\theta, \vec{e}_\phi$; the unit vectors in moving coordinates system, $\vec{e}'_r, \vec{e}'_\theta, \vec{e}'_\phi$

It seems that in the case of nonuniform flow ahead of shock, unit vectors

\vec{e}_γ , \vec{e}_ϕ , \vec{e}_η are not in parallel with \vec{e}'_γ , \vec{e}'_ϕ , \vec{e}'_η , respectively. The moving frame relative to the stationary frame can make not only translational motion, but also rotational motion. So we cannot write the relations between two coordinates like relations (7.15) in general.

In fact, for present case, the small region ahead of the shock is taken as an infinitesimal fluid element, and the moving frame approaches the stationary frame infinitely, which will make the unit vectors in the moving frame parallel with those in the stationary frame, respectively. Therefore, in the infinitesimal fluid element ahead of the shock, we can make the transient transformation of coordinates in the orthogonal curvilinear coordinates. The relations between the stationary and moving frame in orthogonal curvilinear coordinate system can be expressed as follows

$$\begin{cases} S_1 = S'_1 + U \cos \varepsilon_1 \cdot t' \\ S_2 = S'_2 + U \cos \varepsilon_2 \cdot t' \\ S_3 = S'_3 + U \cos \varepsilon_3 \cdot t' \\ t = t' \end{cases} \quad (7.28)$$

where S_1 , S_2 , S_3 are the curvilinear coordinates in the stationary frame, S'_1 , S'_2 , S'_3 are the curvilinear coordinates in the moving frame.

The differential relations between both of the coordinates are given as

$$\begin{cases} \frac{\partial}{\partial S'_1} = \frac{1}{D} \left(D_{s_{11}} \cdot \frac{\partial}{\partial S_1} + D_{s_{21}} \cdot \frac{\partial}{\partial S_2} + D_{s_{31}} \cdot \frac{\partial}{\partial S_3} \right) \\ \frac{\partial}{\partial S'_2} = \frac{1}{D} \left(D_{s_{12}} \cdot \frac{\partial}{\partial S_1} + D_{s_{22}} \cdot \frac{\partial}{\partial S_2} + D_{s_{32}} \cdot \frac{\partial}{\partial S_3} \right) \\ \frac{\partial}{\partial S'_3} = \frac{1}{D} \left(D_{s_{13}} \cdot \frac{\partial}{\partial S_1} + D_{s_{23}} \cdot \frac{\partial}{\partial S_2} + D_{s_{33}} \cdot \frac{\partial}{\partial S_3} \right) \end{cases} \quad (7.29)$$

where

$$D = 1 - Q_1 \alpha_{s_1} - Q_2 \alpha_{s_2} - Q_3 \alpha_{s_3}$$

$$D_{s_{11}} = 1 - Q_2 \alpha_{s_2} - Q_3 \alpha_{s_3}$$

$$D_{s_{21}} = Q_2 \alpha_{s_1}$$

$$D_{s_{31}} = Q_3 \alpha_{s_1}$$

$$D_{s_{12}} = Q_1 \alpha_{s_2}$$

$$D_{s_{22}} = 1 - Q_1 \alpha_{s_1} - Q_3 \alpha_{s_3}$$

$$\begin{aligned} D_{s_{32}} &= Q_3 \alpha_{s_2} \\ D_{s_{13}} &= Q_1 \alpha_{s_3} \\ D_{s_{23}} &= Q_2 \alpha_{s_3} \\ D_{s_{33}} &= 1 - Q_1 \alpha_{s_1} - Q_2 \alpha_{s_2} \end{aligned}$$

§ 7.3 Three-dimensional equations in rectangular coordinates

The three-dimensional equations of shock dynamics include the geometrical relations and the area relation. The vectorial expressions for the geometrical relations in three-dimensional case can be expressed as

$$\nabla \cdot (\frac{\vec{i}}{A}) = 0 \quad (7.30)$$

and

$$[M + m(\vec{n} \cdot \vec{n}_f)]a = \frac{1}{|\nabla \alpha|} \quad (7.31)$$

According to the definition of the unit vector \vec{i} , which has been given in Chapter 6, we can directly obtain three-dimensional geometrical relations denoted by M and θ_i ($i = 1, 2, 3$) from the relations (7.30) and (7.31) instead of the transformation of coordinates. The same method as in Chapter 6 is used for establishing the area relation.

1. The geometrical relations

Substituting (7.9) and (7.12) into (7.30), we get

$$\begin{aligned} \frac{\partial}{\partial x} \left[\frac{M \cos \theta_1 + m \cos \varepsilon_1}{A'L} \right] + \frac{\partial}{\partial y} \left[\frac{M \cos \theta_2 + m \cos \varepsilon_2}{A'L} \right] \\ + \frac{\partial}{\partial z} \left[\frac{M \cos \theta_3 + m \cos \varepsilon_3}{A'L} \right] = 0 \quad (7.32) \end{aligned}$$

By using (7.31), we get the unit vector \vec{n} as

$$\vec{n} = \frac{\nabla \alpha}{|\nabla \alpha|} = [M + m(\vec{n} \cdot \vec{n}_f)]a \nabla \alpha = La \nabla \alpha \quad (7.33)$$

and we have

$$\vec{n} = \cos \theta_1 \cdot \vec{e}_x + \cos \theta_2 \cdot \vec{e}_y + \cos \theta_3 \cdot \vec{e}_z \quad (7.34)$$

By comparing (7.33) with (7.34), we get

$$\begin{cases} \alpha_x = \cos \theta_1 / La \\ \alpha_y = \cos \theta_2 / La \\ \alpha_z = \cos \theta_3 / La \end{cases} \quad (7.35)$$

Considering $\frac{\partial}{\partial x} \alpha_y = \frac{\partial}{\partial y} \alpha_x$, $\frac{\partial}{\partial y} \alpha_z = \frac{\partial}{\partial z} \alpha_y$, we have

$$\frac{\partial}{\partial x} \left(\frac{\cos \theta_2}{La} \right) - \frac{\partial}{\partial y} \left(\frac{\cos \theta_1}{La} \right) = 0 \quad (7.36)$$

$$\frac{\partial}{\partial y} \left(\frac{\cos \theta_3}{La} \right) - \frac{\partial}{\partial z} \left(\frac{\cos \theta_2}{La} \right) = 0 \quad (7.37)$$

2. The area relation

The area relation along a ray tube in the moving frame attached to the infinitesimal fluid element can be written as

$$e \frac{dM}{d\alpha'} + \frac{h}{p} \cdot \frac{dp}{d\alpha'} + \frac{g}{a} \cdot \frac{da}{d\alpha'} + \frac{1}{A'} \cdot \frac{dA'}{d\alpha'} = 0 \quad (7.38)$$

where α' is the curvilinear coordinate along a ray in the moving frame, and we have

$$\begin{cases} x' = x'(\alpha') \\ y' = y'(\alpha') \\ z' = z'(\alpha') \end{cases} \quad (7.39)$$

where x' , y' , and z' are the rectangular coordinates in the moving frame.

Expanding (7.38) by using (7.39), we obtain

$$\begin{aligned} & \left(e \frac{\partial M}{\partial x'} + \frac{h}{p} \frac{\partial p}{\partial x'} + \frac{g}{a} \frac{\partial a}{\partial x'} + \frac{1}{A'} \frac{\partial A'}{\partial x'} \right) \frac{dx'}{d\alpha'} \\ & + \left(e \frac{\partial M}{\partial y'} + \frac{h}{p} \frac{\partial p}{\partial y'} + \frac{g}{a} \frac{\partial a}{\partial y'} + \frac{1}{A'} \frac{\partial A'}{\partial y'} \right) \frac{dy'}{d\alpha'} \\ & + \left(e \frac{\partial M}{\partial z'} + \frac{h}{p} \frac{\partial p}{\partial z'} + \frac{g}{a} \frac{\partial a}{\partial z'} + \frac{1}{A'} \frac{\partial A'}{\partial z'} \right) \frac{dz'}{d\alpha'} = 0 \end{aligned} \quad (7.40)$$

Rearranging (7.40), we get

$$\begin{aligned} & \left(e \frac{\partial M}{\partial x'} + \frac{h}{p} \frac{\partial p}{\partial x'} + \frac{g}{a} \frac{\partial a}{\partial x'} + \frac{1}{A'} \frac{\partial A'}{\partial x'} \right) \\ & + \left(e \frac{\partial M}{\partial y'} + \frac{h}{p} \frac{\partial p}{\partial y'} + \frac{g}{a} \frac{\partial a}{\partial y'} + \frac{1}{A'} \frac{\partial A'}{\partial y'} \right) \frac{dy'}{dx'} \\ & + \left(e \frac{\partial M}{\partial z'} + \frac{h}{p} \frac{\partial p}{\partial z'} + \frac{g}{a} \frac{\partial a}{\partial z'} + \frac{1}{A'} \frac{\partial A'}{\partial z'} \right) \frac{dz'}{dx'} = 0 \end{aligned} \quad (7.41)$$

We now make the transformation of coordinates for relation (7.41) from the moving frame into the stationary one, that is, substituting (7.27) into (7.41), thus we get

$$\left[D_{x_1} + D_{x_2} \left(\frac{dy'}{dx'} \right) + D_{x_3} \left(\frac{dz'}{dx'} \right) \right] \left(e \frac{\partial M}{\partial x} + \frac{h}{p} \frac{\partial p}{\partial x} + \frac{g}{a} \frac{\partial a}{\partial x} + \frac{1}{A'} \frac{\partial A'}{\partial x} \right) +$$

$$\left[D_{y_1} + D_{y_2} \left(\frac{dy'}{dx'} \right) + D_{y_3} \left(\frac{dz'}{dx'} \right) \right] \left(e \frac{\partial M}{\partial y} + \frac{h}{p} \frac{\partial p}{\partial y} + \frac{g}{a} \frac{\partial a}{\partial y} + \frac{1}{A'} \frac{\partial A'}{\partial y} \right) + \\ \left[D_{z_1} + D_{z_2} \left(\frac{dy'}{dx'} \right) + D_{z_3} \left(\frac{dz'}{dx'} \right) \right] \left(e \frac{\partial M}{\partial z} + \frac{h}{p} \frac{\partial p}{\partial z} + \frac{g}{a} \frac{\partial a}{\partial z} + \frac{1}{A'} \frac{\partial A'}{\partial z} \right) = 0 \quad (7.42)$$

(7.42) can be rewritten as

$$\left(e \frac{\partial M}{\partial x} + \frac{h}{p} \frac{\partial p}{\partial x} + \frac{g}{a} \frac{\partial a}{\partial x} + \frac{1}{A'} \frac{\partial A'}{\partial x} \right) \\ + G_1 \left(e \frac{\partial M}{\partial y} + \frac{h}{p} \frac{\partial p}{\partial y} + \frac{g}{a} \frac{\partial a}{\partial y} + \frac{1}{A'} \frac{\partial A'}{\partial y} \right) \\ + G_2 \left(e \frac{\partial M}{\partial z} + \frac{h}{p} \frac{\partial p}{\partial z} + \frac{g}{a} \frac{\partial a}{\partial z} + \frac{1}{A'} \frac{\partial A'}{\partial z} \right) = 0 \quad (7.43)$$

where

$$G_1 = \frac{D_{y_1} + D_{y_2} \left(\frac{dy'}{dx'} \right) + D_{y_3} \left(\frac{dz'}{dx'} \right)}{D_{x_1} + D_{x_2} \left(\frac{dy'}{dx'} \right) + D_{x_3} \left(\frac{dz'}{dx'} \right)}$$

$$G_2 = \frac{D_{z_1} + D_{z_2} \left(\frac{dy'}{dx'} \right) + D_{z_3} \left(\frac{dz'}{dx'} \right)}{D_{x_1} + D_{x_2} \left(\frac{dy'}{dx'} \right) + D_{x_3} \left(\frac{dz'}{dx'} \right)}$$

In Fig. 7.3, we find out the relations among the line elements along the ray in the moving frame and dx' , dy' , dz' .

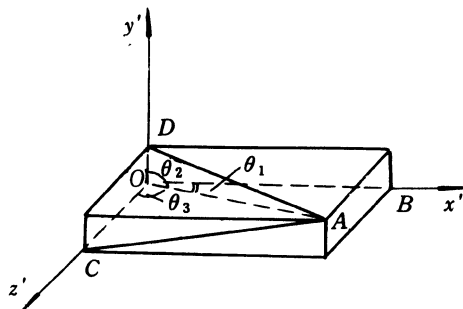


Fig. 7.3 The relations among $Mada'$ and dx' , dy' , dz'

The line element along the ray in moving frame is $Mada'$ which is denoted by line OA in Fig. 7.3. We have the following relations

$$\begin{cases} Mada'\cos\theta_1 = dx' \\ Mada'\cos\theta_2 = dy' \\ Mada'\cos\theta_3 = dz' \end{cases} \quad (7.44)$$

From (7.44), we get

$$\begin{cases} \frac{dy'}{dx'} = \frac{\cos\theta_2}{\cos\theta_1} \\ \frac{dz'}{dx'} = \frac{\cos\theta_3}{\cos\theta_1} \end{cases} \quad (7.45)$$

Substituting (7.45) and the expressions for D_{x1} , D_{x2} , D_{x3} , D_{y1} , D_{y2} , D_{y3} , D_{z1} , D_{z2} , D_{z3} into the expressions for G_1 , G_2 , we get

$$G_1 = \frac{M\cos\theta_2 + m\cos\varepsilon_2}{M\cos\theta_1 + m\cos\varepsilon_1} \quad (7.46)$$

$$G_2 = \frac{M\cos\theta_3 + m\cos\varepsilon_3}{M\cos\theta_1 + m\cos\varepsilon_1} \quad (7.47)$$

Thus we obtain the area relation along a ray tube in the moving frame denoted by stationary coordinates x, y, z as follows

$$\begin{aligned} & \frac{1}{A'} \frac{\partial A'}{\partial x} + G_1 \cdot \frac{1}{A'} \frac{\partial A'}{\partial y} + G_2 \cdot \frac{1}{A'} \frac{\partial A'}{\partial z} \\ &= - \left[\left(e \frac{\partial M}{\partial x} + \frac{h}{p} \frac{\partial p}{\partial x} + \frac{g}{a} \frac{\partial a}{\partial x} \right) + G_1 \left(e \frac{\partial M}{\partial y} + \frac{h}{p} \frac{\partial p}{\partial y} + \frac{g}{a} \frac{\partial a}{\partial y} \right) \right. \\ & \quad \left. + G_2 \left(e \frac{\partial M}{\partial z} + \frac{h}{p} \frac{\partial p}{\partial z} + \frac{g}{a} \frac{\partial a}{\partial z} \right) \right] \end{aligned} \quad (7.48)$$

The above geometrical relations and area relation are summarized as follows

$$\begin{cases} \frac{\partial}{\partial x} \left[\frac{M\cos\theta_1 + m\cos\varepsilon_1}{A'L} \right] + \frac{\partial}{\partial y} \left[\frac{M\cos\theta_2 + m\cos\varepsilon_2}{A'L} \right] \\ \quad + \frac{\partial}{\partial z} \left[\frac{M\cos\theta_3 + m\cos\varepsilon_3}{A'L} \right] = 0 \\ \frac{\partial}{\partial x} \left(\frac{\cos\theta_2}{La} \right) - \frac{\partial}{\partial y} \left(\frac{\cos\theta_1}{La} \right) = 0 \\ \frac{\partial}{\partial y} \left(\frac{\cos\theta_3}{La} \right) - \frac{\partial}{\partial z} \left(\frac{\cos\theta_2}{La} \right) = 0 \\ \cos^2\theta_1 + \cos^2\theta_2 + \cos^2\theta_3 = 1 \\ \frac{1}{A'} \left(\frac{\partial A'}{\partial x} + G_1 \frac{\partial A'}{\partial y} + G_2 \frac{\partial A'}{\partial z} \right) = -(E_x + G_1 E_y + G_2 E_z) \end{cases} \quad (7.49)$$

where

$$\begin{aligned} E_x &= e \frac{\partial M}{\partial x} + \frac{h}{p} \frac{\partial p}{\partial x} + \frac{g}{a} \frac{\partial a}{\partial x} \\ E_y &= e \frac{\partial M}{\partial y} + \frac{h}{p} \frac{\partial p}{\partial y} + \frac{g}{a} \frac{\partial a}{\partial y} \\ E_z &= e \frac{\partial M}{\partial z} + \frac{h}{p} \frac{\partial p}{\partial z} + \frac{g}{a} \frac{\partial a}{\partial z} \end{aligned}$$

The above equations are three-dimensional equations of shock dynamics for a nonuniform flow ahead of a shock.

In the above equations (7.49), the first, second, third and fourth expressions are the geometrical relations; the fifth one is the area relation; the parameters of the flow field ahead of a shock, m , ε_1 , ε_2 , ε_3 and a are given; M , θ_1 , θ_2 , θ_3 and A' are unknown variables.

Substituting the fifth expression of (7.49) into the first expression, we can eliminate A' and considering the fourth expression, we get the three equations with three unknown variables M , θ_1 , θ_2 (or θ_3). If the equations of shock dynamics are used for solving the problem such as unsteady, three-dimensional diffraction of a plane shock wave around a moving body, there are only three unknown functions and three independent variables (x , y , z). While the same problem for gas dynamics is solved, there are five unknown functions and four independent variables (x , y , z , t).

§ 7.4 Three-dimensional equations in cylindrical coordinates

1. The geometrical relations

In cylindrical coordinate system, the unit vectors \vec{n} and \vec{n}_f can be expressed as

$$\vec{n} = \cos \theta_r \vec{e}_r + \cos \theta_\varphi \vec{e}_\varphi + \cos \theta_x \vec{e}_x \quad (7.50)$$

$$\vec{n}_f = \cos \varepsilon_r \vec{e}_r + \cos \varepsilon_\varphi \vec{e}_\varphi + \cos \varepsilon_x \vec{e}_x \quad (7.51)$$

where \vec{e}_r , \vec{e}_φ and \vec{e}_x are the unit vectors in the r , φ and x directions, respectively, θ_r , θ_φ and θ_x are the angles between the unit vector \vec{n} and unit vectors \vec{e}_r , \vec{e}_φ and \vec{e}_x , respectively; ε_r , ε_φ and ε_x are the angles between the unit vector of the direction of the flow ahead of the shock, \vec{n}_f and unit vectors \vec{e}_r , \vec{e}_φ and \vec{e}_x , respectively.

The vector $\vec{M} + \vec{m}$ can be expressed as

$$\begin{aligned} \vec{M} + \vec{m} &= M \vec{n} + m \vec{n}_f \\ &= (M \cos \theta_r + m \cos \varepsilon_r) \vec{e}_r + (M \cos \theta_\varphi + m \cos \varepsilon_\varphi) \vec{e}_\varphi \end{aligned}$$

$$+ (M \cos \theta_x + m \cos \theta_x) \vec{e}_x \quad (7.52)$$

and

$$N = |\vec{M} + \vec{m}| \\ = \left[M^2 + m^2 + 2Mm(\cos \theta_r \cos \varepsilon_r + \cos \theta_\varphi \cos \varepsilon_\varphi + \cos \theta_x \cos \varepsilon_x) \right]^{\frac{1}{2}} \quad (7.53)$$

From (7.52) and (7.53), we can obtain

$$\vec{i} = B_r \vec{e}_r + B_\varphi \vec{e}_\varphi + B_x \vec{e}_x \quad (7.54)$$

where

$$B_r = \frac{1}{N} (M \cos \theta_r + m \cos \varepsilon_r)$$

$$B_\varphi = \frac{1}{N} (M \cos \theta_\varphi + m \cos \varepsilon_\varphi)$$

$$B_x = \frac{1}{N} (M \cos \theta_x + m \cos \varepsilon_x)$$

The cylindrical coordinate system is shown in Fig. 7.4

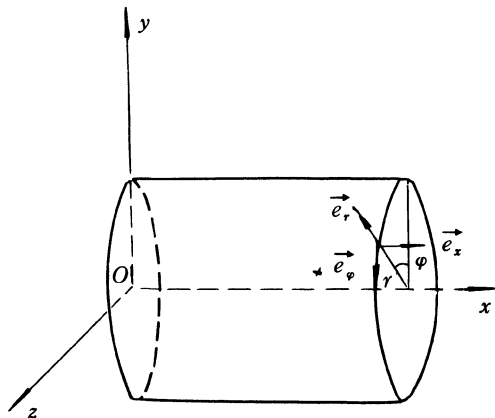


Fig. 7.4 The cylindrical coordinate system

Substituting the expression for \vec{i} into (7.30), we get

$$\frac{\partial}{\partial r} \left(\frac{r B_r}{A} \right) + \frac{\partial}{\partial \varphi} \left(\frac{B_\varphi}{A} \right) + \frac{\partial}{\partial x} \left(\frac{r B_x}{A} \right) = 0 \quad (7.55)$$

or

$$\begin{aligned} & \frac{\partial}{\partial r} \left[\frac{(M \cos \theta_r + m \cos \varepsilon_r)r}{A \cdot N} \right] + \frac{\partial}{\partial \varphi} \left[\frac{(M \cos \theta_\varphi + m \cos \varepsilon_\varphi)r}{A \cdot N} \right] \\ & + \frac{\partial}{\partial x} \left[\frac{(M \cos \theta_x + m \cos \varepsilon_x)r}{A \cdot N} \right] = 0 \end{aligned} \quad (7.56)$$

From Fig.7.1, we have

$$A' \cos \gamma = A' (\vec{n} \cdot \vec{i}) = A \quad (7.57)$$

Substituting (7.50) and (7.54) into (7.57), we get

$$\begin{aligned} \frac{A}{A'} &= \frac{1}{N} [(M \cos \theta_r + m \cos \varepsilon_r) \cos \theta_r + (M \cos \theta_\varphi + m \cos \varepsilon_\varphi) \cos \theta_\varphi \\ &+ (M \cos \theta_x + m \cos \varepsilon_x) \cos \theta_x] \end{aligned} \quad (7.58)$$

or

$$\frac{A}{A'} = \frac{L}{N} \quad (7.59)$$

where $L = [M + m(\cos \theta_r \cos \varepsilon_r + \cos \theta_\varphi \cos \varepsilon_\varphi + \cos \theta_x \cos \varepsilon_x)]$

Substituting (7.59) into (7.56), we get

$$\begin{aligned} & \frac{\partial}{\partial r} \left[\frac{(M \cos \theta_r + m \cos \varepsilon_r)r}{A'L} \right] + \frac{\partial}{\partial \varphi} \left[\frac{(M \cos \theta_\varphi + m \cos \varepsilon_\varphi)r}{A'L} \right] \\ & + \frac{\partial}{\partial x} \left[\frac{(M \cos \theta_x + m \cos \varepsilon_x)r}{A'L} \right] = 0 \end{aligned} \quad (7.60)$$

From (7.31), we can obtain unit vector \vec{n} as

$$\begin{aligned} \vec{n} &= [M + m(\vec{n} \cdot \vec{n}_f)]a \nabla \alpha \\ &= La \left(\alpha_r \vec{e}_r + \frac{1}{r} \alpha_\varphi \vec{e}_\varphi + \alpha_x \vec{e}_x \right) \end{aligned} \quad (7.61)$$

By comparing (7.61) with (7.50), we get

$$\begin{cases} \alpha_r = \frac{\cos \theta_r}{La} \\ \alpha_\varphi = \frac{r \cos \theta_\varphi}{La} \\ \alpha_x = \frac{\cos \theta_x}{La} \end{cases} \quad (7.62)$$

From (7.62), we can obtain

$$\frac{\partial}{\partial x} \left(\frac{\cos \theta_r}{La} \right) - \frac{\partial}{\partial r} \left(\frac{\cos \theta_x}{La} \right) = 0 \quad (7.63)$$

$$\frac{\partial}{\partial r} \left(\frac{r \cos \theta_\varphi}{La} \right) - \frac{\partial}{\partial \varphi} \left(\frac{\cos \theta_r}{La} \right) = 0 \quad (7.64)$$

In addition, we have

$$\cos^2 \theta_r + \cos^2 \theta_\varphi + \cos^2 \theta_x = 1 \quad (7.65)$$

2. The area relation along a ray tube in the moving frame

In any orthogonal curvilinear coordinate system, starting with relation (7.38) and using the following relations

$$\begin{cases} S'_1 = S'_1(\alpha') \\ S'_2 = S'_2(\alpha') \\ S'_3 = S'_3(\alpha') \end{cases} \quad (7.66)$$

By expanding the relation (7.38) and making the transformation of coordinates for (7.38) by using (7.29), we can obtain the following area relation along a ray tube in the moving frame, denoted by the orthogonal curvilinear coordinates in the stationary frame

$$\frac{1}{A'} \frac{\partial A'}{\partial S_1} + G'_1 \frac{1}{A'} \frac{\partial A'}{\partial S_2} + G'_2 \frac{1}{A'} \frac{\partial A'}{\partial S_3} = - \left(E_{s_1} + G'_1 E_{s_2} + G'_2 E_{s_3} \right) \quad (7.67)$$

$$\text{where } E_{s_1} = e \frac{\partial M}{\partial S_1} + \frac{h}{p} \frac{\partial p}{\partial S_1} + \frac{g}{a} \frac{\partial a}{\partial S_1}$$

$$E_{s_2} = e \frac{\partial M}{\partial S_2} + \frac{h}{p} \frac{\partial p}{\partial S_2} + \frac{g}{a} \frac{\partial a}{\partial S_2}$$

$$E_{s_3} = e \frac{\partial M}{\partial S_3} + \frac{h}{p} \frac{\partial p}{\partial S_3} + \frac{g}{a} \frac{\partial a}{\partial S_3}$$

In the cylindrical coordinate system,

$$\begin{cases} dS_1 = dr \\ dS_2 = r d\varphi \\ dS_3 = dx \end{cases} \quad (6.68)$$

Substituting (6.68) into (7.67), we get

$$\frac{1}{A'} \frac{\partial A'}{\partial r} + G'_1 \frac{1}{A'} \frac{\partial A'}{\partial r \partial \varphi} + G'_2 \frac{1}{A'} \frac{\partial A'}{\partial x} = - (E_r + G'_1 E_\varphi + G'_2 E_x) \quad (7.69)$$

where

$$G'_1 = \frac{M \cos \theta_\varphi + m \cos \varepsilon_\varphi}{M \cos \theta_r + m \cos \varepsilon_r}$$

$$G'_2 = \frac{M \cos \theta_x + m \cos \varepsilon_x}{M \cos \theta_r + m \cos \varepsilon_r}$$

$$\begin{aligned} E_r &= e \frac{\partial M}{\partial r} + \frac{h}{p} \frac{\partial p}{\partial r} + \frac{g}{a} \frac{\partial a}{\partial r} \\ E_\varphi &= e \frac{\partial M}{r \partial \varphi} + \frac{h}{p} \frac{\partial p}{r \partial \varphi} + \frac{g}{a} \frac{\partial a}{r \partial \varphi} \\ E_x &= e \frac{\partial M}{\partial x} + \frac{h}{p} \frac{\partial p}{\partial x} + \frac{g}{a} \frac{\partial a}{\partial x} \end{aligned}$$

3. The three-dimensional equations of shock dynamics in the cylindrical coordinates

Summarizing the above equations, (7.60), (7.63), (7.64), (7.65), and (7.69), we can obtain a set of three-dimensional equations in the cylindrical coordinates as follows

$$\left\{ \begin{array}{l} \frac{\partial}{\partial r} \left[\frac{(M \cos \theta_r + m \cos \varepsilon_r) r}{A' L} \right] + \frac{\partial}{\partial \varphi} \left[\frac{(M \cos \theta_\varphi + m \cos \varepsilon_\varphi) r}{A' L} \right] \\ \quad + \frac{\partial}{\partial x} \left[\frac{(M \cos \theta_x + m \cos \varepsilon_x) r}{A' L} \right] = 0 \\ \frac{\partial}{\partial x} \left(\frac{\cos \theta_r}{L a} \right) - \frac{\partial}{\partial r} \left(\frac{\cos \theta_x}{L a} \right) = 0 \\ \frac{\partial}{\partial r} \left(\frac{r \cos \theta_\varphi}{L a} \right) - \frac{\partial}{\partial \varphi} \left(\frac{\cos \theta_r}{L a} \right) = 0 \\ \cos^2 \theta_r + \cos^2 \theta_\varphi + \cos^2 \theta_x = 1 \\ \frac{1}{A'} \frac{\partial A'}{\partial r} + G_1 \frac{1}{A'} \frac{\partial A'}{r \partial \varphi} + G_2 \frac{1}{A'} \frac{\partial A'}{\partial x} = -(E_r + G'_1 E_\varphi + G'_2 E_x) \end{array} \right. \quad (7.70)$$

4. The equations in the case of axially-symmetrical flow

In the case of axially-symmetrical flow, the equations (7.70) can be simplified.

If the flow field in this case has no circumferential flow, i.e., $\theta_\varphi = 90^\circ$, $\varepsilon_\varphi = 90^\circ$, and letting $\theta_x = \theta$, $\varepsilon_x = \varepsilon$, we have

$$\theta_r = 90^\circ - \theta, \quad \varepsilon_r = 90^\circ - \varepsilon \quad (7.71)$$

Substituting (7.71) into (7.70), and noting $\frac{\partial}{\partial \varphi} = 0$, $\theta_x = \theta$, $\varepsilon_x = \varepsilon$, we can obtain the axially-symmetrical equations as

$$\left\{ \begin{array}{l} \frac{\partial}{\partial r} \left[\frac{(M \sin \theta + m \sin \varepsilon) r}{(M + m \cos(\theta - \varepsilon)) A'} \right] + \frac{\partial}{\partial x} \left[\frac{(M \cos \theta + m \cos \varepsilon) r}{(M + m \cos(\theta - \varepsilon)) A'} \right] = 0 \\ \frac{\partial}{\partial x} \left[\frac{\sin \theta}{(M + m \cos(\theta - \varepsilon)) a} \right] - \frac{\partial}{\partial r} \left[\frac{\cos \theta}{(M + m \cos(\theta - \varepsilon)) a} \right] = 0 \\ \frac{1}{A'} \frac{\partial A'}{\partial r} + G' \frac{1}{A'} \frac{\partial A'}{\partial x} = -(E_r + G' E_x) \end{array} \right. \quad (7.72)$$

where $G' = \frac{M\cos\theta + m\cos\varepsilon}{M\sin\theta + m\sin\varepsilon}$

The equations (7.72) are all the same as the equations (6.80) in Chapter 6.

Next, we will derive the three-dimensional equations in spherical coordinates.

§ 7.5 Three-dimensional equations in spherical coordinates

1. The geometrical relations

In the spherical coordinate system (as shown in Fig.7.2), the unit vectors \vec{n} and \vec{n}_f can be expressed as

$$\vec{n} = \cos\theta_r \vec{e}_r + \cos\theta_\varphi \vec{e}_\varphi + \cos\theta_\eta \vec{e}_\eta \quad (7.73)$$

$$\vec{n}_f = \cos\varepsilon_r \vec{e}_r + \cos\varepsilon_\varphi \vec{e}_\varphi + \cos\varepsilon_\eta \vec{e}_\eta \quad (7.74)$$

where \vec{e}_r , \vec{e}_φ and \vec{e}_η are the unit vectors in r , φ , η directions, respectively; θ_r , θ_φ and θ_η are the angles between \vec{n} and \vec{e}_r , \vec{e}_φ , \vec{e}_η , respectively; ε_r , ε_φ and ε_η are the angles between \vec{n}_f and \vec{e}_r , \vec{e}_φ , \vec{e}_η , respectively.

$$\begin{aligned} \vec{M} + \vec{m} &= (M\cos\theta_r + m\cos\theta_r)\vec{e}_r + (M\cos\theta_\varphi + m\cos\varepsilon_\varphi)\vec{e}_\varphi \\ &\quad + (M\cos\theta_\eta + m\cos\varepsilon_\eta)\vec{e}_\eta \end{aligned} \quad (7.75)$$

$$N = |\vec{M} + \vec{m}| = [M^2 + m^2 + 2Mm(\cos\theta_r \cos\varepsilon_r + \cos\theta_\varphi \cos\varepsilon_\varphi + \cos\theta_\eta \cos\varepsilon_\eta)]^{\frac{1}{2}} \quad (7.76)$$

From (7.75) and (7.76), we have

$$\vec{i} = B_r \vec{e}_r + B_\varphi \vec{e}_\varphi + B_\eta \vec{e}_\eta \quad (7.77)$$

$$\text{where } B_r = \frac{1}{N}(M\cos\theta_r + m\cos\varepsilon_r)$$

$$B_\varphi = \frac{1}{N}(M\cos\theta_\varphi + m\cos\varepsilon_\varphi)$$

$$B_\eta = \frac{1}{N}(M\cos\theta_\eta + m\cos\varepsilon_\eta)$$

Substituting (7.77) into (7.30), we get

$$\frac{1}{r^2} \frac{\partial}{\partial r} \left(\frac{r^2 B_r}{A} \right) + \frac{1}{r \sin\eta} \frac{\partial}{\partial \varphi} \left(\frac{B_\varphi}{A} \right) + \frac{1}{r \sin\eta} \frac{\partial}{\partial \eta} \left(\frac{\sin\eta \cdot B_\eta}{A} \right) = 0 \quad (7.78)$$

or

$$\frac{\partial}{\partial r} \left[\frac{(M\cos\theta_r + m\cos\varepsilon_r)}{A \cdot N} \right] + \frac{1}{r \sin\eta} \frac{\partial}{\partial \varphi} \left[\frac{(M\cos\theta_\varphi + m\cos\varepsilon_\varphi)}{A \cdot N} \right]$$

$$\begin{aligned}
& + \frac{1}{r \sin \eta} \frac{\partial}{\partial \eta} \left[\frac{(M \cos \theta_r + m \cos \varepsilon_r) \sin \eta}{A \cdot N} \right] \\
& + \frac{2(M \cos \theta_r + m \cos \varepsilon_r)}{r A \cdot N} = 0
\end{aligned} \tag{7.79}$$

From Fig.7.1, we have

$$A' \cos \gamma = A'(\vec{n} \cdot \vec{i}) = A \tag{7.80}$$

Substituting (7.73) and (7.77) into (7.80), we get

$$\frac{A}{A'} = \frac{L}{N} \tag{7.81}$$

where

$$L = [M + m(\cos \theta_r \cos \varepsilon_r + \cos \theta_\varphi \cos \varepsilon_\varphi + \cos \theta_\eta \cos \varepsilon_\eta)]$$

Substituting (7.81) into (7.79), we have

$$\begin{aligned}
& \frac{\partial}{\partial r} \left[\frac{(M \cos \theta_r + m \cos \varepsilon_r)}{A' L} \right] + \frac{1}{r \sin \eta} \frac{\partial}{\partial \varphi} \left[\frac{(M \cos \theta_\varphi + m \cos \varepsilon_\varphi)}{A' L} \right] \\
& + \frac{1}{r \sin \eta} \frac{\partial}{\partial \eta} \left[\frac{(M \cos \theta_\eta + m \cos \varepsilon_\eta) \sin \eta}{A' L} \right] \\
& + \frac{2(M \cos \theta_r + m \cos \varepsilon_r)}{r A' L} = 0
\end{aligned} \tag{7.82}$$

From (7.31), we can obtain the unit vector \vec{n} as

$$\begin{aligned}
\vec{n} &= [M + m(\vec{n} \cdot \vec{n}_f)] a \nabla \alpha \\
&= La(\alpha_r \vec{e}_r + \frac{1}{r \sin \eta} \alpha_\varphi \vec{e}_\varphi + \frac{1}{r} \alpha_\eta \vec{e}_\eta)
\end{aligned} \tag{7.83}$$

By comparing (7.83) with (7.73), we get

$$\begin{cases} \alpha_r = \frac{\cos \theta_r}{La} \\ \alpha_\varphi = \frac{r \cos \theta_\varphi \sin \eta}{La} \\ \alpha_\eta = \frac{L \cos \theta_\eta}{La} \end{cases} \tag{7.84}$$

From (7.84), we can obtain

$$\frac{\partial}{\partial r} \left(\frac{r \cos \theta_\varphi}{La} \right) - \frac{1}{\sin \eta} \frac{\partial}{\partial \varphi} \left(\frac{\cos \theta_r}{La} \right) = 0 \tag{7.85}$$

$$\frac{\partial}{\partial r} \left(\frac{r \cos \theta_\eta}{La} \right) - \frac{\partial}{\partial \eta} \left(\frac{\cos \theta_r}{La} \right) = 0 \tag{7.86}$$

In addition, we have

$$\cos^2 \theta_r + \cos^2 \theta_\varphi + \cos^2 \theta_\eta = 1 \quad (7.87)$$

2. The area relation along a ray tube in the moving frame

In the spherical coordinate system, the line elements in r, φ, η directions can be expressed as

$$\begin{cases} dS_1 = dr \\ dS_2 = r \sin \eta d\varphi \\ dS_3 = r d\eta \end{cases} \quad (7.88)$$

Substituting (7.88) into (7.67), we can obtain the area relation along a ray tube in the moving frame denoted by spherical coordinates as follows

$$\frac{1}{A'} \frac{\partial A'}{\partial r} + G''_1 \frac{1}{A'} \frac{1}{r \sin \eta} \frac{\partial A'}{\partial \varphi} + G''_2 \frac{1}{A'} \frac{\partial A'}{\partial \eta} = - (E_r + G''_1 E_\varphi + G''_2 E_\eta) \quad (7.89)$$

where

$$\begin{aligned} G''_1 &= \frac{M \cos \theta_r + m \cos \varepsilon_r}{M \cos \theta_r + m \cos \varepsilon_r}, & G''_2 &= \frac{M \cos \theta_\eta + m \cos \varepsilon_\eta}{M \cos \theta_r + m \cos \varepsilon_r}, \\ E_r &= e \frac{\partial M}{\partial r} + \frac{h}{p} \frac{\partial p}{\partial r} + \frac{g}{a} \frac{\partial a}{\partial r}, & E_\varphi &= \frac{1}{r \sin \eta} \left(e \frac{\partial M}{\partial \varphi} + \frac{h}{p} \frac{\partial p}{\partial \varphi} + \frac{g}{a} \frac{\partial a}{\partial \varphi} \right) \\ E_\eta &= \frac{1}{r} \left(e \frac{\partial M}{\partial \eta} + \frac{h}{p} \frac{\partial p}{\partial \eta} + \frac{g}{a} \frac{\partial a}{\partial \eta} \right) \end{aligned}$$

3. The three-dimensional equations in the spherical coordinates

Summarizing the above equations, we can obtain a set of three-dimensional equations in the spherical coordinates as follows

$$\begin{cases} \frac{\partial}{\partial r} \left[\frac{(M \cos \theta_r + m \cos \varepsilon_r)}{AL} \right] + \frac{1}{r \sin \eta} \frac{\partial}{\partial \varphi} \left[\frac{(M \cos \theta_\varphi + m \cos \varepsilon_\varphi)}{AL} \right] + \\ \frac{1}{r \sin \eta} \frac{\partial}{\partial \eta} \left[\frac{(M \cos \theta_\eta + m \cos \varepsilon_\eta) \sin \eta}{AL} \right] + \frac{2(M \cos \theta_r + m \cos \varepsilon_r)}{r AL} = 0 \\ \frac{\partial}{\partial r} \left(\frac{r \cos \theta_\varphi}{La} \right) - \frac{1}{\sin \eta} \frac{\partial}{\partial \varphi} \left(\frac{\cos \theta_r}{La} \right) = 0 \\ \frac{\partial}{\partial r} \left(\frac{r \cos \theta_\eta}{La} \right) - \frac{\partial}{\partial \eta} \left(\frac{\cos \theta_r}{La} \right) = 0 \\ \cos^2 \theta_r + \cos^2 \theta_\varphi + \cos^2 \theta_\eta = 1 \\ \frac{1}{A'} \frac{\partial A'}{\partial r} + G''_1 \frac{1}{A'} \frac{1}{r \sin \eta} \frac{\partial A'}{\partial \varphi} + G''_2 \frac{1}{A'} \frac{\partial A'}{\partial \eta} = - (E_r + G''_1 E_\varphi + G''_2 E_\eta) \end{cases} \quad (7.90)$$

§ 7.6 The equations in the case of axially-symmetrical and self-similar flow field

Under the condition of axially-symmetrical and self-similar flow, the equations (7.72) may be simplified further.

We now introduce the similarity variable η , which satisfies the following relation

$$\eta = \tan^{-1} \frac{r}{x} \quad (7.91)$$

Differentiating (7.91) with respect to x and r , respectively, we get

$$\begin{cases} \frac{\partial}{\partial x} = -\frac{r}{x^2 + r^2} \frac{d}{d\eta} \\ \frac{\partial}{\partial r} = \frac{x}{x^2 + r^2} \frac{d}{d\eta} \end{cases} \quad (7.92)$$

Substituting (7.92) into the first, second, and third expressions of (7.72), respectively, we have

$$\begin{aligned} \frac{d}{d\eta} \left[\frac{M \cos \theta + m \cos \varepsilon}{A'(M + m \cos(\theta - \varepsilon))} \right] - \cot \eta \frac{d}{d\eta} \left[\frac{M \sin \theta + m \sin \varepsilon}{A'(M + m \cos(\theta - \varepsilon))} \right] \\ = \frac{M \sin \theta + m \sin \varepsilon}{A'[M + m \cos(\theta - \varepsilon)] \sin^2 \eta} \end{aligned} \quad (7.93)$$

$$\tan \eta \frac{d}{d\eta} \left[\frac{\sin \theta}{a(M + m \cos(\theta - \varepsilon))} \right] + \frac{d}{d\eta} \left[\frac{\cos \theta}{a(M + m \cos(\theta - \varepsilon))} \right] = 0 \quad (7.94)$$

The third expression of (7.92) can be written as

$$\begin{aligned} \left(\frac{x}{x^2 + r^2} - G' \frac{r}{x^2 + r^2} \right) \frac{1}{A'} \frac{dA'}{d\eta} \\ = - \left(\frac{x}{x^2 + r^2} - G' \frac{r}{x^2 + r^2} \right) \left(e \frac{dM}{d\eta} + \frac{h}{p} \frac{dp}{d\eta} + \frac{g}{a} \frac{da}{d\eta} \right) \end{aligned} \quad (7.95)$$

or

$$\frac{1}{A'} \frac{dA'}{d\eta} = - \left(e \frac{dM}{d\eta} + \frac{h}{p} \frac{dp}{d\eta} + \frac{g}{a} \frac{da}{d\eta} \right) \quad (7.96)$$

If the flow field ahead of the shock is homoentropic, we have the following relations

$$\begin{cases} \frac{1}{a} \frac{da}{d\eta} = -\frac{\gamma-1}{2} \frac{m}{\left(1 + \frac{\gamma-1}{2} m^2\right)} \frac{dm}{d\eta} \\ \frac{1}{p} \frac{dp}{d\eta} = -\frac{\gamma m}{\left(1 + \frac{\gamma-1}{2} m^2\right)} \frac{dm}{d\eta} \end{cases} \quad (7.97)$$

Substituting (7.97) into (7.96), we get

$$\frac{1}{A'} \frac{dA'}{d\eta} = -e \frac{dM}{d\eta} + f \frac{dm}{d\eta} \quad (7.98)$$

$$\text{where } f = \frac{m \left(\frac{\gamma-1}{2} g + \gamma h \right)}{\left(1 + \frac{\gamma-1}{2} m^2 \right)}$$

Summarizing the above equations, we can obtain a set of axially-symmetrical, self-similar equations as follows

$$\begin{cases} \frac{d}{d\eta} \left(\frac{C}{A' \cdot B} \right) - \cot \eta \frac{d}{d\eta} \left(\frac{S}{A' \cdot B} \right) = \frac{S}{A' \cdot B \sin^2 \eta} \\ \tan \eta \frac{d}{d\eta} \left(\frac{\sin \theta}{a \cdot B} \right) + \frac{d}{d\eta} \left(\frac{\cos \theta}{a \cdot B} \right) = 0 \\ \frac{1}{A'} \frac{dA'}{d\eta} = -e \frac{dM}{d\eta} + f \frac{dm}{d\eta} \end{cases} \quad (7.99)$$

where

$$B = M + m \cos(\theta - \varepsilon)$$

$$C = M \cos \theta + m \cos \varepsilon$$

$$S = M \sin \theta + m \sin \varepsilon$$

Expanding the first and second expressions of (7.99), and substituting the third expression into the first expression for eliminating $\frac{1}{A'} \frac{dA'}{d\eta}$, we can obtain the following equations

$$\begin{cases} C_1 \frac{dM}{d\eta} + C_2 \frac{d\theta}{d\eta} = C_3 \frac{dm}{d\eta} + C_4 \frac{d\varepsilon}{d\eta} + C_5 \\ D_1 \frac{dM}{d\eta} + D_2 \frac{d\theta}{d\eta} = D_3 \frac{dm}{d\eta} + D_4 \frac{d\varepsilon}{d\eta} \end{cases} \quad (7.100)$$

where

$$C_1 = \{m[\sin(\eta - \varepsilon) - \cos(\theta - \varepsilon)\sin(\eta - \theta)] - Be[M \sin(\eta - \theta) + m \sin(\eta - \varepsilon)]\}$$

$$C_2 = [M^2 \cos(\eta - \theta) + Mm \cos(\eta - \varepsilon) - m^2 \sin(\theta - \varepsilon)\sin(\eta - \varepsilon)]$$

$$C_3 = -\{[M \sin(\eta - \theta)\cos(\theta - \varepsilon) - M \sin(\eta - \varepsilon)] + Bf[M \sin(\eta - \theta) + m \sin(\eta - \varepsilon)]\}$$

$$C_4 = -[Mm \sin(\eta - \theta)\sin(\theta - \varepsilon) + Mm \cos(\eta - \varepsilon) + m^2 \cos(\eta - \theta)]$$

$$C_5 = -B(M \sin \theta + m \sin \varepsilon) / \sin \eta$$

$$D_1 = 1$$

$$D_2 = -[B \tan(\eta - \theta) + m \sin(\theta - \varepsilon)]$$

$$D_3 = - \left[\cos(\theta - \varepsilon) - \frac{(\gamma - 1)mB}{2 \left(1 + \frac{\gamma - 1}{2} m^2 \right)} \right]$$

$$D_4 = -m \sin(\theta - \varepsilon)$$

Solving for $\frac{d\theta}{d\eta}$ and $\frac{dM}{d\eta}$ from equations (7.100), we get

$$\frac{d\theta}{d\eta} = \left(\frac{C_3 - C_1 D_3}{C_2 - C_1 D_2} \right) \frac{dm}{d\eta} + \left(\frac{C_4 - C_1 D_4}{C_2 - C_1 D_2} \right) \cdot \frac{d\varepsilon}{d\eta}$$

$$+ \frac{C_5}{C_2 - C_1 D_2} \quad (7.101)$$

$$\begin{aligned} \frac{dM}{d\eta} &= \left(\frac{C_2 D_3 - C_3 D_2}{C_2 - C_1 D_2} \right) \frac{dm}{d\eta} + \left(\frac{C_2 D_4 - C_4 D_2}{C_2 - C_1 D_2} \right) \frac{d\varepsilon}{d\eta} \\ &- \frac{D_2 C_5}{C_2 - C_1 D_2} \end{aligned} \quad (7.102)$$

In the equations (7.101) and (7.102), the flow Mach number and flow angle ahead of a shock, m and ε , are given, and $M(\eta)$ and $\theta(\eta)$ are unknown functions, so (7.101) and (7.102) may be expressed as

$$\begin{cases} \frac{d\theta}{d\eta} = f_1(M, \theta, \eta) \\ \frac{dM}{d\eta} = f_2(M, \theta, \eta) \end{cases} \quad (7.103)$$

By using corresponding boundary conditions and shock-shock relations, we can find the solution of the equations (7.103).

§ 7.7 Shock-shock relations in the case of a moving gas ahead of a shock

In Chapter 3, we have derived the shock-shock relations in the case of a quiescent gas ahead of a shock, which include the expressions for tangential and normal derivatives of the function α , that is,

$$\vec{n}_{ss} \times (\nabla \alpha)_0 = \vec{n}_{ss} \times (\nabla \alpha)_1 \quad (7.104)$$

$$\frac{\vec{n}_{ss} \cdot \vec{n}_0}{A_0} = \frac{\vec{n}_{ss} \cdot \vec{n}_1}{A_1} \quad (7.105)$$

where \vec{n}_{ss} is the unit vector normal to the shock-shock surface, the subscripts 0 and 1 denote undisturbed shock and disturbed shock divided by shock-shock, respectively.

In the case of a shock wave moving into a uniform or a nonuniform flow

field, what are the shock-shock relations? We will answer this question as follows.

Firstly, we consider the relation (7.104). In the case of a moving gas ahead of a shock, the value of α along the shock is also the same even across the discontinuity of shock-shock, and the tangential derivatives of α on both sides of the shock-shock must be equal. So we have the same relation as (7.104), but the expression for \vec{n} is different. From relation (7.33), we have

$$\vec{n}_0 = [M_0 + m(\vec{n}_0 \cdot \vec{n}_f)]a(\nabla\alpha)_0 \quad (7.106)$$

$$\vec{n}_1 = [M_1 + m(\vec{n}_1 \cdot \vec{n}_f)]a(\nabla\alpha)_1 \quad (7.107)$$

Substituting (7.106) and (7.107) into (7.104), we have

$$\frac{\vec{n}_{ss} \times \vec{n}_0}{[M_0 + m(\vec{n}_0 \cdot \vec{n}_f)]} = \frac{\vec{n}_{ss} \times \vec{n}_1}{[M_1 + m(\vec{n}_1 \cdot \vec{n}_f)]} \quad (7.108)$$

In the case of two-dimensional flow, the relation can be expressed as

$$\frac{\vec{n}_{ss} \times \vec{n}_0}{[M_0 + m\cos(\theta_0 - \varepsilon)]} = \frac{\vec{n}_{ss} \times \vec{n}_1}{[M_1 + m\cos(\theta_1 - \varepsilon)]} \quad (7.109)$$

Next, we consider the relation (7.105). In the case of a moving gas ahead of a shock, we cannot use this relation, because the rays in this case are not normal to the shock surface. In order to obtain the ratio of the cross-sectional area of the ray of the undisturbed shock to that of the disturbed shock, it is necessary to make a transformation of coordinates from the stationary frame into the moving one, which will make the rays be normal to the shock surface.

An infinitesimal fluid element which includes the triple point (the point of shock-shock disturbance on the shock surface) is chosen, and the moving frame is attached to the flow field ahead of the shocks, which is considered as a uniform region as shown in Fig. 7.5.a (for the convenience of analysis, the figure is drawn in two-dimensional flow). In the moving frame, the relation (7.105) may be written as

$$\frac{\vec{n}'_{ss} \cdot \vec{n}'_0}{A'_0} = \frac{\vec{n}'_{ss} \cdot \vec{n}'_1}{A'_1} \quad (7.110)$$

where the rays in the moving frame are normal to the shock surface.

Since the directions of the shock-shock surface, undisturbed shock and disturbed shock remain unchanged when the transformation of coordinates is made, we have

$$\vec{n}'_{ss} = \vec{n}_{ss} \quad (7.111)$$

$$\vec{n}'_0 = \vec{n}_0 \quad (7.112)$$

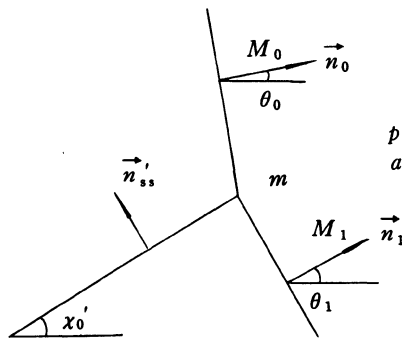


Fig. 7.5 (a) The fluid element

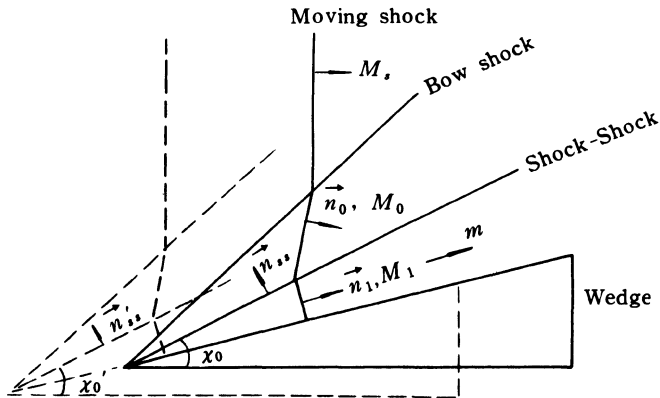


Fig. 7.5 (b) Interaction of a plane moving shock with the bow shock attached to a wedge

$$\vec{n}'_1 = \vec{n}_1 \quad (7.113)$$

and

$$\frac{\vec{n}_{ss} \cdot \vec{n}_0}{A'_0} = \frac{\vec{n}_{ss} \cdot \vec{n}_1}{A'_1}. \quad (7.114)$$

In order to obtain intuitive flow pattern of the shock-shock disturbance propagating on the shock surface, we only consider that a shock wave moves into a uniform, two-dimensional flow field, for example, an interaction of a plane moving shock with the bow shock attached to a wedge, as shown in Fig. 7.5.b.

In this case, the shock-shock trace is a straight line, the angle between the trace and x -axis is denoted by χ_0 . In the moving frame, which is attached to the uniform flow ahead of the shock waves, the flow pattern is illustrated by the dashed lines. Obviously, the shock-shock angle remains unchanged(Han and Yin, 1992), that is,

$$\chi'_0 = \chi_0 \quad (7.115)$$

From Fig. 7.5b, we can obtain

$$\vec{n}_{ss} \cdot \vec{n}_0 = -\sin(\chi_0 - \theta_0) \quad (7.116)$$

$$\vec{n}_{ss} \cdot \vec{n}_1 = -\sin(\chi_0 - \theta_1) \quad (7.117)$$

$$\vec{n}_{ss} \times \vec{n}_0 = \cos(\chi_0 - \theta_0) \vec{v} \quad (7.118)$$

$$\vec{n}_{ss} \times \vec{n}_1 = \cos(\chi_0 - \theta_1) \vec{v} \quad (7.119)$$

where \vec{v} is unit vector normal to the paper surface.

It should be noted that the relations (7.116) through (7.119) are also valid for the cases of curved shock-shock traces in two-dimensional flow and axially-symmetrical flow.

Substituting (7.116) and (7.117) into (7.114), we obtain

$$\frac{\sin(\chi_0 - \theta_0)}{A'_0} = \frac{\sin(\chi_0 - \theta_1)}{A'_1} \quad (7.120)$$

Substituting (7.118) and (7.119) into (7.109), we obtain

$$\frac{\cos(\chi_0 - \theta_0)}{M_0 + m\cos(\theta_0 - \varepsilon)} = \frac{\cos(\chi_0 - \theta_1)}{M_1 + m\cos(\theta_1 - \varepsilon)} \quad (7.121)$$

Next we will discuss the area relation along the ray tube across the shock-shock in the moving frame.

From Chapter 4, we have

$$e \frac{dM}{d\alpha'} + \frac{g}{a_1} \frac{da_1}{d\alpha'} + \frac{h}{p_1} \frac{dp_1}{d\alpha_1} = - \frac{1}{A'} \frac{dA'}{d\alpha'} \quad (7.122)$$

It is evident that there are only the changes in M , θ and A' across the shock-shock trace, that is, the changes in p_1 , a_1 can be negligible. So we have

$$edM = - \frac{dA'}{A'} \quad (7.123)$$

or

$$\frac{A'_1}{A'_0} = \frac{f(M_1)}{f(M_0)} \quad (7.124)$$

Summarizing the above relations, in general case, we have the following shock-shock relations,

$$\begin{cases} \frac{\vec{n}_{ss} \times \vec{n}_0}{[M_0 + m(\vec{n}_0 \cdot \vec{n}_f)]} = \frac{\vec{n}_{ss} \times \vec{n}_1}{[M_1 + m(\vec{n}_1 \cdot \vec{n}_f)]} \\ \frac{\vec{n}_{ss} \cdot \vec{n}_0}{A'_0} = \frac{\vec{n}_{ss} \cdot \vec{n}_1}{A'_1} \\ \frac{A'_1}{A'_0} = \frac{f(M_1)}{f(M_0)} \end{cases} \quad (7.125)$$

In two-dimensional case including that χ_0 is a variable or a constant, the relations (7.125) can be written as

$$\begin{cases} \frac{\cos(\chi_0 - \theta_0)}{M_0 + m\cos(\theta_0 - \varepsilon)} = \frac{\cos(\chi_0 - \theta_1)}{M_1 + m\cos(\theta_1 - \varepsilon)} \\ \frac{\sin(\chi_0 - \theta_0)}{A'_0} = \frac{\sin(\chi_0 - \theta_1)}{A'_1} \\ \frac{A'_1}{A'_0} = \frac{f(M_1)}{f(M_0)} \end{cases} \quad (7.126)$$

It is noted that the relations (7.126) are also valid for axially-symmetrical flow.

We introduce two quantities W_0 and W_1 which are expressed as follows

$$W_0 = M_0 + m\cos(\theta_0 - \varepsilon) \quad (7.127)$$

$$W_1 = M_1 + m\cos(\theta_1 - \varepsilon) \quad (7.128)$$

It is evident that W_0 represents the ratio of the absolute velocity of the undisturbed shock to the speed of sound in the region immediately ahead of the shock at the triple-point, and W_1 represents the ratio for the disturbed shock.

The first and second expressions of (7.126) can be expressed in another form

$$\tan(\theta_1 - \theta_0) = \frac{(W_1^2 - W_0^2)^{\frac{1}{2}}(A'_0{}^2 - A'_1{}^2)^{\frac{1}{2}}}{A'_1 W_1 + A'_0 W_0} \quad (7.129)$$

$$\tan(\chi_0 - \theta_0) = \frac{A'_0}{W_0} \frac{(W_1^2 - W_0^2)^{\frac{1}{2}}}{(A'_0{}^2 - A'_1{}^2)^{\frac{1}{2}}} \quad (7.130)$$

In this section, we have discussed the shock-shock relations for a moving gas ahead of a shock, which are very important for calculating the phenomena of a shock moving into a uniform or a nonuniform flow.

§ 7.8 The application of the equations of shock dynamics to "shock-on-shock interaction"

So-called "Shock-on-Shock Interaction" means the interaction of a moving shock with the bow shock attached to a supersonic vehicle, which is an important research topic in the field of gas dynamics and shock dynamics.

There are three methods that can be used for studying the topic, i.e., experimental method, theoretical method, and numerical method. Of course, the best way is to apply the three methods jointly.

Our purpose in this section is to make an application of the equations of shock dynamics derived before to the calculation of the waves in the interaction of a moving plane shock with the bow shock attached to a cone.

The shock-on-shock interactions can be divided into two types, that is, the head-on interaction and oblique interaction. So-called head-on interaction means that the angle between the normal to the moving plane shock and the axis of vehicle (cone, in present case) is equal to zero. Of course, this is a special case. In more general case, the angle of interaction mentioned above is not equal to zero. We call the case oblique interaction.

1. The head-on interaction

The shock waves of the head-on interaction of the plane moving shock with the bow shock attached to the cone is not only axially-symmetrical, but also self-similar, which is shown in Fig. 7.6.

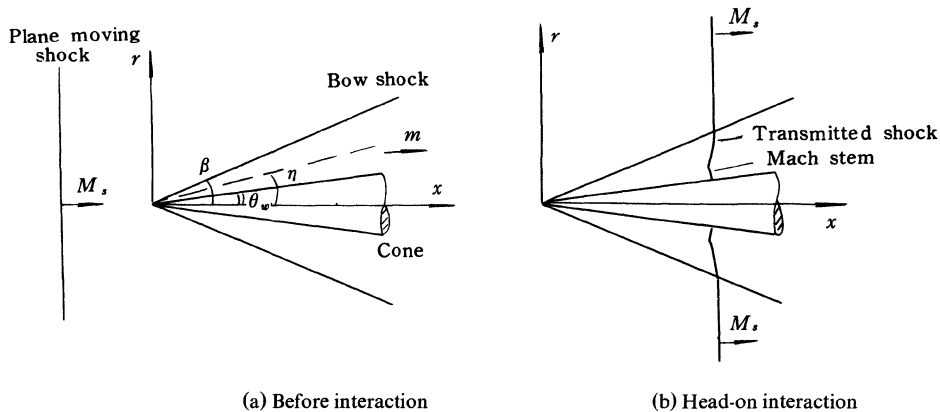


Fig. 7.6 Head-on interaction of a plane moving shock with the bow shock attached to a cone

The procedure of the calculation includes that the first is to find conical flow field around the cone; the second is to calculate the interaction of the plane mov-

ing shock with bow shock; the third is to calculate the transmitted shock from the point where the plane moving shock intersects with the bow shock to the shock-shock; the fourth is to calculate the Mach stem according to shock-shock conditions and boundary conditions on the surface of the cone.

(1) Conical flow field before the interaction

The flow field around the cone may be described by the following equations.

Under the conditions of the axially-symmetrical and self-similar flow, that is, $\frac{\partial}{\partial \varphi} = 0$, $\frac{\partial}{\partial r} = 0$, the equation of continuity in the spherical coordinates can be expressed as

$$\frac{2\rho v_r}{r} + \frac{1}{r \sin \eta} \frac{\partial}{\partial \eta} (\rho v_\eta \sin \eta) = 0 \quad (7.131)$$

or

$$2v_r + v_\eta \cot \eta + \frac{v_\eta}{\rho} \frac{d\rho}{d\eta} + \frac{dv_\eta}{d\eta} = 0 \quad (7.132)$$

Under the same flow conditions, the equation of momentum can be written as

$$\frac{v_\eta}{r} \left[\left(v_r + \frac{dv_\eta}{d\eta} \right) \vec{i}_\eta + \left(\frac{dv_r}{d\eta} - v_\eta \right) \vec{i}_r \right] = - \frac{1}{\rho r} \frac{dp}{d\eta} \vec{i}_\eta \quad (7.133)$$

where \vec{i}_η and \vec{i}_r are the unit vectors in η and r directions, respectively; v_η and v_r are the components of the velocity in η and r directions, respectively.

From (7.133), we get

$$v_\eta = \frac{dv_r}{d\eta} \quad (7.134)$$

$$\frac{v_\eta v_r}{r} + \frac{v_\eta}{r} \frac{dv_\eta}{d\eta} = - \frac{a^2}{\rho r} \frac{dp}{d\eta} \quad (7.135)$$

From (7.132) and (7.135), we can eliminate $d\rho / d\eta$, and then combining (7.134), thus we get following two relations for calculating the flow field around the cone

$$\begin{cases} \left(1 - \frac{v_\eta^2}{a^2} \right) \frac{dv_\eta}{d\eta} + \left(2 - \frac{v_\eta^2}{a^2} \right) v_r + v_\eta \cot \eta = 0 \\ v_\eta = \frac{dv_r}{d\eta} \end{cases} \quad (7.136)$$

The boundary condition on the bow shock may be given as follows:

According to the tangential continuity of the velocity across the bow shock

front, we get

$$v_{rs} = m_1 a_1 \cos \beta \quad (7.137)$$

where the subscript "s" denotes the value immediately behind the bow shock; m_1 and a_1 are the flow Mach number and speed of sound in the region ahead of the bow shock, respectively; β is the angle of the bow shock with the axis of the cone.

The speed of sound ahead of the bow shock, a_1 , can be expressed by

$$a_1 = a_T (1 + \frac{\gamma - 1}{2} m_1^2)^{\frac{1}{2}} \quad (7.138)$$

where a_T is the speed of sound at the stagnation point.

The normal component of the velocity immediately behind the bow shock can be expressed as,

$$v_{\eta s} = m_{sn} \cdot a_s \quad (7.139)$$

where

$$\begin{aligned} a_s &= a_1 \left[\frac{\left(1 + \frac{\gamma - 1}{2} m_1^2 \sin^2 \beta\right) \left(\frac{2\gamma}{\gamma - 1} m_1^2 \sin^2 \beta - 1\right)}{\frac{(\gamma + 1)^2}{2(\gamma - 1)} m_1^2 \sin^2 \beta} \right]^{\frac{1}{2}} \\ m_{sn} &= \left[\frac{m_1^2 \sin^2 \beta + \frac{2}{\gamma - 1}}{\frac{2\gamma}{\gamma - 1} m_1^2 \sin^2 \beta - 1} \right]^{\frac{1}{2}} \\ m_s &= \frac{v_s}{a_s} = \frac{(v_{\eta s}^2 + v_{rs}^2)^{\frac{1}{2}}}{a_s} \end{aligned} \quad (7.140)$$

The boundary condition on the surface of the cone is $v_\eta = 0$.

The flow field around the cone is shown in Fig. 7.7.

(2) The intersection of the plane moving shock with the bow shock

The intersection of the plane moving shock with the bow shock will form a transmitted shock and a deflected shock as shown in Fig. 7.8.

In the vicinity of the intersection point e, the flow field may be divided into five regions, i.e., regions ①, ②, ③, ④, and ⑤, by the moving shock, bow shock, transmitted shock, deflected shock, and contact surface, respectively.

The velocity of the point e along the bow shock may be expressed as

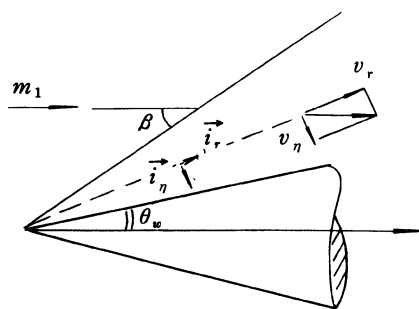


Fig. 7.7 The conical flow field

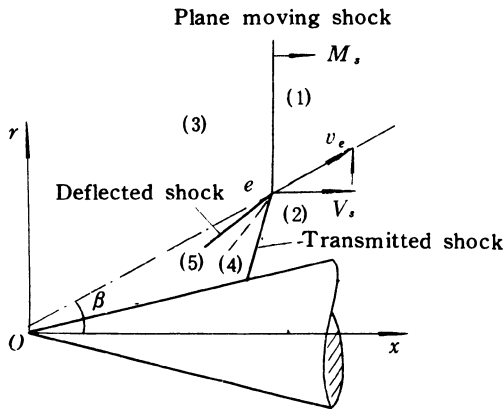


Fig. 7.8 The plane moving shock intersects with the bow shock at point e

$$v_e = \frac{V_s}{\cos \beta} = \frac{(M + m_1)a_1}{\cos \beta} \quad (7.141)$$

In order to transfer the unsteady flow field in the vicinity of the point e into the steady one, it is necessary to be superposed by a velocity $-\vec{v}_e$, that is, a moving frame of reference which is attached to the point e can be used. In the moving frame, the point e is at rest, of course, the velocity $-\vec{v}_e$ will be superposed on the entire flow field, which will change the velocities in the regions mentioned above.

The first thing we have to do before the superposition of the velocity $-\vec{v}_e$

is to find out the parameters in regions ② and ③.

The parameters in region ② refer to that immediately behind the bow shock, which have been given by relations (7.137), (7.138), (7.139), and (7.140).

The parameters in region ③ are given by the following relations

$$p_3 = p_1 \left(\frac{2\gamma}{\gamma+1} M^2 - \frac{\gamma-1}{\gamma+1} \right) \quad (7.142)$$

$$a_3 = a_1 \left[\frac{\left(1 + \frac{r-1}{2} M^2 \right) \left(\frac{2\gamma}{\gamma-1} M^2 - 1 \right)}{\frac{(\gamma+1)^2}{2(\gamma-1)} M^2} \right]^{\frac{1}{2}} \quad (7.143)$$

$$v_3 = m_1 a_1 + \frac{2a_1}{\gamma+1} \left(M - \frac{1}{M} \right) \quad (7.144)$$

$$m_3 = \frac{v_3}{a_3} \quad (7.145)$$

The velocity $-\vec{v}_e$ is superposed in regions ② and ③, thus we get

$$\vec{v}_2 - \vec{v}_e = \vec{v}_{2R} \quad (7.146)$$

$$\vec{v}_3 - \vec{v}_e = \vec{v}_{3R} \quad (7.147)$$

where $\vec{v}_2 = \vec{v}_s$, the velocity immediately behind the bow shock. The subscript "R" refers to the quantities in the moving frame.

(7.146) and (7.147) are divided by $a_2 (= a_s)$ and a_3 , respectively, we get

$$\vec{m}_2 = \vec{M}_{e2} + \vec{m}_{2R} \quad (7.148)$$

$$\vec{m}_3 = \vec{M}_{e3} + \vec{m}_{3R} \quad (7.149)$$

where

$$\vec{m}_2 = \frac{\vec{v}_2}{a_2}, \quad \vec{m}_3 = \frac{\vec{v}_3}{a_3},$$

$$\vec{m}_{2R} = \frac{\vec{v}_{2R}}{a_2}, \quad \vec{m}_{3R} = \frac{\vec{v}_{3R}}{a_3},$$

$$\vec{M}_{e2} = \frac{\vec{v}_e}{a_2}, \quad \vec{M}_{e3} = \frac{\vec{v}_e}{a_3}.$$

From (7.141), (7.148), and (7.149), we have

$$M_{e2} = \frac{(M + m_1)}{\cos\beta} \cdot \frac{a_1}{a_2} \quad (7.150)$$

$$M_{e3} = \frac{(M + m_1)}{\cos\beta} \cdot \frac{a_1}{a_3} \quad (7.151)$$

According to relations (7.148) and (7.149), the geometrical configurations are shown in Fig. 7.9.

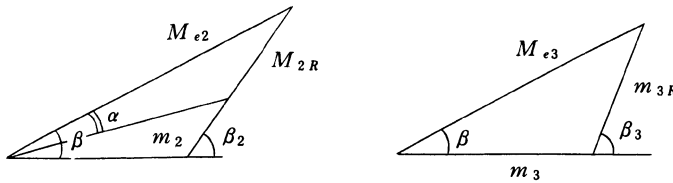


Fig. 7.9 The geometrical configurations

From Fig. 7.9 we can obtain the following relations

$$m_{2R} = (m_2^2 + M_{e2}^2 - 2m_2 M_{e2} \cos\alpha)^{\frac{1}{2}} \quad (7.152)$$

$$m_{3R} = (m_3^2 + M_{e3}^2 - 2m_3 M_{e3} \cos\beta)^{\frac{1}{2}} \quad (7.153)$$

where

$$\alpha = \tan^{-1} \frac{v_{rs}}{v_{\eta s}}$$

$$\beta_2 = \sin^{-1} \left(\frac{m_2 \sin\alpha}{m_{2R}} \right) + \beta \quad (7.154)$$

$$\beta_3 = \sin^{-1} \left(\frac{m_3 \sin\beta}{m_{3R}} \right) + \beta \quad (7.155)$$

Next, we want to find out the directions of the transmitted shock and deflected shock.

In the moving frame of reference attached to point e , we have the following flow field as shown in Fig. 7.10.

In order to find out wave angles, θ_2 and θ_3 , we can write the following six equations from region ② to ④, region ③ to ⑤,

$$\frac{P_4}{P_2} = \frac{2\gamma}{\gamma+1} (m_{2R} \sin\theta_2)^2 - \frac{\gamma-1}{\gamma+1} \quad (7.156)$$

$$\frac{P_5}{P_3} = \frac{2\gamma}{\gamma+1} (m_{3R} \sin\theta_3)^2 - \frac{\gamma-1}{\gamma+1} \quad (7.157)$$

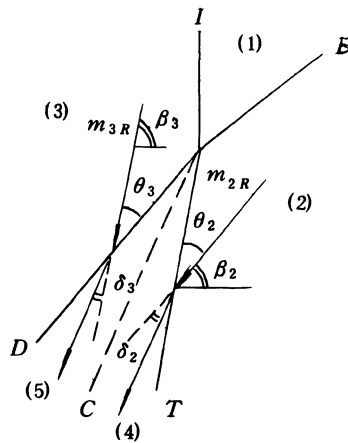


Fig. 7.10 The flow field in the moving frame

I: Moving shock B: Bow shock

T: Transmitted shock D: Deflected shock C: Contact surface

$$\tan \delta_2 = 2 \cot \theta_2 \frac{m_{2R}^2 \sin^2 \theta_2 - 1}{m_{2R}^2 (\gamma + \cos 2\theta_2) + 2} \quad (7.158)$$

$$\tan \delta_3 = 2 \cot \theta_3 \frac{m_{3R}^2 \sin^2 \theta_3 - 1}{m_{3R}^2 (\gamma + \cos 2\theta_3) + 2} \quad (7.159)$$

$$p_4 = p_5 \quad (7.160)$$

$$\delta_2 + \delta_3 = \beta_3 - \beta_2 \quad (7.161)$$

In the above six equations, m_{2R} , m_{3R} , β_2 , β_3 , p_2 and p_3 are given, θ_2 , θ_3 , δ_2 , δ_3 , p_4 and p_5 are unknown. So we can find out the solutions from (7.156) through (7.161).

Now we can obtain the angle between the transmitted shock and the axis of the cone (x -axis) by using $(\theta_2 + \beta_2)$.

It should be noted that the strength and wave direction of the transmitted shock are not influenced by the transformation of coordinates, so the strength of the transmitted moving shock can be expressed as

$$M_T = m_{2R} \sin \theta_2 \quad (7.162)$$

The angle of the transmitted shock, θ_T , can be expressed as

$$\theta_r = (\theta_2 + \beta_2) - 90^\circ \quad (7.163)$$

(3) The transmitted shock propagating in the conical flow field

The results obtained from relations (7.162) and (7.163) can be used as the boundary conditions to calculate the transmitted shock which will move into the nonuniform conical flow field, then by using the equations (7.101), (7.102) and the known parameters of the conical flow field, M and ε , we can find out the M and θ of the transmitted shock at any given η .

(4) The Mach stem in the conical flow field

In the case of head-on interaction, the reflection of the transmitted shock on the surface of the cone is always Mach reflection. So we cannot make the calculation of the transmitted shock directly from the bow shock to the surface of the cone.

In order to satisfy the boundary condition on the surface of the cone, it is necessary to use the shock-shock relations (7.125) or (7.126).

Since the shock-shock angle χ_0 is not known in advance, we first need to assume an angle χ_0 , and then we can find out the Mach number M_1 and wave angle θ_1 of the Mach Stem, at $\eta = \chi_0$. Next, M_1 and θ_1 are used as the boundary condition, we can calculate M and θ of the whole curved Mach stem according to the equations (7.101) and (7.102).

When the Mach stem reaches the surface of the cone, namely, $\eta = \theta_w$ (θ_w is the semi-angle of the cone), the wave angle θ ought to be equal to θ_w . If $\theta \neq \theta_w$ at the surface of the cone, another angle χ_0 will be assumed, and the procedure mentioned above has to be repeated until the Mach stem is normal to the surface of the cone. Thus we can find out the strengths, wave angles and shapes of the transmitted shock and Mach stem, and the transient pressure on the surface of the cone under the condition of the head-on interaction of a plane moving with the bow shock attached to a cone.

2. The oblique interaction

When the angle between the normal to the plane moving shock and the axis of the cone, is not equal to zero, the oblique interaction occurs. This angle is called interaction angle, which is denoted by λ . The wave system of oblique interaction is shown in Fig. 7.11.

The oblique interaction of the plane moving shock with the bow shock attached to a moving body is an unsteady, three-dimensional problem with a complicated flow pattern.

(1) The oblique interaction in the symmetrical plane through the axis of the cone.

If we only want to obtain the wave system of the oblique interaction in the

symmetrical plane through the axis of the cone, the problem may be simplified to some extent. As an approximation, the axially-symmetrical and self-similar equation (7.100) can still be used, if the angle λ is not too large.

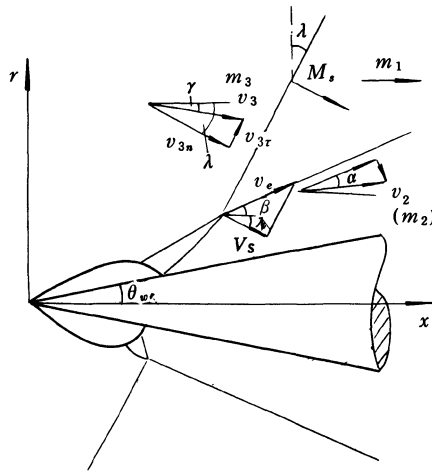


Fig. 7.11 The oblique interaction of plane moving shock with bow shock attached to a cone

Owing to the interaction angle $\lambda \neq 0$, some changes will be made in the calculation of boundary condition on the bow shock.

The velocity of the intersection point e along the bow shock can be expressed as

$$v_e = \frac{V_s}{\cos(\beta + \lambda)} = \frac{(M + m_1 \cos \lambda) a_1}{\cos(\beta + \lambda)} \quad (7.164)$$

$$M_{e2} = \frac{(M + m_1 \cos \lambda) a_1}{\cos(\beta + \lambda)} \frac{a_1}{a_2} \quad (7.165)$$

$$M_{e3} = \frac{(M + m_1 \cos \lambda) a_1}{\cos(\beta + \lambda)} \frac{a_1}{a_3} \quad (7.166)$$

$$\vec{m}_2 = \vec{M}_{e2} + \vec{m}_{2R} \quad (7.167)$$

$$\vec{m}_3 = \vec{M}_{e3} + \vec{m}_{3R} \quad (7.168)$$

where m_2 refers to m_s , which is the flow Mach number immediately behind the bow shock.

$$m_{2R} = (m_2^2 + M_{e2}^2 - 2m_2 M_{e2} \cos \alpha)^{\frac{1}{2}} \quad (7.169)$$

$$m_{3R} = (m_3^2 + M_{e_3}^2 - 2m_3 M_{e_3} \cos(\beta + \gamma))^{\frac{1}{2}} \quad (7.170)$$

where

$$\begin{aligned} \gamma &= \lambda - \tan^{-1} \frac{v_{3\tau}}{v_{3n}} \\ v_{3\tau} &= m_1 a_1 \sin \lambda \\ v_{3n} &= \frac{2a_1}{\gamma + 1} \left(M - \frac{1}{M} \right) + m_1 a_1 \cos \lambda \\ \beta_2 &= \sin^{-1} \left(\frac{m_2 \sin \alpha}{m_{2R}} \right) + \beta \end{aligned} \quad (7.171)$$

$$\beta_3 = \sin^{-1} \left[\frac{m_3 \sin(\beta + \gamma)}{m_{3R}} \right] + \beta \quad (7.172)$$

Next, the same method as the head-on interaction may be used for finding the transmitted and deflected shock.

Finally, the transmitted shock at the intersection point obtained above can be used as the boundary conditions to calculate the transmitted shock which moves into the nonuniform flow field, by using the same equations as the axially-symmetric and self-similar case. By using the equations (7.101) and (7.102) and the known parameters of the conical flow field, m , ε , we can find out the M and θ of the transmitted shock at any given η . If the reflection of the transmitted shock on the surface of the cone is regular reflection, above calculation for the transmitted shock can be directly conducted to the surface of the cone; if the reflection on the surface of the cone is Mach reflection, the shock-shock conditions may be used for calculating the Mach stem.

The same procedure should be followed for calculating M and θ along the curved Mach stem by using the equations (7.101) and (7.102).

(2) The oblique interaction in the general case

The oblique interaction of a plane moving shock with the bow shock attached to a moving body is a three-dimensional, unsteady flow problem. If the body is the cone moving with zero angle of attack, the flow is self-similar, and then the problem may be summed up as three unknown functions and two independent variables.

Starting with the three-dimensional equations in spherical coordinates (7.90), noting that there is no circumferential component of the velocity in the conical flow field, $\varepsilon_\phi = 90^\circ$, $\cos \varepsilon_\phi = 0^\circ$ and the flow field is similar, $\frac{\partial}{\partial r} = 0$, and setting $\varepsilon_r = \varepsilon$, $\varepsilon_\eta = 90^\circ - \varepsilon$, the equations in the present case can be simpli-

fied and expressed as

$$\left\{ \begin{array}{l} \frac{\partial}{\partial \varphi} \left(\frac{M \cos \theta_\varphi}{A'L} \right) + \frac{\partial}{\partial \eta} \left[\frac{(M \cos \theta_\eta + m \sin \varepsilon) \sin \eta}{A'L} \right] \\ \quad + \frac{2(M \cos \theta_r + m \cos \varepsilon) \sin \eta}{A'L} = 0 \\ \frac{\partial}{\partial \varphi} \left(\frac{\cos \theta_r}{La} \right) = \frac{\cos \theta_\varphi}{La} \sin \eta \\ \frac{\partial}{\partial \eta} \left(\frac{\cos \theta_r}{La} \right) = \frac{\cos \theta_\eta}{La} \\ \cos^2 \theta_r + \cos^2 \theta_\varphi + \cos^2 \theta_\eta = 1 \\ -\frac{1}{A'} \left[\frac{\partial A'}{\partial \eta} + \frac{M \cos \theta_\varphi}{(M \cos \theta_\eta + m \sin \varepsilon) \sin \eta} \frac{\partial A'}{\partial \varphi} \right] \\ = \left(e \frac{\partial M}{\partial \eta} - f \frac{\partial m}{\partial \eta} \right) + \frac{M \cos \theta_\varphi}{(M \cos \theta_\eta + m \sin \varepsilon) \sin \eta} \left(e \frac{\partial M}{\partial \varphi} - f \frac{\partial m}{\partial \varphi} \right) \end{array} \right. \quad (7.173)$$

where

$$f = \frac{m \left(\frac{\gamma-1}{2} g + \gamma h \right)}{1 + \frac{\gamma-1}{2} m^2}$$

$$L = [M + m(\cos \theta_r \cos \varepsilon + \cos \theta_\eta \sin \varepsilon)]$$

Expanding the first expression of (7.173), and substituting the fifth expression into the first one, we can eliminate A' .

Taking partial derivative of the fourth expression of (7.173) with respect to φ , we get

$$\sin 2\theta_r \frac{\partial \theta_r}{\partial \varphi} + \sin 2\theta_\varphi \frac{\partial \theta_\varphi}{\partial \varphi} + \sin 2\theta_\eta \frac{\partial \theta_\eta}{\partial \varphi} = 0 \quad (7.174)$$

From the fourth expression of (7.173), we also get

$$\cos \theta_\varphi = \left(1 - \cos^2 \theta_r - \cos^2 \theta_\eta \right)^{\frac{1}{2}} \quad (7.175)$$

$$\sin \theta_\varphi = \left(\cos^2 \theta_r + \cos^2 \theta_\eta \right)^{\frac{1}{2}} \quad (7.176)$$

Substituting (7.175) and (7.176) into (7.174), and rearranging (7.174), we get

$$\frac{\partial \theta_\varphi}{\partial \varphi} = Q_1 \frac{\partial \theta_r}{\partial \varphi} + Q_2 \frac{\partial \theta_\eta}{\partial \varphi} \quad (7.177)$$

where

$$\begin{aligned} Q_1 &= -\left(\frac{\sin 2\theta_r}{\sin 2\theta_\eta}\right) = -\left[\frac{\sin 2\theta_r}{2(\cos^2 \theta_r + \cos^2 \theta_\eta)^{\frac{1}{2}}(1 - \cos^2 \theta_r \cos^2 \theta_\eta)^{\frac{1}{2}}}\right] \\ Q_2 &= -\left(\frac{\sin 2\theta_\eta}{\sin 2\theta_r}\right) = -\left[\frac{\sin 2\theta_\eta}{2(\cos^2 \theta_r + \cos^2 \theta_\eta)^{\frac{1}{2}}(1 - \cos^2 \theta_r \cos^2 \theta_\eta)^{\frac{1}{2}}}\right] \end{aligned}$$

Expanding the equations (7.173), and noting that the flow field ahead of the shock is an axially-symmetrical flow, $\frac{\partial m}{\partial \varphi} = 0$, $\frac{\partial \varepsilon}{\partial \varphi} = 0$, we get following equations

$$\left\{ \begin{array}{l} E_1 \frac{\partial M}{\partial \varphi} + E_2 \frac{\partial M}{\partial \eta} + (E_3 + E_7 Q_1) \frac{\partial \theta_r}{\partial \varphi} + E_4 \frac{\partial \theta_r}{\partial \eta} \\ \quad + (E_5 + E_7 Q_2) \frac{\partial \theta_\eta}{\partial \varphi} + E_6 \frac{\partial \theta_\eta}{\partial \eta} = E_{10} \frac{\partial m}{\partial \eta} + E_{12} \frac{\partial \varepsilon}{\partial \eta} + E_0 \\ F_1 \frac{\partial M}{\partial \varphi} + F_3 \frac{\partial \theta_r}{\partial \varphi} + F_5 \frac{\partial \theta_\eta}{\partial \varphi} = F_0 \\ H_2 \frac{\partial M}{\partial \eta} + H_4 \frac{\partial \theta_r}{\partial \eta} + H_6 \frac{\partial \theta_\eta}{\partial \eta} = H_{10} \frac{\partial m}{\partial \eta} + H_{12} \frac{\partial \varepsilon}{\partial \eta} + H_0 \end{array} \right. \quad (7.178)$$

where

$$\begin{aligned} E_0 &= -2(M \cos \theta_r + m \cos \varepsilon) \sin \eta - (M \cos \theta_\eta + m \sin \varepsilon) \cos \eta, \\ E_1 &= (1 - \frac{M}{L} + M e)(1 - \cos^2 \theta_r - \cos^2 \theta_\eta)^{\frac{1}{2}}, \\ E_2 &= \cos \theta_\eta \sin \eta + e(M \cos \theta_\eta + m \sin \varepsilon) \sin \eta - \frac{1}{L}(M \cos \theta_\eta + m \sin \varepsilon) \sin \eta, \\ E_3 &= \frac{M m \sin \theta_r \cos \varepsilon (1 - \cos^2 \theta_r - \cos^2 \theta_\eta)^{\frac{1}{2}}}{L}, \\ E_4 &= \frac{m(M \cos \theta_\eta + m \sin \varepsilon) \sin \eta \cdot \cos \varepsilon \cdot \sin \theta_r}{L}, \\ E_5 &= \frac{M m \sin \theta_\eta \sin \varepsilon (1 - \cos^2 \theta_r - \cos^2 \theta_\eta)^{\frac{1}{2}}}{L}, \\ E_6 &= \frac{\sin \theta_\eta \sin \eta [m(M \cos \theta_\eta + m \sin \varepsilon) \sin \varepsilon - M]}{L}, \\ E_7 &= -M(\cos^2 \theta_r + \cos^2 \theta_\eta)^{\frac{1}{2}} \end{aligned}$$

$$\begin{aligned}
E_{10} &= f(M \cos \theta_\eta + m \sin \varepsilon) \sin \eta - \sin \varepsilon \cdot \sin \eta \\
&\quad + \frac{(M \cos \theta_\eta + m \sin \varepsilon)(\cos \theta_r \cos \varepsilon + \cos \theta_\eta \sin \varepsilon) \sin \eta}{L} \\
E_{12} &= -m \sin \eta \left[\frac{(M \cos \theta_\eta + m \sin \varepsilon)(\cos \theta_\eta \cos \varepsilon - \cos \theta_r \sin \varepsilon)}{L} - \cos \varepsilon \right] \\
F_0 &= -L \sin \eta (1 - \cos^2 \theta_r - \cos^2 \theta_\eta)^{\frac{1}{2}}, \\
H_0 &= -L \cos \theta_\eta \\
F_1 &= H_2 = \cos \theta_r \\
F_3 = H_4 &= L \sin \theta_r - m \cos \theta_r \sin \theta_r \cos \varepsilon \\
F_5 = H_6 &= -m \cos \theta_r \sin \theta_\eta \sin \varepsilon \\
H_{10} &= \frac{\frac{\gamma-1}{2} m \cos \theta_r L}{1 + \frac{\gamma-1}{2} m^2} - (\cos \theta_r \cos \varepsilon + \cos \theta_\eta \sin \varepsilon) \cos \theta_r \\
H_{12} &= -m \cos \theta_r (\cos \theta_r \sin \varepsilon - \cos \theta_\eta \cos \varepsilon)
\end{aligned}$$

If the subscripts of the coefficients are not the figures given above, the corresponding terms are equal to zero.

It follows from the equations (7.178) that the parameters of the conical flow field ahead of the shock, m , ε are given, the unknown functions are M , θ_r and θ_η . By using the equations (7.178) and corresponding boundary conditions, we can find out M , θ_r and θ_η at any given η and φ .

Up to now, in this course, we have explained and discussed the equations of shock dynamics and some applications in the various conditions, which include the quiescent and moving gases, uniform and nonuniform gases ahead of shocks, one-dimensional case to the three dimensional case.

In the following chapters, we will discuss the recent development of the Mach reflection of shocks on the surface of a wedge, refraction at the interface of gases and shock interactions, and explain some applications of shock dynamics to the fields mentioned above.

Part 3 Dynamic Phenomena of Shock Waves

Chapter 8 Reflections of Shock Waves in Steady and Pseudosteady Flows

§ 8.1 Introduction

The dynamic phenomena of shock waves which we shall discuss in the following chapters include the reflection of shock wave on a solid wall, the diffraction of shock wave around a convex corner, the refraction of shock wave across an interface between different media, and the interaction between two shock waves.

We begin discussing these phenomena since this chapter. Although the phenomena of diffraction and reflection of shocks have been explained briefly in Chapter 2, we need further to discuss them in detail. The reflection of shock waves in steady and pseudosteady flows will be explained in Chapter 8, the reflection in an unsteady flow will be introduced in Chapter 9 and the refraction and interaction of shock waves will be discussed in Chapter 10.

The reflection of shocks on a solid wall is a very important and interesting phenomenon. More than one hundred years ago, Mach(1875) first studied and discovered the Mach reflection effect. Since then, many researchers have studied this subject. von Neumann(1943) systematically analysed the shock reflection. Smith(1945) and White(1951) first observed the complex and double Mach reflections, respectively.

Over last twenty years the research work in the field of shock reflection has been made good progress. The representative works include work of the group around Glass at Toronto (Law and Glass, 1971; Ben-Dor and Glass, 1979, 1980), around Henderson at Sydney (Henderson and Lozzi, 1975, 1979), around Hornung at Göttingen (Hornung *et al.*, 1979, Hornung and Taloy, 1982), and around Takayama at Sendai (Ben-Dor and Takayama, 1985, 1987). Hornung (1986) and Ben-Dor(1988, 1992) gave us recent reviews in this field.

The reflections of shock waves may be divided into steady, pseudosteady and unsteady cases. For example, the reflection of an oblique shock wave generated by a wedge in supersonic wind tunnel on the surface of wall is the steady reflection. The reflections of a plane moving shock on the surface of a wedge or a cone belong to the pseudosteady reflection. However, the reflections of a plane moving shock on the surface of concave or convex wedge, or on the surface of sphere, and the reflection of a spherical shock on a plane surface are the

unsteady reflection.

On the other hand, the reflections of moving shock waves may also be divided into two types: the reflections for shock waves propagating into gases at rest and in motion, respectively.

So far, one has obtained four types of reflections: Regular Reflection (RR), Single Mach Reflection (SMR), Complex Mach Reflection (CMR) and Double Mach Reflection (DMR).

In this chapter, we shall introduce the flow patterns, types, transition criteria of reflections, and some calculation methods for the steady and pseudosteady flows. We first introduce some of oblique shock relations and the shock polar denoted by the pressure ratio and deflected angle, which is very useful for studying various dynamic phenomena of shock waves.

In the steady inviscid flow, the governing equations across the oblique shock are written as follows:

$$\text{continuity: } \rho_1 v_1 \sin\varphi = \rho_2 v_2 \sin(\varphi - \delta) \quad (8.1)$$

Momentum:

$$\text{tangential direction: } v_1 \cos\varphi = v_2 \cos(\varphi - \delta) \quad (8.2)$$

$$\text{normal direction: } p_1 + \rho_1 v_1^2 \sin^2 \varphi = p_2 + \rho_2 v_2^2 \sin^2(\varphi - \delta) \quad (8.3)$$

$$\text{Energy: } h_1 + \frac{1}{2} v_1^2 = h_2 + \frac{1}{2} v_2^2 \quad (8.4)$$

where ρ , p and h are the density, pressure and enthalpy, respectively; v is the flow velocity; φ is the angle between the shock front and the oncoming flow; and δ is the deflected angle of gas flow behind the shock. The subscripts 1 and 2 represent the states ahead of and behind the shock, respectively (see Fig. 8.1.a).

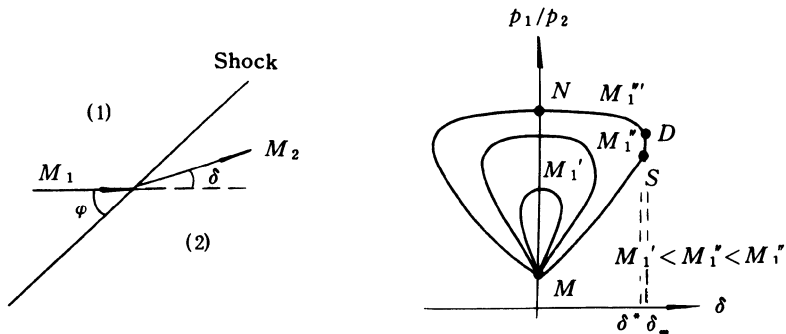


Fig. 8.1 Shock wave and shock polar

For the perfect gas, we have

$$h = C_p T = \frac{\gamma}{\gamma - 1} \frac{p}{\rho} \quad (8.5)$$

state equation: $p = \rho RT \quad (8.6)$

speed of sound: $a^2 = \gamma RT \quad (8.7)$

Mach number $M = v / a \quad (8.8)$

where T , γ and R are the temperature, ratio of specific heats, and gas constant, respectively.

Using (8.1)–(8.4), together with the relations (8.5)–(8.8), we can obtain the oblique shock relations expressed in terms of M_1 and p_2 / p_1 for the perfect gas

$$\xi = p_2 / p_1 \quad (8.9)$$

$$\sin^2 \varphi = \frac{(\gamma + 1)\xi + (\gamma - 1)}{2\gamma M_1^2} \quad (8.10)$$

$$\rho_2 / \rho_1 = \frac{(\gamma + 1)\xi + (\gamma - 1)}{(\gamma - 1)\xi + (\gamma + 1)} \quad (8.11)$$

$$T_2 / T_1 = (a_2 / a_1)^2 = \xi \cdot \frac{(\gamma - 1)\xi + (\gamma + 1)}{(\gamma + 1)\xi + (\gamma - 1)} \quad (8.12)$$

$$M_2^2 = \frac{M_1^2[(\gamma + 1)\xi + (\gamma - 1)] - 2(\xi^2 - 1)}{\xi[(\gamma - 1)\xi + (\gamma + 1)]} \quad (8.13)$$

$$\tan^2 \delta = \left[\frac{\xi - 1}{\gamma M_1^2 - (\xi - 1)} \right]^2 \frac{M_1^2 - \left[1 + \frac{\gamma + 1}{2\gamma} (\xi - 1) \right]}{1 + \frac{\gamma + 1}{2\gamma} (\xi - 1)} \quad (8.14)$$

For a given oncoming flow Mach number, M_1 , we can draw a curve in $\xi-\delta$ plane which is referred to as the pressure-deflected angle shock polar (as shown in Fig. 8.1). In most textbooks the hodograph shock polar has been introduced in more detail. As will be seen later, the $\xi-\delta$ shock polar is specially convenient for analysing problems of the reflection, refraction and interaction of shocks.

We can see from Fig. 8.1 that the shape of $\xi-\delta$ shock polar depends on γ and M_1 . Giving γ and changing M_1 , we get different $\xi-\delta$ shock polars. The polars are symmetrical about the ξ -axis because there are two possible values of δ for a given $\xi = p_2 / p_1$, which are equal in magnitude and opposite in sign. Giving a deflected angle δ , we can obtain two values of pressure which correspond to the strong and weak solutions of the shock wave, respectively.

Each point along the shock polar represents its own state. There are some special points along the polar. The point M corresponds to the Mach wave

with $p_2/p_1=1$ and $\delta=0$. The point N corresponds to the normal shock. The point D is called the maximum deflection point or detachment point. The corresponding deflected angle is referred to as the maximum deflection angle or detachment angle which is denoted by δ_m . It means that if δ is greater than δ_m , no solution may be obtained.

Taking the differential of (8.14) with respect to M_1 and letting $\frac{\partial \delta}{\partial M_1} = 0$,

we get a Mach number at which there is a maximum deflection angle δ_m for a fixed pressure ratio ξ :

$$(M_1^2)_{\text{for } \delta_m} = 2 + (\xi - 1) \quad (8.15)$$

Substituting this relation into (8.14), we obtain the corresponding maximum deflected angle δ_m denoted by the pressure ratio,

$$\tan \delta_m = \frac{1}{\gamma} \frac{(\xi - 1)}{\left[2 \sqrt{1 + \frac{\gamma + 1}{2\gamma}(\xi - 1)} \sqrt{1 + \frac{\gamma - 1}{2\gamma}(\xi - 1)} \right]} \quad (8.16)$$

Taking the differential of (8.14) with respect to ξ and letting $\frac{\partial \delta}{\partial \xi} = 0$, we can obtain the expression for ξ_m at the maximum deflection point in terms of M_1

$$\xi_m = \frac{1}{2} M_1^2 - 1 + \sqrt{\frac{4}{\gamma + 1} + \frac{2(\gamma - 1)}{\gamma + 1} M_1^2 + \frac{1}{4} M_1^4} \quad (8.17)$$

Substituting the relation (8.17) into (8.10), we get

$$\begin{aligned} \sin^2 \varphi_m &= \frac{1}{\gamma M_1^2} \left[\frac{\gamma + 1}{4} M_1^2 - 1 + \right. \\ &\quad \left. \sqrt{(\gamma + 1) \left[1 + \frac{\gamma - 1}{2} M_1^2 + \frac{\gamma + 1}{16} M_1^4 \right]} \right] \end{aligned} \quad (8.18)$$

Another special point in the $\xi-\delta$ diagram is the point S at which the flow behind the shock is exactly sonic. It is referred to as the sonic point. The corresponding deflected angle at the sonic point is denoted by δ^* . For $\gamma=1.4$, the value of δ^* is less than that of δ_m by as much as 0.5° over the entire range of Mach number, M_1 , from unity to infinity. In order to find out the pressure ratio ξ^* at the sonic point, letting $M_2=1$ in (8.13), we have that

$$\xi^* = \frac{1}{2} M_1^2 - \frac{1}{2} + \sqrt{\frac{\gamma + 9}{4(\gamma + 1)} - \frac{3 - \gamma}{2(\gamma + 1)} M_1^2 + \frac{1}{4} M_1^4} \quad (8.19)$$

Substituting the expression (8.19) into (8.10), we have that

$$\sin^2 \varphi^* = \frac{1}{\gamma M_1^2} \left[\frac{\gamma+1}{4} M_1^2 - \frac{3-\gamma}{4} + \sqrt{(\gamma+1) \left[\frac{9+\gamma}{6} - \frac{3-\gamma}{8} M_1^2 + \frac{\gamma+1}{16} M_1^4 \right]} \right] \quad (8.20)$$

The expressions (8.16)–(8.20) are useful for us to calculate the reflection, refraction and interaction of shock waves.

§ 8.2 Flow pattern

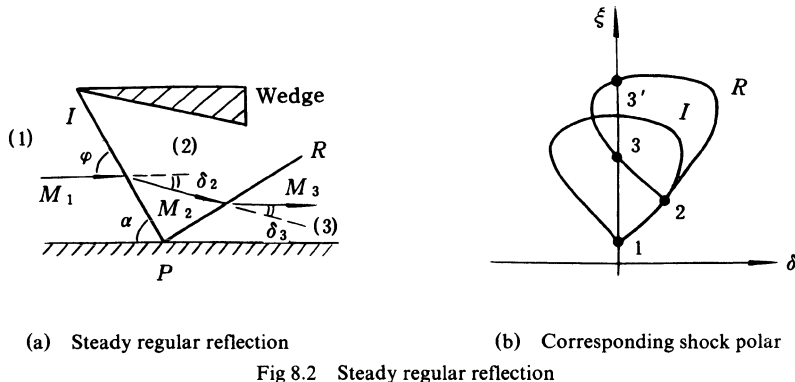
In this section we shall introduce some basic wave system about the reflection of a plane shock on the surface of wall in steady and pseudosteady cases, respectively. In the steady case, there exist regular reflection and single Mach reflection only. However, in the pseudosteady case, there are four types of reflections.

1. Steady inviscid flow

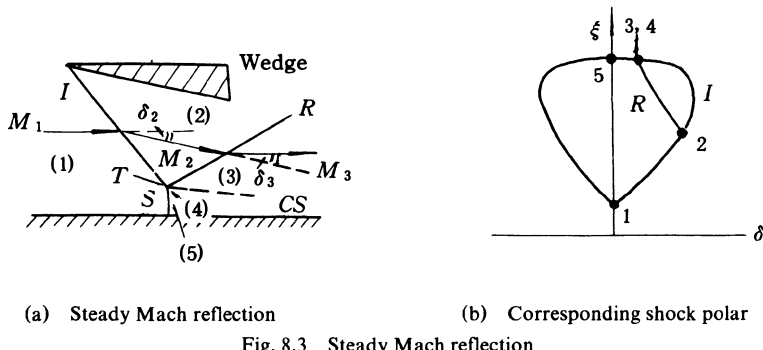
Consider the reflection of an oblique shock generated by a wedge in steady flow on the surface of wall (Fig. 8.2). The incident shock I deflects the freestream clockwise by angle δ_2 . Thus the flow direction in the region 2 behind the incident shock is not parallel to the wall. In order to satisfy the boundary condition on the wall, it is necessary for the reflected shock R to deflect the flow in region 2 anticlockwise by the same angle ($\delta_3 = -\delta_2$). This kind of reflection is called regular reflection (RR) which consists of two-shock configuration (an incident shock I and a reflected shock R).

The graphical solution to the regular reflection with the aid of the shock polar is shown in Fig. 8.2b. The point 2 represents the state of region 2 behind the incident shock, it lies on the incident shock polar I with $M = M_1$ and below the sonic point. From the point 2, we may draw the reflected shock polar R with $M = M_2$. There are two intersection points between the shock polar R and the ξ -axis which are the points 3 and 3'. The points 3 and 3' correspond to the weak and strong solutions of the reflected shock, respectively. In general, the weak solution of the reflected shock occurs, that is, the regular reflection shown in Fig. 8.2a should be represented by the points 1–2–3 in Fig. 8.2b.

If the incident angle α , which is the angle between the incident shock and the wall, is small, the regular reflection described above is possible. However, with the angle α increasing, the point 2 moves up along the polar I (because of increasing in δ_2) and the reflected shock polar R becomes small (because of decreasing in M_2). If the angle α is larger than some value, the reflected shock polar R may no longer intersect with the ξ -axis, so that the regular reflection become impossible and an irregular reflection takes place.



In the irregular reflection, there are four discontinuities. A near normal shock S (called Mach stem) connects with the incident shock I and reflected shock R at point T (called triple point) which lies above the wall and a contact surface CS (or, called slip line or vortex sheet) emanates from the point T (see Fig. 8.3.a). The contact surface separates the gas flow passing through I and R from that passing through S . The gases on both sides of the contact surface CS have the same pressure and flow direction. As the gases have passed through shocks of different strength, they have incurred different entropy increases and have different speeds. The contact surface is therefore a very thin region of concentrated vorticity. This kind of shock reflection is referred to as the Mach reflection (MR) which was first investigated by E.Mach (1878).



In the $\xi-\delta$ diagram, Fig. 8.3b, the reflected shock polar R intersects the incident shock polar I at point 3. As the pressure and flow direction in region 4

behind the Mach stem S are the same as that in region 3, the point 4 must be coincident with the point 3 in the $\xi-\delta$ plane. It is evident in Fig. 8.3 that in the vicinity of the point T the flow direction in regions 3 and 4 is inclines to the wall, but on the surface of wall it must be parallel to the wall. It means that in general the Mach stem is curved, which is represented by the part 4–5 of the polar I in Fig. 8.3.b.

2. Pseudosteady inviscid flow

Consider a plane shock moving from right to left into a gas at rest with shock Mach number M_s , and striking a wedge at rest with a semiapex angle, θ_w . If the wedge angle θ_w is sufficiently large (or the angle α is sufficiently small), the regular reflection (RR) occurs. Fig. 8.4.a shows the flow pattern of regular reflection which consists of two shock waves. The plane incident shock I strikes the surface of wedge at the point P . The reflected shock R , which, unlike the incident shock, is curved, emanates from the reflected point P , terminates on the horizontal surface and is normal to it. The intersection point P between the incident shock I and the surface of wedge moves at the following velocity

$$V_p = M_s \cdot a_1 / \cos\theta_w = M_s \cdot a_1 / \sin\alpha \quad (8.21)$$

where a_1 is the speed of sound in the region ahead of the moving shock. Since M_s , a_1 , and θ_w are constants, the velocity of the point P is also a constant, that is, the distance d increases linearly with time. This phenomenon is referred to as self-similar. In the absence of viscosity and heat flux, the only characteristic length of the boundary condition is d , which is a linear function of time. All physical parameters depend on the x/t and y/t . Therefore, the phenomenon is also called pseudosteady reflection.

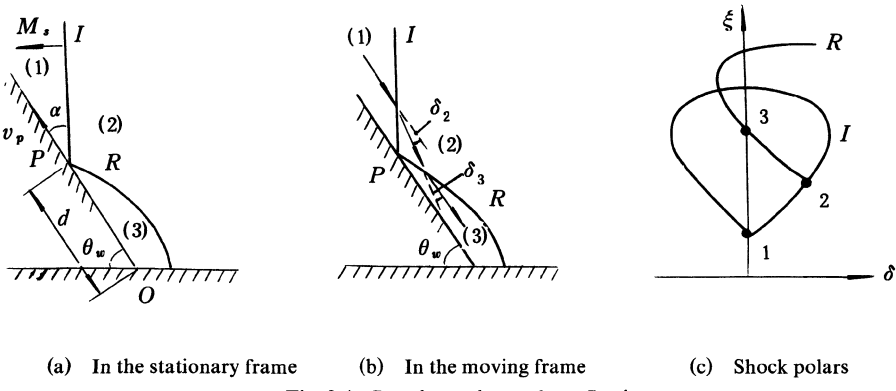
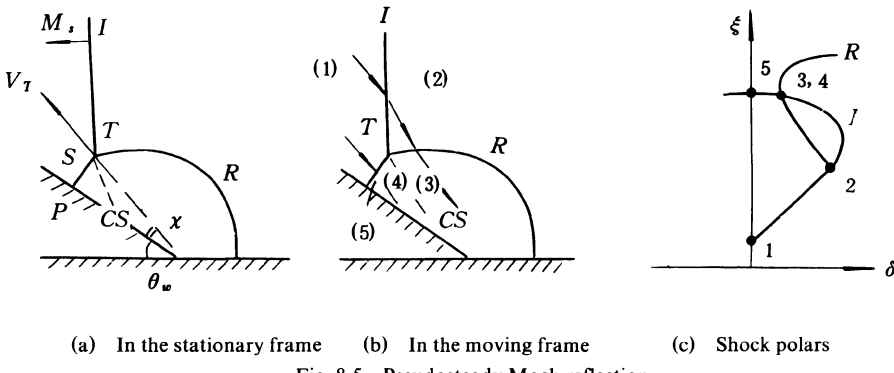


Fig. 8.4 Pseudosteady regular reflection

The pseudosteady shock reflection can be investigated using steady flow concept. In a frame of reference attached to and moving with the point P , the flow in the vicinity of the point P is steady. Figure 8.4.b shows the flow parameters in the moving frame of reference. The flow in region 1, which moves parallel to the wedge surface with Mach number $M_1 = M_s / \cos\theta_w$, is deflected towards the wedge surface by angle of δ_2 , passing through the incident shock I . The reflected shock deflects the flow in region 2 by angle of δ_3 in opposite direction, and the flow becomes again parallel to the wedge surface. Thus, $\delta_3 = \delta_2$. Figure 8.4.c shows the corresponding shock polar representation.

If the wedge angle θ_w decreases (α increases) and exceeds some critical value, the Mach reflection (MR) takes place (Fig. 8.5). MR consists of four discontinuities: the incident shock I , the reflected shock R , the Mach stem S and the slip surface CS , which meet at the point T (called the triple point). The Mach stem emanates from the point T and terminates on the wedge surface at the point P . In general the Mach stem is curved. The angle between the triple-point trace and the surface of wedge is denoted by χ and called trajectory angle of the triple point. The flow is self-similar and the triple-point T moves at a constant speed V_T .

$$V_T = M_s \cdot a_1 / \cos(\theta_w + \chi) \quad (8.22)$$



(a) In the stationary frame (b) In the moving frame (c) Shock polars

Fig. 8.5 Pseudosteady Mach reflection

In the moving frame of reference attached to the point T , the flow in the vicinity of T becomes steady. (Fig. 8.5.b) The corresponding shock polar is shown in Fig. 8.5.c.

The Mach reflection can be further subdivided into three types. One shown in Fig. 8.5 is called Single Mach Reflection (SMR) which consists of an incident shock I , a continuously curved reflected shock R , a Mach stem S , and a contact

surface CS . The other two are referred to as the Complex Mach Reflection (CMR) and Double Mach Reflection (DMR) which are shown in Fig. 8.6.a and b, respectively. CMR is characterized by a kinked reflected shock which consists of a piece of straight shock and a piece of curved shock. The intersection point of the two shocks is called the kink (K). DMR has two reflected shocks, two Mach stems, two contact surfaces and two triple points. The trajectory angle of the second triple point is denoted by χ'

In the steady supersonic wind tunnel experiments, only RR and SMR have been observed. In the unsteady case one has observed RR, SMR, CMR and DMR. Studying this problem, Ben-Dor and Glass(1979) concluded that in nonstationary flow shock reflections depend on two processes taking place simultaneously: the incident shock is reflected on the wedge surface, whereas the induced nonstationary flow behind it is deflected by the wedge. The interaction between the reflection and diffraction cause CMR and DMR to occur in nonstationary flows in addition to RR and SMR observed in steady flows.

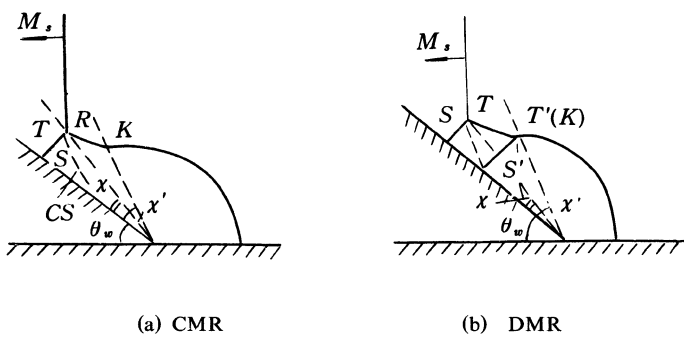


Fig. 8.6 CMR and DMR

§ 8.3 Some basic concept and analytic method

In this section we shall give the definitions of the weak and strong shock reflections, further analyse the shock polar and apply the shock polar to the shock reflections in the steady case. This analysis, of course, can be used to the pseudosteady case.

1. Special values of $\alpha(M, \gamma)$ in inviscid steady flow.

In the steady flow, the parameters influencing the types of reflection are Mach number of oncoming flow M_1 , incident angle α , and ratio of specific heats γ . There are some special values of α for given M_1 and γ .

First one is α_d which is called the maximum deflection condition or

detachment condition. Given M_1 and γ , when the incident angle α is equal to α_d , the reflected shock polar is just tangent to the ξ -axis as shown by the solid lines in Fig. 8.7. The pressure at the point of tangency of the reflected shock polar with the ξ -axis may be lower or higher than that at the normal shock point of the incident shock polar, depending on M_1 and γ . Accordingly, it is referred to as "weak" or "strong" reflection, respectively. Later we shall discuss another definition.

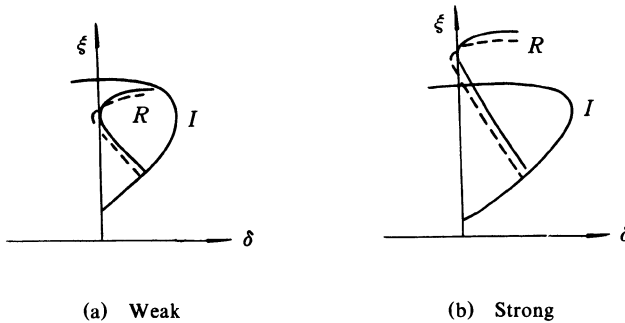


Fig. 8.7 Detachment condition(Solid lines) and sonic condition(dashed lines)

Just below the value of α_d , there is another special value of α at which the sonic point of the reflected shock polar lies on the ξ -axis. It is called the sonic condition and denoted by α_s . It is indicated by the dashed lines in Fig. 8.7.

The Third special value of α is defined as the condition that the intersection point between the reflected shock polar and the ξ -axis just lies at the normal shock point of the incident shock polar in ξ - δ plane, as shown in Fig. 8.8. The condition is named after von Neumann who first recognized its importance. The von Neumann condition is denoted by α_N .

There are two kinds of definitions of boundary between the weak and strong shock reflections. One corresponds to the condition that the detachment point coincides with the von Neumann point, that is, $\alpha_N = \alpha_d$. The other corresponds to the condition that the sonic point coincides with von Neumann point, that is, $\alpha_N = \alpha_s$. They occur at particular values of $M_1(\gamma)$ which is a function of the ratio of specific heats. The boundaries between weak and strong shocks are shown as follows for the two definitions, respectively.

Table 8.1 Two kinds of definitions of boundary between weak and strong shocks

	γ	5 / 3	7 / 5	9 / 7
$M_1(\gamma)$	$\alpha_N = \alpha_d$	2.47	2.20	2.10
	$\alpha_N = \alpha_s$	2.75	2.40	2.28

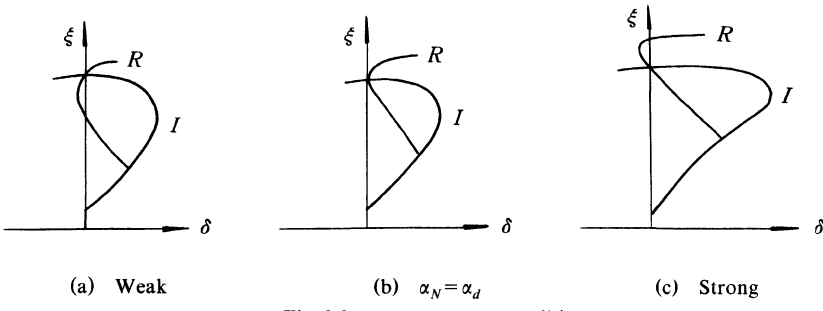


Fig. 8.8 von Neumann condition

2. Possible types of reflections in steady flow for $\gamma = 1.4$ (Hornung, 1986)

The factors influencing the shock reflection have M_1 , α , and γ . For the gas with $\gamma = 1.4$, we have two variables M_1 and α . In the following discussion, we shall analyse the shock polars and the corresponding possible types of shock reflections in different ranges of M_1 , respectively.

(1) $1 < M_1 < 1.25$:

In this range the polar of the reflected shock is inside that of the incident shock. We shall discuss two cases, $\alpha < \alpha_d$ and $\alpha > \alpha_d$, respectively.

$\alpha < \alpha_d$: As shown in Fig. 8.9.a by the curve(I), when $\alpha < \alpha_d$, the reflected shock polar intersects with the ξ -axis. We know that the regular reflection is possible in this case.

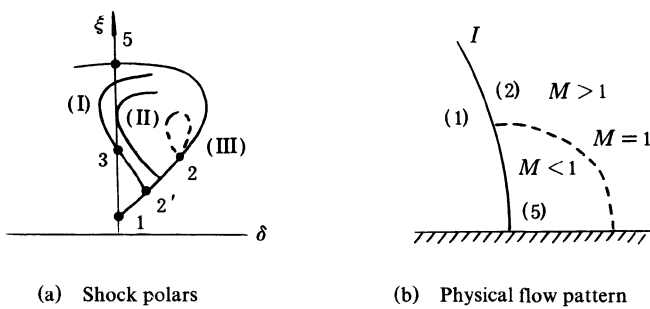


Fig. 8.9 $1 < M_1 < 1.25$

$\alpha > \alpha_d$: For the case $\alpha > \alpha_d$, the reflected shock polar intersects with neither the ξ -axis nor the incident shock polar, as shown in Fig. 8.9.a by the dashed line. in the physical plane for this case (Fig. 8.9.b), the incident shock should be curved and normal to the surface of wall. In the regions behind the incident shock there may exist a supersonic part (region 2) and a subsonic part (region 5)

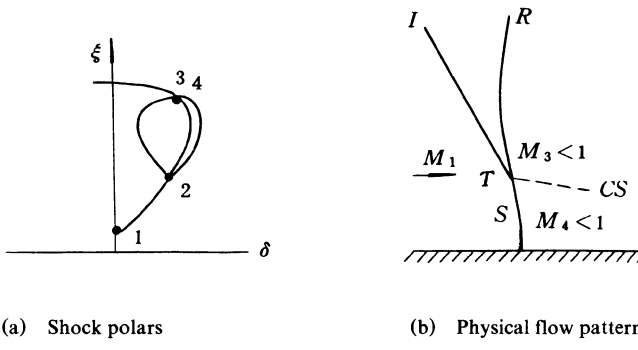
which are represented by the part 2–5 of the incident shock polar in the $\xi-\delta$ plane.

(2) $1.25 < M_1 < 1.48$:

In this range we shall discuss two cases, $\alpha < \alpha_d$ and $\alpha > \alpha_d$, respectively.

$\alpha < \alpha_d$: Similarly, the regular reflection is possible.

$\alpha > \alpha_d$: As shown in Fig. 8.10.a, in this case there exists an intersection point between the polars of the reflected and incident shocks and the intersection point lies to the right of the symmetric line of the reflected shock polar. It means that the gas behind the incident shock is again deflected toward the wall through the reflected shock. In the physical plane Fig. 8.10.b, the reflected shock should be inclined forward, the Mach stem is inclined backward and the contact surface slopes toward the wall in the vicinity of the triple point T .



(a) Shock polars

(b) Physical flow pattern

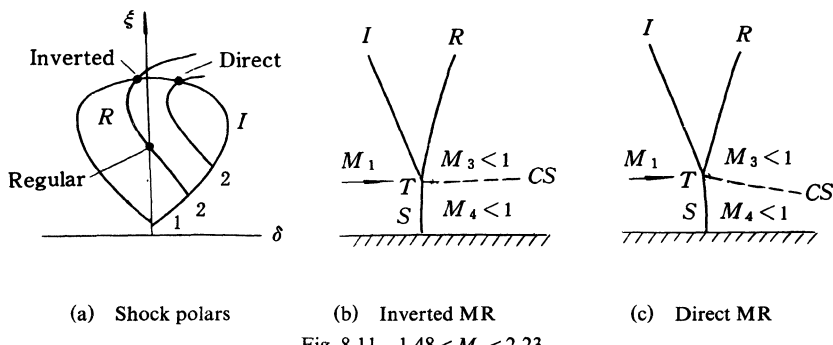
Fig. 8.10 $1.25 < M_1 < 1.48$

(3) $1.48 < M_1 < 2.20$:

In this range, we shall discuss three cases, $\alpha < \alpha_N$, $\alpha > \alpha_d$, $\alpha_N < \alpha < \alpha_d$, respectively.

$\alpha < \alpha_N$: We can see from Fig. 8.11.a that when $\alpha < \alpha_N$ there are two possible solutions. One is the intersection point between the reflected shock polar R and the ξ -axis. We know that this is a regular reflection. Another is the intersection point between the reflected shock polar R and the incident shock polar I . We can see from Fig. 8.11.a that the intersection point between two shock polars lies to the left of the ξ -axis in this case. It means that in the physical plane the contact surface CS slopes away from the wall and the Mach stem S is convex toward the upstream direction at the triple point T , as shown in Fig. 8.11.b. This kind of reflection is referred to as the inverted Mach reflection. We shall see this type of reflection in next chapter.

$\alpha > \alpha_d$: The condition $\alpha > \alpha_d$ means that there is no intersection point between the reflected shock polar and ξ -axis. But in this case the intersection point between the reflected and incident shock polars occurs, which lies to the left of the symmetric line of the reflected shock polar, as shown in Fig. 8.11.a. This kind of reflection is referred to as the direct Mach reflection. In the physical plane Fig. 8.11.c, the contact surface CS slopes to the wall, the Mach stem S is concave, and the reflected shock R is inclined downstream. If the angle α increases away from α_d , the case shown in Fig. 8.10 may occur.

Fig. 8.11 $1.48 < M_1 < 2.23$

$\alpha_N < \alpha < \alpha_d$: It is evident that in this range there are two possibilities: regular reflection and direct Mach reflection.

(4) $M_1 = 2.20$:

This is a special case. In this case $\alpha_d = \alpha_N$ (Fig. 8.8.b). The contact surface is parallel to the wall surface and the Mach stem is straight and normal to the wall. This kind of reflection is referred to as stationary Mach reflection.

(5) $M_1 > 2.40$:

In all the cases discussed above, if MR occurs, the gases on both sides of the contact surface are subsonic. For the case $M_1 > 2.40$, if MR occurs, the contact surface separates the supersonic region 3 from the subsonic region 4.

3. Summary

As a brief summary, the various reflections discussed above are shown in Fig. 8.12. Although these boundaries only apply to the inviscid flow with $\gamma = 1.4$, no qualitative difference occurs when γ is changed to other values. In the figure there are some regions in which both MR and RR are possible. Later we shall discuss which one will take place in fact and the transition criteria from RR to MR and from MR to RR.

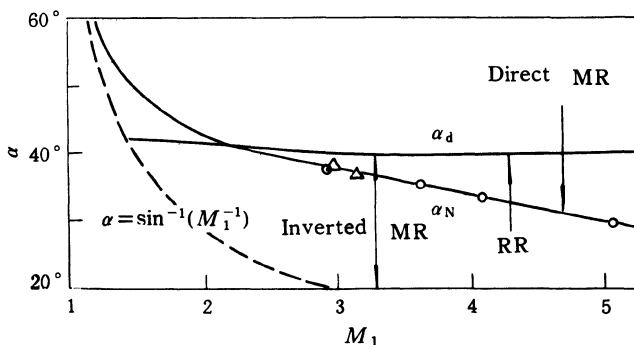


Fig. 8.12 The various reflection types in steady flow(Hornung, 1986)

§ 8.4 Transition criteria RR \rightleftharpoons MR in steady and pseudosteady flows

von Neumann(1943) first studied systematically the transition RR \rightleftharpoons MR in steady and pseudosteady flows. Since then, this subject has attracted many researchers. Up to now there are three transition criteria for RR \rightleftharpoons MR. In this section we shall discuss them.

1. Detachment criterion and sonic criterion

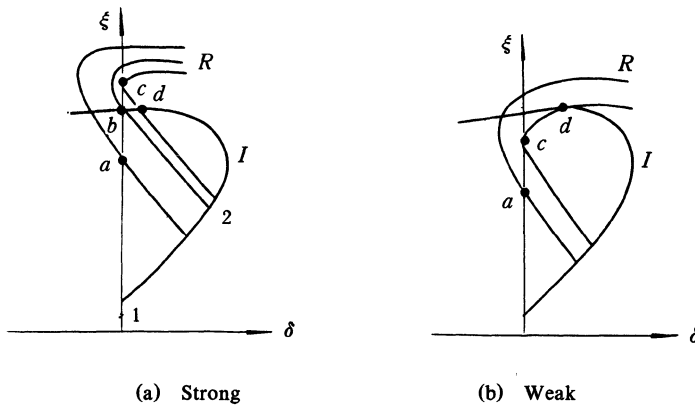
von Neumann deduced the well-known detachment criterion that the transition from RR to MR occurs when the flow deflected angle δ_2 through the incident shock exceeds the maximum flow deflected angle δ_{3m} through the reflected shock. It can mathematically be expressed as

$$\delta_2 - \delta_{3m} = 0 \quad (8.23)$$

In shock polars shown in Fig. 8.13, the state in region 3 behind the reflected shock is represented by the point a for RR. As the incident angle α increases for steady case (or the wedge angle θ_w decreases for pseudosteady case), the point a moves up along the ξ -axis until the polar R is tangent to the ξ -axis (point c). Upon a further increase in α (or decrease in θ_w), the polar R does not intersect the ξ -axis anymore and RR becomes impossible. Therefore the detachment criterion corresponds to the point c in the shock polars.

There is another transition criterion which is called the sonic criterion. It means that the transition from RR to MR takes place when the flow behind the reflected shock reaches local speed of sound with respect to the reflected point P (see Fig. 8.2 and 8.4). It is expressed as

$$\delta_2 - \delta_{3s} = 0 \quad (8.24)$$



The difference between δ_{3s} and δ_{3m} is very small, so that it is difficult to distinguish them experimentally

2. Mechanical equilibrium criterion

The mechanical equilibrium criterion, which was first suggested by von Neumann, was reinitiated by Henderson and Lozzi(1975). We can see from Fig. 8.13 that when RR terminates and MR forms, the pressure behind the reflected shock jumps from the point c (RR) to the point d (MR), if the detachment criterion is accepted. It means that there is a sudden pressure change during the transition. Henderson and Lozzi considered that such a sudden pressure change must be supported by either a compression wave or an expansion wave. But neither of these additional wave structures was observed experimentally. It is concluded that the pressure change in the system should be gradual during the transition and the system should remain in mechanical equilibrium. By this reason, the transition $RR \rightleftharpoons MR$ takes place at the point b shown in Fig. 8.13, that is, the polar R for reflected shock intersects the ξ -axis at the normal shock point of the incident shock polar I . According to the mechanical equilibrium criterion, with the angle α increasing, the procedure from RR to MR should be $a \rightarrow b \rightarrow d$ in Fig. 8.13. It can be formulated as

$$\delta_2 - \delta_3 = \delta_4 = 0 \quad (8.25)$$

As mentioned above, for the weak shock the tangency point of the polar R with the ξ -axis is inside the polar I and for the strong shock the tangency point is outside the polar I (Fig. 8.7). That is, there is no solution for the mechanical equilibrium criterion over the region of the weak shock.

3. Length scale criterion

Hornung *et al.*(1979) introduced another criterion which is referred to as the length scale criterion. Difference between RR and MR includes a length scale, namely the length of Mach stem. They argued that in order for MR to form, information about the characteristic length must reach the reflected point P , i.e., pressure signals must be communicated to the reflected point P of RR. This argument leads to different transition lines for steady and pseudosteady cases, respectively.

We first consider the case of regular reflection in pseudosteady flow(see Fig. 8.4). The reflected point P moves away from the tip of wedge O at a constant speed. When the velocity of flow behind the reflected shock with respect to the reflected point P is equal to or less than the local speed of sound, the information from the tip of wedge can reach the reflected point P . In other words, the length scale criterion in pseudosteady flow corresponds to the sonic criterion, that is,

$$\delta_2 - \delta_{3s} = 0$$

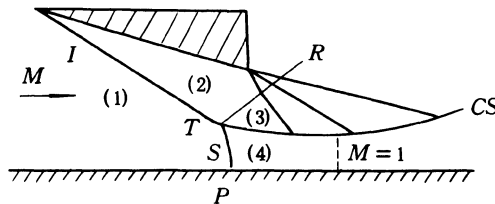


Fig. 8.14 Steady Mach reflection

In steady flow, the length scale criterion leads to two different transition criteria depending on whether the shock is a weak shock and a strong shock. For the strong shock, the flow pattern of Mach reflection is shown in Fig. 8.14. There are the supersonic region 3 and subsonic region 4 on two sides of the slip surface CS . The expansion wave emanating from the trailing edge of the wedge with a finite length is refracted by the reflected shock and strikes the slip surface CS . If there did not exist the expansion wave, the slip surface would asymptotically approach a line parallel to the wall. The expansion wave causes the slip surface CS to curve more strongly away from the wall and a sonic throat forms between CS and the wall. Thus the information path exists from the trailing edge along the leading characteristic of the expansion wave to the subsonic region upstream of the throat and thus to the point P . According to the discussion above, the transition takes place very first time MR becomes

theoretically possible, that is, the length scale criterion corresponds to the mechanical equilibrium criterion for the strong shock in steady flow. For the weak shock, the mechanical equilibrium criterion does not exist, and thus the length scale criterion leads to the sonic criterion.

4. Summary

The transition criteria discussed above is summarized as follows:

Table 8.2 Various transition criteria

Criteria	Investigators	Steady		Pseudosteady	
		Weak	Strong	Weak	Strong
Detachment	von Neumann (1943)	$\delta_2 - \delta_{3m} = 0$	$\delta_2 - \delta_{3m} = 0$	$\delta_2 - \delta_{3m} = 0$	$\delta_2 - \delta_{3m} = 0$
Mechanical Equilibrium	Henderson and Lozzi(1975)	unknown	$\delta_2 - \delta_3 = \delta_4 = 0$	unknown	$\delta_2 - \delta_3 = \delta_4 = 0$
Length-scale	Hornung <i>et al.</i> (1979)	$\delta_2 - \delta_{3s} = 0$	$\delta_2 - \delta_3 = \delta_4 = 0$	$\delta_2 - \delta_{3s} = 0$	$\delta_2 - \delta_{3s} = 0$

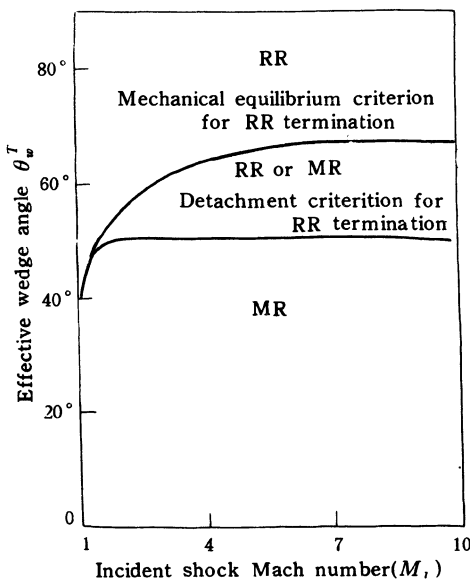


Fig. 8.15 Possible domains of RR and MR(from Ben-Dor, 1988)

5. Experimental results

Figure 8.15 shows the regions in which MR and RR are theoretically possible, where the angle θ_w^T is equal to $90^\circ - \varphi_2$ (the significance of φ_2 is shown in Fig. 8.19). It is evident that the area of disagreement between the detachment and mechanical equilibrium criteria is very large. Note that if the sonic criterion

had been added to the figure, it would have lain slightly above the detachment transition line.

In order to verify which criterion is correct, extensive experimental investigations were made in supersonic wind tunnel and shock tube. In general, experimental results in both steady and pseudosteady flows suggest that in steady flows the RR \rightleftharpoons MR transition agree with the condition given by the mechanical equilibrium criterion, while in pseudosteady flows the RR \rightleftharpoons MR transition seem to agree with the detachment or sonic criterion.

But there exist some disagreements between the experimental results and theoretical results predicted by the two-shock or three-shock theories suggested by von Neumann. In pseudosteady flows the experiments show that the RR structure persists not only inside the dual solution region shown in Fig. 8.15, but also slightly below the detachment transition line, where RR is theoretically impossible. For the weak shock the persistence is up to 5° , while for the strong shock RR extends to about 2° below its theoretical limit. In particular, in some regions of the weak shock von Neumann theory has no physically acceptable solutions and yet the experiments show that Mach reflection exists. This rather remarkable discrepancy is referred to as 'von Neumann paradox'.

As will be shown later, the disagreement between the detachment criterion and experiments in pseudosteady flow can be attributed to the viscous effect. In the strong shock region, the real gas effect also plays a significant role. In last section of this chapter we will present some research results for the von Neumann paradox of weak Mach reflection.

§ 8.5 CMR, DMR and their transition

1. Studies of CMR and DMR

When RR terminates, three different types of Mach reflections may occur in the pseudosteady flow. They are SMR, CMR and DMR. (See Figs. 8.5 and 8.6). CMR and DMR were first observed by Smith (1945) and White (1951), respectively.

Glass and his co-operators studied SMR, CMR, DMR and their transition experimentally and analytically. They suggested that SMR \rightleftharpoons CMR transitions occur when the flow behind the reflected shock is sonic with respect to the first triple point T and CMR \rightleftharpoons DMR transitions occur when the flow behind the reflected shock is sonic with respect to the kink K (or the second triple point T). These transition criteria are mathematically expressed as

$$M_{3T} = 1.0 \quad \text{for } \text{SMR} \rightleftharpoons \text{CMR} \quad (8.26)$$

$$M_{3K} = 1.0 \quad \text{for } \text{CMR} \rightleftharpoons \text{DMR} \quad (8.27)$$

Using these assumed criteria, the domains and transition boundaries of va-

rious reflections in the $(M_s, \theta_w + \chi)$ plane can be obtained (Fig. 8.16). Glass (1987) conducted a lot of experiments in the shock tube to study the various reflections in N_2 , Ar, CO_2 , Freon-12 and SF_6 over the range of M_s from 1.8 to 10.2. They also investigated the real-gas effects due to the excitation of the internal degrees of freedom, vibration, dissociation and ionization in the strong shock case. The comparison of the experimental results with the analytical prediction was given in their papers.

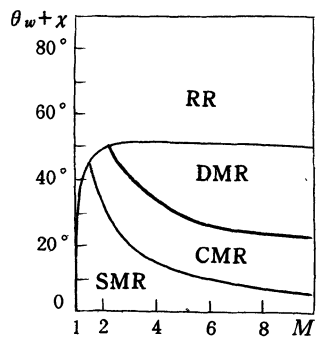


Fig. 8.16 The domains and boundaries of various reflection

It should be mentioned here that Glass and his group found that DMR could be subdivided into four subtypes depending on the trajectory angle of the second triple point, χ' (Fig. 8.17). If $\chi' > \chi$, it is denoted as DMR^+ , if $\chi' < \chi$, it is denoted as DMR^- , and the transition boundary between DMR^+ and DMR^- is $\chi' = \chi$. When the second triple point T' lies on the surface of wedge ($\chi' = 0$), the second Mach stem disappears, which is referred to as Terminal Double Mach Reflection (TDMR). This phenomenon may take place in the gases with low values of γ , such as Freon-12 and SF_6 , whereas it is impossible in the perfect monatomic, diatomic and triatomic gases.

The criteria mentioned above rely directly on the calculation of the first and second triple points, whereas all computations depend upon the reasons for the occurrence of CMR and DMR. It should be pointed out that the physical interpretations of the above mentioned work are somewhat ambiguous, even though the predicted boundaries agree quite well with the experimental data for some gases.

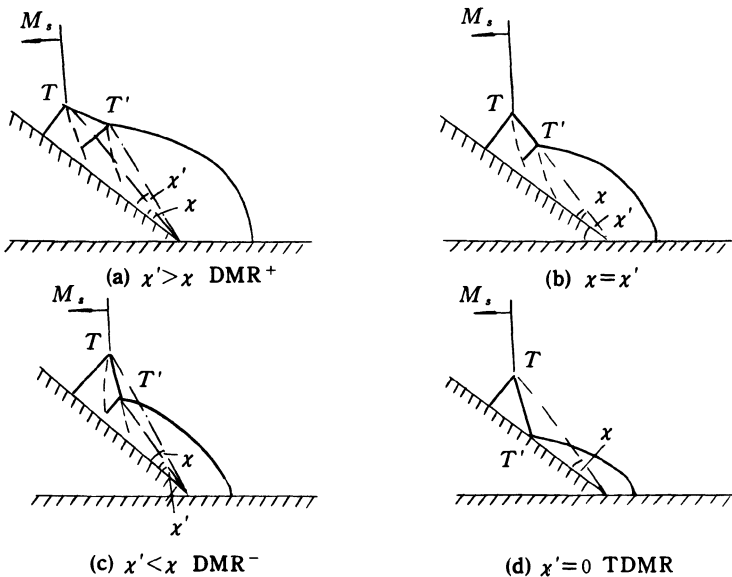


Fig. 8.17 Four types of DMR

2. Reason for the occurrence of CMR and DMR

CMR and DMR are doubtlessly very complicated reflection phenomena. Their mechanism has not been clear up to now. Lee and Glass considered that the occurrence of CMR and DMR were because interaction between the reflection and deflection processes (see § 8.3). Henderson and Lozzi suggested that a band of compression waves must exist in CMR, these compression waves finally converged to a shock wave and DMR occurred when the flow behind the reflected shock with respect to the point T was supersonic.

Hornung(1986) thought that the occurrence of DMR was due to the interaction of the contact surface CS with the solid wall. As shown in Fig. 8.5, in the frame of reference attached to T , the flow in region 3 is supersonic, provided θ_w is small or M_s is large. If we assume that the flow in region 4 is uniform (Mach stem is straight), TB is a straight vortex sheet which strikes on the wall at the point B as shown in Fig. 8.18. The flow velocities on both sides of the contact surface have the same direction and different magnitude. Note that the flow velocity in region 4 is equal to the velocity of the point B in the fixed frame of reference. Therefore, in the moving frame of reference with B , the flow direction in region 3 is not parallel to the wall, while the wall impermeability condition needs that the flow in region 3 is deflected to the

direction parallel to the wall. In the strong reflection range, the flow velocity in region 3 with respect to B is positive ($v_3 - v_B = v_3 - v_4 > 0$). That is to say, the flow in region 3 has to be decelerated and deflected toward the wedge tip. If the relative speed $v_3 - v_4$ is less than the speed of sound a_3 , the deflection takes place without shock and, it corresponds to SMR or CMR depending on whether the Mach number in region 3 with respect to T (M_{3T}) is less or greater than one. If $v_3 - v_4 > a_3$, then the deflection occurs via a shock, which is DMR. According to these, the transition criteria should be modified as

$$M_{3T} = 1.0 \quad \text{for SMR} \Leftrightarrow \text{CMR} \quad (8.28)$$

$$M_{3B} = 1.0 \quad \text{for CMR} \Leftrightarrow \text{DMR} \quad (8.29)$$

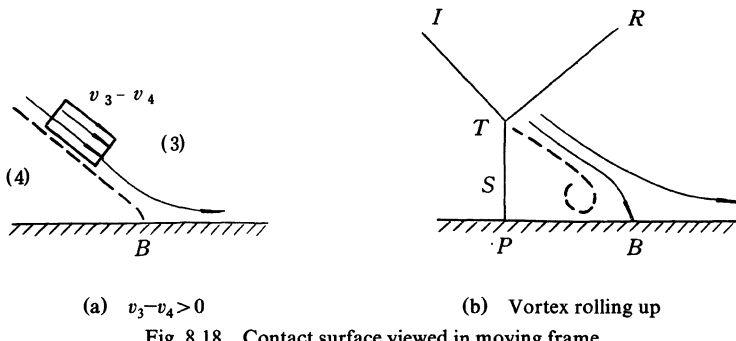


Fig. 8.18 Contact surface viewed in moving frame

In the frame of reference moving with point B , the gas in region 4 is at rest, whereas the flow in region 3 is decelerated through compression wave or shock. Thus, the pressure on the right of the point B (P_3) is higher than that on the left of it (P_4) in the vicinity of the point B . The pressure gradient forces the vortex sheet to curl up (Fig. 8.18).

§ 8.6 Calculation of χ and χ'

1. Calculation of χ

In the study of Mach reflection, it is important to estimate the height of Mach stem or the angle χ of triple point trajectory. There are two analytical methods to calculate χ : shock dynamic method and three-shock theory. The former is presented in Chapter 2. Here we will introduce the three-shock theory(Ben-Dor, 1980).

As shown in Fig. 8.19, in the frame of reference attached to the triple point T , the flow in the vicinity of T can be treated as a steady flow. Using the well-known oblique shock relations across I , R and S , one can obtain the

equations as follows

$$\rho_i \tan \varphi_j = \rho_j \tan(\varphi_j - \delta_j) \quad (8.30)$$

$$\rho_i v_i \sin \varphi_j = \rho_j v_j \sin^2(\varphi_j - \delta_j) \quad (8.31)$$

$$p_i + \rho_i v_i^2 \sin^2 \varphi_j = p_j + \rho_j v_j^2 \sin(\varphi_j - \delta_j) \quad (8.32)$$

$$h_i + \frac{1}{2} v_i^2 \sin^2 \varphi_j = h_j + \frac{1}{2} v_j^2 \sin^2(\varphi_j - \delta_j) \quad (8.33)$$

where ρ , p , v , and h are the density, pressure, velocity with respect to the point T , and enthalpy, respectively. φ is the angle between the oncoming flow and shock surface, δ is the deflected angle of the flow across the shock, $i=1, j=2$ for the incident shock I , $i=2, j=3$ for the reflected shock R and $i=1, j=4$ for the Mach stem S , as shown in Fig. 8.19.

The states in region 3 and 4 across the contact surface satisfy the following relations

$$p_3 = p_4 \quad (8.34)$$

$$\delta_4 = \delta_2 \pm \delta_3 \quad (8.35)$$

The above 14 equations consist of 22 independent variables ($\rho_1 \rho_2 \rho_3 \rho_4$, $p_1 p_2 p_3 p_4$, $h_1 h_2 h_3 h_4$, $v_1 v_2 v_3 v_4$, $\varphi_2 \varphi_3 \varphi_4$, $\delta_2 \delta_3$, and δ_4). Consequently, in general, 8 out of the 22 parameters should be known in order to solve the remaining 14. However, ρ , h , p are no longer independent due to the thermodynamic relations. Therefore, 4 out of the 12 thermodynamic variables vanish. There are 14 equations with 18 independent parameters.

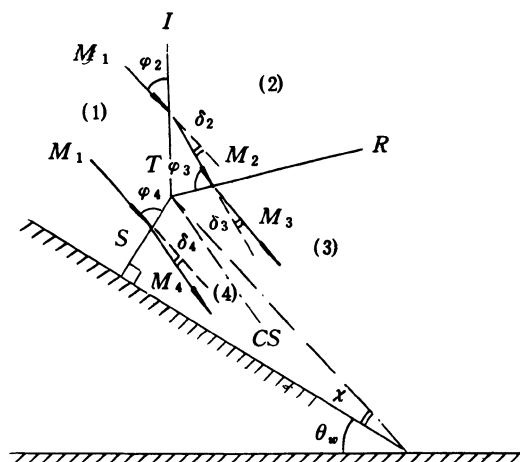


Fig 8.19 Flow field in vicinity of T

When χ is calculated by using the three-shock theory, it is assumed that the Mach stem is straight and normal to the surface of wedge. Thus we have the geometric relations as follows

$$\varphi_2 = \frac{\pi}{2} - (\theta_w + \chi) \quad (8.36)$$

$$\varphi_4 = \frac{\pi}{2} - \chi \quad (8.37)$$

$$\text{and } v_1 = M_s \sec(\theta_w + \chi) \cdot a_1 \quad (8.38)$$

In summary, we have 17 equations with 21 variables (included M_s , θ_w and χ). Giving M_s , p_1 , a_1 and θ_w , the angle χ and flow parameters near T are solvable.

The experimental results show that the above assumption is good in the range $5^\circ < \theta_w < 45^\circ$. However, it is not valid for $M_s < 2$ and $\theta_w < 5^\circ$. It is because the Mach stem, in fact, is curved and this tendency is more prominent for smaller wedge angle and lower shock Mach number.

2. Calculation of χ'

At present, we have not got any analytical method to predict the angle χ' . Ben-Dor(1980) suggested an empirical method to estimate the location of the second triple point. It is assumed that the second triple point T' moves at the same horizontal velocity as the induced flow behind the incident shock in the fixed frame. According to the assumption, we can get

$$\frac{l}{L} = \frac{\rho_1}{\rho_2} \quad (8.39)$$

where l is horizontal distance between two triple points; L is the distance between T and the tip of wedge; ρ_1 / ρ_2 is density ratio across the incident shock.

The experimental study found that the above assumption was good only in the range of $\theta_w < 40^\circ$. The experimental data for $\theta_w > 40^\circ$ indicated that the ratio l / L decreases and approached zero as θ_w increases.

If the incident shock travels the distance L from the moment it collides with the tip of wedge, the time passed is

$$\Delta t = L / W_s \quad (8.40)$$

where W_s is the velocity of the incident shock.

Thus

$$v_T = W_s \operatorname{cosec} \varphi_2$$

$$\text{or } v_{Tx} = W_s, \quad v_{Ty} = W_s \cot \varphi_2 \quad (8.41)$$

where v_T is the velocity of point T in the fixed frame. The velocity of T' with respect to T is denoted by $v_{TT'}$ with the direction along the straight reflected shock TT' (see Fig. 8.20).

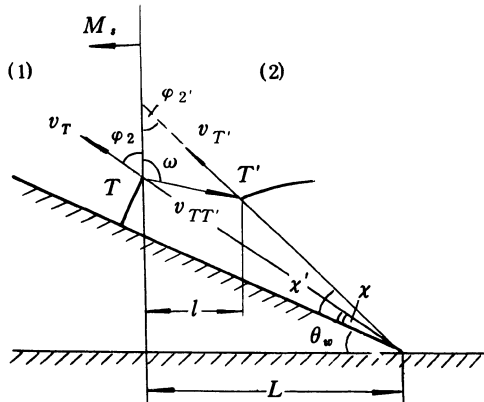


Fig. 8.20 Calculation of χ'

$$v_{TT'} = \frac{l}{\Delta t} \cdot \sec(\omega - \frac{\pi}{2}) = \frac{\rho_1}{\rho_2} \cdot W_s \cdot \sec(\omega - \frac{\pi}{2})$$

$$\text{or } v_{T'T_x} = \frac{\rho_1}{\rho_2} \cdot W_s, \quad v_{T'T_y} = \frac{\rho_1}{\rho_2} \cdot W_s \cdot \tan\left(\omega - \frac{\pi}{2}\right) \quad (8.42)$$

In the fixed frame, the velocity of T' , $v_{T'}$, is

$$v_{T'_x} = W_s(1 - \rho_1 / \rho_2)$$

$$v_{T'_y} = W_s \left[\cot\varphi_2 - \rho_1 / \rho_2 \tan(\omega - \frac{\pi}{2}) \right]$$

$$\text{and } \varphi'_2 = \tan^{-1} \frac{v_{T'_x}}{v_{T'_y}} = \frac{1 - \rho_1 / \rho_2}{\cot\varphi_2 + (\rho_1 / \rho_2) \cot\omega} \quad (8.43)$$

From Fig. 8.20, we have

$$\chi' = \frac{\pi}{2} - \theta_w - \varphi'_2 \quad (8.44)$$

hence

$$\chi' = \frac{\pi}{2} - \theta_w - \tan^{-1} \left[\frac{1 - \rho_1 / \rho_2}{\cot\varphi_2 + (\rho_1 / \rho_2) \cot\omega} \right] \quad (8.45)$$

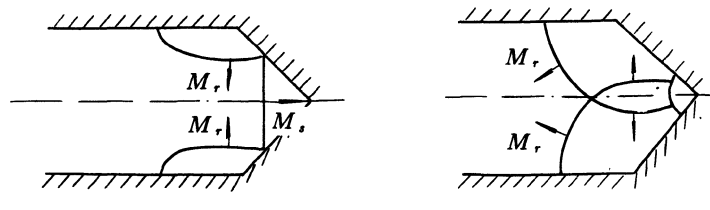
It should be pointed out that the boundaries in Fig. 8.16 are calculated by using the above approximate methods of calculation of χ and χ' with the

addition of the criteria expressed by (8.23), (8.26) and (8.27).

§ 8.7 Effect of viscosity in pseudosteady flow

1. Effect of wall boundary layer

In experiments about the reflection of moving shocks on the surface of wedge, the results show that the regular reflection persists beyond the boundary predicted by the detachment criterion. However, by using the symmetrical configuration shown in Fig. 8.21, which replaces the wedge surface by the plane of symmetry, the transition RR=MR is in agreement with the theory. The difference between both experiments is that the former has the boundary layer on the wall, the latter cancels it. On the basis of these experimental results, Hornung *et al.* (1982) suggested a possible mechanism for the persistence of regular reflection beyond α_d .



(a) Relation of shock on the end wall (b) Interaction between reflected shocks

Fig. 8.21 Experiment of shock reflection to avoid viscous effects.

While the incident shock travels through a wedge and reflects on the surface, a viscous boundary layer forms from the reflection point P along the wall surface, which is an unsteady boundary layer. For the inviscid mode, in the frame of reference attached to the point P , the flow in the vicinity of P is steady and the wall moves at velocity v_1 , as shown in Fig. 8.22.a. The boundary layer forming downstream of P along the wedge surface in region 3 has a velocity profiles as shown in Fig. 8.22.b because $v_1 > v_3$. In the moving frame there is a negative displacement thickness of magnitude $\delta^*(x)$. The flow direction can therefore have a significant component perpendicular to the inviscid wall in region 3 (In Fig. 8.22.b, the dashed line represents the inviscid wall). This time, we have

$$\delta_2 - \delta_3 = \varepsilon > 0 \quad (8.46)$$

This causes the maximum deflection condition on the reflected shock to be shifted to a larger value of α . In the shock polars shown in Fig. 8.22.c, Mach reflection may take place at the point A according to the inviscid detachment

criterion (dashed line), but, in fact, the transition $RR \rightleftharpoons MR$ is postponed to the point B due to the effect of the viscous boundary layer. Here the persistence of RR beyond the value predicted by using the inviscid assumption has qualitatively been explained. Hornung and Taylor (1982) calculated the value of displacement thickness δ^* , and explained successfully the von Neumann paradox for strong reflection. Takayama *et al.*(1981) performed experiments with different kinds of roughness of wall. Their experiments verified the effect of viscosity. But the persistence of RR in weak reflection is still unsolved.

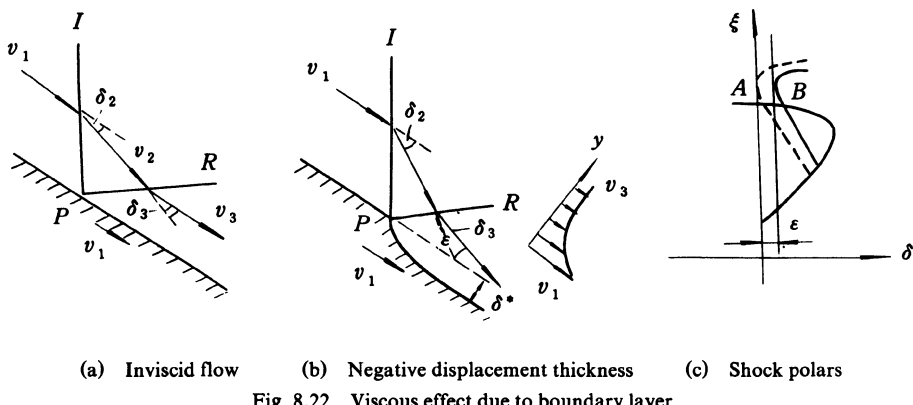


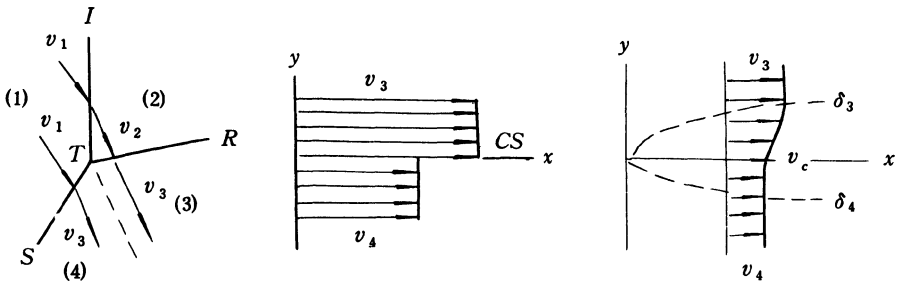
Fig. 8.22 Viscous effect due to boundary layer

2. Effect of viscosity on contact surface

For MR, viscous effects are dominant not only along the wedge surface, but also on both sides of the contact surface. Viscous effects on the contact surface are important as they affect the flow field in the vicinity of the triple point.

According to the assumption of inviscid flow, the contact surface CS is regarded as an infinitely thin discontinuity and the gas flows on both sides of CS have different velocities, v_3 and v_4 , as shown in Fig. 8.23.b.

In the real flow, due to the effect of viscosity, the boundary layer develops in both streams to result in a continuous change in velocity as shown in Fig. 8.23.c. When the Mach reflection is calculated by using the three-shock theory with the inviscid assumption described in § 8.6, the evident discrepancies between the results of the calculation and experiments are found. Ben-Dor (1987) calculated the flow pattern by using the three-shock theory with viscous effects and obtained the satisfactory results.



(a) Flow in the vicinity of triple point \$I\$ (b) Velocities on both sides of \$CS\$ without viscous effects (c) Velocities on both sides of \$CS\$ with viscous effects.

Fig. 8.23 Contact surface with and without viscous effects

Assuming that the flow inside the boundary layer is laminar, one can use the following velocity profile:

$$u = ay^3 + by^2 + cy + d \quad (8.47)$$

where \$u\$ is the velocity inside the boundary layer; \$x\$ is a distance measured from the triple point \$T\$ along the constant surface \$CS\$, \$y\$ is direction normal to \$x\$ direction. With the following boundary condition in regions above and below the contact surface respectively:

$$u|_{y=\delta_3} = v_3, \quad u|_{y=0} = v_c, \quad \frac{\partial u}{\partial y} \Big|_{y=\delta_3} = 0, \quad \frac{\partial^2 u}{\partial y^2} \Big|_{y=0} = 0 \quad (8.48)$$

and

$$u|_{y'=\delta_4} = v_4, \quad u|_{y'=0} = v_c, \quad \frac{\partial u}{\partial y'} \Big|_{y'=\delta_4} = 0, \quad \frac{\partial^2 u}{\partial y'^2} \Big|_{y'=0} = 0 \quad (8.49)$$

we obtain the velocity profiles inside both boundary layers

$$u_3 = \frac{v_c - v_3}{2} \left(\frac{y}{\delta_3} \right)^3 - \frac{3(v_c - v_3)}{2} \left(\frac{y}{\delta_3} \right) + v_c \quad (8.50)$$

$$u_4 = \frac{v_c - v_4}{2} \left(\frac{y'}{\delta_4} \right)^3 - \frac{3(v_c - v_4)}{2} \left(\frac{y'}{\delta_4} \right) + v_c \quad (8.51)$$

where \$\delta_3\$ and \$\delta_4\$ are the boundary layer thicknesses above and below \$CS\$, respectively. \$v_3\$ and \$v_4\$ are the flow velocities outside both boundary layers, \$y\$ and \$y'\$ are the directions that both boundary layers grow, and \$v_c\$ is flow velocity along \$CS\$.

Defining

$$\eta_3 = \frac{v_c}{v_3} \quad 0 < \eta_3 < 1 \quad (8.52)$$

and

$$\eta_4 = \frac{v_c}{v_4} \quad \eta_4 > 1 \quad (8.53)$$

and substituting (8.52) and (8.53) into (8.50) and (8.51), respectively, we have

$$u_3 = \frac{v_3(\eta_3 - 1)}{2} \left(\frac{y}{\delta_3} \right)^3 - \frac{3v_3(\eta_3 - 1)}{2} \left(\frac{y}{\delta_3} \right) + \eta_3 v_3 \quad (8.54)$$

$$u_4 = \frac{v_4(\eta_4 - 1)}{2} \left(\frac{y'}{\delta_4} \right)^3 - \frac{3v_4(\eta_4 - 1)}{2} \left(\frac{y'}{\delta_4} \right) + \eta_4 v_4 \quad (8.55)$$

Using the definitions in (8.52) and (8.53), we have

$$\frac{\eta_3}{\eta_4} = \frac{v_4}{v_3} \quad (8.56)$$

For the sake of simplicity it is assumed that the pressure and density changes are negligible on both sides of *CS* along *CS*. It is quite safe to assume in a very short distance along *CS* because it is of the order of the shock wave thickness in the present analytical model. The von Karman integral momentum equation is

$$\mu \left(\frac{\partial u}{\partial y} \right) \Big|_{y=0} = \frac{\partial}{\partial x} \int_0^\delta (u^2 - uv) dy \quad (8.57)$$

Inserting the velocity profiles (8.54) and (8.55) into (8.57), respectively, we can obtain the boundary layer thicknesses on both sides of *CS*,

$$\frac{\delta_3}{x} = \sqrt{\frac{280}{22\eta_3 + 13}} (Re_{3x})^{-\frac{1}{2}}, \quad Re_{3x} = \frac{\rho_3 v_3 x}{\mu_3} \quad (8.58)$$

and

$$\frac{\delta_4}{x} = \sqrt{\frac{280}{22\eta_4 + 13}} (Re_{4x})^{-\frac{1}{2}}, \quad Re_{4x} = \frac{\rho_4 v_4 x}{\mu_4} \quad (8.59)$$

Then inserting (8.54) and (8.55) into following equations

$$v_3 \delta_3^* = \int_0^{\delta_3} (v_3 - u_3) dy \quad \text{and} \quad v_4 \delta_4^* = \int_0^{\delta_4} (u_4 - v_4) dy'$$

where δ^* is displacement thickness, results in

$$\delta_3^* = \frac{3}{8}(1 - \eta_3)\delta_3 \quad (8.60)$$

and

$$\delta_4^* = \frac{3}{8}(\eta_4 - 1)\delta_4 \quad (8.61)$$

Inserting the expressions of boundary layer thickness (8.58) and (8.59) into (8.60) and (8.61), respectively, results in

$$\frac{\delta_3^*}{x} = \frac{3}{8}(1 - \eta_3)\sqrt{\frac{280}{22\eta_3 + 13}}(Re_{3x})^{-\frac{1}{2}} \quad (8.62)$$

and

$$\frac{\delta_4^*}{x} = \frac{3}{8}(\eta_4 - 1)\sqrt{\frac{280}{22\eta_3 + 13}}(Re_{4x})^{-\frac{1}{2}} \quad (8.63)$$

At any given distance x , δ_3^* must be equal to δ_4^* , thus we have

$$\frac{1 - \eta_3}{\eta_4 - 1}\sqrt{\frac{22\eta_4 + 13}{22\eta_3 + 13}} = \left(\frac{\mu_4}{\mu_3} \frac{\rho_3}{\rho_4} \frac{v_3}{v_4}\right)^{\frac{1}{2}} \quad (8.64)$$

Using $\frac{\mu}{\mu_0} = (\frac{T}{T_0})^k$, $\rho = \frac{P}{RT}$ and $p_3 = p_4$, together with $\frac{v_3}{v_4} = \frac{M_3}{M_4} \left(\frac{T_3}{T_4}\right)^{\frac{1}{2}}$, results in

$$\frac{1 - \eta_3}{\eta_4 - 1}\sqrt{\frac{22\eta_4 + 13}{22\eta_3 + 13}} = \left[\left(\frac{T_4}{T_3}\right)^{\frac{1}{2}+k} \cdot \frac{M_3}{M_4}\right]^{\frac{1}{2}} \quad (8.65)$$

and

$$\frac{\eta_3}{\eta_4} = \frac{M_4}{M_3} \left(\frac{T_4}{T_3}\right)^{\frac{1}{2}} \quad (8.66)$$

The above two equations provide a way for calculating η_3 and η_4 , provided T_3 , T_4 , M_3 and M_4 are known.

Once η_3 and η_4 are known, the angular displacement of CS can be solved by using

$$\varepsilon = \tan^{-1} \left. \frac{\delta^*}{x} \right|_{x=10\lambda}$$

where λ is the mean free path. If ε is known, the deflection of flow across the reflected shock must be changed from δ_3 to $\delta_3 + \varepsilon$, while across Mach stem must

be changed from δ_4 to $\delta_4 - \varepsilon$.

Ben-Dor (1987) calculated MR flow pattern for $M_s = 2.71$, $\varphi_1 = 39.9^\circ$, $T_1 = 296$ K, $p_0 = 0.1$ MPa, by using the above method. The results are shown in Table 8.3

Table 8.3 Comparison between calculating results with and without viscous effects and experiments (from Ben-Dor, 1987)

	ω_{ir}	ω_{is}	ω_{rc}
Experiment	$118^\circ \pm 1^\circ$	$132^\circ \pm 1^\circ$	$32^\circ \pm 1$
Inviscid	123.19° ($+5.19^\circ$)	132.74° ($+0.74^\circ$)	27.16° (-4.84°)
With viscous effect	118.02° ($+0.02^\circ$)	131.70° (-0.30°)	32.32° ($+0.32^\circ$)

where ω_{ir} is the angle between the incident shock and reflected shock, ω_{is} is that between the incident shock and Mach stem and ω_{rc} is that between the reflected shock and contact surface. The values in brackets are the differences between the calculated and measured values.

It is evident from the table that when the viscous model is used, the agreement between the calculated results and the experimental results is excellent, and the viscous effect on slip surface in MR should be accounted.

Except the viscous effect, for strong shock, the real gas effect and the thermal conduction effect also play an important role. In addition, the effects of surface condition which includes rough surface, perforated surface, porous surface and liquid surface are subjects being progressing.

§ 8.8 von Neumann paradox of weak Mach reflection

As mentioned earlier, the comparison of the results predicted by von Neumann theory with the experimental data indicates that for strong and weak RR, and also for strong MR, the agreements are generally satisfactory, except that RR apparently persists beyond the boundary predicted by mechanical equilibrium and detachment criteria. The reason for RR to persist can be known by effects of viscosity, real gas and thermal conduction for strong shocks. For weak MR, the theory almost always failed to agree with experiments. In the

range near the weak / strong boundary, the wave angles at the triple point calculated by the theory deviate from the experimental values. The discrepancy between them is much larger than the experimental error. For the weaker shock, the von Neumann theory gives no physically acceptable solutions, and yet experiment shows that MR, or MR-like, does in fact exist. These suggest that the physical model of MR used by von Neumann be incorrect. This subject, called von Neumann paradox of weak MR, has attracted many researchers whose work includes analytical, experimental and numerical studies.

For weak shocks the effects of real gas and thermal conduction is negligible. The causes for the failure of von Neumann theory of weak MR may, in general, include the effects of viscosity, unsteadiness, nonlinearity and nonuniformity in the flow.

von Neumann theory is based on the assumption that the gas is inviscid. The experimental and numerical results indicate that for weak MR the viscous effects are only dominant near the tip of wedge. When the incident shock first encounters the tip, the initial reflection appears to be of the regular type, and after 100–150 mean free path lengths from the tip, the Mach reflection appears. In other words, the viscous effects near the tip make the trajectory of triple point not pass through the tip of wedge. Further away, viscous effects appear to be at most of secondary importance and mainly due to the wall boundary layer.

Other assumption of von Neumann theory is that the flows in the vicinity of the triple point are uniform. For strong MR the flow is supersonic and uniform downstream of the reflected shock, so that theory is applicable. For weak shocks the flows downstream of the triple point are subsonic and nonuniform, and thus the entire flow field can affect the flow near the triple point. This implies that von Neumann theory cannot be applied and the entire flow field must be taken into account in order to determine the flow near the triple point.

In particular, the experimental and numerical results of Colella and Henderson (1990) show that when the angle between the reflected shock and the slip surface is larger than 90° or the three-shock theory has no physically acceptable solutions, a different flow pattern forms, which they called von Neumann reflection' (NR). In NR, the incident and Mach shocks appear to be a single wave with a smoothly turning tangent near the triple point, instead of slop discontinuity in MR. The curvature of the Mach shock is noticeably large. The reflected wave becomes a curved compression band with finite thickness near the triple point. All of these violate the physical model used by von Neumann.

Chapter 9 Reflections of Shock Waves in Unsteady Flow

§ 9.1 Introduction

The reflection of shock waves in unsteady flow is more complicated than that in steady and pseudosteady flows. Figure 9.1 illustrates three different types of unsteady reflections. When an incident shock I propagating from left to right collides with a convex half cylinder, the transition process of reflections is from the head-on collision, through regular reflection, to Mach reflection (Fig. 9.1a). When an incident shock I strikes a concave half cylinder, an opposite transition process takes place, i.e., from Mach reflection to regular reflection (Fig. 9.1b). In both cases the incident shock Mach number remains constant and only the wedge angles θ_w change. Figure 9.1c shows that a spherical shock is reflected on a plane surface, in which both the incident shock Mach number and the reflected wedge angle decrease and the transition from regular to Mach reflections takes place.

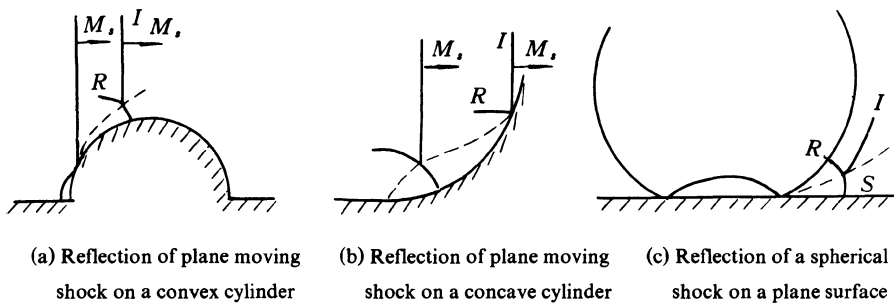


Fig. 9.1 Unsteady shock reflections

§ 9.2 Shock reflection on the cylindrical surface

In this section, we shall discuss the reflection of constant velocity shock on the concave and convex cylindrical surface, respectively. A lot of experimental investigations conducted in the shock tube show that this type of unsteady shock reflection has different properties from the reflection of a plane moving

shock on a straight wedge discussed in the previous chapter. The transition RR \rightleftharpoons MR in this case depends not only on the incident shock Mach number, but also on both the radius of curvature of the cylindrical wedge R and the initial wedge angle θ_{wi} .

1. Shock reflection on the cylindrical concave surface

Figure 9.2 shows experimental results of transition angle θ_w^T of shock reflection over the cylindrical concave surface (MR \rightarrow RR) together with theoretical transition line AB predicted by the mechanical equilibrium criterion and AC by the detachment criterion. We can see from the figure that (1) all the experimental transition angles lie above the transition line AB ; (2) as the radius of curvature R increases, the transition angle decreases; (3) as the radius of curvature approaches infinity ($R \rightarrow \infty$), the transition angle approaches the transition line AB appropriate to the steady flow; and (4) with the initial wedge angle θ_{wi} increasing, the transition angle θ_w^T decreases.

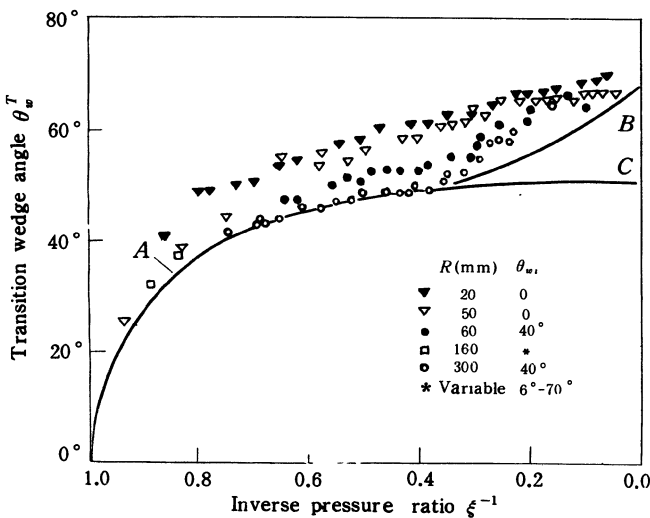


Fig. 9.2 Shock reflection over cylindrical concave surface
(from Ben-Dor, 1988)

2. Shock reflection on the cylindrical convex surface

Figure 9.3 shows experimental results of transition angle θ_w^T for shock reflection on the cylindrical convex surface (RR \rightarrow MR). In the figure the lines AB and AC are theoretical transition lines for the mechanical equilibrium and the detachment criteria, respectively. The experimental results indicate that (1)

all the experimental transition angles θ_w^T lie below the theoretical transition line AC ; (2) as the radius of curvatures increases, the transition angle increases; (3) as the radius of curvatures approaches infinity ($R \rightarrow \infty$), the transition angle approaches the transition line AC appropriate to the pseudosteady flow; and (4) with initial wedge angles decreasing, the transition angle decreases, but the effects of initial wedge angle is not evident, compared with the case of concave cylindrical surface.

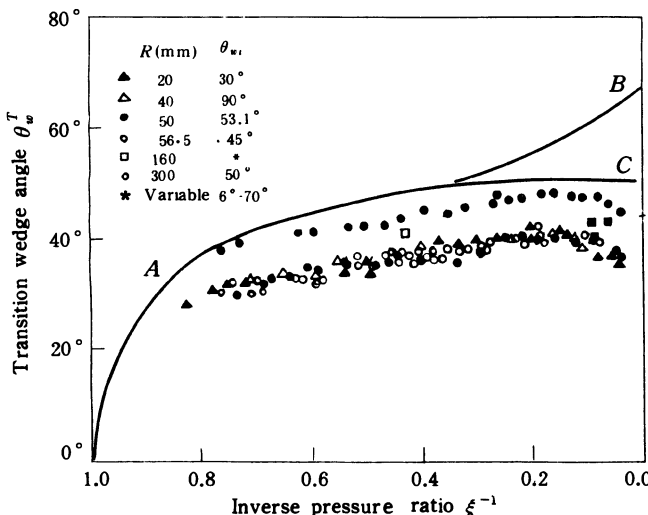


Fig. 9.3 Shock reflection over cylindrical convex surface
(from Ben-Dor, 1988)

3. Triple point trajectory

When a plane moving shock is reflected on the cylindrical concave surface and transition $MR \rightarrow RR$ occurs, the triple point trajectory can be shown in Fig. 9.4. We can see that the trajectory is not a straight line. The length of the Mach stem, λ , increases from $\lambda = 0$ to a maximum, and then decreases from the maximum to $\lambda = 0$ where transition $MR \rightarrow RR$ forms. Thus, the triple point trajectory may be divided into two parts: $d\lambda / ds > 0$ and $d\lambda / ds < 0$, where s is a distance measured along the wedge surface. As indicated above, the reflection of a plane shock on the surface of concave cylinder undergoes following processes: a direct Mach reflection, a stationary Mach reflection, an inverse Mach reflection and a regular reflection (see § 8.3).

If the unsteady flow is divided into a sequence of momentarily pseudosteady states, the shock polars can be used to describe the phenomenon.

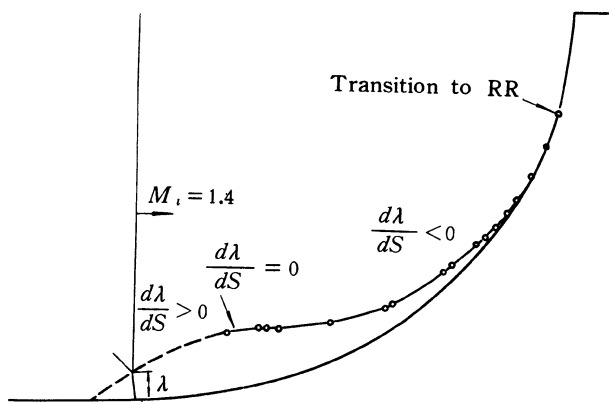


Fig. 9.4 Triple point trajectory of shock reflection on cylindrical concave surface (from Ben-Dor, 1988)

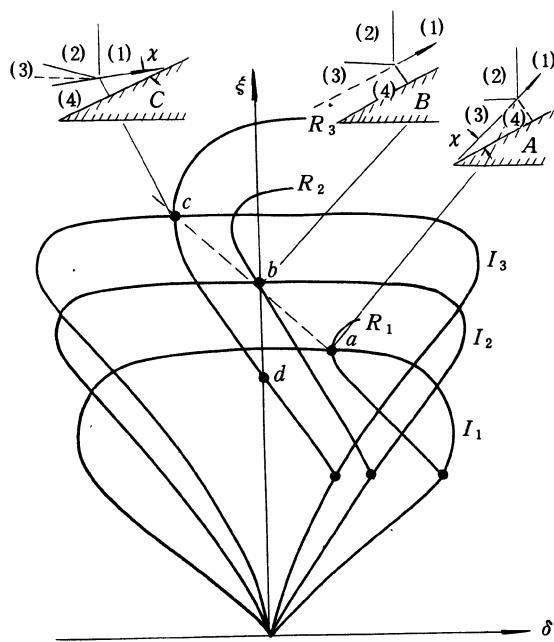


Fig. 9.5 Multi-shock polar diagram (from Ben-Dor, 1988)

Because the effective wedge angle increases when the constant velocity shock propagates along the cylinder, the oncoming flow Mach number with respect to

the triple point increases. Figure 9.5 shows the shock polars corresponding to three different moments. Since the pressure behind the incident shock remains constant, all polars of the reflected shock emanate from their corresponding I -polars at the same pressure. For the part of $d\lambda / ds > 0$, R -polar intersects with I -polar at the point a (the right portion of I -polar), for $d\lambda / ds = 0$, the intersection point is the point b (normal shock point of I -polar), and for $d\lambda / ds < 0$, the intersection point is the point c (the left portion of I -polar). When RR occurs, the solution corresponds to the point d . Therefore, the reflection processes of $MR \rightarrow RR$ is $a \rightarrow b \rightarrow c \rightarrow d$.

It should be noted that the transition $MR \rightarrow RR$ corresponds to $c \rightarrow d$ and pressure drop exists. As mentioned above, If a pressure jump occurs during transition, then an unsteady compression or expansion wave will be generated in the flow. Such an additional shock wave indeed appears in experimental photographs.

For the shock reflection on the cylindrical convex surface, the triple point trajectory always has $d\lambda / ds > 0$ and only direct Mach reflection occurs.

§ 9.3 Prediction of transition $RR \rightarrow MR$ on cylindrical convex surface

A lot of experimental results indicate that the transition $RR=MR$ in the unsteady flow is different from that in the steady and pseudosteady flows and the transition from RR to MR for the convex cylinder is also different from the transition from MR to RR for the concave cylinder. In this section, we shall discuss some methods used to predict the transition from RR to MR over the cylindrical convex surface.

1. Application of shock dynamics

In Chapter 3 we have studied the reflection of a plane shock on the cylindrical convex surface using shock dynamic method. There we assume that the Mach stem has an infinitesimal length in the region of RR. In this section our purpose is to study the transition from RR to MR by using the shock dynamic method.

Heilig (1969) first used the shock dynamics developed by Whitham to predict the transition $RR \rightarrow MR$ for the convex cylinder. Itoh *et al.*(1981) modified his theory.

Figure 9.6 illustrates the shock wave system in the vicinity of $RR \rightarrow MR$ transition point (the reflected shock is omitted). From the geometry, we get the following relations

$$L = M_s a_0 \delta t, \quad L_s = M_w a_0 \delta t, \quad L' = L_s \cos \theta_w^T \quad (9.1)$$

where a_0 is the speed of sound ahead of the incident shock, M_s and M_w are

the shock Mach numbers of the incident shock and the Mach stem, respectively, and δt is an infinitesimal time interval. The significances of L , L' and L_s are shown in the figure (OZ is the tangential line to the wall surface at the point O). When the transition RR→MR takes place at the point O , we have

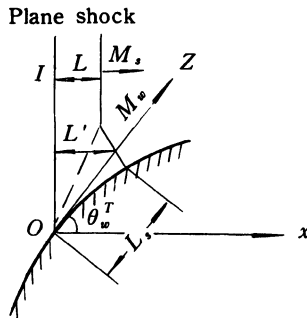


Fig. 9.6 Application of shock dynamics to transition RR→MR
for convex cylinder

$$L' = L + 0, \quad \text{i.e.,} \quad \frac{M_w}{M_s} \sin \theta_w^T = \tan \theta_w^T \quad (9.2)$$

By description in Chapter 2, we get the relation between M_w and θ_w by using the relation of simple wave of the shock dynamics,

$$\theta_w^T = \int_{M_s}^{M_w} \frac{dM}{AC} \quad (9.3)$$

Note that this is an approximate expression. In fact, the shock-shock relation should be used. In (9.3), A is the area of the ray tube and C is characteristic speed. Substituting the following $A - M$ relation into (9.3)

$$\frac{dA}{A} = \frac{-2MdM}{(M^2 - 1)K(M)}$$

and supposing that $K(M)$ is a constant and equal to n , we get the integration of (9.3)

$$\begin{aligned} \frac{M_w}{M_s} &= \frac{1}{2M_s} \left\{ \left[(M_s^2 - 1)^{\frac{1}{2}} + M_s \right] \exp \left[\left(\frac{1}{2}n \right)^{\frac{1}{2}} \theta_w^T \right] \right. \\ &\quad \left. + \left[(M_s^2 - 1)^{\frac{1}{2}} + M_s \right] \exp \left[\left(\frac{1}{2}n \right)^{\frac{1}{2}} \theta_w^T \right] \right\}^{-1} \end{aligned} \quad (9.4)$$

Substituting (9.4) into (9.2), we obtain

$$\frac{1}{2M_s} \left\{ \left(\sqrt{M_s^2 - 1} + M_s \right) \exp \left(\sqrt{\frac{n}{2}} \theta_w^T \right) \right. \\ \left. + \left[\left(\sqrt{M_s^2 - 1} + M_s \right) \exp \left(\sqrt{\frac{n}{2}} \theta_w^T \right) \right]^{-1} \right\} \sin \theta_w^T = \tan \theta_w^T \quad (9.5)$$

From (9.5), we can find θ_w^T iteratively.

2. Application of disturbance propagating concept

Hornung *et al.* (1979) argued that the reason of formation of the Mach stem was that a disturbance signal caught up with the reflected point. Li(1988) calculated the transition RR→MR over a convex cylinder by both concept of disturbance propagation and shock dynamic theory.

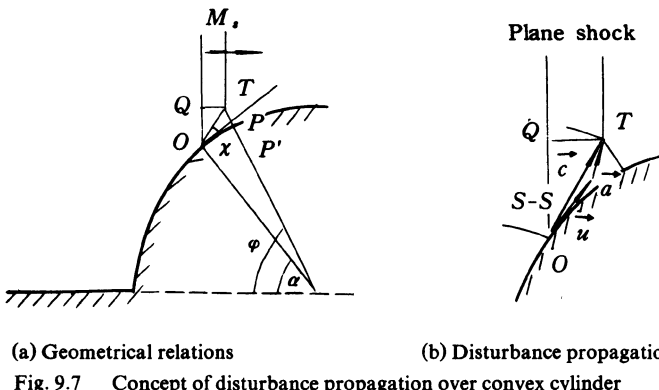


Figure 9.7 shows the shock system in the vicinity of the point O . Assuming that the transition RR \rightarrow MR occurs at the point O , the angle α is critical angle α_t ($\alpha_t = 90^\circ - \theta_w^T$), M_s and M_w are the Mach numbers of the incident shock and the Mach stem, respectively. The point T is the triple point. OP is tangent to the surface of the cylinder. The angle TOP is referred to as the triple point trajectory angle χ . Assuming that the disturbance from the point O propagates at the speed of sound, a , with respect to flow and catches up with the triple point T , and the path of signal propagation is along the triple point trajectory (see Fig. 9.7), the velocity c of the signal propagation is expressed as

$$\vec{c} = \vec{u} + \vec{a} \quad (9.6)$$

where \vec{u} is flow velocity behind the reflected shock at point O , which direction is

along OP and a is the speed of sound behind the Mach stem. Thus, we have

$$c = u\cos\chi + (a^2 - u^2 \sin^2 \chi)^{1/2} \quad (9.7)$$

From Fig. 9.7, we know that TQ is the propagating distance of the incident shock at interval Δt

$$TQ = M_s a_0 \Delta t$$

where a_0 is the undisturbed speed of sound. Thus, we can get

$$c \Delta t \sin(\alpha_t - \chi) = M_s a_0 \Delta t$$

or

$$u\cos\chi + (a^2 - u^2 \sin^2 \chi)^{1/2} = M_s a_0 / \sin(\alpha_t - \chi) \quad (9.8)$$

This is the equation derived from the viewpoint of disturbance propagation. In order to solve the transition angle α_t , we have to find the angle χ using the shock dynamic method. As shown in Fig. 9.7, the propagating distances of the incident shock and the Mach stem at interval Δt are, respectively,

$$M_s a_0 \Delta t = TQ = R \cos \alpha_t - (R + \lambda) \cos \varphi \quad (9.9)$$

$$M_w a_0 \Delta t = R(\varphi - \alpha_t) \quad (9.10)$$

where R is the radius of the cylinder, λ is the length of the Mach stem. The areas of the ray tube for the incident shock and Mach stem are defined, respectively, as

$$A_s = OQ = (R + \lambda) \sin \varphi - R \sin \alpha_t \quad (9.11)$$

$$A_w = \lambda \quad (9.12)$$

The angle χ is expressed as

$$\tan \chi = \frac{TP}{OP} = \frac{(R + \lambda) - R / \cos(\varphi - \alpha_t)}{R \tan(\varphi - \alpha_t)} \quad (9.13)$$

Let $\delta = \varphi - \alpha_t$, if $\Delta t < < 1$, then λ / R can be expressed as

$$\lambda / R = \lambda_1 \delta + \lambda_2 \delta^2 + o(\delta^3) \quad (9.14)$$

where λ_1 , λ_2 are coefficients. Substituting (9.14) to (9.9)–(9.13) and neglecting the terms of δ^2 , we get

$$\frac{M_s}{M_w} = \sin \alpha_t - \lambda_1 \cos \alpha_t \quad (9.15)$$

$$\frac{A_w}{A_s} = \frac{\lambda_1}{\lambda_1 \sin \alpha_t + \cos \alpha_t} \quad (9.16)$$

$$\tan \chi = \lambda_1$$

From (9.15) and (9.16), eliminating λ_1 results in

$$\sin \alpha_t = \frac{A_w / A_s + M_s / M_w}{1 + M_s / M_w \cdot A_w / A_s} \quad (9.17)$$

$$\tan \chi = \frac{A_w}{A_s} \left[\frac{1 - (M_s / M_w)^2}{1 - (A_w / A_s)^2} \right]^{1/2} \quad (9.18)$$

where $A - M$ relation is expressed as

$$\frac{A_w}{A_s} = \frac{f(M_w)}{f(M_s)} \quad (9.19)$$

From (9.8) and (9.17)–(9.19), we can solve α_t for given M_s iteratively.

3. Comparison with experimental results

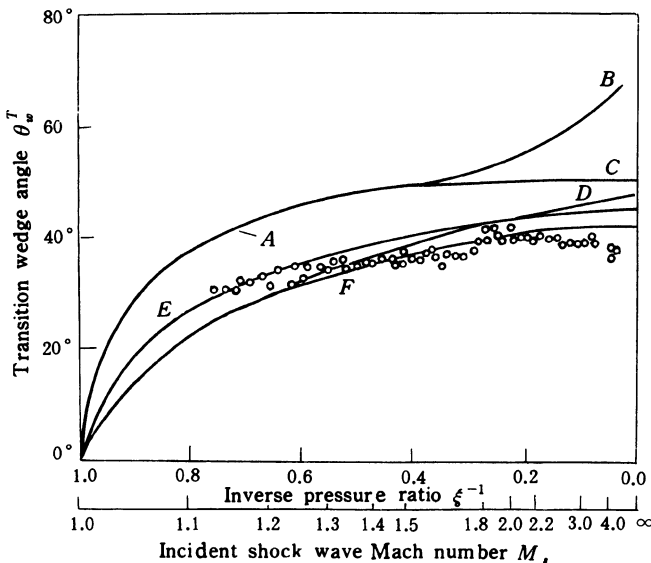


Fig. 9.8 Comparison between various criteria and experimental results
(from Ben-Dor, 1988)

Finally, we give the comparison between the experimental and theoretical

results. In Fig. 9.8, lines *D* and *E* are the transition lines calculated by Heilig and Itoh who used the shock dynamics, respectively, and line *F* is calculated by Li who used the disturbance propagation concept. From the figure we can see that the line *F* seems more accurate, but these methods cannot explain the effect of radius of curvature on the transition.

§ 9.4 Prediction of transition MR → RR over cylindrical concave surface

1. Application of shock dynamic theory

Itoh *et al.* (1981) first studied the transition MR→RR for the reflection of a plane shock on the surface of a concave cylinder by using the shock dynamic theory.

Consider a plane shock *I* reflected on the surface of a concave cylinder with an initial wedge angle θ_{wi} (Fig. 9.9). From the Witham's theory, we have

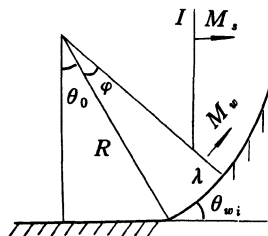


Fig. 9.9 Application of shock dynamics to the transition
MR→RR for a concave cylinder

$$M = \frac{1}{|\nabla \alpha|} \quad (9.20)$$

where α is the shock surface function and M is the shock Mach number. Since α is continuous at the shock-shock and is given by the undisturbed shock, we have

$$\alpha = a_0 t = \frac{(R - \lambda) \sin(\theta_{wi} + \varphi)}{M_s} - \frac{R \sin \theta_{wi}}{M_s} \quad (9.21)$$

where M_s is the Mach number of the incident shock, a_0 is the speed of sound ahead of the incident shock, t indicates the time measured from the instant the shock strikes the leading edge of cylinder, R is the radius of the cylinder, φ is an angle which indicates position of shock at time t , and λ is the length of Mach stem which is a function of φ

$$|\nabla \alpha| = \left| \frac{\partial \alpha}{\partial r} \vec{i}_r + \frac{\partial \alpha}{\partial \varphi} \vec{i}_\varphi \right| = \frac{1}{r} \frac{d\alpha}{d\varphi} \quad (9.22)$$

where \vec{i}_r and \vec{i}_φ are the unit vectors of coordinates. The Mach number M at radius r is given by

$$\frac{1}{M} = |\nabla \alpha| = \frac{1}{r} \frac{d\alpha}{d\varphi}$$

For the Mach stem, taking the mean position, we have

$$\frac{1}{M_w} = \frac{1}{R - \lambda/2} \cdot \frac{d\alpha}{d\varphi} \quad (9.23)$$

where M_w is the Mach number of the Mach stem. From (9.21), we have

$$\frac{d\alpha}{d\varphi} = \frac{1}{M_s} \left[(R - \lambda) \cos(\theta_{wi} + \varphi) - \sin(\theta_{wi} + \varphi) \frac{d\lambda}{d\varphi} \right] \quad (9.24)$$

Substituting (9.24) to (9.23) and rearranging them, we get

$$\frac{d\lambda}{d\varphi} = \frac{R - \lambda}{\tan(\theta_{wi} + \varphi)} - \frac{R - \lambda/2}{\sin(\theta_{wi} + \varphi)} \frac{M_s}{M_w} \quad (9.25)$$

If assuming $R = 1$, (9.25) becomes

$$\frac{d\lambda}{d\varphi} = \frac{1 - \lambda}{\tan(\theta_{wi} + \varphi)} - \frac{1 - \lambda/2}{\sin(\theta_{wi} + \varphi)} \frac{M_s}{M_w} \quad (9.26)$$

In order to obtain the length of Mach stem, the value of M_s / M_w has to be estimated. Itoh *et al.* (1981) again used the continuous wave relation of the shock dynamics

$$\theta_w = \varphi + \theta_{wi} = \int_{M_s}^{M_w} \frac{1}{AC} dM$$

where θ_w is the angle between the normal to the Mach stem and the horizontal line, and the $A - M$ relation modified by Milton (1975), which includes the effects of the reflected shock and the contact surface. The following relation can be obtained

$$\theta_w = \int_{M_s}^{M_w} \left[\frac{2}{(M^2 - 1)K(M)} + \frac{\eta}{M^2} \right]^{1/2} dM \quad (9.27)$$

where the expression of η can be found in Chapter 1. Using (9.27) and (9.26), the length of Mach stem at φ can be obtained. When $\lambda = 0$, the angle φ is defined as the transition angle from MR to RR, which is denoted by φ_{tr} .

2. Analytic method on the basis of disturbance propagation

According to the disturbance propagation concept, for Mach reflection to exist, the corner signals generated at the tip of the reflecting wedge must catch up with the incident shock. On the contrary, if the corner signal cannot catch up with the incident shock, then the regular reflection occurs. The concept is valid for both the steady and pseudosteady flows. Ben-Dor and Takayama (1985) applied this concept to the reflection of shock on the surface of a concave cylinder.

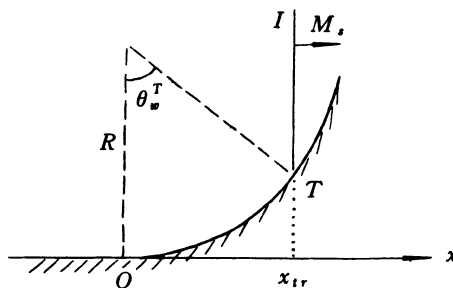


Fig. 9.10 Disturbance propagation for transition MR→RR

As the incident shock propagates over the concave cylinder, the termination of MR occurs at the point T where it becomes impossible for the corner-generated signals to catch up with the incident shock (Fig. 9.10). The corner signals generated at the tip of the cylinder move with the velocity $u+a$. In general, the value of $u+a$ changes inside the flow field behind the reflected shock. If Δt is the time for the signals to propagate from the tip of the cylinder to the transition point T , then during this time the signals have propagated the distance of

$$S = \int_0^{\Delta t} (u + a) dt \quad (9.28)$$

If assuming that the reflected shock is weak, we can approximately get

$$u + a = u_1 + a_1 \quad (9.29)$$

where u_1 and a_1 are the velocity and speed of sound behind the incident shock, respectively. The integration of (9.28) can be carried out, resulting in

$$S = (u_1 + a_1) \Delta t \quad (9.30)$$

and

$$\Delta t = \frac{x_{tr}}{w_s} = \frac{R \sin \theta_w}{M_s a_0} \quad (9.31)$$

where x_w is the horizontal distance that the incident shock propagates from the tip of the cylinder, O , to the transition point T , θ_w^T is the transition wedge angle, and w_s is the velocity of the incident shock.

Substituting (9.31) into (9.30) results in

$$S = \frac{R \sin \theta_w^T}{M_s a_0} (u_1 + a_1) \quad (9.32)$$

where R is the radius of the cylinder, M_s is the incident shock Mach number, and a_0 is the speed of sound ahead of the incident shock.

How to determine S ? Ben-Dor and Takayama used two modes.

In mode A, it is assumed that the path of the signal propagation is very close to the circular arc OT . Thus, we have

$$S = R \theta_w^T \quad (9.33)$$

Substituting (9.33) into (9.32) and rearranging them, we get

$$\frac{\sin \theta_w^T}{\theta_w^T} = \frac{M_s a_0}{u_1 + a_1} \quad (9.34)$$

where u_1 and a_1 are the functions of M_s ,

$$u_1 = \frac{2a_0(M_s^2 - 1)}{(\gamma + 1)M_s} \quad (9.35)$$

$$a_1 = \frac{\gamma - 1}{\gamma + 1} \frac{a_0}{M_s} \left[\left(\frac{2\gamma M_s^2}{\gamma - 1} - 1 \right) \left(M_s^2 + \frac{2}{\gamma - 1} \right) \right]^{1/2} \quad (9.36)$$

Using (9.34) (9.35) and (9.36), θ_w^T can be solved.

In mode B, it is assumed that the path of the signal propagation is close to the line OT . Thus we have

$$S = 2R \sin \frac{\theta_w^T}{2} \quad (9.37)$$

Substituting (9.37) into (9.32), finally we get

$$\cos \frac{\theta_w^T}{2} = \frac{M_s a_0}{u_1 + a_1} \quad (9.38)$$

If the concave cylinder have an initial angle, θ_0 , then (9.34) and (9.38) are

respectively written as

$$\frac{\sin\theta_w^T - \sin\theta_0}{\theta_w^T - \theta_0} = \frac{M_s a_0}{u_1 + a_1} \quad (9.39)$$

$$\frac{\sin\theta_w^T - \sin\theta_0}{\frac{1}{2}(\theta_w^T - \theta_0)} = \frac{2M_s a_0}{u_1 + a_1} \quad (9.40)$$

3. Comparison with experimental results

Figure 9.11 shows comparison between the various transition criteria and experimental results. Lines *D* and *E* are results predicted by modes A and B of Ben-Dor and Takayama, respectively. Line *F* is given by using shock dynamics. It is evident that the line *D* is quite good in the range $1.25 < M_s < 4$, while line *E* exhibits good agreement only for weak shocks.

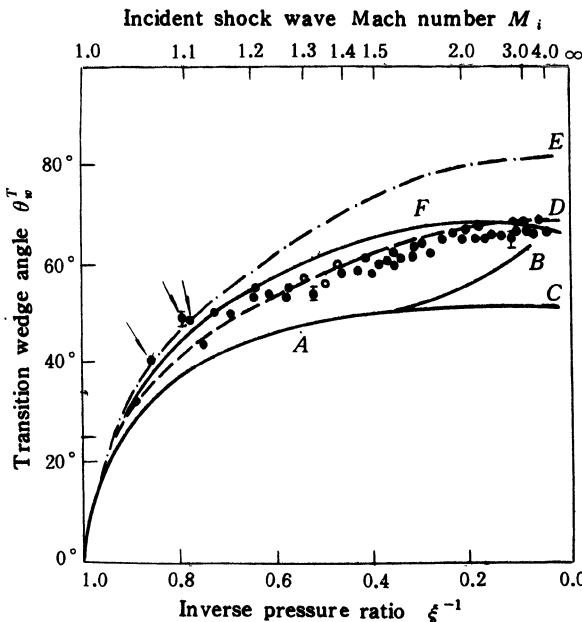


Fig. 9.11 Comparison between various transition criteria and experimental results (from Ben-Dor, 1988)

§ 9.5 Reflection of plane shock on double wedge

In order to further understand the shock reflection on the concave and convex cylindrical surfaces, Ben-Dor, Dewey and Takayama (1987) studied the shock reflection over double wedge with a single increase or decrease of the wedge angle (Fig. 9.12). In their investigation, seven different shock configurations were predicted analytically and verified by sequences of shadowgraphs and schlieren photographs. The seven regions in the (θ_w^1, θ_w^2) plane which identify the different reflection processes of the shock over the double wedge are shown in Fig. 9.13 and corresponding reflection processes are summarized in Table 9.1.

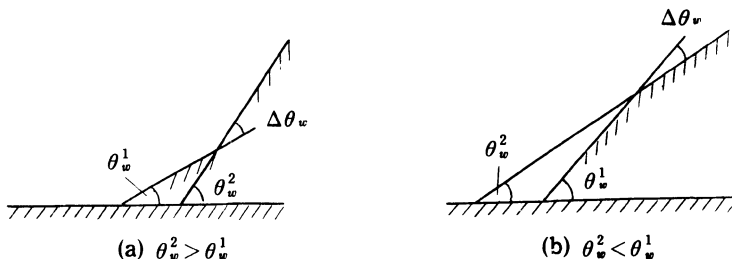


Fig. 9.12 Double wedges

Table 9.1 Various reflections of shock waves over double wedge (from Ben-Dor *et al.*, 1987)

	θ_w^1	θ_w^2	$\Delta\theta_w$	First surface	Second surface	Region
Convex	> det	> det	—	RR	RR	2
	< det	< det	—	MR	MR	3
	> det	< det	—	RR	MR	4
Concave	> det	> det	—	RR	RR	1
	< det	> det	> det	MR	RR → RR	5
	< det	< det	< det	MR	MR → MR	6
	< det	> det	< det	MR	MR → RR	7

where θ_w^{det} is the transition angle according to the detachment criterion. The seven kinds of reflection processes have the very complicated structures of the

shock wave system. In general, the sudden pressure changes exist as the reflections move from first to second wedge. The measured transition angles are different from that predicted by the present criteria. The transition criteria for the double wedge case have not yet been established, it is a subject of continuing studies.

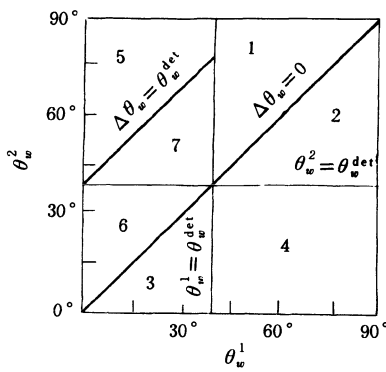


Fig. 9.13 Seven reflection processes of shock over double wedge
(from Ben-Dor, 1987)

Chapter 10 Refractions of Shock Waves at Interface Between Different Media and Interaction Between Shocks

§ 10.1 Introduction

The interaction of shock waves with nonuniform media occurs in many fields of science. For example, sonic boom propagation through Earth's turbulent atmosphere, shock-boundary layer interaction on transonic airfoils, blast wave reflection and refraction on the water surface, shock interaction with flame fronts, and shock propagation through a gas-liquid stratified system in nuclear reactors.

It is clear that such phenomena are very complicated. In order to understand the mechanism and rule of these phenomena, one often studied some simple models extracted from them.

Jahn (1956), Abd-el-Fattah and Henderson (1978, 1979), Abd-el-Fattah, Henderson and Lozzi (1979) investigated experimentally the refraction of shock waves at plane gas interfaces, Catherasoo and Sturtevant (1983), and Schwendeman (1988) studied the refraction of shocks by shock dynamic method, Markstein (1957) and Rudinger (1958) studied the interaction of shock wave with curved flame fronts, Haas and Sturtevant (1987) investigated the interactions of weak shock waves with cylindrical and spherical gas inhomogeneities.

In view of the complexity of the refraction phenomenon, we have to pay our attention to the refraction of a plane shock at the interface between gases with different speeds of sound. In this chapter, we introduce various flow patterns of the shock refraction, their corresponding shock polars and applications of shock dynamic methods to the shock refraction.

In addition, the interaction between two shock waves is also presented in this chapter.

§ 10.2 Flow patterns of shock refraction and their shock polars

In this section, we shall introduce the refraction of a moving shock at a plane interface across which the gases are at rest and have the same pressure, but have different speeds of sound.

In general, when a plane moving shock strikes at an interface, processes of both refraction and reflection take place simultaneously. The reflected wave may be shock or expansion wave. If the incident shock, transmitted shock and reflected wave meet all at the same point on the interface, the refraction is called regular refraction, on the contrary, it is called irregular refraction. The property of shock refraction depends on the strength of incident shock, the angle between the incident shock and interface, and the properties of gases on both sides of the interface.

The interface can be divided into “fast-slow” and “slow-fast”. So-called “fast-slow” means that the speed of sound of the gas in which the incident shock moves is larger than that in which the transmitted shock moves (for example, air / SF₆, He / CO₂). If the speed of sound in the incident gas is less than that in the transmitted gas, then it is referred to as “slow-fast” (for example, CO₂ / He, CO₂ / CH₄)

Next, we shall discuss the cases of the “fast-slow” and “slow-fast” interfaces, respectively.

This section is written on the basis of works of Abd- el- Fattah and Hendersor, (1978, 1979).

1. “fast-slow” gas interface

We first present the refraction of shock at the fast-slow gas interface. In general, for different shock strengths the refraction has different physical flow pattern. We will dissuss the cases of “very weak”, “weak”, “strong” and “stronger” incident shocks, respectively.

(1) The very weak group

If the strength of the incident shock is held constant and the incident angle ω_0 is changed, we will obtain a series of flow patterns. When the incident angle is small, the refraction is regular. It consists of the incident shock I , transmitted shock T and reflected shock R . The experiments show that the phenomenon is self-similar. Therefore, in the frame of reference moving with the point P the flow is steady; and the three-shock theory and the shock polar method can again be used (Fig. 10.1). In the $\xi-\delta$ plane, we draw the polar i of incident shock and the polar t of the transmitted shock. The polar i is smaller than the polar t because the interface is fast-slow. The intersection point between them is denoted by A_1 . We can draw a reflected shock polar r from the point 1 which represents the state behind the incident shock. There are two intersection points α_1 and α_2 between the polars t and r . The weaker solution α_1 always occurs in experiments. Such regular refraction with the reflected shock is denoted by RRR (as shown in Fig. 10.1a).

With the incident angle ω_0 increasing, the point 1 moves up along the polar i , and the intersection point A_1 moves down because the polar i becomes

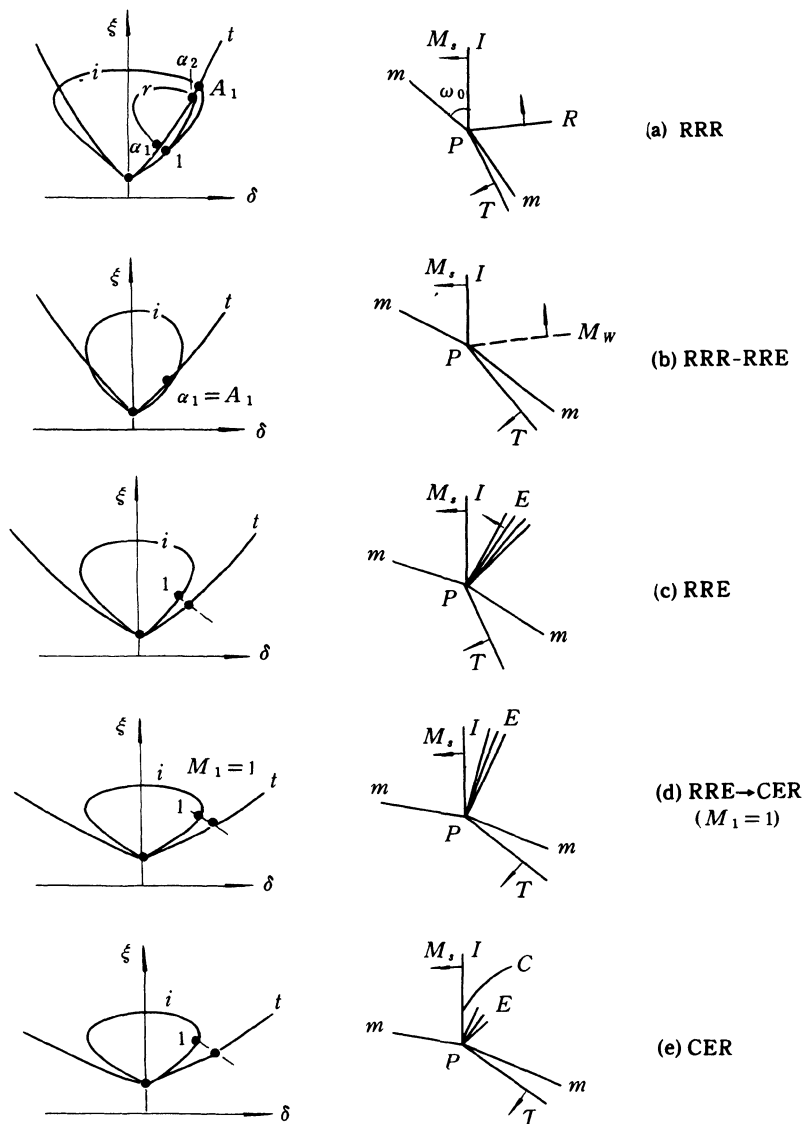


Fig. 10.1 Shock refraction at fast-slow interface for very weak group

small. While the intersection point α_1 coincides with the point A_1 , the reflected shock degenerates to a Mach wave (Fig. 10.1b). It corresponds to the case that the gases on both sides of the interface have the same shock impedances. If the incident angle ω_0 again increases, the pressure in region 1 behind the incident shock becomes higher than that behind the transmitted shock, and thus the reflected wave is an expansive wave which is denoted by RRE(Fig. 10.1c).

As ω_0 further increases, the flow behind the incident shock increases to $M_1=1$, that is , the point 1 coincides with the sonic point of polar i , the transition from regular to irregular refractions takes place (Fig. 10.1d). Beyond the value of the critical incident angle, an irregular refraction called centred expansion irregular refraction (CER) forms (as shown in Fig. 10.1e).

(2) The weak group

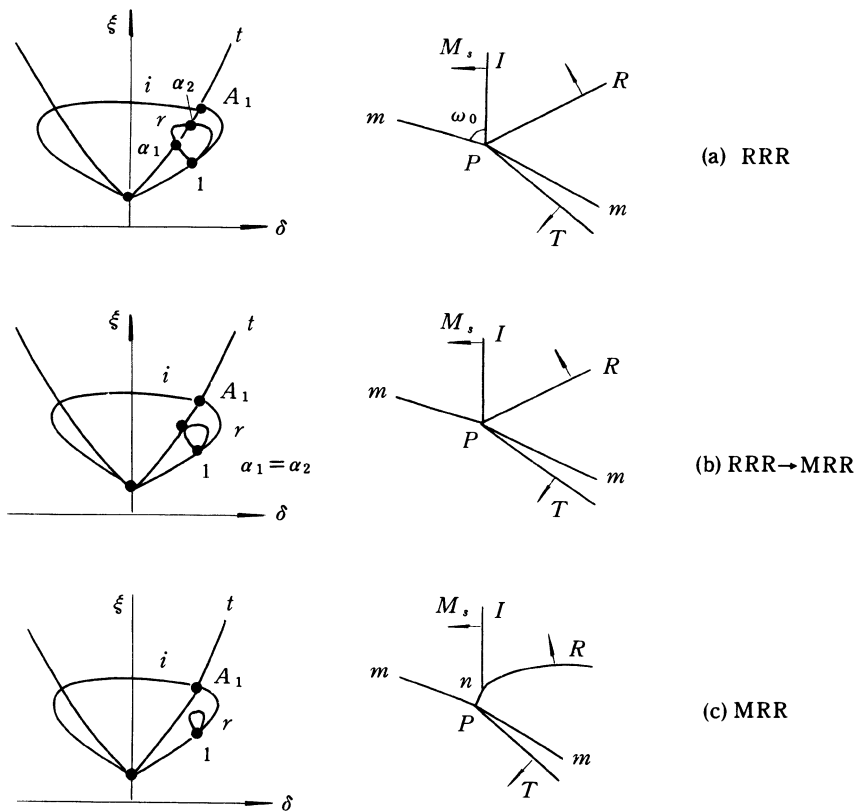


Fig. 10.2 Shock refraction at fast-slow interface for weak group

For a given shock Mach number, the incident angle ω_0 is changed similarly to the case of the very weak group. We first obtain RRR for small incident angle (Fig. 10.2a). When the incident angle ω_0 increases, the two intersection points between the polars r and t (α_1, α_2) approach each other and finally coincide, as shown in Fig. 10.2b. If the angle ω_0 again increases, in shock polar diagram, there is no intersection point between the shock polars r and t . In the physical plane, a Mach stem normal to the interface meets with the incident and reflected shocks at triple point above the interface. Such refraction is referred to as Mach type irregular refraction (MRR) shown in Fig. 10.2c. For larger ω_0 , MRR can no longer exist and there must be a further transition to other irregular refraction.

(3) The strong group

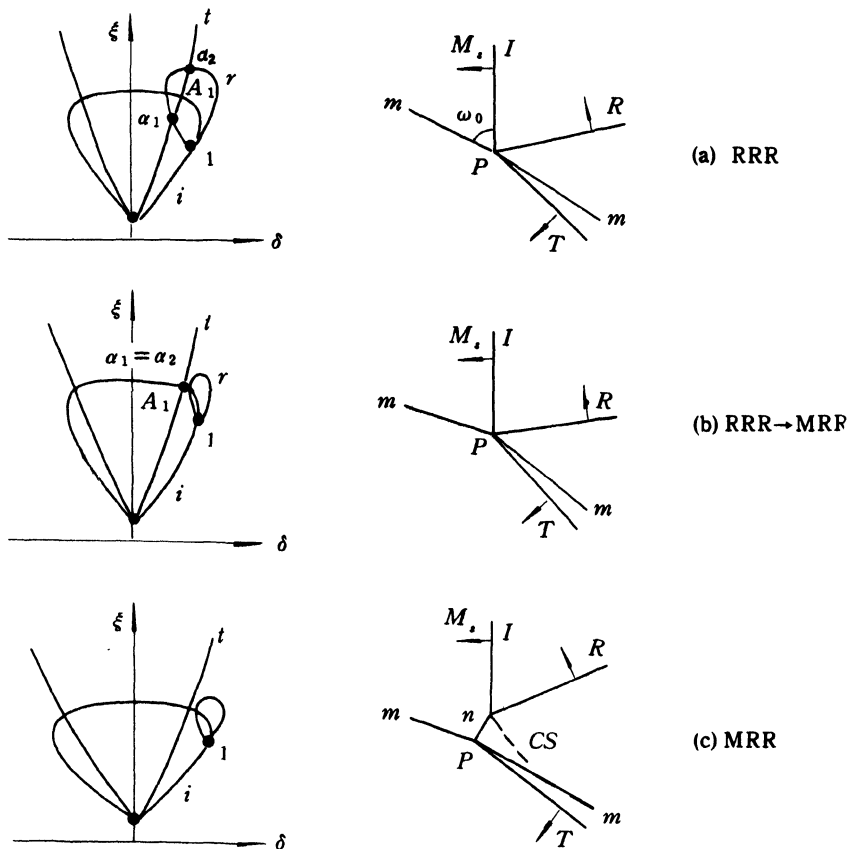


Fig. 10.3 Shock refraction at fast-slow interface for strong group

Figure 10.3 shows the refractions of a strong shock. We obtain the flow patterns similar to the weak group. When the incident angle ω_0 increasing for given shock Mach numbers, RRR and MRR are observed. It is important to note that when the transition from RRR to MRR takes place, the pressure at the tangent point ($\alpha_1 = \alpha_2$) between the polars r and t is higher than that at intersection point A_1 between the polars i and t for the strong shock group. For larger ω_0 , we have $M_1 < 1$ and the Mach reflection can not exist, so there is a further transition to another irregular system. The experimental results show that for this case the incident shock I and Mach stem n become a continuous wave which is concave forwards. This irregular system is called concave forwards irregular refraction denoted by CFR. In the system, the reflected shock is dispersed into a band of weaker wavelets and there is a reflected expansion wave emanating from the intersection point between the incident shock and the interface. The CFR is also found in the weak group.

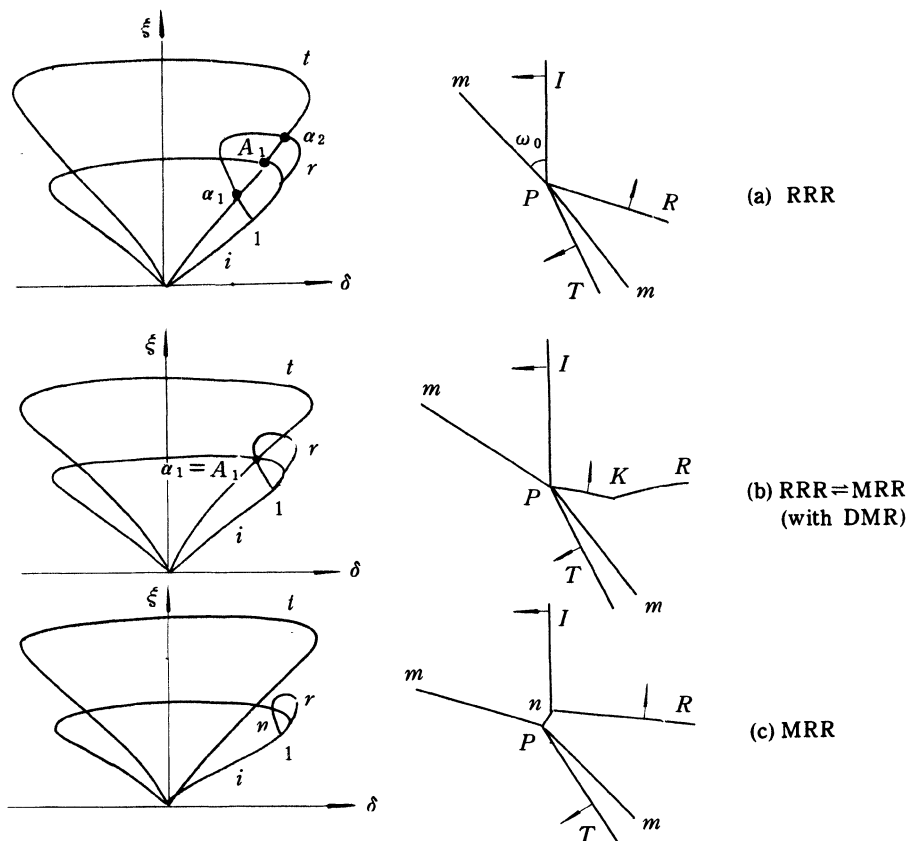


Fig. 10.4 Shock refraction at fast-slow interface for stronger group

(4) The stronger group

For the given stronger shock, we first obtain RRR at small ω_0 as shown in Fig. 10.4a. With ω_0 increasing, the polar r for reflected shock intersects with the polar t of transmitted shock at the point A_1 , which is intersection point between polars i and $t(\alpha_1 = A_1)$. The transition RRR \rightarrow MRR forms. For this group, the flow behind the reflected shock may be supersonic ($M_2 > 1$) with respect to the triple point in small range of ω_0 . We have known from the previous chapter that CMR or DMR may form for $M_2 > 1$ in the shock reflection on rigid wall. Similarly, the shock refraction with DMR is called double-Mach-reflection type of refraction. Beyond this range of ω_0 and continuously increasing in ω_0 , MRR and CFR, similar to the case in the strong group, are obtained.

Figure 10.5 shows the regions of various refraction at air / SF₆ interface.

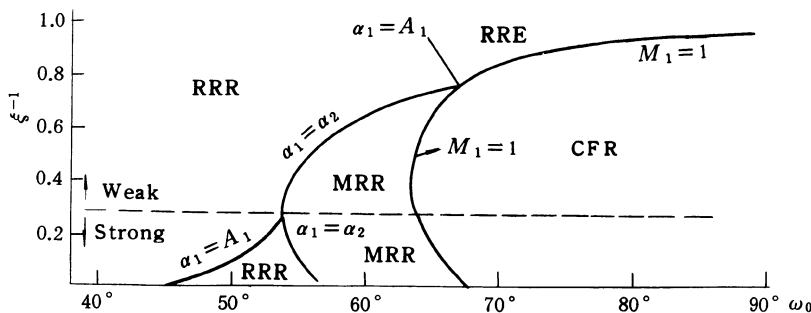


Fig. 10.5 Various refraction at fast-slow interface (from Abd- el- Fattah and Henderson, 1978)

2. Slow-fast interface

For the refraction of shocks at the slow-interface, the flow patterns are much more complicated than that at the fast-slow interface. Here we only discuss some main parts. The discussion will be made for the very weak, weak and strong incident shocks, respectively.

(1) The very weak group

If the incident shock Mach number is held constant and the incident angle ω_0 is changed, a series of flow patterns are shown in Fig. 10.6 for the very weak incident shock. When ω_0 is small, we first obtain the regular refraction with the reflected expansion (RRE), as shown in Fig. 10.6a. In shock polars, the transmitted shock polar t is smaller than the incident shock polar i because the interface is slow-fast. The intersection point between them is denoted by A_1 . In Fig. 10.6a, the pressure behind the incident shock is higher than that behind the transmitted shock. Therefore the reflected wave is an expansion wave.

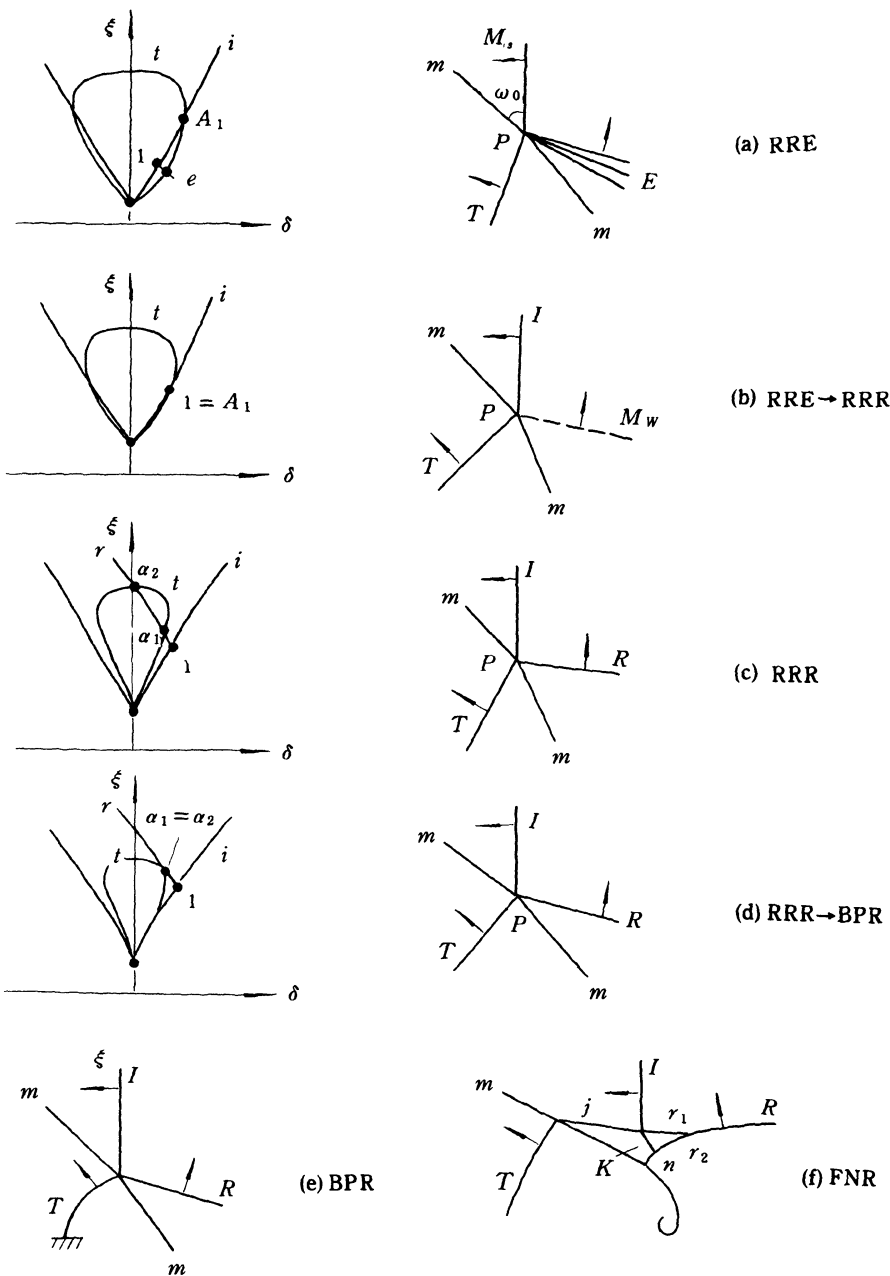


Fig. 10.6 Shock refractions at slow-fast interface for very weak group

While the point 1 coincides with the intersection point A_1 in shock polars as ω_0 increasing, the reflected wave degenerates to Mach wave (Fig. 10.6b) and the transition from RRE to RRR takes place. In Fig. 10.6c, the polar r for the reflected shock intersects with the transmitted shock polar t at two points α_1 and α_2 . In general, the weak solution α_1 occurs. It is regular refraction with the reflected shock (RRR). As ω_0 further increases, the reflected shock polar r is tangent with the transmitted shock polar t and the transition from regular to irregular refraction occurs (Fig. 10.6d). For still larger ω_0 , two types of irregular refractions form, as shown in Fig. 10.6e and f. One is called “bound precursor refraction” (BPR), in which the transmitted shock is always ahead of the incident shock and proceeds along the interface at nearly the same velocity as that of the incident shock. The other is referred to as “free precursor von Neumann refraction” (FNR), in which the transmitted shock being faster than the incident shock is itself refracted at the interface, a new shock j transmits back into the incident gas and a very complicated flow pattern forms.

(2) The weak group

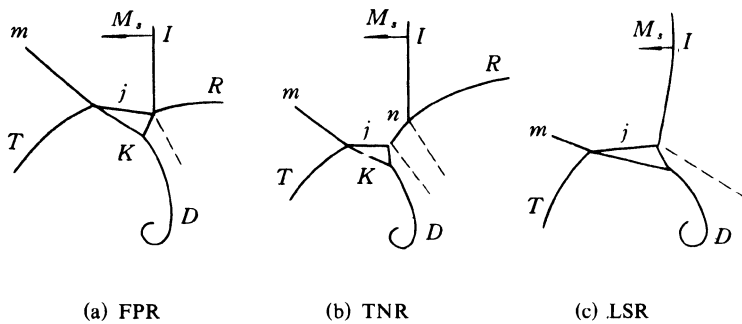


Fig. 10.7 Three types of ‘free precursor refractions’

For this group, with ω_0 increasing, we can obtain RRE, RRR and BPR, respectively. Beyond the BPR range, there are three types of “free precursor refractions” as shown in Fig. 10.7. They are “free precursor refraction” (FPR), “twin von Neumann refraction” (TNR) and “lambda shock refraction” (LSR). FPR is similar to FNR (in the very weak group). In both cases the transmitted shock t is refracted back to the incident gas at the interface and interacts with the incident shock i . The difference between them is that in FNR the modified shock K undergoes a new Mach reflection at the interface, but in FPR the shock K propagates undisturbedly to the interface. With ω_0 increasing, the interaction of shock j with the incident shock i becomes irregular, and TNR as shown in Fig. 10.7b forms, in which there are two triple points and two slip sur-

faces. At still larger ω_0 , the flow Mach number behind the incident shock I approaches unity and the reflected shock R degenerates to Mach wave. The LSR system forms as shown in Fig. 10.7c, in which one triple point has been degenerated.

(3) The strong group

In this group, with ω_0 increasing, the refraction processes similar to the weak group are obtained except RRR and FPR. They are RRE, BPR, TMR and LSR respectively. The twin Mach refraction (TMR) has a flow pattern similar to TNR, but now the shock is strong. TMR is different from DMR in the reflection of shock on solid wall. In DMR the Mach reflections are in series with each other and appear in the disturbed flow downstream of the incident shock, whereas in TMR they are in parallel and appear in the undisturbed gas.

Finally some ranges of various refraction for $\text{CO}_2 / \text{CH}_4$ interface are shown in Fig. 10.8.

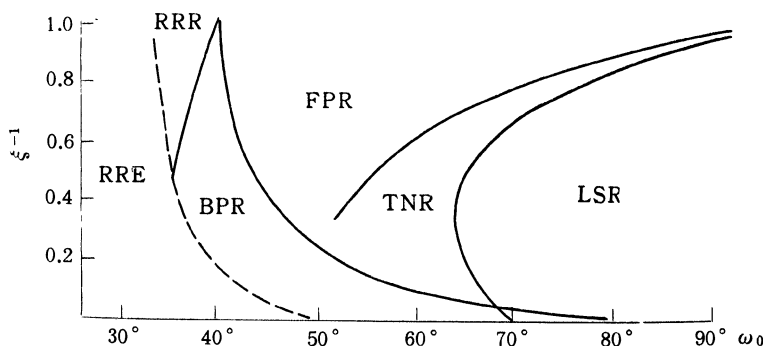


Fig. 10.8 Various refractions at slow-fast interface (from Abd-el-Fattah and Henderson, 1979)

§ 10.3 Refraction of moving shock at slip surface

In previous section, we discussed a series of phenomena of shock refraction at interface, in which the gases on both sides of the interface are at rest. If there are moving media on both sides of interface or one side is moving gas and the other side is quiescent gas, the interfaces is referred to as slip surface. When a plane moving shock strikes at a slip surface, the shock wave will also be refracted. The property of refraction depends not only on the strength of an incident shock, incident angle and speed of sound on both sides of slip surface, but also on the flow velocities of gas on both sides of the slip surface.

Yang, Han and Yin (1991) studied experimentally the refraction of a moving shock at slip surface in a combination facility of a shock tube and shock tunnel. In the experiment, the shock tube with a rectangular cross section is connected obliquely with the test section of a shock tunnel and the upper and bottom walls of both facilities are kept coincident as shown in Fig. 10.9. After the shock tunnel starts, a steady supersonic flow in the test section with M_∞ , p_∞ , a_∞ forms and a slip surface AB being parallel to the axis of tunnel occurs at exit of nozzle, provided the initial pressure is controlled carefully. The gases on both sides of the slip surface have the same pressure, but have different speeds of sound and flow velocities.

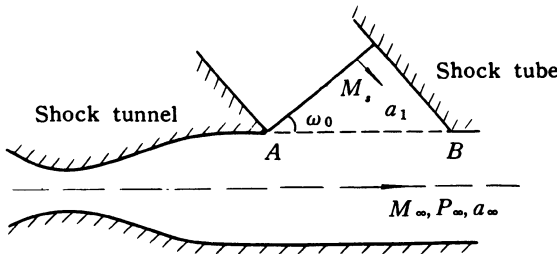


Fig. 10.9 Combination of shock tube and shock tunnel

Consider a plane moving shock in the shock tube striking the slip surface with angle ω_0 at point P . The velocity of the point P is

$$V_p = \frac{M_s a_1}{\sin \omega_0}$$

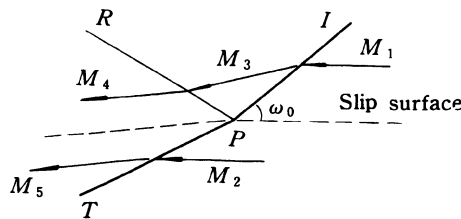


Fig. 10.10 Flow pattern in moving reference system

In a reference system attached to the point P and moving with it, a steady flow field in the vicinity of the point P is obtained, as shown in Fig. 10.10.

The oncoming flow Mach number, M_1 , for the incident shock i and M_2 for the transmitted shock are, respectively,

$$M_1 = \frac{M_s}{\sin \omega_0}$$

and

$$M_2 = \frac{M_s}{\sin \omega_0} \frac{a_1}{a_\infty} - M_\infty$$

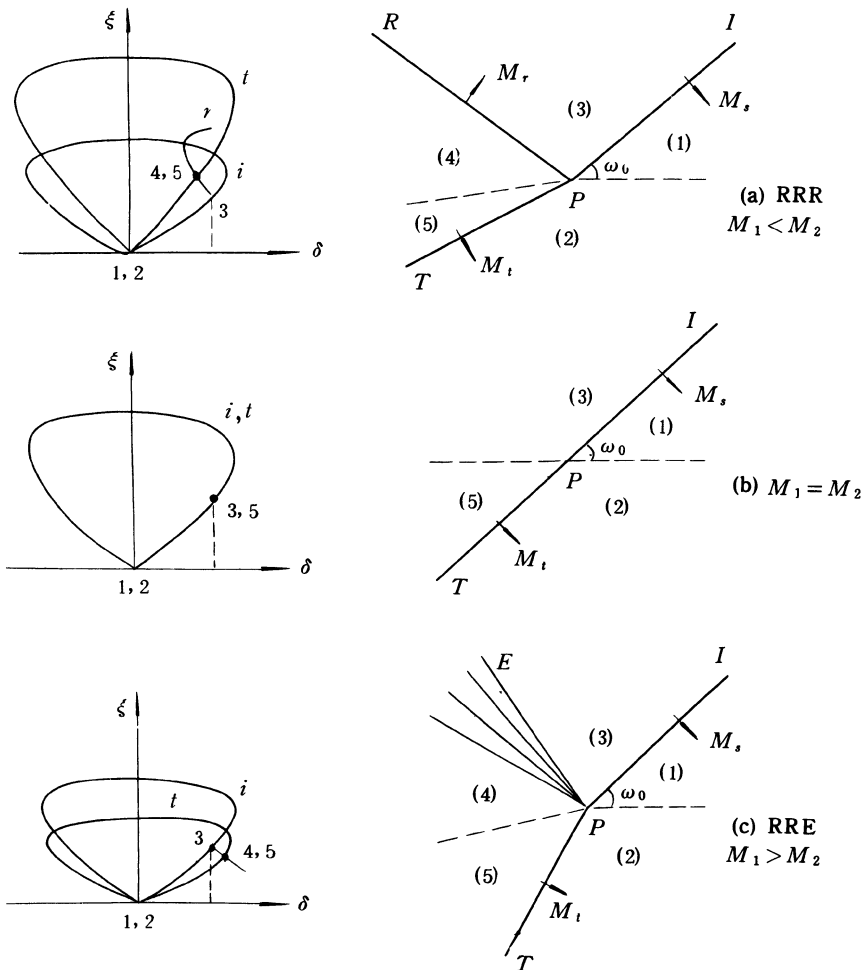


Fig. 10.11 A few of refraction of shock at slip surface

In the experiment, $a_1 = 353 \text{ m/sec}$, $a_\infty = 194.9 \text{ m/sec}$, $M_\infty = 5.0$ and $\omega_0 = 40^\circ$. For the given parameters, the incident shock strength being changed, a serious phenomena of shock refraction is obtained.

For stronger incident shock, $M_1 < M_2$. This case is similar to the 'fast-slow' interface mentioned in the previous section. The transmitted shock T refracts backwards and the reflected wave is a shock wave (RRR). (Fig. 10.11.a). With the strength of incident shock decreasing, both M_1 and M_2 decrease, but M_2 decreases faster. At some critical value, M_2 can be equal to M_1 . In this case, both the shock polars, i and t , are coincident. The incident shock passes through the slip surface with no refraction and the reflected shock degenerates to Mach wave (Fig. 10.11.b). It is easy to find that the critical shock Mach number is

$$M_{sc} = \frac{M_\infty a_\infty \sin \omega_0}{a_1 - a_\infty}$$

This phenomenon cannot be found in the case of quiescent gas. Beyond the critical value, with M_s decreasing, $M_1 > M_2$ is obtained and the regular refraction with the reflected expansion wave (RRE) is observed (Fig. 10.11.c). It corresponds to 'slow-fast' interface in the case of quiescent gas, although now the speed of sound in the incident gas is larger than that in the refracted gas. For weaker incident shock, in $\xi-\delta$ diagram, characteristic from point 3 is tangent to the polar t of the transmitted shock. Transition from the regular to the irregular refraction takes place. For the still weaker incident shock, the irregular refraction occurs. The transmitted shock moves faster than the incident shock. But the detailed pattern was not obtained in the experiment, because the turbulent level in the slip surface is too large. If the incident shock strength decreases continuously, we can get $M_2 = 1$, $M_2 < 1$, $M_2 = 0$ and so on.

§ 10.4 Application of shock dynamics to shock refraction

In Chapter 4, we have got the relations among the shock Mach number, M , the cross-section area of tube, A , and the thermodynamic parameters ahead of shock, a, p, γ . That is

$$\frac{2M}{(M^2 - 1)K(M)} dM + \frac{dA}{A} + f dy + g \frac{da}{a} + h \frac{dp}{p} = 0 \quad (10.1)$$

where $K(M, \gamma) = 2 \left(1 + \frac{2}{\gamma + 1} \frac{1 - \mu^2}{\mu} \right)^{-1} \left(1 + 2\mu + \frac{1}{M^2} \right)^{-1}$

$$f(M, \gamma) = \frac{g(M, \lambda)}{\gamma(\gamma + 1)} (\mu - \gamma)$$

$$g(M, \gamma) = 1 + \frac{2\mu(M^2 - 1)}{(\gamma - 1)M^2 + 2}$$

$$h(M, \gamma) = \frac{1}{2\gamma(M^2 - 1)} \{2(M^2 - 1) + \mu[2\gamma M^2 - (\gamma - 1)]\}$$

$$\mu(M, \gamma) = \left[\frac{(\gamma - 1)M^2 + 2}{2\gamma M^2 - (\gamma - 1)} \right]^{\frac{1}{2}}$$

Now, we consider a plane shock moving through an interface across which there are discontinuities in thermodynamic parameters of gases. The interface is inclined at an angle δ_I to the x -axis, as shown in Fig. 10.12, and the gases ahead of the shock are at rest. The discontinuities of thermodynamic parameters across the interface cause the changes in the strength and direction of the transmitted shock waves.

Plane moving shock

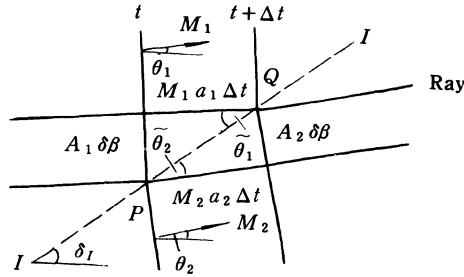


Fig. 10.12 Shock refraction at interface

For simplicity, we can introduce a parameter $\tilde{\theta}$

$$\tilde{\theta} = \theta - \delta_I \quad (10.2)$$

which are the angles between the rays and the interface.

We can see from the expressions of the line segment PQ that

$$U \propto \cos \tilde{\theta} \quad A \propto \sin \tilde{\theta} \quad (10.3)$$

where U is the normal velocity of the shocks.

If assuming infinitesimal changes in a , p , γ across the interface, then

$$\frac{dU}{U} = -\tan \tilde{\theta} d\tilde{\theta}, \quad \frac{dA}{A} = \cot \tilde{\theta} d\tilde{\theta} \quad (10.4)$$

By eliminating $d\tilde{\theta}$, we have

$$\frac{dA}{A} = -\cot^2 \tilde{\theta} \frac{dU}{U} \quad (10.5)$$

Substituting (10.5) into (10.1) and using

$$\frac{dU}{U} = \frac{dM}{M} + \frac{da}{a} \quad (10.6)$$

we have

$$(\tan^2 \tilde{\theta} - v^2) \frac{dM}{M} = v^2 \left[(1 - g \tan^2 \tilde{\theta}) \frac{da}{a} - \tan^2 \tilde{\theta} (fdy + h \frac{dp}{p}) \right] \quad (10.7)$$

where $v = \frac{1}{M} \left[\frac{(M^2 - 1)K(M)}{2} \right]^{\frac{1}{2}}$

Now this relation is used to the interface across which there is a different speed of sound only, while the pressure, p , and ratio of specific heats, γ , are uniform. Then the last two terms in (10.7) vanish and the equation reduces to an ordinary differential equation in M and a ,

$$\frac{dM}{da} = v^2 M (U^2 - g V^2) / a (V^2 - v^2 U^2) \quad (10.8)$$

where $U = aM$, $V^2 = K^2 - U^2$, $K = \frac{M_1 a_1}{\cos \tilde{\theta}_1}$

If M_1 and θ_1 are known, then the unknown Mach number M_2 across the interface may be found by integrating (10.8) from a_1 to a_2 . The unknown $\tilde{\theta}_2$ is given by

$$U_1 / \cos \tilde{\theta}_1 = U_2 / \cos \tilde{\theta}_2 \quad (10.9)$$

In the derivation of (10.8) the slow changes in U , A and a across the interface is assumed. But the above equation can work well so long as the jump in θ and M is not too large. For large jump, M_2 may not be given accurately.

As the first example, we choose the simplest configuration in which the interface is wedge-shaped with one of the sides aligned parallel to the undisturbed shock front and other lying at an angle δ_1 with x -axis, as shown in Fig. 10.13. For ‘slow-fast’ refraction, that is, the shock moves from the side of lower speed of sound to the side of higher speed of sound ($a_1 < a_2$), the shock refraction is studied. After the shock transmits through the vertical portion of the interface, the strength of shock in region 2 can be calculated exactly from the equations of one-dimensional, unsteady gasdynamics and provides the lower boundary condition in this problem.

We know from § 10.2 that for large interface angle δ (or small incident angle ω_0), the regular refraction (RRE) is first obtained (Fig. 10.13a). The

transmitted shock is refracted forwards. From the viewpoint of shock dynamics the disturbance from trip of interface propagates along shock-expansions of opposite family (C^+ and C^-). Using the interface jump conditions (10.8) and (10.9), the refracted shock in region 3 is solved (including the strength and direction of refracted shock). Using one-dimensional, unsteady relations, the shock in region 2 is solved. Thus, the shock in region 4 can be found by using the characteristic relations of two-dimensional shock dynamics in quiescent gas and boundary conditions in region 3 and 2.

While the interface angle δ_I decreases and approaches the uppermost characteristic of shock expansion C^+ , the transition from the regular to the irregular refraction occurs. In this case (Fig. 10.13b), the region 3 vanishes and this results in the formation of a shock-shock which lies above the interface at an angle χ_1 with the x -axis. As the interface angle decreases further, the upper shock expansion C^+ vanishes (Fig. 10.13c), which corresponds to FPR.

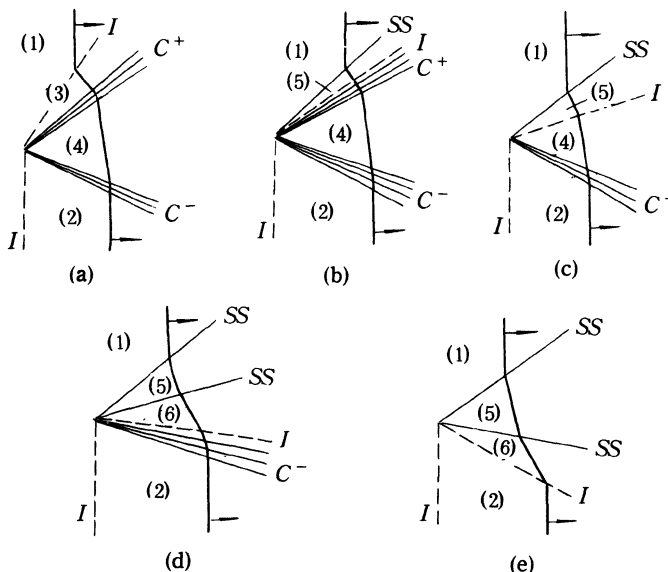


Fig. 10.13 Shock refraction at slow-fast interface.(from Catherasoo and Strutevant, 1983)

For the irregular refraction cases, since none of the conditions in the two regions adjacent to the interface are known as a priori, it is necessary to make a guess of one quantity, say the Mach number M in region 5, above the interface and then to solve the problems by using the shock-shock relation across SS ,

interface jump conditions across I , and characteristic relations of shock dynamics iteratively.

If the slope of the interface decreases further and the uppermost characteristic of the lower shock expansion C^- approaches the interface, the second transition takes place. In this case, the region 4 vanishes and the second shock-shock forms above the interface at an angle χ_2 with the x -axis (Fig. 10.13d). If the interface angle decreases further, finally the lower shock expansion C^- vanishes, the problem involves only two shock-shocks of opposite families (Fig. 10.13e), which corresponds to TNR.

It is worth while noticing that the transition from the regular to irregular refraction arises naturally in the shock dynamic theory in terms of the slopes of characteristics. The calculated results by shock dynamics show very good agreement with the experimental data and the results predicated by three-shock theory (Catherasoo and Sturtevant, 1983).

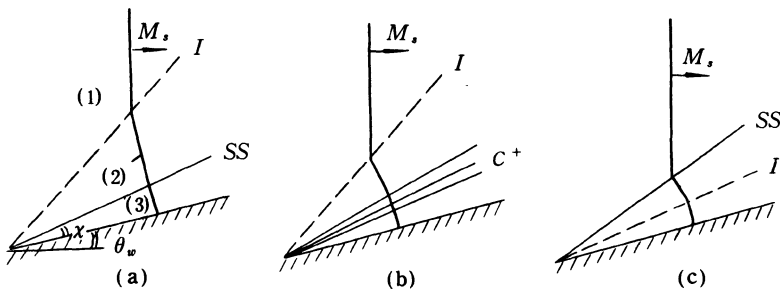


Fig. 10.14 Shock refraction at slow-fast interface with solid wall.

The second example applied shock dynamics is that a solid wall is introduced below the slow-fast interface I , at an angle θ_w with the x -axis as shown in Fig. 10.14. For the large interface angle δ_I and the small wall angle θ_w , the regular refraction occurs at the interface and a shock-shock lies between the interface and the wall, similar to the reflection of shock on a wedge surface. (Fig. 10.14a). For the given strength of the incident shock and condition of interface, solving equations (10.8) and (10.9), we can find the Mach number and direction of the shock in region 2. Then, the Mach number of the shock normal to the wall is found by using the shock-shock relation. As the interface angle δ_I decreases, the shock-shock weakens, vanishes and degenerates C^+ characteristics (Fig. 10.14b). The transition from shock-shock to shock-expansion corresponds to the case that the transmitted shock in region 2 is normal to the wall. While the interface angle decreases below the

C^+ characteristics, the irregular refraction takes place and the shock-shock occurs above the interface (Fig. 10.14c).

Shock dynamics is successfully applied to the ‘slow-fast’ shock refraction. But for the refraction of shock at the ‘fast-slow’ interface, the theory does not give out analytic results (Catherasoo and Sturtevant, 1983).

§ 10.5 Numerical shock dynamics

The shock dynamic equations can be calculated numerically, instead of analytically. In this section we introduce the new method which is advantageous in its simplicity and can be applied to a wide variety of problems, (Henshaw, *et al.*, 1986).

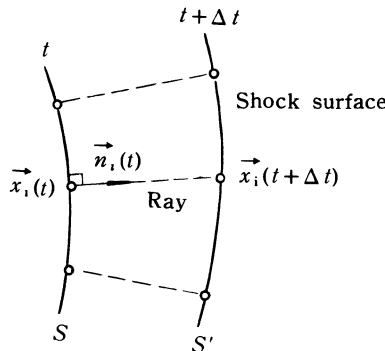


Fig. 10.15 Shock front positions at t and $t + \Delta t$ and approximate rays

According to the two-dimensional shock dynamic equations, along a ray, we have

$$\frac{\partial x}{\partial \alpha} = M \cos \theta \quad \frac{\partial y}{\partial \alpha} = M \sin \theta \quad (10.10)$$

Writing the above equations in vectorial form and eliminating α in favour of time t , the equations (10.10) become

$$\frac{\partial}{\partial t} \bar{x}(\beta, t) = a(\beta, t) M(\beta, t) \bar{n}(\beta, t) \quad (10.11)$$

where $\bar{x} = (x, y)$ is the position of the shock front and $\bar{n} = (\cos \theta, \sin \theta)$ is the normal to the shock front.

Discretization of (10.11) in space yields a system of N ordinary differential equations for the discrete shock front positions $\bar{x}_i(t)$, $i=1, \dots, N$. We then integrate the system of ODE in time using the two-step leap-frog scheme

$$\bar{x}_i(t + \Delta t) = \bar{x}_i(t - \Delta t) + 2\Delta t a_i(t) M_i(t) \bar{n}_i(t) \quad i = 1, \dots, N \quad (10.12)$$

where $t = n \Delta t$, for $n = 0, \dots, T / \Delta t$, and $a_i(t)$, $M_i(t)$, and $\bar{n}_i(t)$ are the discrete speed of sound, Mach number and shock front normal at $\bar{x}_i(t)$, respectively.

For the shock propagation in uniform media, the speed of sound a in (10.12) is constant. The Mach number $M_i(t)$ is found by solving the A - M relation

$$\frac{A_i(t)}{A_i(0)} = \frac{f(M_i(t))}{f(M_0(t))} \quad \text{for } i = 1, \dots, N \quad (10.13)$$

The area $A_i(t)$ in (10.13) is given by a centred scheme about the point $\bar{x}_i(t)$ in the interior and an one-sided scheme at the endpoints

$$A_i(t) = \frac{1}{2} \begin{cases} S_{i+1}(t) - S_i(t) & i = 1 \\ S_{i+1}(t) - S_{i-1}(t) & i = 2, \dots, N-1 \\ S_i(t) - S_{i-1}(t) & i = N \end{cases} \quad (10.14)$$

where $S_i(t)$ is the discrete arclength given by

$$S_i(t) = \begin{cases} 0 & i = 1 \\ S_{i-1}(t) + |\bar{x}_i(t) - \bar{x}_{i-1}(t)| & i = 2, \dots, N \end{cases} \quad (10.15)$$

The normal to the shock front $\bar{n}_i(t)$ in (10.12) is determined by differentiating two cubic splines fitted to the data $(S_i(t), x_i(t))$ and $(S_i(t), y_i(t))$, $i = 1, \dots, N$, respectively. Let $\tilde{x}(S)$ and $\tilde{y}(S)$ denote these two cubic spline interpolants, respectively. The smooth curve $(\tilde{x}(S), \tilde{y}(S))$ is an approximation to the shock front at time t . Therefore, $\bar{n}_i(t)$ is given by

$$\bar{n}_i(t) = \frac{(y'(S_i), -x'(S_i))}{[(x'(S_i))^2 + (y'(S_i))^2]^{\frac{1}{2}}} \quad i = 1, \dots, N \quad (10.16)$$

where the primes denote the derivative with respect to S .

While the shock propagates in nonuniform media, for example, there is only nonuniformity of the speed of sound, for simplicity, the Mach number $M_i(t)$ can be obtained from the integral

$$\int_0^t \left\{ \frac{2M}{(M^2 - 1)K} \frac{\partial M}{\partial t} + \frac{1}{A} \frac{\partial A}{\partial t} + \frac{g}{a} \frac{\partial a}{\partial t} \right\} dt = 0 \quad (10.17)$$

We integrate (10.17) along the ray tube and (10.17) becomes

$$-\log \frac{f(M_i(t))}{f(M_i(0))} + \log \frac{A_i(t)}{A_i(0)} + \int_0^t \frac{g(M(t))}{a(t)} \frac{\partial a}{\partial t} dt = 0 \text{ for } i = 1, \dots, N \quad (10.18)$$

where the expressions of $f(M)$ and $g(M)$ is the same as in (10.1). The last term in (10.18) can be handled approximately. As a first step, we note that if $g(M) \approx g(M_0) = \text{constant}$, we can integrate it to give

$$\frac{f(M_i(t_1))}{f(M_i(0))} = \frac{A_i(t_1)}{A_i(0)} \left[\frac{a_i(t_1)}{a_i(0)} \right]^{g(0)} \quad (10.19)$$

where $g(0) \equiv g(M_i(0))$. In the numerical scheme, we can take $g(M) \approx \text{constant}$ at each time step. Then the $A-M$ relation is given

$$\frac{f(M_i(t))}{f(M_i(0))} = \frac{A_i(t)}{A_i(0)} \prod_{k=1}^N \left[\frac{a_i(k\Delta t)}{a_i((k-1)\Delta t)} \right]^{g(k-1)} \quad (10.20)$$

where $g(k) \equiv g(M_i(k\Delta t))$. Inverting $f(M)$ gives $M_i(t)$ for $i = 1, \dots, N$. The other processes are the same as in the case of uniform media.

Initially, the shock position $\bar{\chi}_i(0)$ and Mach number $M_i(0)$ at $t=0$ are given. An explicit one-step scheme is used to begin the two-step leap-frog time marching scheme.

The parameters N and Δt are chosen by the following rules

$$\text{Rule 1} \quad \Delta S_{\text{avg}} = \frac{1}{N} \sum_{i=2}^N \Delta S_i(0) = \frac{S_N(0)}{N} = K_1 \ll 1 \quad (10.21)$$

$$\text{Rule 2} \quad \frac{\Delta t}{\Delta S_{\min}} = \frac{\Delta t}{\min \Delta S_i(t)} = \frac{\Delta t}{d \Delta S_{\text{avg}}} < K_2 = O(1) \quad (10.22)$$

where $\Delta S_i(t) = S_i(t) - S_{i-1}(t)$ and d is a minimum tolerance on $\Delta S_i(t)$.

On the wall boundaries, the shock must be normal to the walls at the wall boundaries. The point at the boundary is then determined such that the line segment between the endpoint and its neighbouring point is normal to the wall.

In expansive regions of the shock front, the points tend to spread out, and in compressive regions, the points tend to cluster. In order to ensure the numerical stability (10.22) in compressive region and to avoid the ray crossing as shock-shock forms, it is necessary to delete the points. In order to maintain the shockfront resolution (10.21) in expansive region, inserting points is required. We must check periodically the point spacing $\Delta S_i(t)$ and we require

$$d \leq \frac{\Delta S_i(t)}{\Delta S_{\text{avg}}} \equiv \sigma_i(t) \leq D \quad \text{for all } i = 2, \dots, N \quad (10.23)$$

where $d = \frac{1}{2}$ and $D = \frac{3}{2}$. If $\sigma_i(t) < d$, point $\bar{x}_i(t)$ is removed and if $\sigma_i(t) > D$, point $\bar{x}_{i-\frac{1}{2}}(t)$ is added using the cubic-spline interpolant evaluated at $\frac{1}{2}(S_i(t) + S_{i-1}(t))$. Finally, after every 10–50 time steps, a simple two-step smoothing procedure is used in order to reduce the high-frequency numerical errors.

Henshaw, *et al.* (1986) and Schwendeman (1988) used the numerical shock dynamic method to many examples, including the reflection of a shock on the surface of wedge and curve wall, the diffraction of a shock by cylinder and sphere, the focusing of a shock and the refraction of shock on plane, cylindrical and spherical interfaces.

The comparison of the numerical results with the exact solutions of the geometrical shock dynamic equations and the experimental investigations shows that the numerical shock dynamic method has simplicity with good accuracy and can be used to solve wide variety of problems of shock propagation. For calculating refraction of shock, this method can be used not only in the slow-fast interface, but also in the fast-slow case. It is also used to calculate the refraction of a shock on cylindrical and spherical interfaces. It is interesting that except the regular and irregular refractions, the precursor wave is found in calculation. On the other hand, the numerical scheme requires no prior knowledge of the solution, and the shock-shock, shock-expansion, shock-compression and precursor wave form naturally in calculation.

§ 10.6 Interaction between shocks

Interaction between shocks is sometimes called shock impingement or shock intersection. It may be one of the most important phenomena of shock dynamics. If we can find a coordinate system in which all wave systems keep stationary, the interaction is referred to as “steady interaction”, otherwise, it is called “unsteady interaction”.

1. steady shock interaction

Two-dimensional, steady shock interaction has been studied experimentally and numerically by many investigators since 1960s. In general, it includes six possible types of interactions, which depend on freestream Mach number, strength of shocks, shape of object, and position of interaction point(Edney, 1968).

Consider a two-dimensional cylinder lying in a stationary supersonic flow at zero angle of attack and a wedge generating an oblique shock. When the oblique shock impinges on the bow shock of the cylinder, six types of

interactions are possible, depending on the position of the impinging point. Figure 10.16 shows the possible regions in which the different types of interactions take place on the bow shock. Next we briefly discuss their flow patterns, as shown in Fig. 10.17.

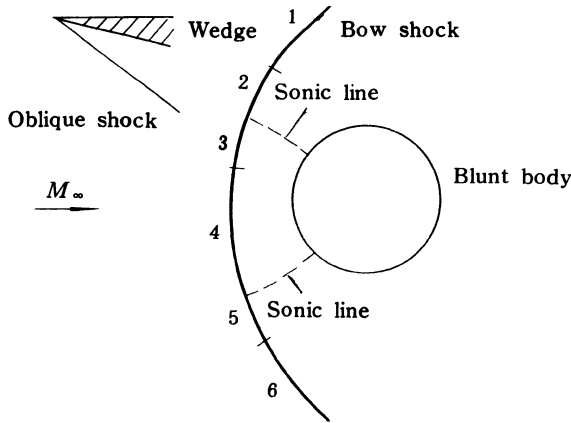


Fig. 10.16 Possible range of six types of steady shock interactions

Type 1: If the impinging shock and the bow shock which are an opposite family of shock intersect at position downstream and far from the upper sonic point, the interaction is regular and is called type 1. In this case the angle between the impinging shock I and the bow shock B is smaller. After the interaction two transmitted shocks and a slip surface form. Four shocks and the slip surface intersect at the same point Q and divide the flow field in the vicinity of the point Q into five uniform regions. In the $\xi-\delta$ diagram, the polars for M_2 and M_3 have two intersection points. In general the weaker one exists in experiment. The points 4 and 5 represent states on both sides of the slip surface, which have the same pressure and the same direction of flow. The relations shown in § 7.8 can be used to calculate the parameters in each region.

Type 2: When the impinging point Q approaches the upper sonic point, the inclined angle of bow shock increases and Mach number M_3 in the region 3 behind the bow shock decreases. In the $\xi-\delta$ diagram, the point 3 moves upward along the polar for M_1 , the polar for M_3 shrinks and there is no intersection point between the polars for M_2 and M_3 . The interaction becomes irregular. A curved Mach shock connects with the impinging shock I and the bow shock B at the points Q and P , respectively. Five-shock configuration divides the flow field into six regions and there is a nonuniform subsonic flow behind the

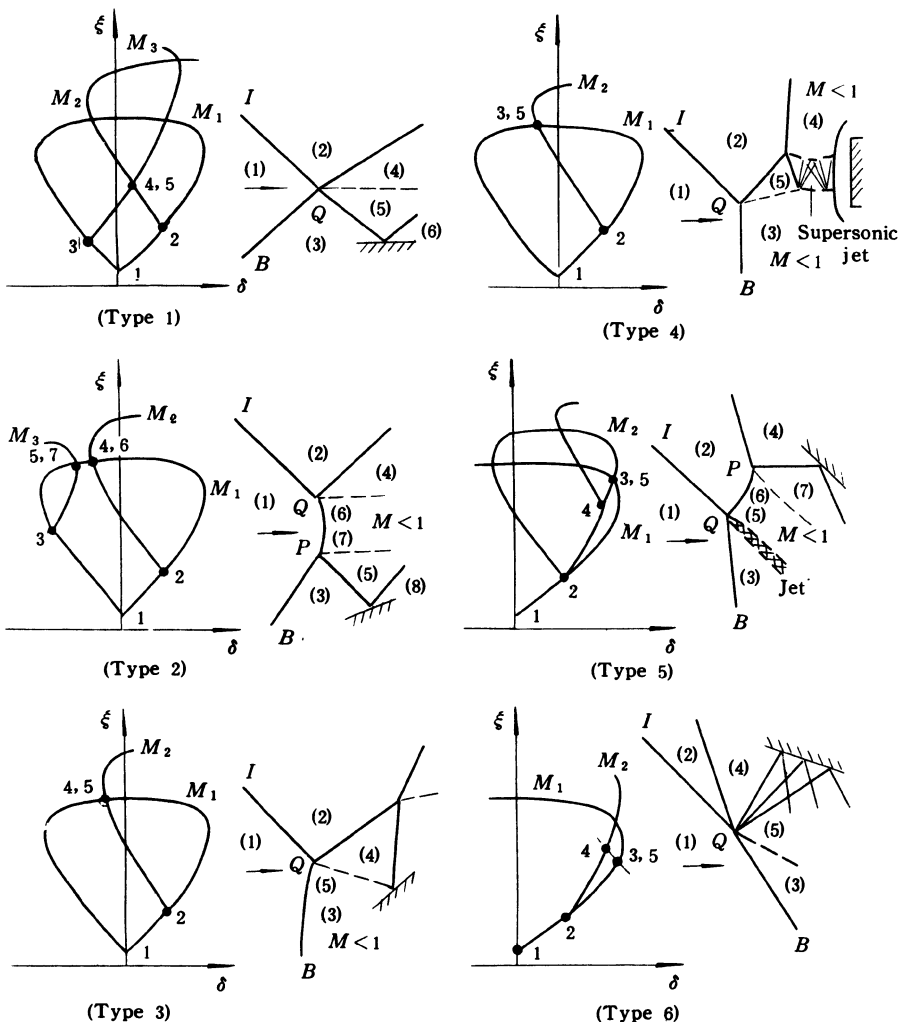


Fig. 10.17 Six types of shock intersections and their shock polars

Mach shock PQ .

Type 3: When the impinging point Q moves to the position below and near the upper sonic point, the flow in the region 3 behind the bow shock is subsonic and the flow pattern in the vicinity of the point Q degenerates to the three-shock configuration.

Type 4: This type of interaction takes place near the stagnation point.

Difference of it from the type 3 is that after the interaction a supersonic jet forms and strikes the object surface.

Type 5: This type is similar to the type 2, but in this case two intersecting shocks are the same family. The interaction is still irregular and the five-shock configuration forms.

Type 6: When the impinging point Q moves downstream and far from the lower sonic point, two shocks being the same family interact. Unlike the type 1, an expansion wave forms and strikes the object surface.

2. Unsteady shock interaction

In unsteady shock interaction, a typical example is the interaction of a plane moving shock with a bow shock attached to a vehicle flying at supersonic speed. If the object is a wedge or a sharp cone at zero angle of attack, the problem is self-similar. If the object has a complicated shape, the problem is three-dimensional, unsteady interaction.

Solving the problem includes three parts: intersection of the moving shock with the bow shock, propagation of transmitted shock in nonuniform flow field and reflection of transmitted shock on object surface.

Since 1960s the interaction of moving shock with bow shock attached to a cone has been studied experimentally and numerically. Merritt (1967) in shock tube and ballastic range and Ruetenik in rocket propelled sled conducted the experiments respectively. Han *et al.* (1987) performed successfully the oblique interaction of a plane moving shock with a bow shock attached to a cone in an electrically controlled double driver shock tunnel. In § 7.8 of this book we present the method of calculation about this problem in the symmetric meridian plane. In order to calculate the shock interaction in all meridian planes by using the method of shock dynamics, it is necessary as mentioned above to calculate the three-dimensional shock intersection, propagation of the three-dimensional shock in a nonuniform flow field and three-dimensional reflection of shock on surface. The latter two items can be solved by the three-dimensional equation of shock dynamics and the three-dimensional shock-shock the relation in moving gas described in Chapter 7. Next we will introduce the problem of the three-dimensional shock intersection.

3. Three-dimensional shock intersection

The three-dimensional shock intersection is much more complicated than the two-dimensional problem. The three-dimensional curved shock has some different properties from the two-dimensional shock. First, in the three-dimensional case it is convenient to denote the flow velocity and orientation of the shock surface by a vector \vec{V} and a unit normal vector \vec{n} to the shock surface. Second, a small smooth part of the curved shock can be treated as a plane shock. Thus, the states on both sides of the curved shock

surface can be solved by the shock relations across a plane shock being tangential to it. Third, the vector of the free stream velocity can arbitrarily be decomposed into a tangential component and an oblique component to the plane. Therefore, description of a three-dimensional shock by shock polar ($\xi-\delta$) has some arbitrariness. Finally, the three-dimensional shock intersection takes place along a spatial curved line, and thus its property depends not only on the strength of shock and the freestream Mach number, but also on the orientation of the intersection line.

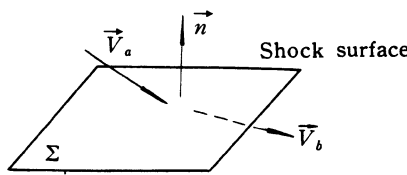


Fig. 10.18 Three-dimensional shock surface

Consider a shock surface Σ with a normal vector \vec{n} (the positive direction points at low pressure side). We can write a vectorial relation of flow velocity across the shock Σ for invicid, perfect gas

$$\vec{V}_b = \vec{V}_a - \frac{2}{\gamma + 1} \left[1 - \frac{a_a^2}{(\vec{V}_a \cdot \vec{n})^2} \right] (\vec{V}_a \cdot \vec{n}) \vec{n} = \vec{V}_a - B_a \vec{n} \quad (10.24)$$

where \vec{V} , a and γ represent the flow velocity, speed of sound, and ratio of specific heats. The subscripts a and b refer to the regions ahead of and behind the shock, respectively. B_a is a constant depending on the state ahead of the shock. This equation considers continuity equation, momentum equation in tangential direction, state equation and Prandtl relation across the oblique shock. The thermodynamic parameters across the shock satisfy the following scalar expressions

$$p_b / p_a = 1 + \frac{\gamma}{a_a^2} \cdot \vec{V}_a \cdot (\vec{V}_a - \vec{V}_b) \quad (10.25)$$

$$a_b^2 / a_a^2 = 1 + \frac{\gamma - 1}{2a_a^2} (\vec{V}_a \cdot \vec{V}_a - \vec{V}_b \cdot \vec{V}_b) \quad (10.26)$$

$$\rho_b / \rho_a = (\gamma + 1) / [(\gamma - 1) + 2a_a^2 / (\vec{V}_a \cdot \vec{n})^2] \quad (10.27)$$

Next we introduce the calculation method of the three-dimensional shock intersection in terms of an example that a plane moving shock intersects

obliquely a bow shock attached to a cone.

Let a cone with semi-apex angle θ_w fly at zero angle of attack with M_∞ and a plane moving shock with M_s strike obliquely the bow shock. The intersection line is an ellipse as shown in Fig. 10.19. Choose a reference system fixed at the cone, the x -axis coinciding with the oncoming flow direction and the angle between the moving shock and the $y-z$ plane being λ . The phenomenon is self-similar. Assuming that the moment that the moving shock strikes the tip of cone is taken as $t=0$, we make the analysis in $(x/t, y/t, z/t)$ system. For simplicity, only the regular intersection is studied. We have the following known quantities

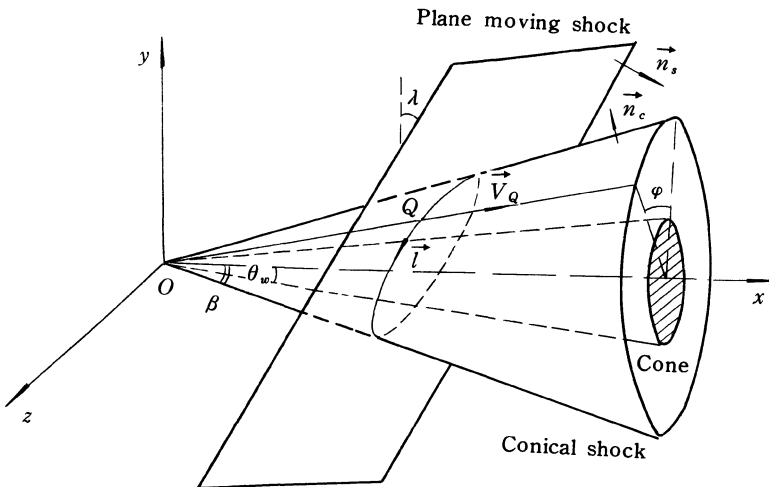


Fig. 10.19 Intersection of plane moving shock with bow shock attached to cone

$$\vec{n}_s = (\cos\lambda, -\sin\lambda, 0) \quad (10.28)$$

$$\vec{n}_c = (-\sin\beta, \cos\beta\cos\varphi, \sin\varphi\cos\beta) \quad (10.29)$$

$$\vec{V}_\infty = M_\infty a_\infty (1, 0, 0) \quad (10.30)$$

where \vec{n}_c is the unit vector normal to the conical shock with a semi-apex angle β , \vec{n}_s is the unit vector normal to the plane moving shock, φ is the angle between the meridian plane studied and the vertical meridian plane. Taking the point Q along the intersection line, we have the tangential unit vector \vec{l} to the intersection line at Q

$$\vec{l} = \frac{\vec{n}_s \times \vec{n}_c}{|\vec{n}_s \times \vec{n}_c|} \quad (10.31)$$

The velocity of the point Q , \vec{V}_Q , has the direction

$$\vec{e}_{v_Q} = (\cos\beta, \sin\beta\cos\varphi, \sin\beta\sin\varphi)$$

Cosine of the angle between it and \vec{n}_s is

$$\vec{e}_{v_Q} \cdot \vec{n}_s = \cos\lambda\cos\beta - \sin\lambda\sin\beta\cos\varphi$$

Thus the velocity of the point Q is expressed as

$$\vec{V}_Q = \frac{(M_s + M_\infty \cos\lambda)a_\infty}{\cos\lambda\cos\beta - \sin\lambda\sin\beta\cos\varphi} \vec{e}_{v_Q} \quad (10.33)$$

In the reference system moving with the point Q , we obtain a stationary flow in the neighbourhood of the point Q and the flow pattern as shown in Fig. 10.20. After transformation of coordinates, we have

$$\vec{V}_1 = \vec{V}_Q - \vec{V}_\infty \quad (10.34)$$

Now, \vec{V}_1 , p_1 , a_1 , \vec{n}_s , \vec{n}_c , \vec{l} are the known quantities from the expressions (10.28)–(10.34).

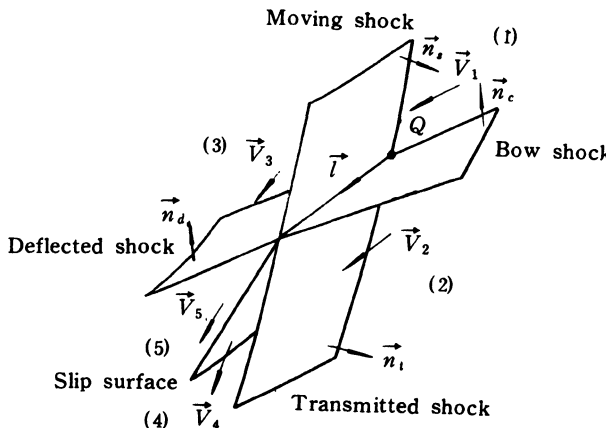


Fig. 10.20 Flow pattern in moving reference system

Using the shock relations (10.24–10.26), we have for the moving shock,

$$\begin{cases} \vec{V}_3 = \vec{V}_1 - B_1 \vec{n}_s \\ p_3 = p_1 \left[1 + \frac{\gamma}{a_1^2} \vec{V}_1 \cdot (\vec{V}_1 - \vec{V}_3) \right] \\ a_3^2 = a_1^2 \left[1 + \frac{\gamma-1}{2a_1^2} (V_1^2 - V_3^2) \right] \end{cases} \quad (10.35)$$

for the bow shock,

$$\begin{cases} \vec{V}_2 = \vec{V}_1 - B_1 \vec{n}_c \\ p_2 = p_1 \left[1 + \frac{\gamma}{a_1^2} \vec{V}_1 \cdot (\vec{V}_1 - \vec{V}_2) \right] \\ a_2^2 = a_1^2 \left[1 + \frac{\gamma-1}{2a_1^2} (V_1^2 - V_2^2) \right] \end{cases} \quad (10.36)$$

for the transmitted shock,

$$\begin{cases} \vec{V}_4 = \vec{V}_2 - B_2 \vec{n}_t \\ p_4 = p_2 \left[1 + \frac{\gamma}{a_2^2} \vec{V}_2 \cdot (\vec{V}_2 - \vec{V}_4) \right] \\ a_4^2 = a_2^2 \left[1 + \frac{\gamma-1}{2a_2^2} (V_2^2 - V_4^2) \right] \end{cases} \quad (10.37)$$

for the deflected shock,

$$\begin{cases} \vec{V}_5 = \vec{V}_3 - B_3 \vec{n}_d \\ p_5 = p_3 \left[1 + \frac{\gamma}{a_3^2} \vec{V}_3 \cdot (\vec{V}_3 - \vec{V}_5) \right] \\ a_5^2 = a_3^2 \left[1 + \frac{\gamma-1}{2a_3^2} (V_3^2 - V_5^2) \right] \end{cases} \quad (10.38)$$

where \vec{n}_{bt} and \vec{n}_d are the unit vectors normal to the transmitted and deflected shock, respectively.

For the regular intersection, the four shocks intersect at the same intersection line, the geometric relation meets

$$\vec{n}_t \cdot \vec{l} = 0, \quad \vec{n}_d \cdot \vec{l} = 0 \quad (10.39)$$

The compatible conditions of the three-dimensional contact surface can be expressed as

$$p_4 = p_5 \quad (10.40)$$

$$(\vec{V}_4 \times \vec{V}_5) \cdot \vec{l} = 0 \quad (10.41)$$

In summary, we have total 24 unknown quantities ($\vec{V}_2, \vec{V}_3, \vec{V}_4, \vec{V}_5, p_2, p_3, p_4, p_5, a_2, a_3, a_4, a_5, \vec{n}_s, \vec{n}_d$) and 24 equations (10.35)–(10.41). The system is closed. (note that \vec{n}_s, \vec{n}_d are unit vectors and have only two independent components for each one).

There is another method of calculation that is more intuitive. We know from the discussion above that for the regular intersection of shocks, all the four shock surfaces have a common intersection line, which tangential unit vector is denoted by \vec{l} . Thus

$$\vec{l} \cdot \vec{n}_s = \vec{l} \cdot \vec{n}_c = \vec{l} \cdot \vec{n}_t = \vec{l} \cdot \vec{n}_d = 0 \quad (10.42)$$

Making scalar product of \vec{l} on both sides of equation (10.24), we have

$$\vec{V}_1 \cdot \vec{l} = \vec{V}_2 \cdot \vec{l} = \vec{V}_3 \cdot \vec{l} = \vec{V}_4 \cdot \vec{l} = \vec{V}_5 \cdot \vec{l} = V_l \quad (10.43)$$

It means that the flow velocities in all regions in the vicinity of the intersection line have the same tangential component of velocity along the intersection line. If one moves with the intersection point, then a two-dimensional shock interaction in the plane normal to the vector \vec{l} can be got. Figure 10.21 shows the flow pattern in the plane D normal to vector \vec{l} . In § 7.8 we have seen the similar pattern. The parameters in region 1 can be found as follows

$$\begin{aligned} \vec{V}_l &= (\vec{V}_1 \cdot \vec{l}) \vec{l} & \vec{V}_{1D} &= \vec{V}_1 - \vec{V}_l \\ \theta_{2D} &= \frac{\pi}{2} - \cos^{-1} \left(\frac{\vec{V}_{1D} \cdot \vec{n}_c}{V_{1D}} \right) & \theta_{3D} &= \frac{\pi}{2} - \cos^{-1} \left(\frac{\vec{V}_{1D} \cdot \vec{n}_s}{V_{1D}} \right) \end{aligned} \quad (10.44)$$

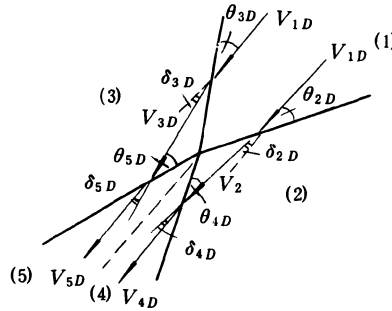


Fig. 10.21 Two-dimensional shock intersection in plane D

Thus we can solve the two-dimensional shock interaction as shown in § 7.8 and get the parameters in each region in the plane D . Assuming the unit vector of

flow velocity direction ahead of and behind the shock are denoted by \vec{e}_{aD} and \vec{e}_{bD} , we can find \vec{e}_{bD} from following relations (\vec{e}_{aD} , \vec{l} , and δ_{bD} are known)

$$\begin{cases} \vec{e}_{aD} \cdot \vec{e}_{bD} = \cos\delta_{bD} \\ \vec{e}_{bD} \cdot \vec{l} = 0 \\ |\vec{e}_{bD}| = 1 \end{cases} \quad (10.45)$$

The flow velocity in the reference system with the point Q is

$$\vec{V}_b = V_{bD} \vec{e}_{bD} + \vec{V}_l$$

In the laboratory coordinates, the velocity is

$$\vec{V} = \vec{V}_b + \vec{V}_Q$$

The unit normal vectors of the transmitted and deflected shocks can be found respectively, by using

$$\begin{cases} \vec{e}_{2D} \cdot \vec{n}_t = -\sin\theta_{4D} \\ \vec{n}_t \cdot \vec{l} = 0 \\ |\vec{n}_t| = 1 \end{cases} \quad \text{and} \quad \begin{cases} \vec{e}_{3D} \cdot \vec{n}_d = -\sin\theta_{3D} \\ \vec{n}_d \cdot \vec{l} = 0 \\ |\vec{n}_d| = 1 \end{cases} \quad (10.46)$$

The method mentioned in this section also applies to the irregular intersection of shocks, but the equations is not closed and we need to know some information about the Mach shock. In principle, the method can also be used for either steady or unsteady shock interaction(Yin and Aihara, 1990).

After getting the Mach number of and the unit vector normal to the transmitted shock, we can use them as the boundary condition for solving the three-dimensional equations of shock dynamics given in Chapter 7.

References

- Abd-el-Fattah, A.M., Henderson, L.F. and Lozzi, A., Precursor shock waves at a slow-fast gas interface. *J. Fluid Mech.*, **76**(1976), 157–176.
- Abd-el-Fattah, A.M. and Henderson, L.F., Shock wave at a fast-slow gas interface. *J. Fluid Mech.*, **86**(1978), 15–32.
- Abd-el-Fattah, A.M. and Henderson, L.F., Shock wave at a slow-fast gas interface. *J. Fluid Mech.*, **89**(1979), 79–95.
- Aiello, G.F., A simplified model of shock-on-shock interaction. *AD-A087247*, 1976.
- Bazhenova, T.V., Gvozdeva, L.G. and Nettleton, M.A., Unsteady interactions of shock waves. *Prog. Aerosp. Sci.*, **21**(1984), 249–331.
- Ben-Dor, G. and Glass, I.I., Domains and boundaries of nonstationary oblique shock wave reflexions. 1. Diatomic gas. *J. Fluid Mech.*, **92**(1979), 459–496.
- Ben-Dor, G. and Glass, I.I., Domains and boundaries of nonstationary oblique shock wave reflexions. 2. Monatomic gas. *J. Fluid Mech.*, **96**(1980), 735–756.
- Ben-Dor, G., Analytical solution of double Mach reflection. *AIAA J.*, **18**(1980), 1036–1043.
- Ben-Dor, G., Takayama, K. and Kawauchi, T., The transition from regular to Mach reflexion and from Mach to regular reflexion in truly nonstationary flows. *J. Fluid Mech.*, **100**(1980), 147–160.
- Ben-Dor, G. and Dewey, J.M., The Mach reflection phenomenon—a suggestion for an international nomenclature. *AIAA J.*, **23**(1985), 1650–1652.
- Ben-Dor, G. and Takayama, K., Analytical prediction of transition from Mach to regular reflection over cylindrical concave wedges. *J. Fluid Mech.*, **158**(1985), 365–380.
- Ben-Dor, G., Dewey, J.M. and Takayama, K., The reflection of a planar shock wave over a double wedge. *J. Fluid Mech.*, **176**(1987A), 483–520.
- Ben-Dor, G., Dewey, J.M. and Takayama, K., The influence of surface roughness on the transition from regular to Mach reflection in pseudosteady flow. *J. Fluid Mech.*, **176**(1987B), 333–356.
- Ben-Dor, G., Takayama, K. and Dewey, J.M., Further analytical considerations of weak planar shock wave reflections over concave wedges. *Fluid Dyn. Res.*, **2**(1987C), 77–85.
- Ben-Dor, G., A reconsideration of the three-shock theory for a pseudosteady Mach reflection. *J. Fluid Mech.*, **181**(1987), 467–484.
- Ben-Dor, G., *Phenomena of shock reflections*, Springer-Verlag, 1992.
- Bingham, G.F. and Davidson, T.E., Simulation of the interaction of a hypersonic body and a blast wave. *AIAA J.*, **3**(1965), 564–566.
- Bleakney, W. and Taub, A.H., Interaction of shock waves. *Rev. Mod. Phys.*, **21**(1949), 584–605.
- Brown, E.A. and Mullaney, G.J., Technique for studying the shock-on-shock problem. *AIAA J.*, **3**(1965A), 2167–2168.
- Brown, E.A. and Mullaney, D.J., Experiments on the head-on shock-shock interaction. *AIAA J.*, **3**(1965B), 2168–2170.
- Bryson, A.E. and Gross, R.W.F., Diffraction of strong shocks by cones, cylinders and spheres. *J. Fluid Mech.*, **10**(1961), 1–6.
- Catherasoo, C.J. and Sturtevant, B., Shock dynamics in non-uniform media. *J. Fluid Mech.*, **127**(1983), 539–561.
- Chen, Q. and Xia, N., A method for calculating oblique blast wave interaction with a supersonic cone. *Acta Aero. Sinica*, **4**(1982), 94–101 (in Chinese).
- Chester, W., The quasi-cylindrical shock tube. *Phil. Mag.*, **45**(1954), 1293–1301.
- Chester, W., The propagation of shock waves along ducts. *Adv. in Appl. Math.*, **6**(1960), 119–152, New York.
- Chisnell, R.F., The normal motion of a shock wave through a non-uniform one dimensional medium. *Proc. Roy. Soc. Ser. A*, **232**(1955), 350–370.

- Chisnell, R.F., The motion of shock wave in a channel, with applications to cylindrical and spherical shock waves. *J. Fluid Mech.*, **2**(1957), 286–298.
- Chisnell, R.F., A note on Whitham's rule. *J. Fluid Mech.*, **22**(1965), 103–104.
- Chisnell, R.F. and Yousaf, M., The effect of the overtaking disturbance on a shock wave moving in a non-uniform medium. *J. Fluid Mech.*, **120**(1982), 523–533.
- Clarke, J.F., Regular reflection of a weak shock wave from a rigid porous wall. *Q.J. Mech. Appl. Math.*, **37**(1984), 87–111.
- Colella, P. and Henderson, L.F., The von Neumann paradox for the diffraction of weak shock waves. *J. Fluid Mech.*, **213**(1990), 71–94.
- .Collins, R. and Chen, H.T., Propagation of a shock wave of arbitrary strength in two half planes containing a free surface. *J. Comp. Phys.*, **5**(1970), 415–422.
- Collins, R. and Chen, H.T., Motion of a shock waves through a non-uniform fluid. *Proc. 2nd Int. Conf. on Numerical Methods in Fluid Dynamics*, 1971.
- Courant, R. and Friedrichs, K.O., *Supersonic flow and shock waves*. Interscience, New York, 1948.
- Dewey, J.M. and McMillin, D.J., Observation and analysis of the Mach reflection of weak uniform plane shock waves, Part 1. Observations. *J. Fluid Mech.*, **152**(1985A), 49–66.
- Dewey, J.M. and McMillin, D.J., Observation and analysis of the Mach reflection of weak uniform plane shock waves, Part 2. Analysis. *J. Fluid Mech.*, **152**(1985B), 67–81.
- Duong, D.Q., Shock wave movement in axisymmetric area contractions. Ph.D. Thesis, Uni. New South Wales, Australia, 1982.
- Duong, D.Q. and Milton, B.E., The Mach reflection of shock waves in converging cylindrical channels. *Exp. in Fluid*, **3**(1985), 161–168.
- Edney, B., Anomalous heats transfer and pressure distributions on blunt bodies at hypersonic speeds in the presence of an impinging shock. *FFA Rept. 115.*, The Aeronautical research Institute of Sweden, 1968.
- Fu, Z.Q., Investigation of aerodynamic interaction of a plane moving shock wave with a conical body at supersonic speeds. *Acta Aero. Sinica*, **3**(1982), 108–113 (in Chinese).
- Gale, H.W., Unsteady flow with shock waves: application to gas dynamic lasers. *AIAA J.*, **15**(1977), 681–685.
- Glass, I.I., Some aspects of shock wave research. *AIAA J.*, **25**(1987), 214–229.
- Griffith, W.C., Shock waves. *J. Fluid Mech.*, **106**(1981), 81–101.
- Haas, J.F. and Sturtevant, B., Interaction of weak shock waves with cylindrical and spherical gas inhomogeneities. *J. Fluid Mech.*, **181**(1987), 41–75.
- Han, Z.Y. et al, An experimental technique of electrically controlled double driver shock tube for studying head-on moving shock–bow shock interaction. *Acta Mech. Sinica*, **4**(1982), 394–400 (in Chinese).
- Han, Z.Y. et al, An investigation of oblique shock–shock interaction on a stationary model in a shock tube. *Acta Aero. Sinica*, **4**(1983), 120–126 (in Chinese).
- Han, Z.Y., Yin, X.Z. and Wang, K., A method for calculating the waves interactions and experimental conditions in an electrically controlled double driver shock tube and shock tunnel. *Acta Aero. Sinica*, **4**(1986), 120–126 (in Chinese).
- Han, Z.Y. et al, A method for producing oblique shock–bow shock interaction in double driver shock tunnel. *Science in China, Ser. A*, **30**(1987), 620–628.
- Han, Z.Y. and Yin, X.Z., Two dimensional equations of shock dynamics for moving gas ahead of shock wave. *Science in China, Ser. A*, **32**(1989A), 1333–1344.
- Han, Z.Y. and Yin, X.Z., Three dimensional equations of shock dynamics for moving gas ahead of shock wave. *Proc. 17th Int. Symp. on Shock Waves and Shock Tubes*, Lehigh, U.S. 1989B.
- Han, Z.Y. and Yin, X.Z., Equation of shock dynamics and shock–shock relations for a moving gas ahead of shock wave. *Proc. 4th Copper Mountain Conf. on Multigrid Methods*, Colorado, U.S., 1990.
- Han, Z.Y. Feng, J.Q. and Yin, X.Z., A new method for calculating head-on interaction of a moving shock with a cone flying at supersonic. *J. of Chinese Soc. of Astro.*, **4**(1990), 1–6.
- Han, Z.Y., Shock dynamics description of reflected shock waves. *Proc. 18th Int. Symp. on Shock Waves. Sendai*, Japan, 1991.
- Han, Z.Y. and Chow, C.Y., A method for studying shock wave–vortex interaction. *1st Chinese–Soviet*

- Workshop on Complex Fields of Gas Flow.* Beijing, China, 1991.
- Han, Z.Y., Development of shock dynamics. *Advance of Modern Fluid Mechanics*, Science Press, China, 1991 (in Chinese)
- Han, Z.Y., Milton, B.K. and Takayama, K., The Mach reflection triple point locus for internal and external conical diffraction of a moving shock wave. *Shock Waves—an International Journal*, 2(1992), 5–12.
- Han, Z.Y. and Yin, X.Z., Shock–shock relations for moving gas ahead of shocks. *Science in China, Ser. A*, (1992)7, 725–733 (in Chinese).
- Heilig, W.H., Diffraction of shock wave by a cylinder. *Phys. Fluids Supl.*, 12(1967), 154–157.
- Henderson, L.F., On the confluence of three shock waves in a perfect gas. *Aero. Q.*, 15(1964), 181–197.
- Henderson, L.F., On shock impedance. *J. Fluid Mech.*, 40(1970), 719–735.
- Henderson, L.F. and Lozzi, A., Experiments on transition of Mach reflexion. *J. Fluid Mech.*, 68(1975), 139–155.
- Henderson, L.F. and Lozzi, A., Further experiments on transition to Mach reflexion. *J. Fluid Mech.*, 94(1979), 541–559.
- Henderson, L.F., On the Whitham theory of shock wave diffraction at concave corners. *J. Fluid Mech.*, 99(1980), 801–811.
- Henderson, L.F. and Gray, P.M., Experiments on the diffraction of strong blast waves. *Proc. Roy. Soc. London, Ser. A*, 377(1981), 363–378.
- Henderson, L.F., Exact expressions for shock reflection transition criteria in a perfect gas. *Z.A.M.M.*, 62(1982), 258–261.
- Henderson, L.F., Regions and boundaries for diffracting shock wave systems. *Z.A.M.M.*, 67(1987), 73–86.
- Henderson, L.F., On the thermodynamic stability of steady state adiabatic systems. *J. Fluid Mech.*, 189(1988), 509–529.
- Henderson, L.F., On the refraction of shock waves. *J. Fluid Mech.*, 198(1989), 365–386.
- Henshaw, W.D., Smyth, N.F. and Schwendemann, D.W., Numerical shock propagation using geometrical shock dynamics. *J. Fluid Mech.*, 171(1986), 519–545.
- Hornung, H.G., Oertel, H. and Sademan, R.J., Transition to Mach reflexion of shock waves in steady and pseudosteady flow with and without relaxaton. *J. Fluid Mech.*, 90(1979), 541–560.
- Hornung, H.G. and Taylor, J.R., Transition from regular to Mach reflelion of shock waves. Part 1, The effect of viscosity in the pseudosteady case. *J. Fluid Mech.*, 123(1982), 143–153.
- Hornung, H.G. and Robinson, M.L., Transition from regular to Mach reflection of shock waves. Part 2, The steady flow criterion. *J. Fluid Mach.*, 123(1982), 155–164.
- Hornung, H.G., Regular and Mach reflection of shock waves. *Ann. Rev. Fluid Mech.*, 18(1986), 13–58.
- Huppert, H.E. and Miles, J.W., A note on shock diffraction by a supersonic wedge. *J. Fluid Mech.*, 31(1968), 455–458.
- Itoh, S., Okazaki, N. and Itaya, M., On the transition between regular and Mach reflection in truly non-stationary flows. *J. Fluid Mech.*, 108(1981), 384–400.
- Jahn, G., The refraction of shock waves at gaseous interface. *J. Fluid Mech.*, 1(1956), 457–489.
- Jones, D.A., Martin, P.M. and Thornhill, C.K., A note on the pseudostationary flow behind a strong shock diffracted or reflected at a corner. *Proc. Roy. Soc. London, Ser. A*, 209(1951), 238–248.
- Kawamura, R. and Saito, H., Reflection of shock waves. I. Pseudo–stationary case. *J. Phys. Soc., Japan*, 11(1956), 584–592.
- Kireev, V.T., Motion of shock waves in an inhomogeneous gas. *Fluid Dynamics*, 1(1981), 175–178.
- Kutler, P., Sakell, L. and Aiello, G., On the shock–on–shock interaction problem. *AIAA paper*, 74–524, 1974 (also see, Two dimentional shock–on–shock interaction problem. *AIAA J.*, 13, 361).
- Kutler, P. and Sakell, L., Three dimentional shock–on–shock interaction problem. *AIAA paper*, 75–49, 1975 (also see *AIAA J.*, 13, 1360).
- Law, C.K. and Glass, I.I., Diffraction of strong shock waves by a sharp compressive corner. *CASI tran.*, 4(1971), 2–12.
- Li, H.D., Study of transition criteria from RR to MR in truly nonstationary flow. Thesis, Univ. of Scie. and Tech. of China, 1988.
- Lighthill, M.J., On the diffraction of blast I. *Proc. Roy. Soc. London, Ser. A*, 198(1949), 454–470.

- Liu, Z.N., Yin, X.Z. and Han, Z.Y., An experimental investigation of shock diffraction over a convex corner in the case of non-uniform flow ahead of shock. *Proc. Int. Conf. on Exp. Fluid Mech.*; Chengdu, China, 1991.
- Mach, E., Über den verlauf von funkenwellen im der ebene und in raume. *Akad. Wiss. Wien.*, **77**(1878), 819–838.
- Marconi, F., Shock reflection transition in three dimensional steady flow about interfering bodies. *AIAA J.*, **21**(1983), 707–713.
- Markstein, G.H., A shock tube study of flame front–pressure wave interaction. *6th Int. Comb. Symp.*, 387–398, Reinhold, 1957.
- Merritt, D.L., Study of blast–bow wave interaction in a wind tunnel. *AIAA paper*, 65–5, 1965.
- Merritt, D.L. and Aronson, P.M., Free flight shock interaction studies. *AIAA paper*, 66–57, 1966.
- Merritt, D.L. and Aronson, P.M., Technique for studying oblique shock–on–shock interaction in free flight. *Fifth Hypervelocity Techniques Symp.*, 1967, 325–346.
- Miles, J.W., A note on shock–shock diffraction. *J. Fluid Mech.*, **22**(1965), 95–102.
- Milton, B.E. and Archer, R.D., Generation of implosions by area change in shock tube. *AIAA J.*, **7**(1969), 779–780.
- Milton, B.E., Shock wave motion and focusing in area contractions. Ph.D. thesis, Uni. New South Wales, Australia, 1971.
- Milton, B.E., Mach reflection using ray shock theory. *AIAA J.*, **13**(1975A), 1531–1533.
- Milton, B.E., Simplified ray–shock theory parameters for use with diatomic gases. *UNSW 1975 / FMT / 2*, 1975B.
- Milton, B.E., Duong, D.Q. and Takayama, K., Multiple, internal conical Mach reflections. *Proc. 15th Int. Symp. on Shock Waves and Shock Tubes*, 1985.
- Nicholson, J.E., Oblique blast wave interaction with a supersonic vehicle. *AIAA paper*, 67–180, 1967.
- Oshima, K. et al., Diffraction of a plane shock wave around a corner. Rept. No. 393, Inst. of Space and Aero. Scie., 1965, Univ. of Tokyo.
- Pack, D.C., The reflexion and diffraction of shock waves. *J. Fluid Mech.*, **18**(1964), 549–576.
- Rosciszewski, J., Calculation of the motion of non-uniform shock waves. *J. Fluid Mech.*, **8**(1960), 337–367.
- Rudinger, G., Shock wave and flame interaction. *Comb. and Propu., 3rd AGARD Coll.*, London, Pergamon, 1958.
- Ruetenik, J.R. and Lemek, B., Study of blast–bow wave interactions in a shock tube and shock tunnel. *AIAA paper*, 66–409, 1966.
- Russell, D.A., Shock wave strengthening by area convergence. *J. Fluid Mech.*, **27**(1967), 305–314.
- Sakurai, A., et al., On the von Neumann paradox of weak Mach reflection. *Fluid Dyn. Res.*, **4**(1989), 333–346.
- Schwendeman, D.W., Numerical shock propagating in non-uniform media. *J. Fluid Mech.*, **188**(1988), 383–410.
- Setchell, R.E., Storm, E. and Sturtevant, B., An investigation of shock strengthening in a conical convergent channel. *J. Fluid Mech.*, **56**(1972), 505–522.
- Shapiro, A.M., *The dynamics and thermodynamics of compressible fluid flow*. Ronald, New York, 1953.
- Skews, B.W., The shape of a diffracting shock wave. *J. Fluid Mech.*, **29**(1967A), 297–304.
- Skews, B.W., The perturbed region behind a diffracting shock wave. *J. Fluid Mech.*, **29**(1967B), 705–719.
- Smith, L.G., Photographic investigation of the reflection plane shock in air. OSRD Rep. No. 6271, 1945.
- Smith, W.R., Mutual reflection of two shock waves of arbitrary strengths. *Phys. Fluids*, **2**(1959), 533–541.
- Takayama, K., Ben-Dor, G. and Dotoh, J., Regular to Mach reflection transition in truly nonstationary flow–influence of surface roughness. *AIAA J.*, **19**(1981), 1238–1240.
- Takayama, K. and Sekiguchi, H., Triple point trajectory of a strong spherical shock wave. *AIAA J.*, **19**(1981), 815–817.
- Takayama, K. and Sasaki, M., Effects of radius of curvature and initial angle on the shock transition over concave and convex wall. *Rep. Int. High Speed Mech.*, Tohoku Uni., 1983.
- von Neumann, J., Oblique reflection of shocks. *Explos. Res. Rep. No. 12*, Washington, DC, 1943 (also see *Collected Works*, **6**, 238–299, Oxford, 1963)

- Wang, J.H., *Some problems on two dimensional unsteady fluid dynamics*. Beijing, 1984 (in Chinese)
- White, D.R., An experimental survey of the Mach reflection of shock waves. Princeton Univ. Dept. Phys. Tech. Rep. II-10, 1951.
- Whitham, G.B., A new approach to problems of shock dynamics, Part I, Two dimensional problems. *J. Fluid Mech.*, 2(1957), 146-171.
- Whitham, G.B., On the propagation of shock waves through regions of non-uniform area or flow. *J. Fluid Mech.*, 4(1958), 337-360.
- Whitham, G.B., A new approach to problems of shock dynamics, Part II, Three dimensional problems. *J. Fluid Mech.*, 5(1959), 369-386.
- Whitham, G.B., A note on shock dynamics relative to a moving frame. *J. Fluid Mech.*, 31(1968), 449-453.
- Whitham, G.B., *Linear and nonlinear waves*, Wiley-Interscience, New York, 1973.
- Whitham, G.B., On shock dynamics *Proc. Indian Acad. Sci.(Math. Sci.)* 96(1987), 71-73.
- Yang, J.M. and Han, Z.Y., Some problemes on shock propagation in ducts *Proc. 4th National Symp. on Shock Tube and Shock Waves*, 1987, 50-55 (in Chinese).
- Yang, J.M., Han, Z.Y. and Yin, X.Z., Shock tunnel-shock tube combination and some applications. *Proc. Int. Conf. on Exp. Fluid Mech.*, Chengdu, China, 1991A.
- Yang, J.M., Han, Z.Y. and Yin, X.Z., An investigation of the refraction of moving shock at slip-surface in combination facility. *Proc. 18th Int. Symp. on Shock Waves*. Sendai, Japan, 1991B.
- Yin, X.Z. and Han, Z.Y., Investigation of Mach reflection of plane shock propagating into uniform supersonic flow around wedge. *Acta Aero. Sinica.*, 7(1989), 67-74.
- Yin, X.Z. and Aihara, Y., A method on calculating three dimensional shock interaction, Part 1, regular case. *Trans. of Japan for Aero. Space Scie.*, 33(1990), 100.
- Yousaf, M., The effect of overtaking disturbances on the motion of converging shock waves *J. Fluid Mech.*, 66(1974), 577-591.

NOMENCLATURE

- A cross sectional area of ray tube, cross-sectional area of one-dimentional tube
 a speed of sound
 b length of Mach stem
 C disturbance velocity of shock-shock
 c velocity of disturbance
 C^+, C^- characteristics
 e coefficient in area relation
 \vec{e} unit vector
 f friction force per unit mass of gas, coefficient in area relation
 g coefficient in area relation
 h coefficient in area relation, enthalpy, height of Mach stem in internal conical diffraction
 \vec{i} unit vector for ray direction
 J_+, J_- Riemann invariants in shock dynamics
 K slowly varying function
 K_1, K_2 Riemann invariants in gasdynamics
 k vortex strength
 \vec{l} unit vector along intersection line of shock surfaces
 M Mach number
 m flow Mach number in the region ahead of shock wave
 \vec{n} unit vector normal to shock, unit vector normal to contact surface
 \vec{n}_f unit vector of flow velocity
 \vec{n}_{ss} unit vector normal to shock-shock surface
 p pressure
 q heat transfer rate per unit mass of gas
 R gas constant, radius
 r coordinate
 R_u universal gas constant
 Re Reynolds number
 S surface surrounding ray tube, moving discontinuity surface
 s entropy, distance along wall, distance along characteristic direction, path of disturbance propagation
 T temperature
 t time
 U velocity
 u flow velocity
 V volume of ray tube, flow velocity
 W_s shock speed
 W_d speed of disturbance wave propagating along shocksurface
 x, y, z coordinates
 α function of shock surface, curvilinear coordinates, incident angle
 β ray, curvilinear coordinates, angle between bow shock and x axis
 γ ratio of specific heat, angle between \vec{n} and \vec{i}
 δ deflected angle of flow across shock wave, thickness of boundary layer
 δ^* displacement thickness of boundary layer
 ϵ internal energy, angle of flow direction change caused by viscous effect
 η coordinates, similar variable, correct coefficient
 θ angle between normal to shock and x axis

λ	length of Mach stem
μ	Mach number of moving shock with respect to flowbehind shock, molecular weight
ν	angle between characteristics and normal to shock surface
ξ	pressure ratio across shock wave
ρ	density
\vec{t}	unit vector tangent to shock surface
φ	coordinates, velocity potential function, anglebetween oncoming flow and shock wave
χ	angle of triple point trajectory
χ'	angle of second triple point trajectory
ψ	stream function
ω	angle, angular speed

subscripts

0	undisturbed quantity, stagnation state
$1, 2, 3, \dots$	coordinates, characteristic, regions in flow field
a	ahead of
b	behind
k	kink
M	moving frame of reference
n	normal to
r	reflected wave
s	shock, entropy, sphere, stationary frame of reference
ss	shock-shock surface
T	triple point, transition point, transmitted shock
T'	second triple point
w	wall surface, wedge
I, II, III	characteristics
prime'	small perturbation, in moving frame of reference

INDEX

A

angle,
 between characteristic and x -axis 56
 between direction of flow and x -axis 171, 188
 between first disturbance and x -axis 56, 158
 between \vec{t} and \vec{n} 141, 174, 191
 between normal to shock and x -axis 152
 between shock-shock trace and surface of wedge 66
flow deflected, 234
 maximum, 236
triple point trajectory, 110, 240, 253

area,
 of shock cut out by ray tube 136, 140, 192
ray tube, 44, 79, 136

B

boundary layer,
 displacement thickness 257, 261
 laminar, 259
 thickness 259

C

characteristic
 curves 15, 99, 125, 163
 relations 47, 125, 128, 148, 156, 163, 183
 expressed by du and $d\rho$ 15
 expressed by du and $d\rho$ 16
 in rectangular coordinates 49, 128

characteristics,

C^+ 30
 C^- 30
 in $x - r$ plane 96
 p 30
 two families of, 46

condition

 boundary, 77, 84
 compatible, 26, 223, 307
 detachment, 242
 maximum deflection, 241
 Rankine-Hugoniot, 38, 40
 sonic, 242
 von Neumann, 242

contact surface 24, 38, 252, 307
coordinates

 cylindrical, 180, 202

fixed, 12, 135
moving, 21, 135
orthogonal curvilinear, 42, 45, 48, 125, 196
rectangular, 42, 48, 128
relation between two, 170, 193
spherical, 207, 226
transformation of, 22, 48, 146, 169
 transient, 172, 192
cubic spline 298

D

density 2, 76
diffraction,
 external conical, 105
 internal conical, 102
 of plane shock 50
 over body 75
 over circular cylinder 87
 over concave wall 63
 over cone 74, 82
 over convex mall 51
 over convex sharp corner 54, 60, 154
 over slender cone 100
 over sphere 90
 over thin or slender body 92
 over wedge 66
 of spherical shock,
 over horizontal plane 75

direction,

 of ray 45, 145
 of flow behind shock 145

disturbance, 46

 propagation concept 270, 275
 propagating on shock 46, 157
 re-reflected, 24, 29
 small, 1, 93

disturbance point

 first, 55, 151, 158
 last, 55, 158, 159

E

effect,
 of real gas 262
 of viscosity, 257
 on boundary layer 257
 on contact surface 258
entropy 3

disturbance of, 16

equation

continuity, 1, 22, 71, 76, 234

energy, 1, 22, 234

Euler, 1, 22, 76, 234

in plane flow case 72

in axially symmetric case 73, 82

in self-similar case 82

one dimensional homoentropic unsteady, 7

one dimensional unsteady, 14, 294

ordinary differential, 83, 211, 218, 294, 297

state, 1, 22, 235

von Karmann integral momentum, 260

wave, 2

F

flow

axially symmetrical, 92, 218

double wave, 7

irrotational, steady supersonic, 75

isentropic, 5

non-isentropic, 5, 6

non-uniform, 165, 187

 ahead of shock wave 165, 179, 191

one dimensional steady, 13

one dimensional unsteady continuous, 1, 13

steady, inviscid, 237, 241

steady state, 7

three dimensional, 79

uniform,

 ahead of shock wave 144

flow field

 axially symmetrical, 219

 conical, 218

 self-similar, 210, 218, 240

 steady, 187, 218, 300

form

 vectorial, 123, 304

frame of reference

 moving, 135, 169, 193

 stationary, 135, 169, 193

 transformation of, 135

 two types of, 135

free propagating 24, 28

function

 of shock surface 72, 75

stream, 77

 of velocity potential 75

G

gas

 nonuniform quiescent, 118, 121

 uniform quiescent, 21, 68, 72

gas constant 3, 22

universal, 3

gas particle 12

path of, 11, 16, 30

I

interaction

 between two shocks 300

 steady, 300

 unsteady, 303

 shock-on-shock, 217

 head-on, 217

 oblique, 217, 224

 shock wave-vortex, 187

interface

 fast-slow, 281

 slow-fast, 281, 294

intersection,

 between two shocks 219, 300

 irregular, 301

 regular, 301

 three-dimensional, 303

 two-dimensional, 219, 308

isentropic process 3

K

kink 241, 251

M

Mach cone 95

Mach number

 critical shock, 292

 flow, 13, 25

 shock, 21, 69

Mach stem 38, 103, 224, 238

 length of, 84, 92, 102, 248

medium

 non-uniform moving, 165, 191

 non-uniform quiescent, 118

 uniform moving, 135

 uniform quiescent, 21, 42, 68

method

 Chester's, 118

 Chisnell's, 24, 118

 numerical, 297

 of shock dynamics 268, 273

 of small perturbations 93

 Whitham's, 30, 118, 165

motion of piston 11, 51

N

normal,

 derivatives of α 78, 214

 to moving surface 68

 to shock 126

- to surface of ray tube 139
- P**
- plane
symmetrical, 224
 $x-t$, 1, 25
 $\alpha-\beta$ 48
- point,
detachment, 236
Mach wave, 235
maximum deflection, 236
normal shock, 235
sonic, 236
triple, 253
 trajectory 66, 81, 99, 110, 267
- pressure, 2
 ratio 26, 236
signal 248, 270, 275
- R**
- ray 42
 direction of, 65, 69, 145
- ray tube 42, 44
 end surface of, 70
 diameter of, 70, 140
 side surface of, 70
 surface of, 69, 139
- reflection,
 Mach, 87, 238, 240
 complex, 241, 250
 direct, 245, 266
 double, 241, 251
 inverted, 244, 266
 single, 240
 stationary, 245, 266
- of plane shock
 over cylindruc concave surface 265
 over cylindruc convex surface 265
 over double wedge 278
 over wedge 151
- pseudosteady, 239
- regular, 87, 151, 237, 239
- steady, 237
- unsteady, 264
- von Neumann, 263
- refraction,
 at slip surface 289
 across interface 280, 292
- irregular,
 bound precursor, 288
 centred expansion, 283
 concaver forwards, 285
 double Mach reflection type, 286
 free precursor, 288
- free precursor von Neumann, 288
lambda, 288
Mach type, 283
twin Mach, 289
twin von Neumann, 288
- regular,
 with reflected shock 281, 292
 with expansion wave 283, 292
- relation,
 between frames of reference 135, 170, 193
 between \vec{t} and A 122
 between \vec{t} and \vec{n} 141, 144, 173
 between M, θ and α 68, 121, 142, 175
 differential, 137
geometric, 42, 45, 222, 254
of $A-M$, 32, 167
 Milton's modified, 38, 274
of homoentropic steady flow 165
ray tube area, 42, 46, 118, 176, 199
- Skew's, 61
- shock, 23, 31, 304
 oblique, 235, 254
Whitham's, 61
- Riemann invariables 8, 9, 48
- S**
- shock,
 bow, 217, 301, 303, 307
 deflected, 219, 307
 incident, 239, 265, 281, 306
 oblique, 146
 opposite family of, 301
polar
 hodograph, 235
 pressure-deflected angle 235, 268, 280
- reflected, 153, 307
 formation of, 153
 orientation of, 154
 shape of, 154
 strength of, 154
 same family of, 301
 transmitted, 219, 224, 307
- shock dynamics
 kinematic relation of, 42, 76
 kinetic relation of, 42
- equations of,
 axisymmetrical, 103, 161, 181, 206
 denoted by M and θ 123, 142, 175
 denoted by α 123, 138, 172
 in moving frame 138, 172
 in stationary frame 139, 173
 three dimensional, 68, 121, 198, 202, 207, 226
 two dimensional, 45, 120, 138, 142, 148, 172,

175, 179, 297
 numerical, 297
 shock compression 51, 64
 shock expansion 51, 62, 154, 295
 shock-shock, 64, 295
 area relation across, 215
 formation of, 62
 relations 64, 79, 212
 trace 66, 81, 99
 angle 215, 253
 shock wave 17, 21
 disturbed, 65, 212
 incident, 24
 formaton of, 17
 of constant strength 21
 of variable stength 24, 30
 orientation of, 53
 reflected, 38
 shape of, 28, 50, 56
 stregh 28, 50, 53
 strong, 27, 55, 67, 242
 three dimensional, 303
 transmitted, 25
 undisturbed, 64
 weak, 27, 242
 similarity variable 82, 210
 sonic point 242, 301
 sound circle 60
 center of, 152
 radius of, 152
 sound wave
 first, 151
 speed,
 of disturbance wave propagating on shock 51, 128
 of nonlinear disturbance wave on shock 48
 of sound, 1, 2, 43, 275

T

tangential derivatives of α 79
 theory
 CCW, 21
 linearized, 92
 of sound 60, 151
 small perturbation, 33
 two-shock, 152, 250
 three-shock, 250, 253, 258
 transition
 point 115
 boundary 245, 250, 272, 286, 289
 criteria SMR \rightarrow CMR 250, 253
 criteria CMR \rightarrow DMR 250, 253
 criterion RR \rightarrow MR 246
 detachment, 246

in shock dynamic theory 158
 length scale, 248
 mechanical equilibrium, 247
 sonic, 246
 MR \rightarrow RR over concave surface 273
 RR \rightarrow MR over convex surface 268
 triple point locus 102, 240, 266
 tube,
 of constant cross sectional area 1, 7, 14
 slowly varying cross sectional area, 38
 soli wall, 165
 with small area change 24
 with variable cross sectional area 14

U

unit vector,
 \vec{i} 141, 144, 173
 in x -axis 72, 74
 in y -axis 72
 in r -axis 74
 normal to surface of shock-shock 79
 of flow ahead of shock 145
 of the normal to shock 72, 74, 305
 of ray direction 69, 122
 tangential to intersection line 305

V

viewpoint,
 field, 4
 gas dynamic, 50
 particle, 4
 shock dynamic, 50, 153
 von Neumann paradox, 250
 of weak Mach reflection 262
 vortex 187

W

wall
 concave, 50
 convex, 50
 surface 78
 wave,
 cylindrical disturbance, 50
 left traveling, 3, 5, 9, 12, 16
 nonlinear, 46
 pressure, 7
 propagating on shock 46
 right traveling, 3, 5, 9, 12, 16
 simple,
 expression of, 10
 formation of, 10
 relations of, 26
 small disturbance, 1
 sound, 1, 50, 60

compression, 1, 11

rarefaction, 1, 11

Mechanics

SOLID MECHANICS AND ITS APPLICATIONS

Series Editor: G.M.L. Gladwell

Aims and Scope of the Series

The fundamental questions arising in mechanics are: *Why?*, *How?*, and *How much?* The aim of this series is to provide lucid accounts written by authoritative researchers giving vision and insight in answering these questions on the subject of mechanics as it relates to solids. The scope of the series covers the entire spectrum of solid mechanics. Thus it includes the foundation of mechanics; variational formulations; computational mechanics; statics, kinematics and dynamics of rigid and elastic bodies; vibrations of solids and structures; dynamical systems and chaos; the theories of elasticity, plasticity and viscoelasticity; composite materials; rods, beams, shells and membranes; structural control and stability; soils, rocks and geomechanics; fracture; tribology; experimental mechanics; biomechanics and machine design.

1. R.T. Haftka, Z. Gürdal and M.P. Kamat: *Elements of Structural Optimization*. 2nd rev.ed., 1990 ISBN 0-7923-0608-2
2. J.J. Kalker: *Three-Dimensional Elastic Bodies in Rolling Contact*. 1990 ISBN 0-7923-0712-7
3. P. Karasudhi: *Foundations of Solid Mechanics*. 1991 ISBN 0-7923-0772-0
4. N. Kikuchi: *Computational Methods in Contact Mechanics*. (forthcoming) ISBN 0-7923-0773-9
5. *Separate title.*
6. J.F. Doyle: *Static and Dynamic Analysis of Structures*. With an Emphasis on Mechanics and Computer Matrix Methods. 1991 ISBN 0-7923-1124-8; Pb 0-7923-1208-2
7. O.O. Ochoa and J.N. Reddy: *Finite Element Analysis of Composite Laminates*. ISBN 0-7923-1125-6
8. M.H. Aliabadi and D.P. Rooke: *Numerical Fracture Mechanics*. ISBN 0-7923-1175-2
9. J. Angeles and C.S. López-Cajún: *Optimization of Cam Mechanisms*. 1991 ISBN 0-7923-1355-0
10. D.E. Grierson, A. Franchi and P. Riva: *Progress in Structural Engineering*. 1991 ISBN 0-7923-1396-8
11. R.T. Haftka and Z. Gürdal: *Elements of Structural Optimization*. 3rd rev. and exp. ed. 1992 ISBN 0-7923-1504-9; Pb 0-7923-1505-7
12. J.R. Barber: *Elasticity*. 1992 ISBN 0-7923-1609-6; Pb 0-7923-1610-X
13. H.S. Tzou and G.L. Anderson (eds.): *Intelligent Structural Systems*. 1992 ISBN 0-7923-1920-6
14. E.E. Gdoutos: *Fracture Mechanics*. An Introduction ISBN 0-7923-1932-X
15. J.P. Ward: *Solid Mechanics*. An Introduction. 1992 ISBN 0-7923-1949-4
16. M. Farshad: *Design and Analysis of Shell Structures*. 1992 ISBN 0-7923-1950-8
17. H. S. Tzou and T. Fukuda (eds.): *Precision Sensors, Actuators and Systems*. 1992 ISBN 0-7923-2015-8
18. J. R. Vinson: *The Behavior of Shells Composed of Isotropic and Composite Materials*. 1993 ISBN 0-7923-2113-8

Mechanics

FLUID MECHANICS AND ITS APPLICATIONS

Series Editor: R. Moreau

Aims and Scope of the Series

The purpose of this series is to focus on subjects in which fluid mechanics plays a fundamental role. As well as the more traditional applications of aeronautics, hydraulics, heat and mass transfer etc., books will be published dealing with topics which are currently in a state of rapid development, such as turbulence, suspensions and multiphase fluids, super and hypersonic flows and numerical modelling techniques. It is a widely held view that it is the interdisciplinary subjects that will receive intense scientific attention, bringing them to the forefront of technological advancement. Fluids have the ability to transport matter and its properties as well as transmit force, therefore fluid mechanics is a subject that is particularly open to cross fertilisation with other sciences and disciplines of engineering. The subject of fluid mechanics will be highly relevant in domains such as chemical, metallurgical, biological and ecological engineering. This series is particularly open to such new multidisciplinary domains.

1. M. Lesieur: *Turbulence in Fluids*. 2nd rev. ed., 1990 ISBN 0-7923-0645-7
2. O. Métais and M. Lesieur (eds.): *Turbulence and Coherent Structures*. 1991 ISBN 0-7923-0646-5
3. R. Moreau: *Magnetohydrodynamics*. 1990 ISBN 0-7923-0937-5
4. E. Couston (ed.): *Turbulence Control by Passive Means*. 1990 ISBN 0-7923-1020-9
5. A.A. Borissov (ed.): *Dynamic Structure of Detonation in Gaseous and Dispersed Media*. 1991 ISBN 0-7923-1340-2
6. K.-S. Choi (ed.): *Recent Developments in Turbulence Management*. 1991 ISBN 0-7923-1477-8
7. E.P. Evans and B. Coulbeck (eds.): *Pipeline Systems*. 1992 ISBN 0-7923-1668-1
8. B. Nau (ed.): *Fluid Sealing*. 1992 ISBN 0-7923-1669-X
9. T.K.S. Murthy (ed.): *Computational Methods in Hypersonic Aerodynamics*. 1992 ISBN 0-7923-1673-8
10. R. King (ed.): *Fluid Mechanics of Mixing*. Modelling, Operations and Experimental Techniques. 1992 ISBN 0-7923-1720-3
11. Z. Han and X. Yin: *Shock Dynamics*. 1993 ISBN 0-7923-1746-7
12. L. Svarovsky and M.T. Thew (eds.): *Hydroclones*. Analysis and Applications. 1992 ISBN 0-7923-1876-5
13. A. Lichatarowicz (ed.): *Jet Cutting Technology*. 1992 ISBN 0-7923-1979-6
14. F.T.M. Nieuwstadt (ed.): *Flow Visualization and Image Analysis*. 1993 ISBN 0-7923-1994-X
15. A.J. Saul (ed.): *Floods and Flood Management*. 1992 ISBN 0-7923-2078-6
16. D.E. Ashpis, T. B. Gatski and R. Hirsh (eds.): *Instabilities and Turbulence in Engineering Flows*. 1993 ISBN 0-7923-2161-8